Computational aspects of on-line machine monitoring.

MILNE, A.J.

1984

COMPUTATIONAL ASPECTS OF ON-LINE MACHINE MONITORING

ALAN J MILNE

A thesis submitted in partial fulfilment of the requirements of the Council for National Academic Awards for the Degree of Doctor of Philosophy (Ph D).

DECLARATION

I hereby declare that this thesis is a record of work undertaken by myself, that it has not been the subject of any previous application for a degree and that all sources of information have been duly referenced.

In the course of the research, the following were included in an approved programme of advanced studies.

1. RGIT course on "Computer Engineering"

2. RGIT course on "Electronic Instrumentation".

3. RGIT course on "Microprocessor and Microcomputer Systems".

4. IEE/SRC Vacation school on "Digital Signal Processing", held at the School of Engineering and Applied Sciences, University of Sussex in September 1982.

5. One day seminar on the "Fundamentals of signal analysis", held at the South Queensferry plant of The Hewlett-Packard Company , March, 1981.

6. United Kingdom Machine Health Monitoring Group, three day course on "On-condition maintenance", held in Aberdeen, April 1981.

A J Milne
August 1984.

CONTENTS   Page

                                            Number

CHAPTER 7.

Appendix: Conference Papers.

ACKNOWLEDGEMENTS

ABSTRACT

COMPUTATIONAL ASPECTS OF ON-LINE MACHINE MONITORING

The detection of the fault phenomena found on three phase induction motors, as widely used in industry, from an electrical engineering viewpoint has been investigated. Various transducers are used, on a real motor, to establish connections between known fault and measurable changes in the signals from these transducers. It is shown that these signals may be processed in a very powerful, yet conceptually simple way, to allow various fault conditions to be diagnosed. A fault condition may be due to one or more individual faults.

In this thesis, the development of a general purpose, user friendly minicomputer based system to carry out fault detection is reported. The establishment of such a system is necessary to provide a framework within which to develop signal processing regimes which are suited to the task of condition monitoring.

Having established the desired links between the controlled faults and measurable changes in the signals from the various transducers used, and the signal processing needed to detect these changes, a dedicated microprocessor implementation has been devised.

The results of this research are directly applicable to industry, and would allow considerable savings on maintenance costs. This is due to the continuous indication of the working state of the machine, so that maintenance may be planned in advance, thus saving on costly downtimes. It will also save time and costs on regular maintenance strategies, as it allows for a motor to be left in service, with complete confidence in its performance, without the need to withdraw it from service and examine it at regular, but possibly otherwise unnecessary intervals.

CHAPTER 1

1.1   Introduction to the Thesis.

It is intended, in this work, to develop the techniques of computer and microprocessor based signal processing which are appropriate to the task of condition monitoring. This monitoring is to be carried out on three-phase asynchronous induction motors, and is to deal with electrical faults.

Although considerable work has been done in the field of condition monitoring, it has been confined to the diagnosis of purely mechanical faults. Certain aspects of the signal processing developed for this end are very powerful and are shown to be directly applicable to the detection and diagnosis of electrical faults. This is an important feature of the work, as it allows a grounding for the development of an instrument which would be capable of handling both mechanical and electrical fault mechanisms, based on a common set of signal procesing techniques.

Because of the interest, here, in electrical faults, the underlying mechanisms must be investigated, and the effects of mechanical and electrical phenomena thereby separated. This is done by the use of different test signals, which reflect features of either source. For example, the vibration of the case of a motor may be caused by purely mechanical means, as well as by the electrical conditions within the machine, by way of electro-magnetic forces. To allow these to be separated, and thus the fundamental mechanism involved to be understood, the current in the supply lines and the magnetic flux are also observed, these being electrical in their origins.

Investigation of these two aspects of a motor, in conjunction with each other allows the fundamental fault mechanisms to be established, and thereby leads to efficient signal processing to monitor for faults, based on machine fundamentals. This property makes the diagnosis applicable to a range of motors, with the minimum of change to the processing.

Each chapter deals with a specific topic within this area. Chapter 2 gives a background to three-phase rotating machine theory, and provides an insight into the fundamental mechanisms involved in the formation of the signals which are measured in the condition monitoring analysis, and the changes to be expected in these, under various fault conditions. In Chapter 3, the various methods of signal processing which may be applied to the problem are discussed and the reasons behind the choice of a particular solution are outlined. This includes a discourse on the use of Walsh Transforms as an alternative to Fourier Transform methods. The former have the advantage of being based on the values of plus and minus unity only, so being attractive for a microprocessor implementation. It is shown, however, that they also have disadvantages associated with them, which out-weigh the advantages for condition monitoring. Chapter 4 is concerned with the development of a general purpose, mini-computer based signal processing system. This is used for all of the research into the fault mechanisms investigated, and provides a flexible means of determining the signal processing which is required to diagnose electrically based faults. The results of this investigation, along with details of the solution implemented for the detection of machine faults are discussed in

Chapter 5. This consists of a collection of signal processing units, configured to give single figure "confidence factors" for each of the faults. These are shown to give a reliable determination of the presence, and type of fault(s) under all load conditions.

As the system for this is based on a general purpose mini-computer and a commercial spectrum analyser, a microprocessor implementation is then undertaken. Chapter 6 discusses this, and gives details of the specific ways in which a microprocessor can be applied to condition monitoring. This includes a careful consideration of the time involved in performing the analysis, and shows how steps can be taken to minimise this, by performing the operations in a particular order, and by the use of hardware to allow more than one operation to proceed at the same time.

1.2   Review of Condition Monitoring.

All items of machinery have a finite life span. This implies that no matter how reliable or well designed a system may be, it is likely to fail at some time. These failures cause problems in production industries by reducing the capacity of plant, and also by occurring at random times.

Condition monitoring seeks to alleviate these problems. This is achieved by monitoring the condition of a machine — either continuously, or at intervals. The results of the various tests carried out during this process may then be analysed, to provide information on the health of the machine. To be

3

meaningful, the results must say more than just "a fault may be present". The nature and severity of the fault is also to be contained in the information given by the analysis.

This research intends to perform these tasks for electrical faults in three-phase induction motors. This is a new field for condition monitoring, as the majority of the work to date has been related to purely mechanical systems, as shown in references [1 - 12].

These forms of analysis have been channelled towards bearing and gear faults, and dynamic balance problems. The main input for the analysis in [1 - 12] has been vibration. This is due to the complex nature of its source - any movement within a mechanical system will be reflected by the vibration at some point. Choosing the correct point at which to take the measurements is of course part of the analysis, as for example, bearing vibration will be best sampled at a point as close as possible to the bearing pedestal. Acoustic noise has also been used [2], and has the same properties as the vibration, as it is the vibration of the casing and internal parts of a machine which will cause this noise. It is not generally as useful as vibration, though, as it may be easily contaminated by extraneous sources.

These all deal with mechanical faults in mechanical systems. The work here is involved with electrical faults, and thus a different set of signals has to be used. This has been done by investigating electrical signals, for example magnetic flux and supply currents, but also by investigating the machine vibration.

This is examined here, as it is a very good source of information, and also because of the fact that it is useful for diagnosing mechanical faults. If proven to be effective for electrical faults as well, then both mechanical and electrical condition monitoring may be possible from a single class of signal.

1.3   Conclusions.

A brief discussion of the research aims, and the contents of this thesis have been presented. These show the direction of the work, and point out that the field of electrical condition monitoring is a new one. The various machine parameters which are to be examined have been outlined, along with the reasons for their choice, as inputs to a condition monitoring scheme.

CHAPTER 2.

ASYNCHRONOUS INDUCTION MOTORS.

2.1   Introduction.

In this Chapter, three-phase induction motors and their theory, relevant to condition monitoring, are examined. This is done in order that the signal processing may be developed to diagnose faults, based on the fundamental mechanisms behind the faults, so that it will be applicable to more than one machine. Had this not been done, and the processing developed merely with reference to one individual motor, then the characteristics of this may allow an inferior process to give good results, in that particular case.

2.2   Induction Motors - A Summary of their Characteristics.

In industry, there is a need for a reliable source of rotary power. This, generally, is provided through the use of asynchronous induction motors. These are the obvious choice due to their construction.

In such machines, a rotating magnetic field is set up by a set of stationary windings, no power being directly supplied to the rotor. There are thus no moving parts other than the rotor and its associated bearings. The rotor itself is commonly made in a single aluminium casting, around the laminated core. This construction, known from its shape as a "squirrel cage" motor is clearly very robust, relatively simple to manufacture, and free from electrical discharges, as would be found in brush-type

motors. They may also be sealed for longer life, or for use in hazardous areas, and are thus suitable for use when completely submerged.

These physical properties make it a very versatile machine. Its electrical properties, to a first analysis, are also desirable. The torque to turn the rotor is produced by the interaction of two magnetic fields, both essentially set up by the stator windings. These produce a uniform rotating field in the air gap between the rotor and the stator. This field couples with the rotor windings, normally bars shorted by solid end rings, and induces currents in these by transformer action. This action takes place at all times when the rotor sees a changing field. This means that torque is produced at standstill, so that the motors are always self starting. At the other end of the speed range, the rotor will turn in synchronism with the stator field. Thus the rotor is "locked" to the stator field, and so does not see a changing field. No transformer action can then take place, and the rotor field is lost. No torque is produced at synchronous speed which means that the maximum speed is known, for a given set of conditions, as discussed in the next section. At full load, the speed is determined by the design of the machine. In order to produce torque, the rotor must couple with a changing magnetic field, so that it must always turn at a lower frequency than the synchronous field of the stator. The rotor is then said to "slip" through the stator field . This gives rise to induced currents in the rotor conductors at the difference − or slip − frequency. This is commonly between one and five Hertz.

7

2.3   Machine Theory for Condition Monitoring.

Certain aspects of the theory relating to three-phase induction motors must be examined so that the mechanisms behind the faults to be investigated may be understood. This is under taken with reference to Alger [13].

Assuming that the machine is to be run from a 50Hz. supply, then the major component in any frequency analysis would be expected to be at this frequency. If this were the only component, then little information would be available for analysis. Because of the way in which a three-phase motor is constructed, and any imperfections in its design or construction, other frequencies will be present. It is the study of these which is of interest in condition monitoring. Two major components have already been brought to light, namely the synchronous and slip frequencies. The slip frequency is determined from the synchronous and full load speeds. Synchronous speed is found by considering the supply frequency and the number of pairs of magnetic poles in the machine — normally two. This gives a synchronous speed of 50 * 60 / 2 = 1500 rpm. for a 4-pole motor running on a 50Hz. supply. The full load speed is determined by the rating and design of the machine. This may be of the order of 1470 rpm. The slip corresponding to this condition is then found by the calculation:

$$s = \frac{1500 - 1470}{1500}$$

to give a Figure of 0.02. The slip frequency is then given by

twice the product of the slip and the supply (Sf = 2sF) to give 2Hz. in this example.

The windings in the machine are not evenly distributed, but lie in discrete slots, to ease the problems of winding the stator coils. The presence of these discrete slots gives rise to further freqencies, known as the slot harmonics. These again depend on the design of the machine, in terms of the number of slots in the stator and rotor.

The flux in the air-gap may be calculated, and several principal components are seen to result. The number of slots in the stator and rotor are referred to by the letters "S" and "R" respectively. Taking the number of pairs of magnetic poles (P) into account, then five major rotating fields are set up, as indicated in Figure 2.1. As the force due to any magnetic field is proportional to the square of the flux density of that field, the magnetic forces within the machine may be represented by the equation shown in Figure 2.2, which is the square of the equation shown in Figure 2.1, taking only the low order products. Considering the terms inside the cosine components of this, all of which represent rotating magnetic fields, the slot harmonic frequencies are derived. Thus the principal frequencies are given by evaluating the expression given in Figure 2.3. For a typical machine, as used in this project, P = 2 pairs of poles, R = 51 rotor slots and S = 36 stator slots, and the principal slot harmonics are as shown in Figure 2.3, for a full load speed of 1430 rpm., giving a slip value s = 0.046.

9

In these calculations, the fields produced by the rotor and stator are assumed to be balanced and uniform. If however, the rotor contains a bar which is broken, then this will not be the case. This has the effect that the broken bar carries no current, and those on either side of it must carry more. This not only increases the heating of these bars, but also disturbs the flux distribution around the rotor. This is reflected in the machine forces again through a square law relationship. Thus an extra term is placed in equation shown in Figure 2.2, and takes the form of a frequency modulation, at twice the slip frequency. It is at this frequency, as the current in the rotor will always be of slip frequency, and the squaring of this value to find the force results in a frequency doubling.

Thus, if a bar breaks, the slot harmonics become frequency modulated. In order to show this effect to good advantage, it has been necessary to used a technique known as "Zoom" transformation - this is a normal frequency analysis, but with the frequency scale expanded by a factor (here) of ten. This has two disadvantages for condition monitoring.

Firstly, it involves a significant increase in computation, so making the diagnosis time longer. More importantly, however, it must be done around a slot harmonic. This implies knowledge of the machine design, so that a monitoring system cannot be applied to a range of machines, without some modification. A solution to this problem must therefore be sought.

In the equations discussed earlier, only the low order terms have been considered. There are components which extend throughout the spectrum. Further to this, the direct means of modulating the frequency spectrum of the machine, ie by the changes in the flux and thereby in the force, is not the only route by which this effect can be seen in the vibration. As the force on the rotor has been changed from a uniform nature to a modulated one, the torque, and thus the speed will also be frequency modulated. This is then mirrored in the vibration. The end result of taking these further factors into the analysis is that the whole of the frequency spectrum may be expected to show the modulation resulting from a broken bar.

It is thus possible to relate the nature of a normal frequency analysis to the presence of a broken bar, without recourse to zoom analysis. This has only been considered with respect to the vibration. However, since the mechanism of the fault is electrically based, it will be reflected by other parameters. As the flux has been disturbed, then the effect should be visible in the stray and axial flux measurements. The flux also couples with the stator windings, and so should be reflected in the current. The vibration, however, has the expected advantage of containing a higher level of modulation, as it has more than one source, and is also easily measured by non-invasive techniques. This is important to condition monitoring, as any modification to a machine is to be avoided.

The motors in question are three phase types. This, under normal conditions, gives a single rotating field in the air-gap, due to the mechanical and electrical distribution of the stator windings. The three fields, one due to each phase, are combined by vector addition to give this result. If one of these phases should fail, then the addition becomes unbalanced, and the rotating field is replaced by a static one, varying in amplitude at the supply frequency. This is the same as if a single phase supply were to be applied to two of the three connections to the stator, and so the fault is known as "Single Phasing". The motor will continue to produce a torque, providing that it is already running, but to a lesser degree than under normal conditions. This creates a heating problem in both the stator and the rotor, and must be detected as soon as possible.

The supply lines will normally be protected by over-current circuit breakers. However, in the interests of reliability, these may be set at too high a level, particularly when the motors are started direct on line, and so drawing large surge currents on start-up.

The pulsating field will be mirrored in the parameters mentioned above, of vibration, current and flux. Thus it would seem feasible to detect this fault by analysis of these signals. The effect will be an increase in the supply frequency component, due to the unbalanced nature of the magnetic field - the steady field of a balanced supply system producing a much smaller component at the supply frequency. This will of course be at twice supply, in the vibration. Again, this is indeed the case, and is examined in Chapter 5.

2.4   Conclusions.

In order that the underlying mechanisms behind any fault investigated may be taken into account, the fundamental theory must be examined. This Chapter has done this, with reference to single phasing and broken rotor bars. The diagnosis of these faults may then be performed in relation to the basic causes of any changes in the signals from the machine. This must be done, so that the analysis developed is not coloured by the particular responses of an individual machine.

A short discourse has also been given on the general characteristics of these machines, to point out the reasons for their widespread use, and thus the benefits that would accrue from reliable condition monitoring.

The air-gap flux density will be given by:

$$B = B_0 \cos (Px - \omega t)$$

$$+ B_1 \cos \left[(S - P)x + \omega t \right]$$

$$+ B_2 \cos \left[(S - P)x - \omega t \right]$$

$$+ B_3 \cos \left\{ (R - P)x + \omega t \left[1 - R (1 - s) / P \right] \right\}$$

$$+ B_4 \cos \left\{ (R + P)x - \omega t \left[1 + R (1 - s) / P \right] \right\}$$

where :-

ω = supply frequency (rads /sec.)

x = rotor position (radians)

R = number of rotor slots

S = number of stator slots

P = number of pairs of poles

s = slip

Figure 2.1

$$B^2 = \frac{B_0^2}{2} \cos 2 \left(Px - \omega t \right)$$

$$+ B_2 B_3 \cos \left\{ \left(R - S - 2P \right) x + \omega t \left[2 - R \left(1 - s \right) / P \right] \right\}$$

$$+ \left(B_1 B_3 + B_2 B_4 \right) \cos \left[\left(R - S \right) x - \omega t R \left(1 - s \right) / P \right]$$

$$+ B_1 B_4 \cos \left\{ \left(R - S + 2P \right) x - \omega t \left[2 + R \left(1 - s \right) / P \right] \right\} + \cdots$$

Figure 2.2

Summarising 2.2 gives the rotor slot harmonic frequencies as :-

$$f_{SH} = \left[\frac{R}{P} \left(1 - S \right) \pm n_f \right] f$$

where n_f is the order of a supply harmonic for vibration, $n_f = 0, 2, 4, 8, \ldots$.

For a motor with:

P = 2, R = 51, S = 0.046, and f = 50Hz, the slot harmonics will appear at :-

n_f = 0   1216.35Hz

n_f = ± 2   1116.35, 1316.35 Hz

n_f = ± 4   1016.35, 1416.35 Hz

n = ± 8   816.35, 1616.35 Hz

Figure 2.3

CHAPTER 3.

SIGNAL PROCESSING TECHNIQUES.

3.1   Introduction.

It is the main objective of this research to develop the techniques of signal processing, with reference to electrical machine faults. There are several routes which may be followed to this end, and this Chapter provides a review of these, and the reasons for choosing a particular path. Although the chosen route is one based on frequency domain analysis, time domain procedures have also been considered. Both techniques are discussed.

3.2   Time Domain Analysis.

In this form of analysis, it is the signal itself which is processed. This entails recording, or sampling the signal, and performing a mathematical appraisal of this data. Frequency domain analysis, on the other hand, requires that a large number of calculations are done on the data before it is actually processed. Although this may seem to give time domain analysis an advantage it will be shown, for machine condition monitoring, that operating in the frequency domain is most appropriate.

If it is desired to consider the effects of a cyclic phenomenon, some form of correlation will have to be carried out. This involves the multiplication of a given signal with itself, as in autocorrelation, or with another, as in cross correlation. For a long time record, this obviously involves a large amount

computation. The result is then a new signal, whose peaks will correspond to the "sameness", or correlation between the two signals. This new data, has also to be interpreted, and does not normally give any direct information in the present environment — consisting mainly of related cyclic waveforms.

In some cases, there will be some foreknowledge of the signal being processed, and specific frequencies may be of interest. Defining the contribution of this particular frequency to a given signal may be carried out by the methods mentioned above, or more probably by some form of filtering. With the recent advances in micro-processor technology, this would normally be implemented digitally [15 - 17]. Digital filters can be given very well defined characteristics, and be very selective. However, this very property ie. good selectivity may act against them. If the signal changes, so that the component of interest changes in frequency, then a new filter would need to be designed. Furthermore, this research includes the task of defining those frequencies that are of particular interest, so that a filtering regime would be less desirable than other available methods, due to its inflexibility.

3.3   Frequency Domain Analysis.

As mentioned previously, frequency domain analysis cannot be carried out directly on a signal. Before any meaningful information can be obtained from the signal, it must be "frequency analysed", as shown in Figure 3.1. This pre-processing burdens the overall processing with a very large overhead of computation. There are benefits, however, in

choosing this path. An extra benefit of this is that many of the time domain techniques may be implemented via the frequency domain. Although this may seem to give an even larger computational overhead, it does not. To illustrate this, a table is given in Figure 3.2 which contrasts the numbers of multiplications required by commonly used functions. The frequency domain (FFT) method is then seen to be more efficient, as less operations, overall, are required. This aspect is discussed in references [18, 28], and the data given in Figure 3.2 was derived from [28]. It is known that the signal source is of a cyclic nature - the motor rotates in a fixed path, and so the signals obtained there from are to be expected to be repetitive. Thus the main advantage of frequency domain analysis is clear. In the time domain, a signal cannot be stationary, unless is is a direct voltage, which will contain little information. It is thus necessary to deal with ever-changing data, before any attempt is made at analysis. In the frequency domain on the other hand, a cyclic signal of a fixed period, and hence constant frequency will appear static, varying only in magnitude (and phase), as shown in Figure 3.3. It is then possible to observe a particular component of a signal, with no further post-processing. If this component should vary in frequency, perhaps as the motor speed changes with load, then a scalar movement along the frequency spectrum will allow its new contribution to be assessed.

When a signal is produced, it may consist of many sources, and be modified by its surroundings. An example of this is the effect of the flux within a machine on the case vibration. The

16

waveform of the flux will be modified by the response of the case, and will thus reflect characteristics of both. This modification may be modelled, and the various components convolved together to obtain the final signal. Convolution is a very complex operation, and to de-convolve a signal into its constituent factors is even more involved. It is a property of the transformation from a time to a frequency domain that convolution becomes multiplication, in the new domain. Further more, if the frequency domain result is scaled logarithmically - as it would on a decibel scale - this multiplication becomes addition. The large overheads involved in producing the frequency domain representation of the signal therefore gives an advantage to any further procesing. If the case of a filter - as might be found in any part of an experiment - were to be considered, a time domain analysis would first have to account for the action of this filter. This would have to be done by a convolution calculation. In the frequency domain, however, the effects of the filter may be removed, simply by subtracting its own frequency response from the spectrum of the system being measured. If now, a filter is applied to a signal which has a rich harmonic content, only a single frequency can be extracted. If the same signal were to be analysed in the frequency domain, this harmonic nature would become apparent, as shown in Figure 3.4.

It is clear, then, that when a complex signal is to be resolved into its component parts, a frequency domain route is more rewarding than a time domain one.

3.4   Orthogonal Transforms.

It has been made clear, that although a frequency domain processing regime is most suited to condition monitoring, the signal cannot be processed directly, but must first be "pre-processed". This processing takes the form of a transformation from the time domain into the frequency domain. This is carried out by use of a set of functions known as "Orthogonal Transforms".
Fourier analysis is an established member of this set of transforms.

An orthogonal function, derives its name by the property of having constituent phasors which are at right-angles to each other, as shown in Figure 3.5. A example of this property is readily observable in sine and cosine functions. When all other properties are identical, these two can be distinguished by their right-angled - or Orthogonal - phase relationship.

If corresponding sine and cosine components are multiplied, in a vector sense, the result will be zero, as shown in Figure 3.6. Thus, if a signal is composed entirely, and only, of these two, the contribution of each to the total signal may be assesed, by multiplying the signal by each of the constituents in turn. The result of each multiplication will be the product of the magnitudes of the signal and multiplying component, plus the product with the other signal component. This latter part, as noted above, will be zero.

If, instead of a single pair of sine and cosine functions, a continuous spread is considered, differing only in their frequency component, and the calculation performed for all of them, then the amounts of each present in the signal will be defined. As mentioned earlier, this process is an established one, viz. that of a Fourier Transform.

Having defined the reason for using an orthogonal transform, it must be noted that Fourier analysis is only one member of a large family of transforms. It should also be noted that although a sine and cosine based analysis is normally the automatic choice from a mathematical point of view, it may not be entirely suitable in all fields. In computer technology, all data is stored in binary format. It is not possible, then, to store or calculate values for sine or cosine series, with absolute accuracy. This forces the problem of transform noise on the situation, since no matter what the word-length the particular computer may have, truncation errors will result. It would seem desirable, therefore, to attempt to fit the problem to its solution, if possible. Here, this would entail the use of a transform which is based not on sines and cosines, with their irrational values, but on a simplified set of numbers. The set of orthogonal transforms contains within it several functions which meet this need. Not only are they based on two values, so immediately look attractive for a digital implementation, but these values are plus and minus unity. This gives the advantage that the process of multiplication, which consumes relatively large amounts of computing time and effort, is reduced simply to additions and subtractions. The savings in computational time,

from this property are very large indeed.

3.5   Walsh Transforms.

A set of two valued functions were first described by Walsh in 1923 [29]. At that time, and for a lengthy period afterwards, they remained as a mathemetical concept, without any serious practical application. More recently, their basis on the values of plus and minus unity, have made them of great interest in microprocessor-based environments, due to the absence of multiplication computations. An overview of the general properties of Walsh transforms is to be found in Frankel [37]. As discussed earlier, any orthogonal transform will effect a change of domain, by analysing the original signal, in terms of the components of the particular transform. Such is the case with Fourier Transforms, where the signal is assumed to be composed exclusively of sine and cosine functions - the constituents of the Fourier transform. Walsh transforms, on the other hand, are based on a set of rectangular functions, and thus the signal will be analysed in these terms. The standard mathematical representation of both Fourier and Walsh Transforms are shown in Figure 3.7. The important properties of both classes of function are summarised in Figure 3.8. In order to give a means of distinguishing between Walsh and Fourier domains, it has become customary to call the Fourier domain "frequency", and the Walsh domain "sequency". They have similar meanings, and allude mainly to the process used between the time and transform domains. The similarity between Fourier and Walsh components is strengthened by taking the Walsh terms in pairs, viz.

0,1; 2,3; 4,5 and so on. These are then named "CAL" for the even and "SAL" for the odd numbered pairs. The new names are chosen to underline the similarity with Cosine and Sine and have similar properties in the Walsh domain as sine and cosine have in the Fourier domain. The first 16 Walsh functions, with both terminologies are shown in Figure 3.9. These two may be unified by the concept of "Generalised Frequency", as in Harmuth [36]. Here, the term "frequency" is defined, not in the normal sense as being the number of complete cycles in a given time, but as half the number of zero crossings per time period. For sine and cosine waves, this is evidently the same as "normal" frequency. In the case of the Walsh functions, with their more complex form, the new term has more meaning.

The set of Walsh functions, then, may also be used as a basis for a transform from the time to frequency domains. As the Walsh Transforms are based on a rectangular set of functions, they are more suited to analysing signals which have a rectangular basis [39]. The signals considered for condition monitoring of electrical machines are, however, sinusoidally based and so the Walsh Transforms may not be suitable for their analysis. As an exapmle of this, Figures 3.10 and 11 show the Fourier and Walsh Transforms of a sine and a square wave. Further to this, the "energy" in a Walsh function is not constant with sequency. This is seen from the fact that a sine wave of a higher frequency may be formed simply by taking an existing one and "compressing" it in the time axis, until another, identical wave can be "fitted in at the end". There is no corresponding property between Walsh transforms, as is seen for example with

21

Wal(13,t) in Figure 3.9. This has the effect that for a fixed amplitude signal, swept in sequency, a varying amplitude will result in the sequency spectrum, thereby making the interpretation of the data a difficult task, as shown in Figure 3.12.

This task is further impeded by the complex nature of the transform output. In Fourier analysis, the transform will generally result in a single peak, corresponding to a single input frequency. Such is not the case with Walsh transforms. This is illustrated in Figure 3.13, and can also been seen in the actual transforms shown in Figures 3.10 and 11, and also in reference [40]. An area of higher sequency energy also appears, as shown in Figure 3.14. The presence of this higher sequency energy only hinders the interpretation of the data. If this contribution could be removed from its place in the sequency spectrum, and put where it would be "expected", then the advantages of the Walsh transform could be further realised. It is significant, that this area of higher sequency energy appears close to the third harmonic sequency of the main peak, with a pronounced trough at near the second harmonic, as shown in Figure 3.14. As mentioned, the results are interpreted in a way which is biased, due to their more frequent use, towards Fourier transforms. If a Walsh function itself is Fourier transformed, it will appear in the frequency spectrum as an area of energy at the fundamental frequency of the Walsh function, plus energy at the third, fifth, and so on harmonic frequencies. This is similar to the case of a sine function being Walsh transformed, and underlines the importance of choosing the most suitable

22

transform for any given application. This particular similarity, however, may allow for the area of higher sequency energy to be directly explained, and with further mathematical analysis, could lead to a modified form of the Walsh transform which will give the advantages of speed and accuracy of calculation, without the disadvantages of a more complex result.

Another property of Fourier analysis which is not mirrored in the Walsh domain, is that of cyclic invariancy [40]. If a signal to which a Fourier analysis is to be applied is given a pure delay, then this will be shown in the frequency domain as a change in phase, without effecting the amplitude spectrum in any way. In the Walsh domain, however, a pure delay cannot be directly modelled as it can in any Fourier analysis, as shown in Figure 3.15. It then becomes more difficult to interpret any data, unless some form of synchronisation is available, such that the signal can always be sampled at the same point in its cycle. This will generally require that the machine under test will have to be modified. This is to be avoided if possible, as the condition monitoring system must be applicable to any machine, with as little modification as possible. When the signal is non-cyclic, the problem is aggravated, and although Fourier analysis does assume that a signal is exactly periodic within the sample time, the effect of this characteristic is very small by comparison.

The main attraction of Walsh analysis has been its speed of calculation, and its suitability for digital processing environments. They may be derived by several means [30, 34] and lend themselves to special purpose hardware implementaions.

23

These can give extremely fast execution times [38].

It has been concluded that any analysis based on Walsh transforms are most suited to signals of a stepped form, and that the sampling time needs to be synchronised closely with the data, to mininise the unwanted side effects of the transform properties. As the signals dealt with are emanating from an electrical machine, driven by a sinusoidal supply and performing uniform circular motion, the signals will also have a sinusoidal basis. This fact makes the Walsh transform less applicable to condition monitoring.

It is, however, possible to perform a Walsh transform, with its high speed of calculation, and then post-process the results to find the Fourier transform. This is discussed in references [31, 32, 33, 35, 42]. These show that for small numbers of samples, that this route may be advantageous. Tadokoro and Higuchi [42] derive a formula for the number of multiplications required for this route. This is that for N sample points, ($N * N - S$) / 6 multiplications are required to calculate S Fourier coefficients via the Walsh domain. Comparing this with the N log N form for a direct Fast Fourier transform, this method requires 174,762 as opposed to 10240 multiplications for the direct form, for the 1024 point transform which is to be used.

Also, when considering the transformed representations of a signal, Blachman [35] shows that a Walsh transform will require significantly more points in order to represent the signal to the same accuracy as a Fourier transform.

24

3.6   Cepstrum Analysis.

The inherent properties of a frequency domain analysis can be exploited to yield information about the machine signals appropriate to condition monitoring. It was shown earlier that the complex task of convolution in the time domain is modelled by multiplication in the frequency domain. When a logarithmic scale is employed, this is further simplified to addition. A signal may then be examined in terms of related components, as are harmonics of a single fundamental, and in terms of different components – combined by superposition – to give the original signal. The possible harmonic structure is much more readily seen in the frequency domain. There are, however, effects which do not show themselves readily in this domain. Where a signal has been produced at source, and then modified by some filtering process, before it is analysed, a frequency analysis cannot be assured to separate the two effects, so that either could be examined. A further level of convolution is involved. Another situation which cannot be directly handled by a simple frequency analysis is that of a modulated signal. Here, there will be a fundamental signal, plus equally separated sidebands, as shown in Figure 3.16. These sidebands may be difficult to deal with, since they may lie very close to the fundamental, and have relatively little energy themselves. The fact that frequency modulating a signal does produce equally spaced sidebands is derived with the aid of Bessel functions, as is shown in equations 3.1 to 3.10, below.

In both these cases, it is conceptually a simple step to perform a second frequency analysis - treating the output of the first as the input for the second. At a first sight, this may seem to return to the original signal, since two forward transforms are the same (except for a phase inversion and a scale factor) as a forward followed by an inverse transform. If all the data were preserved throughout, then this would indeed result in the recovery of the original signal. The output of the first transform may, however, be logarithmically scaled. The second transform then gives its results in the time domain, but because of the logarithmic transform, the output of the overall process is not the original signal.

This process is called Cepstrum analysis [27, 42, 43], and, as with the Walsh transforms, a new terminology has been devised for its use. (The name comes from "spectrum", with the first letters reversed.) This modification is carried through all of the terms, some of which are listed below:

1. SPECtrum   becomes   CEPStrum,

2. FREQuency   "   "   QUEFrency,

3. PHASE   "   "   SAPHE,

4. HARmonic   "   "   RHAmonic, and so on.

In machine condition monitoring, the resonance of the casing effects the original vibration signal; the process is similar to filtering. A Cepstrum analysis on such a complex signal enables the individual effects to be separated. (An analogy can be

26

found in the production of human voice signals. The sounds are created by two effects. The throat produces the initial sound, which is then modified, or filtered, by the cavities within the head. Applying a Cepstrum analysis to such a signal separates the two effects, so that each may be studied completely separated from the other, as shown in Figure 3.17.)

Where modulation is the effect to be considered, the justification is somewhat simpler. As the output from the first transform is used as the input to the second, it may be directly considered as a signal. It is known that a modulated waveform will have sidebands, and that these will appear as equally spaced peaks in the frequency domain. If this is considered as a signal, the fact that it contains evenly spaced peaks implies that it is periodic. It is periodic, however in frequency. A further analysis of this signal will produce a single peak for each modulation frequency, as shown in Figure 3.18. It is thus possible to determine the effects of the fundamental and its modulating function quite separately. This is very powerful when the modulation itself is of interest, and is in a considerably lower frequency range to the carrier. In such a case, the carrier will be "lost" in the cepstrum, leaving the information in the modulation completely separated from the carrier information.

A useful property of the cepstrum process comes to light when the scaling is considered. In the case of the first stage of a Cepstrum transform, the "x-axis" is scaled linearly in frequency. When the second transform is applied to this, this axis is scaled in time – and thus in frequency, with an inverse

27

law. This gives the additional property of compressing the high frequency components towards the origin, and the scale then gradually expands as the frequency falls. The result of this is excellent noise immunity, since the noise is generally high frequency, and thus becomes separated from the low frequencies which are of interest.

As an extension to this, any of the peaks in the Spectrum or Cepstrum may be removed during the processing, and the resulting data inversely transformed. It is then possible to study the effects on the signal of removing individual components.

Signals from the test machine were Cepstrum analysed, and the results are presented in Chapter 5, where the power of this technique is clear when determining the modulated nature of the signal when a broken rotor bar is present in the machine, as compared to the much cleaner signal from a machine in good condition.

In terms of a Cepstrum analysis, a further disadvantage of a Walsh based transform becomes apparent. Any modulated signal will consist of two components - a "carrier" and "modulating signal". To obtain the final signal, these are multiplied together. In a sine based environment, this multiplication results in pairs of difference products, or sidebands, as shown in Figure 3.19(a). In the case of a Walsh environment however, these difference products do not occur, as shown in Figure 3.19(b). Thus Walsh modulation does not exhibit the sidebands, and the technique thus not suited to the analysis of machine signals.

28

3.7   Conclusions.

It has been shown that in relation to electrical machine test signals, which are cyclic, modulated and sinusoidal in form, a frequency domain analysis is the correct choice. Time domain analysis is unsuitable due to its inflexibility and the lower overall computational overheads attainable by using frequency analysis. Although Fourier functions are normally chosen for this task, Walsh functions have also been investigated. These have the desirable properties of being capable of high speed calculation and of giving a "quiet" transform, due to the absence of multiplications and rounding errors, respectively. When analysing sinusoidally based signals, as here, the Walsh transform has many undesirable properties, such as cyclic non-invariance, and non-constant output in the sequency domain with varying frequency. This makes interpretation of the data a very complex task, when compared to their Fourier counterparts.

It has been shown, then, that frequency domain analysis, by the use of orthogonal transforms, is the preferable route. It is also shown that even with the penalties of complex calculation and inherent noise from truncation errors, Fourier transforms have advantages over other members of the set of orthogonal transforms which make them the obvious choice for the transformation of the signal from the time to frequency domain.

Cepstrum analysis is an extension to frequency domain techniques, and is well suited to the analysis of convolved or modulated signals. Its use in condition monitoring is in its power to determine the modulated nature of the signals under

"fault" and "good" conditions.

Time domain

Pre-processing:

Frequency

analysis

Frequency domain
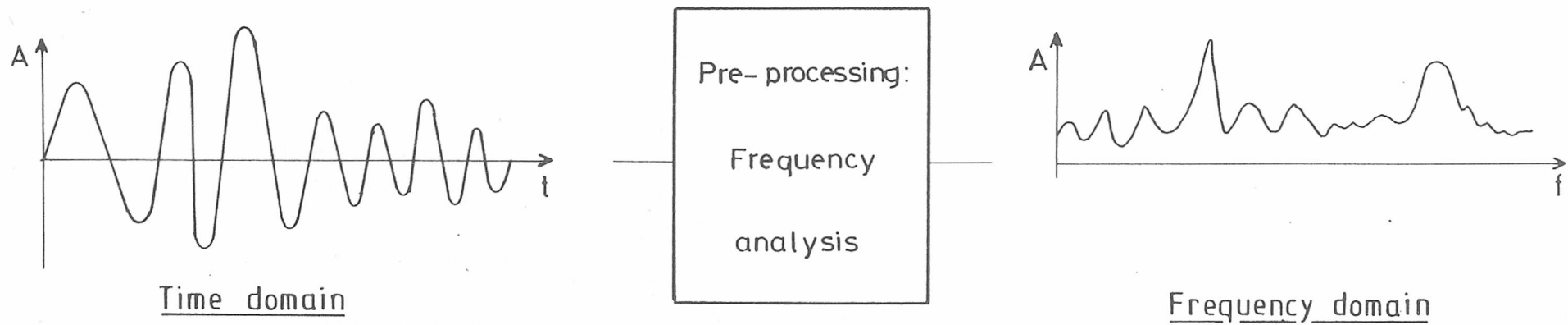
For Frequency analysis the signal must be "pre-processed"

Figure 3.1

operation	formula	approximate maximum number of multiplications	
		DIRECT	FFT
Fourier transform	$$\sum_{k=0}^{N-1} X_k \, e^{-2\pi j r k}$$ $r = 1,2 \ldots\ldots N-1$	N^2	$2N \log_2 N$
Convolution (filtering)	$$\sum_{k=0}^{N-1} X_k \, Y_{u-k}$$ $u = 0,1 \ldots\ldots N-1$	N^2	$3N \log_2 N$
Autocorrelation functions	$$\sum_{k=0}^{N-1} X_k \, X_{r+k}$$ $r = 0,1 \ldots\ldots N-1$	$\dfrac{N}{4}\left(\dfrac{N}{2}+3\right)$	$3N \log_2 N$

Comparison of computational effort for Direct and FFT methods in signal processing

Figure 3.2
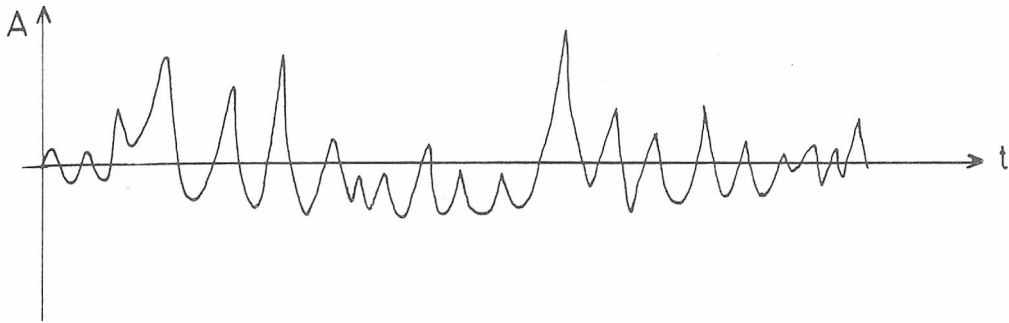
(a) in time domain, the data is constantly
changing
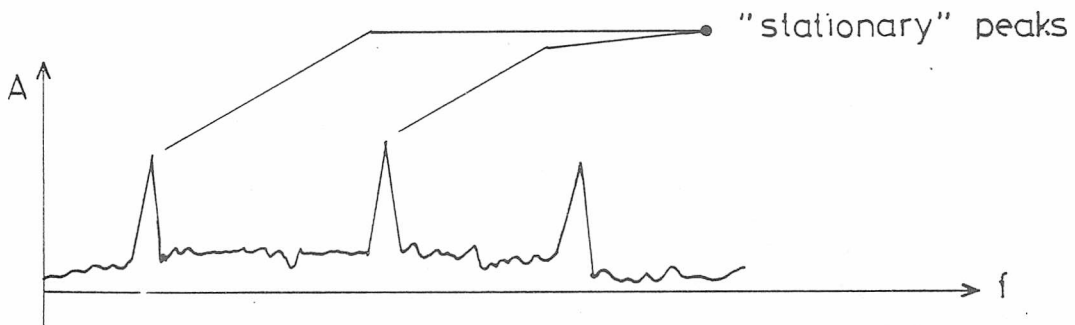
(b) in frequency domain, the data is more
constant

Figure 3·3
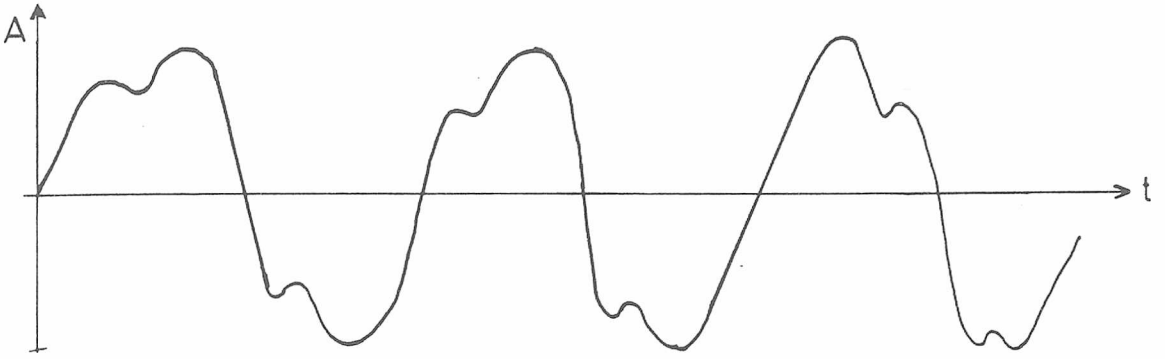
(a)   harmonically   rich   signal
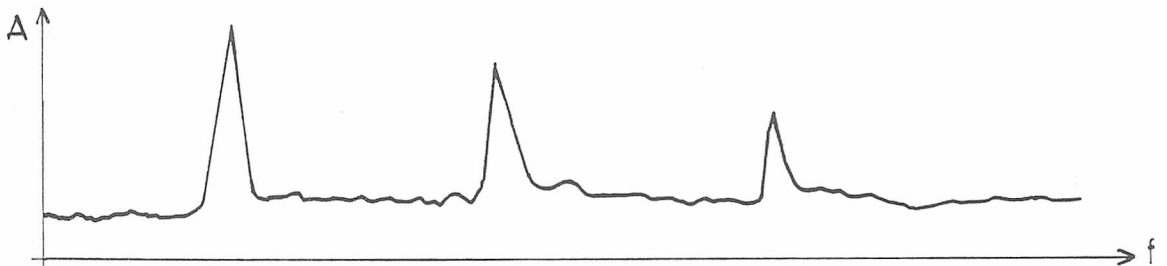
(b)   the   harmonic   structure   is
      clear   in   the   frequency
      domain

Figure   3·4

Rotating at ω radians/second
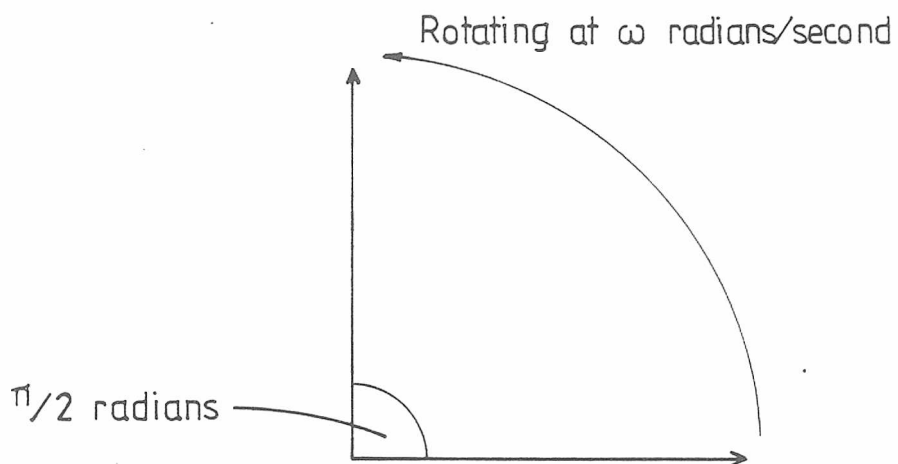
$\pi/2$ radians

Two rotating vectors, separated by $\pi/2$ radians are said to be "ORTHOGONAL"

Figure 3.5
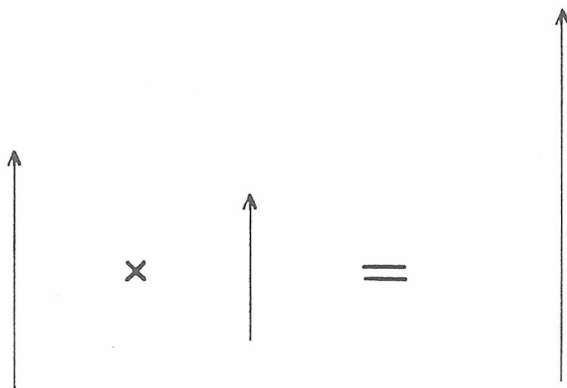
(a) Vectors at the same angle give a finite product
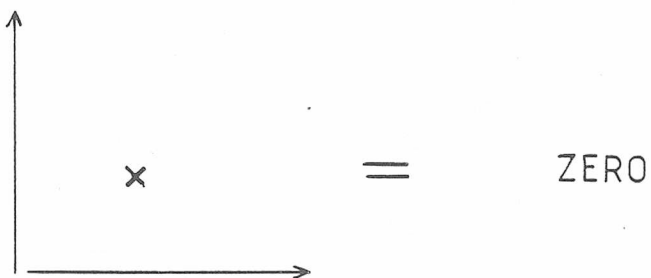
ZERO

(b) Orthogonal vectors give a zero product

Figure 3.6

• • • a signal f may be represented by:

$$f(t) = a_o + \sum_{n=1}^{\infty} a_c \cos n\omega t$$

$$f(\theta) = a(0) + \text{Wal}(0,\theta)$$

$$+ \sum_{n=1}^{\infty} a_s \sin n\omega t$$

$$+ \sum_{n=1}^{\infty} \left[a_c(i) \, \text{Cal}(i,\theta) + a_s(i) \, \text{Sal}(i,\theta) \right]$$

where:-

$$a_o = \frac{1}{T} \int_0^T f(t) \, dt$$

where:-

$$a(0) = \int_{-1/2}^{1/2} f(t) \, \text{Wal}(0,t) \, dt = \int_{-1/2}^{1/2} f(t) \, dt$$

$$a_c = \frac{2}{T} \int_0^T f(t) \cos n\omega t \, dt$$

$$a_c(i) = \int_{-1/2}^{1/2} f(t) \, \text{Cal}(i,t) \, dt$$

$$a_s = \frac{2}{T} \int_0^T f(t) \sin n\omega t \, dt$$

$$a_s(i) = \int_{-1/2}^{1/2} f(t) \, \text{Sal}(i,t) \, dt$$

using Fourier transform methods

using Walsh transform methods

Figure 3·7

A frequency modulated signal may be represented by:

$$e(t) = A\cos(\omega_c t + \phi(t)) \quad \cdots \cdots \cdots \cdots \quad 3.1$$

where
$$A = \text{peak amplitude}$$
$$\omega_c = \text{carrier frequency (in radians/second)}$$
$$\phi(t) = \text{carrier phase (in radians)}$$

thus the instantaneous phase will be:
$$\left(\omega_c t + \phi(t)\right)$$

and by differentiation the instantaneous frequency will be given by:

$$\frac{d}{dt}\left(\omega_c t + \phi(t)\right)$$
$$= \omega_c + \frac{d\phi(t)}{dt} \quad \cdots \cdots \cdots \cdots \quad 3.2$$

In frequency modulation, it is the $d\phi(t)$ term which is controlled:

$$\frac{d\Theta(t)}{dt} = Ke_m(t) \quad \cdots \cdots \cdots \cdots \quad 3.3$$

where $e_m(t)$ modulating signal

expanding 3.1 with 3.3 allowing e_m to be a sinusoid:

$$e(t) = A\cos\left(\omega_c t + \frac{Ke_m}{\omega_m}\sin\omega_m t\right)$$
$$= A\cos\left(\omega_c t + mf\sin\omega_m t\right) \quad \cdots \cdots \cdots \quad 3.4$$

where
$$mf = \frac{Ke_m}{\omega_m} \quad \cdots \cdots \cdots \cdots \quad 3.5$$

and is the Modulation Index of $e(t)$

3.4 may be extended using

$\cos(A+B) = \cos A \cos B - \sin A \sin B$ to give:

$$e(t) = A\left[\cos\omega_c t \cos\left(mf \sin\omega_m t\right)\right.$$

$$\left. - \sin\omega_c t \sin\left(mf \sin\omega_m t\right)\right] \quad \cdot \; \vdots \; \cdot \; \cdot \; \cdot \; \cdot \; \cdot \quad 3 \cdot 6$$

To further expand 3.6, Bessel Functions must be used, thus the terms of 3.6 may be represented as:

$$\cos\left(mf \sin\omega_m t\right) = J_0(mf) + 2J_2(mf)\cos 2\omega_m t$$

$$+2J_4(mf)\cos 4\omega_m t \quad \cdot \; \cdot \; \cdot \; \cdot \; \cdot \; \cdot \; \cdot \; \cdot \quad 3 \cdot 7$$

$$\sin\left(mf \sin\omega_m t\right) = 2J_1(mf)\sin\omega_m t$$

$$+2J_3(mf)\sin 3\omega_m t$$

$$+2J_5(mf)\sin 5\omega_m t \quad \cdot \; \cdot \; \cdot \; \cdot \; \cdot \; \cdot \; \cdot \quad 3 \cdot 8$$

Using these relations, the F.M. signal representation becomes:

$$e(t) = A\left[J_0(mf)\cos\omega_c t + J_2(mf)\cos(\omega_c + \omega_m)t\right.$$

$$-J_1(mf)\cos(\omega_c - \omega_m)t + J_2(mf)\cos(\omega_c + 2\omega_m)t$$

$$\left. + J_2(mf)\cos(\omega_c - 2\omega_m)t + \cdot \; \cdot \; \cdot \; \cdot \; \cdot \; \cdot \right] \quad \cdot \; \cdot \; \cdot \; \cdot \quad 3 \cdot 9$$

Thus, in terms of frequency components, $e(t)$ is seen to be:

$$\omega_c \pm N\omega_m, \qquad N = 0 \rightarrow \infty \quad \cdot \; \cdot \; \cdot \; \cdot \; \cdot \quad 3 \cdot 10$$

which represents a single carrier $\left(\omega_c\right)$

plus sidebands

spaced at

$\pm N\omega_m$

$$X_f = \frac{1}{N} \sum_{i=0}^{N=1} X_i e^{(-j2\pi i f/N)} \quad f = 0, 1, 2 \cdots N-1$$

the discrete Fourier transform

The kernal of the Fourier transform is complex, and
has N possible values

$$(-j2\pi i f/N)$$

Figure 3.8 (a)

$$f(t) = a_o \mathrm{Wal}(0,t) + \sum_{i=1}^{N/2} \sum_{j=1}^{N/2} \left(a_i \mathrm{Sal}(i,t) + b_j \mathrm{Cal}(j,t) \right)$$

The kernal of the Walsh transform has two
interesting properties

(1) Possible values are limited to ±1

(2) Sal and Cal cannot be combined
to a complex form, as can
Sine and Cosine.

Figure 3.8 (b)

(a)

(b)

Figure 3.9 First 16 Walsh functions
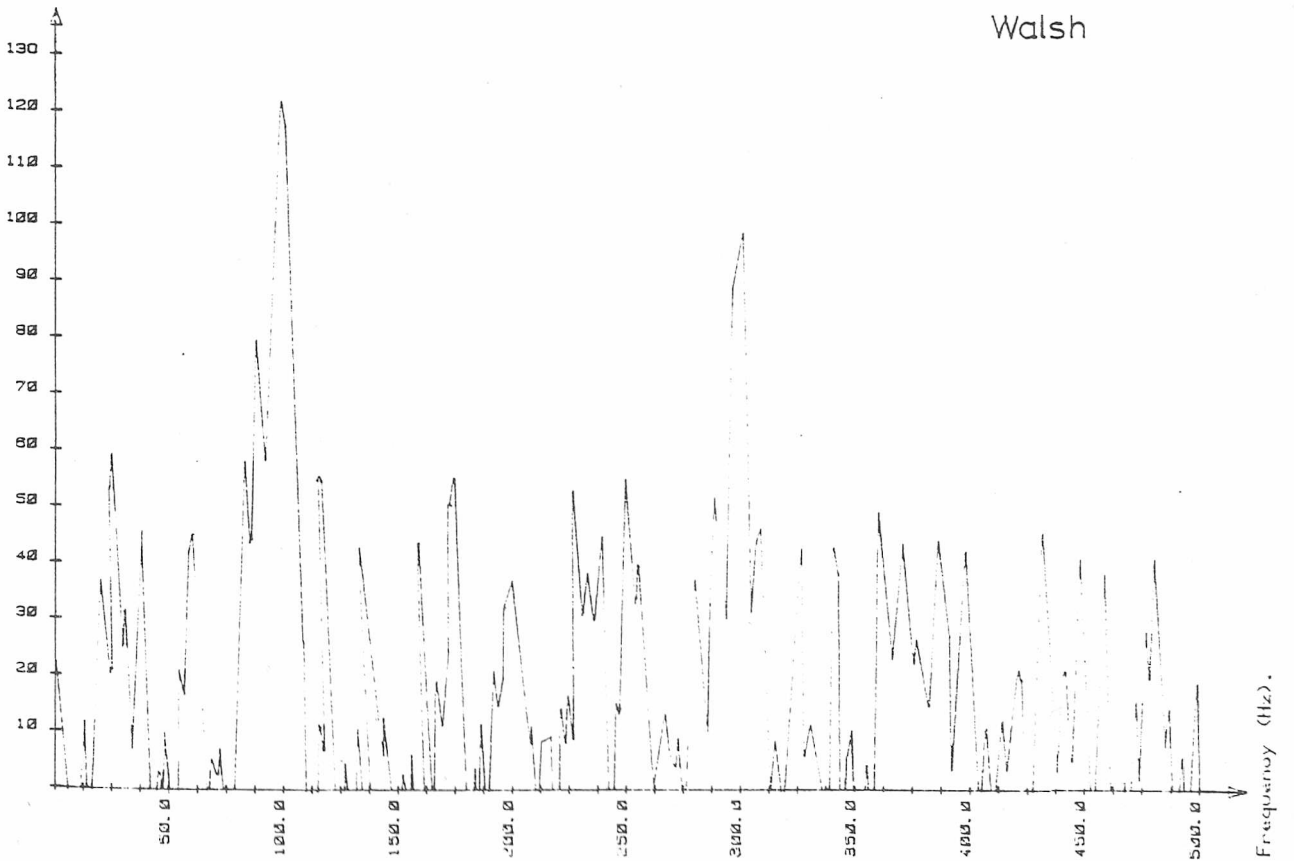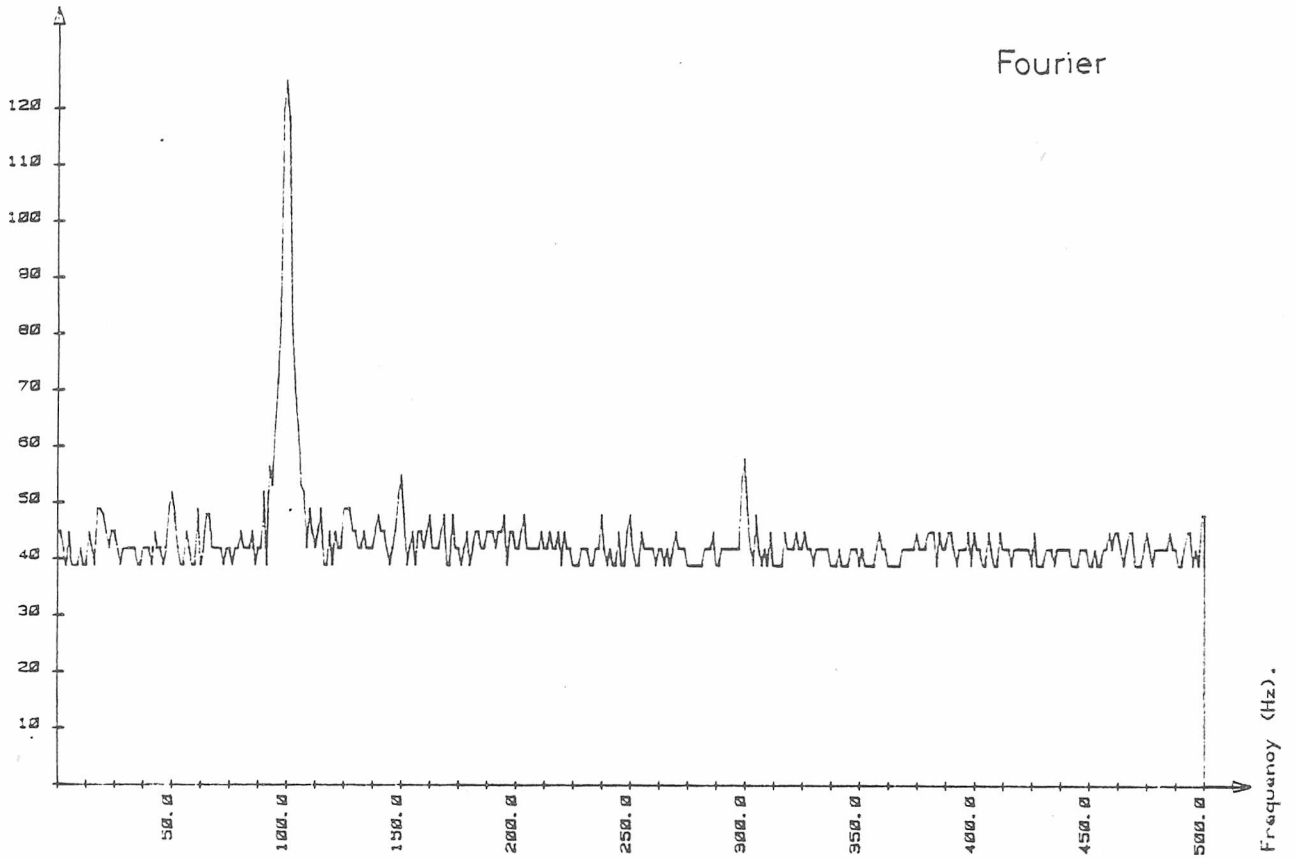
Figure 3.10   Transforms of a sinewave
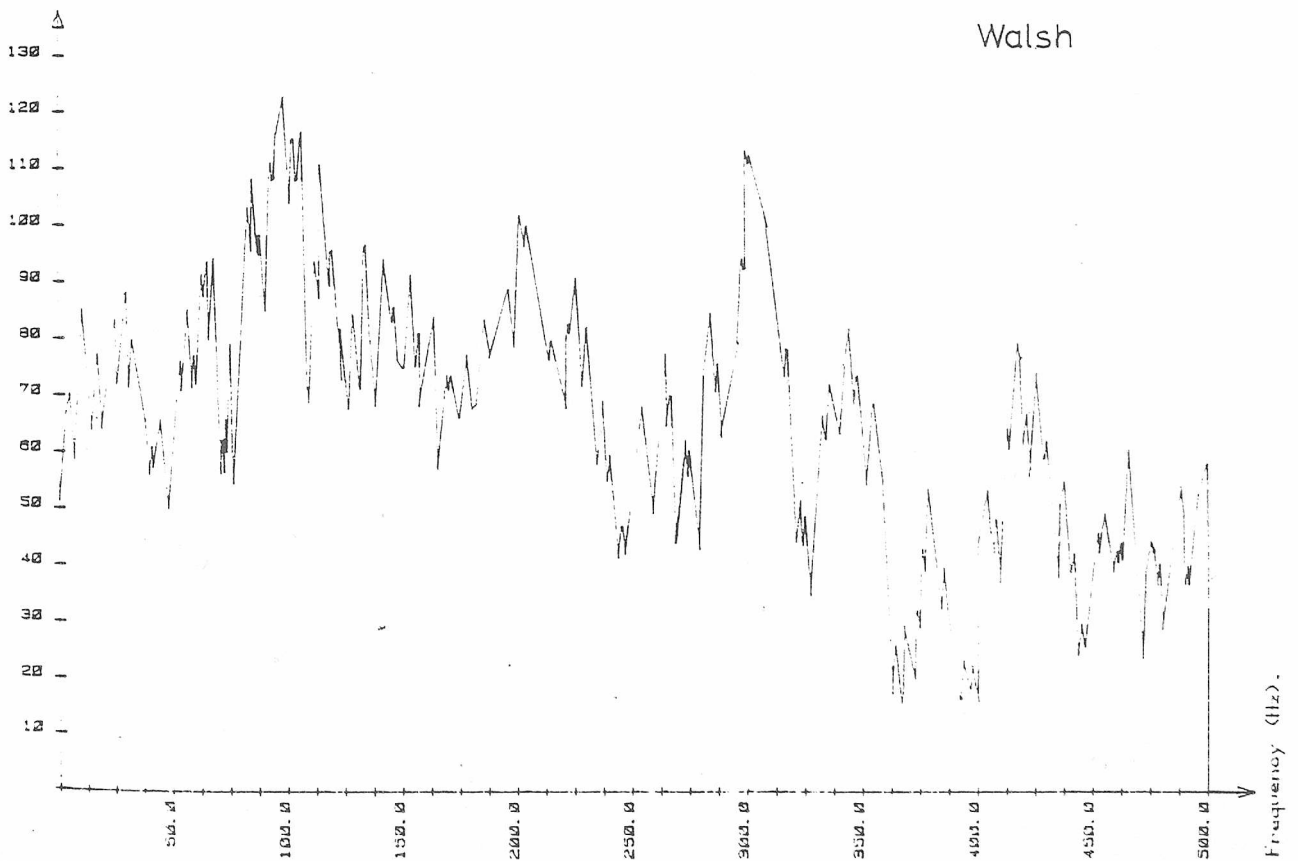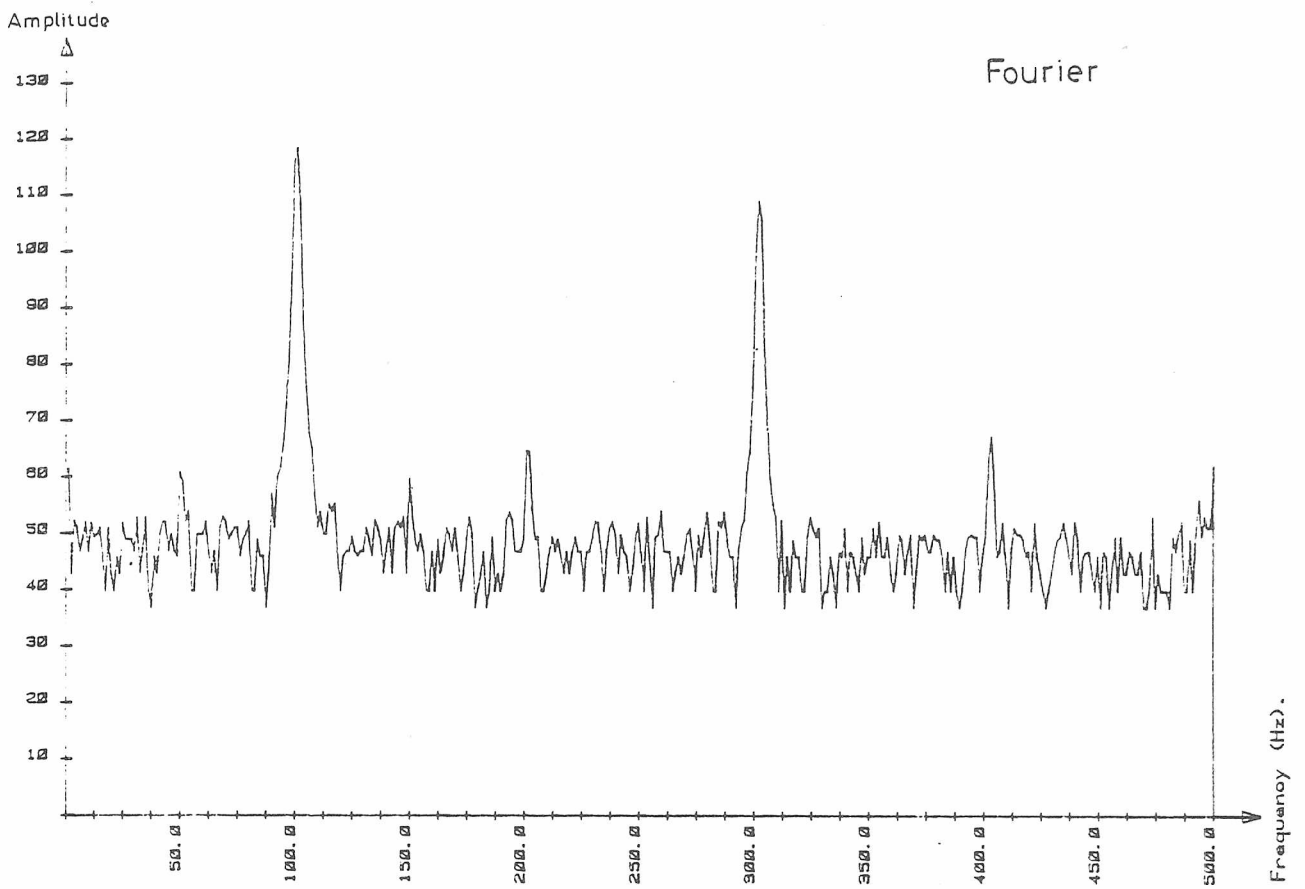
Figure 3·11   Transforms   of   a   squarewave

A ↑ — — — — — — — — — — — — — — — constant amplitude swept · frequency

A ↑ — — — — — — — — — — — — — — — constant

FOURIER

A ↑   varying
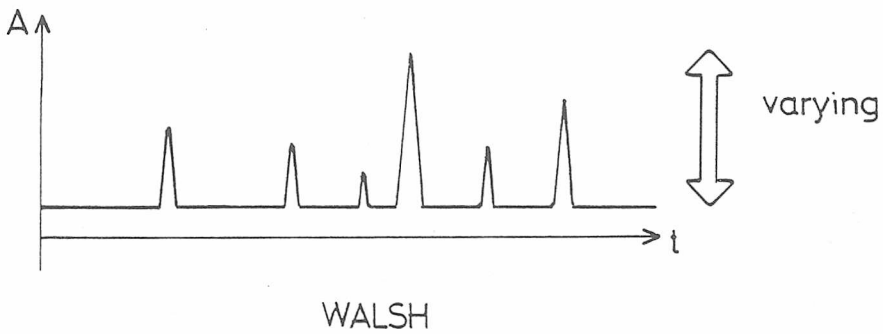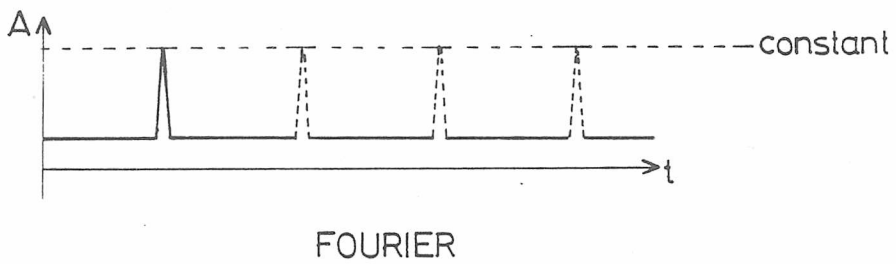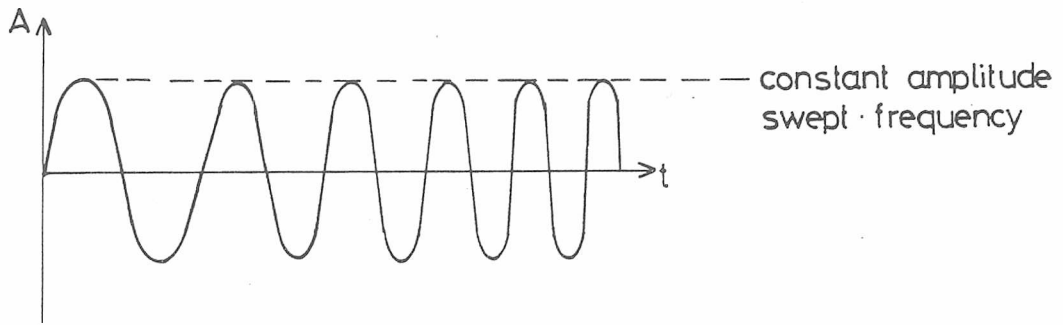
WALSH

WALSH transform output varies with frequency.
FOURIER transform output is constant.

Figure 3·12
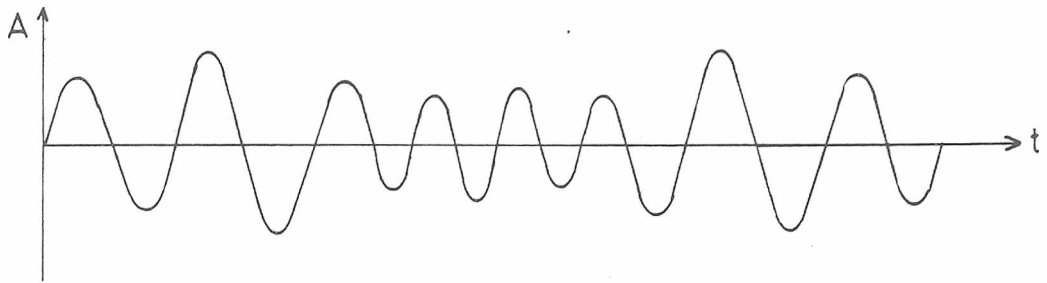
(a) signals from the machine are sinusoidally based
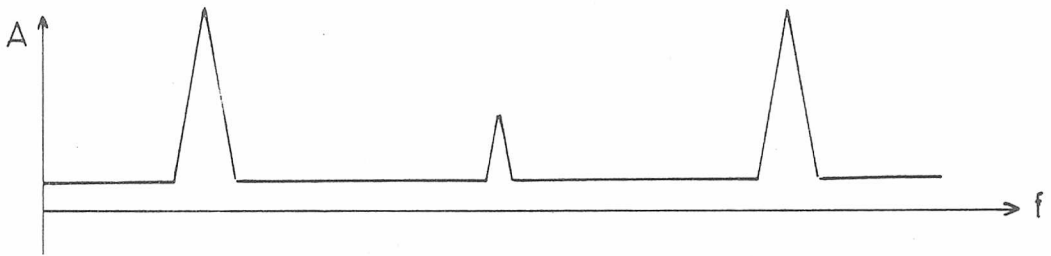
(b) Fourier transform then gives a relatively clean output
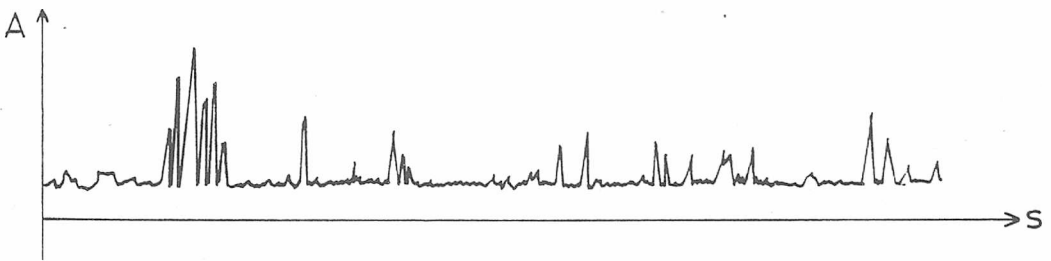
(c) Walsh transform gives a very complex output

Figure 3.13
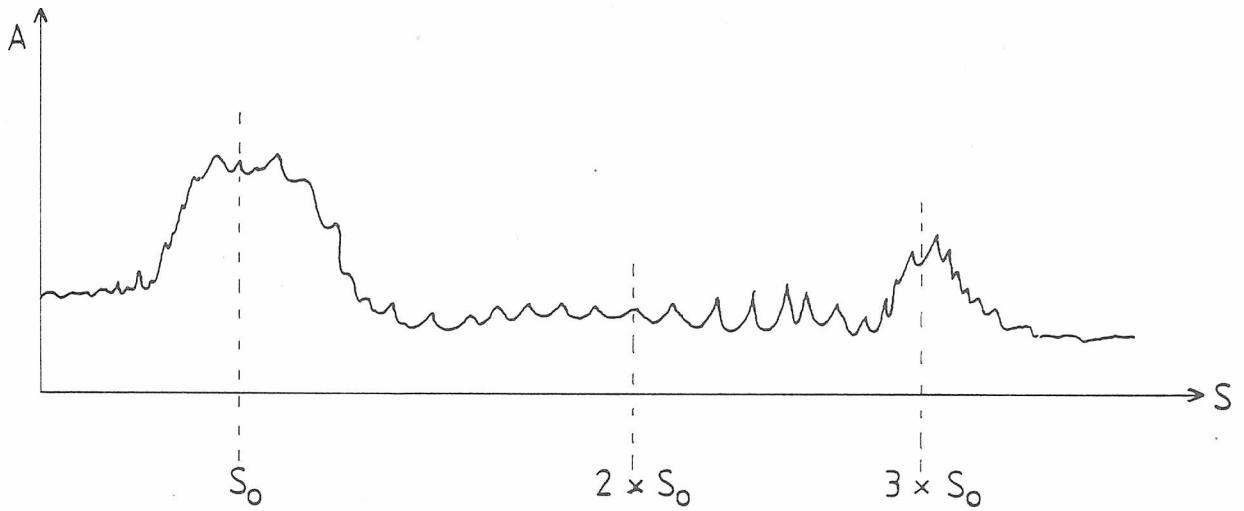
A Walsh transform has an area of higher sequency energy —
— at around the third harmonic of the fundamental, S_o
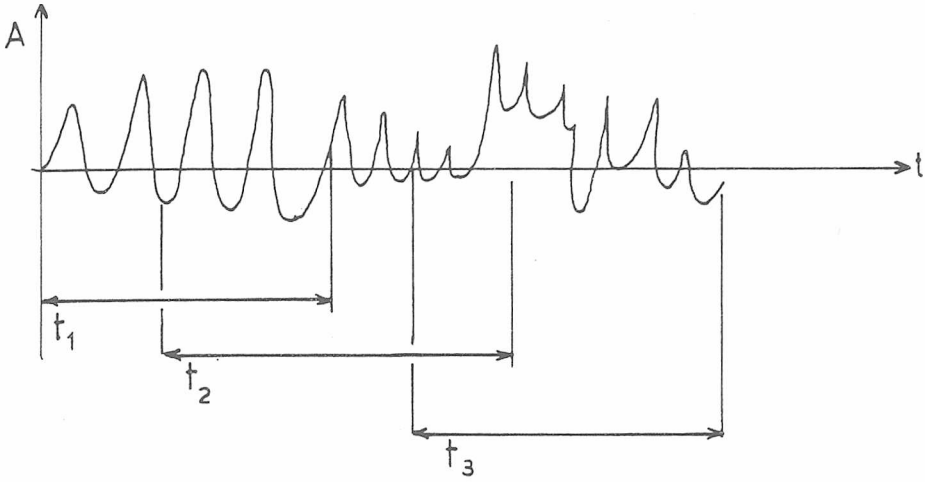
Figure 3·14

A signal may be sampled at different times
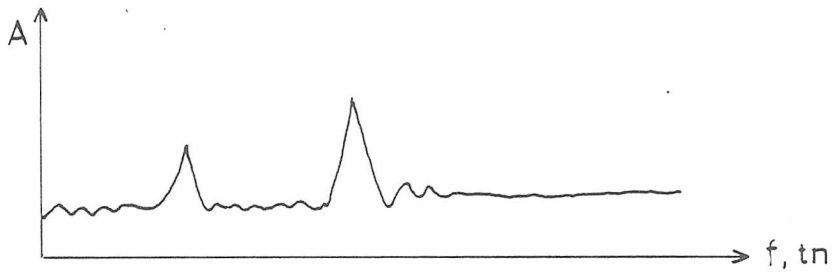
(a)   A Fourier transform is not affected
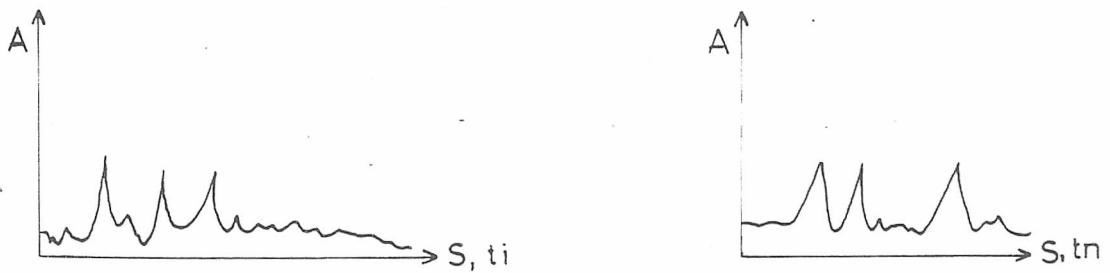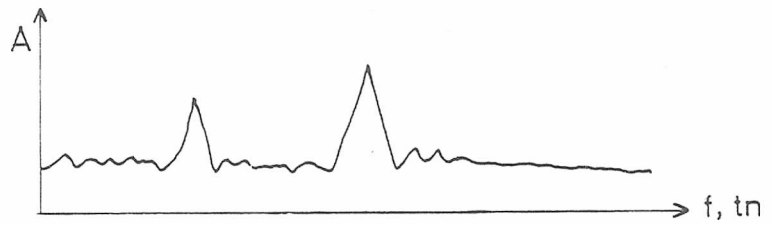
(b)   A Walsh transform will vary with different sample times

Figure 3·15

(a)   a   frequency   modulated   signal
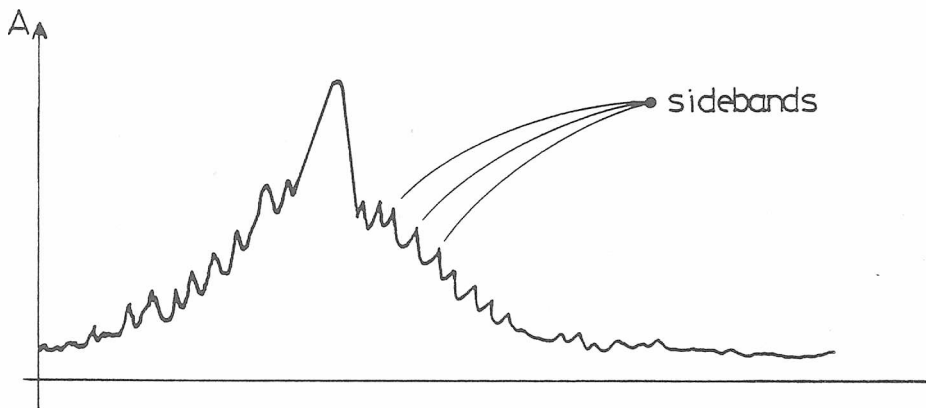
sidebands

(b)   the   spectrum   of   this   signal
       may   contain   many   closely-
       spaced   sidebands

Figure   3·16

(a) original signal

filter

(b) filtered signal

due to original
signal

due to the effects
of the filter

t (Quefrency)
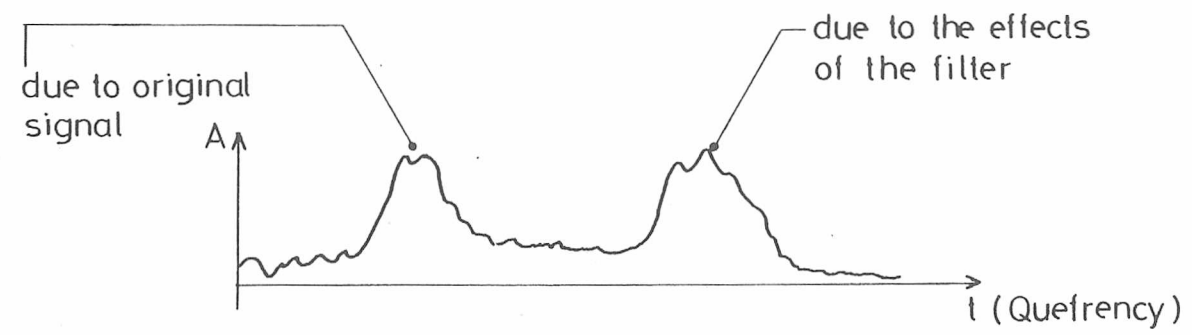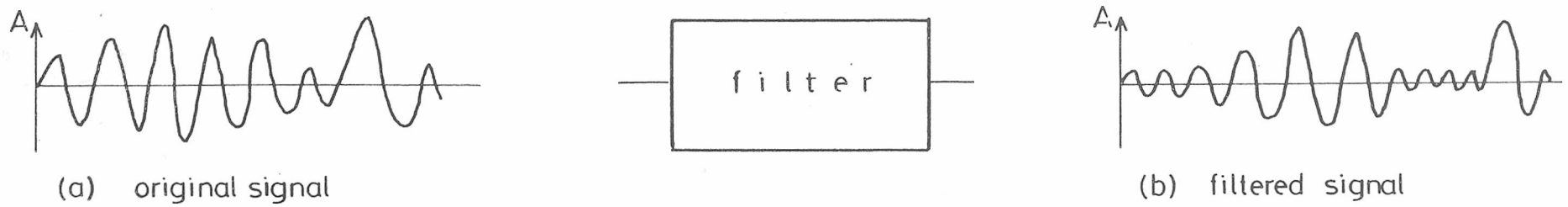
(c) the cepstrum can separate the effects
of the filter, and the original signal

Figure 3·17

constant amplitude
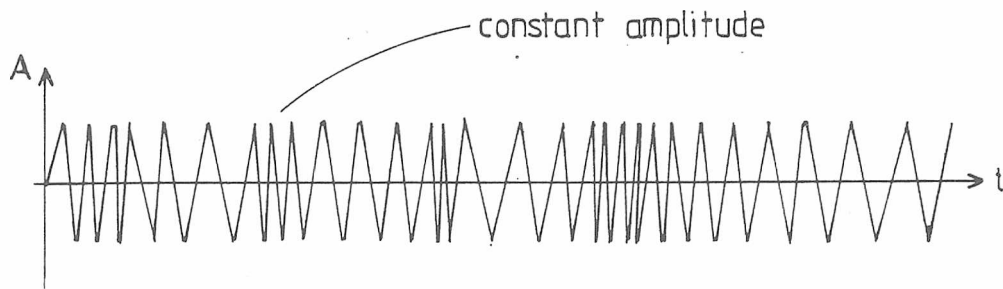
(a)   a frequency modulated signal
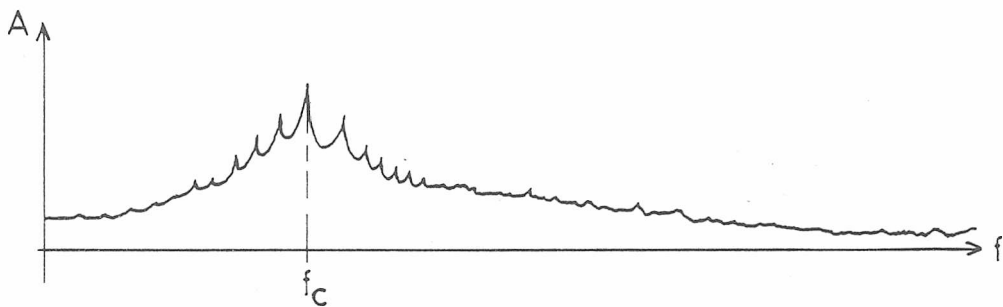
(b)   the spectrum is also complex, peaking around the carrier frequency, f_c
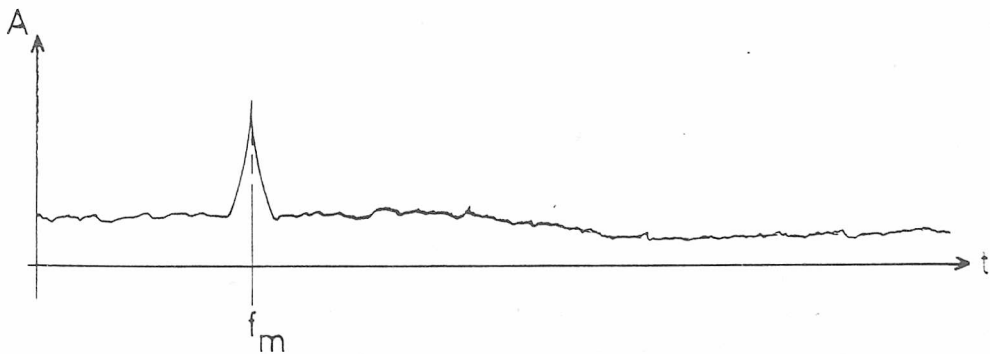
(c)   the cepstrum gives a single peak, at the modulating frequency, f_m

Figure 3·18

$$2 \cos i\theta \cos k\theta = \cos(i-k)\theta + \cos(i+k)\theta$$

$$2 \sin i\theta \cos k\theta = \sin(i-k)\theta + \sin(i+k)\theta$$

$$2 \cos i\theta \sin k\theta = -\sin(i-k)\theta + \sin(i+k)\theta$$

$$2 \sin i\theta \sin k\theta = \cos(i-k)\theta - \cos(i+k)\theta$$

A carrier $(i\theta)$ multiplied by modulation
$(k\theta)$ gives two sidebands $(i+k, i-k)$

Figure 3.19(a) Sine modulation

$$cal(i,\theta)cal(k,\theta) = cal(i \oplus k,\theta)$$

$$sal(i,\theta)cal(k,\theta) = sal\{[k \oplus (i-1)]+1,\theta\}$$

$$cal(i,\theta)sal(k,\theta) = sal\{[i \oplus (k-1)]+1,\theta\}$$

$$sal(i,\theta)sal(k,\theta) = cal\{[i \oplus (k-1)],\theta\}$$

$\oplus$ indicates addition, modulo 2

A carrier (i) multiplied by modulation (k)
does not result in the "split" form,(above).
This Walsh modulation does not produce
sidebands.

Figure 3.19 (b) Walsh modulation

CHAPTER 4.

THE CASPAR PROGRAM.

4.1   Introduction.

The exact nature of the particular signal processing requirements for condition monitoring was unknown at the start of the research project, and so a flexible signal processing facility was required. This could have been achieved by the use of sophistocated programming techniques, and writing specific routines for each process to be tested.

Whilst this may be a good approach to the design of a suite of programs to perform some specific and predefined task, it is impractical in this context. What is required is a main program framework, into which specific routines may be placed and tested. It must handle all necessary protocols, data flow and operator entry automatically. The normal form for such a framework is the so called "menu driven" program. The program developed for this research, named CASPAR (Computer Aided Signal Processing And Recording), is an example of such a scheme.

4.2   The main routines in CASPAR.

As an introduction to the facilities allowed by the CASPAR
program, a list is presented of the routines which it contains:

A) Read a full spectrum from the analyser.

B) Read a reduced spectrum from the analyser.

C) Set the analyser to display its memory.

D) Write a spectrum back to the analyser.

E) Produce a print out of the spectrum.

F) Produce a single plot of the spectrum.

G) Perform multi-plotting.

H) Wait for a time, then continue.

I) Use the "Recorder Start" button as a trigger.

J) Ring the terminal bell.

K) Set up the attenuators on the analyser.

L) Clear the interface.

M) Find the "energy" in the spectrum.

N) Normalize the spectrum.

O) Set a noise threshold on the spectrum.

P) Find the peak in the spectrum.

R) Perform autocorrelation on the spectrum.

S) Stop at any point and return to the start of the program.

T) Talk to the analyser

U) Produce a cepstrum.

V) Read a spectrum from disc.

W) Write a spectrum to disc.

X) Use the "RETURN" button as a trigger.

Y) Store a spectrum in memory.

Z) Recall a spectrum from memory.

&) This allows continuation of a line, keeping all data valid.

A summary is now presented of the main routines suported by the program. Firstly, data must be acquired. Two routines are provided for this. As a first choice, the data is read from the analyser as two blocks of data. One of these contains the spectral values, and the other contains details of the settings on the analyser. These are used when interpreting and recording the data, and include the sampling frequency and full-scale amplitude settings. If a number of spectra are to be read without changing the settings, then the second routine would be used. This transfers the spectra only, and does so in a much faster data format.

After the data has been processed, it must be examined. Several possibilities are presented. Firstly, the result may be passed back to the analyser for display. Again two data transfer protocols exist, and are exactly analogous to those for reading data. If a paper record is needed, the data may be printed on the operator's console (and thereby on a printer) in list form. When a graphical representation is desired, the plotter is brought into action on the same IEEE interface as the analyser. This gives a plot of the data, fully annotated and scaled. A further facility is allowed here. It may be necessary to observe a phemomenon which changes with time. For this, spectra may be recorded at intervals, each one individually processed, and then the group of them placed on the same plot, with offsets in the "X" and "Y" directions.This generates a "surface", and so simulates a pseudo-three-dimensional repsesentation of the data.

As any condition monitoring exercise proceeds in time, long term records are needed. This facility is provided by recording the spectra on disc. The operator may request disc storage and provided that a valid disc is in the computer, the data will be recorded. This recording is permanent, and no means exists in the program for erasing or overwriting it. Thus, once on a disc, the results cannot be lost. To aid record keeping, the discs are all provided with a unique number, recorded on the disc, and the spectrum is given a serial number as it is recorded. This number is displayed on the operator's console. To retrieve this data, the disc reading choice is placed in the input line, and the serial number will be requested by the program.

4.3   The Command Level Loop.

The main control of the program is carried out by the "Command Level Loop", as shown in Figure 4.1. It is the function of this part of the program to allow execution of a particular set of routines, selected from the "menu", and to control the program during this period.

The command structure is also able to allow extra facilities, not offered as normal input choices.

At the start of every program run, the operator is given four choices of action:

34

1. Y   Yes, print the menu.

2. N   No, do not print the menu.

3. C   Continue, re-using the last choice.

4. S   STOP.

All of these, as with the choices for the routine input string, are entered as a single letter, so keeping continuity throughout the program.

The last of these, "STOP" is self explanatory, and terminates the program. It must be noted, however, that typing an "S" in the choice line will not terminate the whole program, but only the present input string. This gives the operator a simple route back to the start of the command loop, should this become necessary. This is shown in Figure 4.1 by the "reset route". The other three choices have the following functions:

1. Yes, print the menu. This gives a listing, on the operator's console, of the currently available processing routines.

2. No, do not print the menu. This gives the means of entering a string of routines, without the menu being printed each time.

3. Continue, and re-use the last choice. This allows a simple method of repeating a given process, without the need to retype it every time.

Once the desired reply is given to these questions, and the menu given, if requested, the operator is free to design a process. This is done by entering a string of characters which relate to the process, in the appropriate order. There are no restrictions on what may be typed in - all necessary protocols are handled by the program, and illegal characters (anything other than letters and numbers) are reported to the operator, so that the string may be corrected without any processing taking place.

Having entered the command string, the operator is prompted for the number of times that it is to be repeated. This differs to the "C" response above, in that it is specified before, rather that after the processing, and allows for any number of repeats, as shown in Figure 4.2. The "C" respone is intended to allow for the re-use of a past process, without the need to explicitly re-type it.

4.4   Program Framework.

If any processing is to take place on the signals read from the spectrum analyser, there must be some simple and fixed means by which these may be gathered, processed and either displayed or recorded. CASPAR allows for this, and other features suited to research in signal processing.

Firstly, the spectra produced by the spectrum analyser must be transferred into the computer. This is done here via an IEEE standard interface bus, all the software for running this having been writen as a part of this work. This allows the whole system

36

to be automated. The software that drives the interface is written in a mixture of FORTRAN and machine language. This gives the advantages of both. The machine coded section allows access to the computer at a level suited to driving the hardware for the interface bus, whilst the FORTRAN sections allow ease of access to the bus, and greatly simplifies the passing of large amounts of data.

When developing such a program, it is normal practice to perform the tasks of interfacing between instruments and general data transfer by the use of subroutines. These may then be nested until whole blocks of data can be transfered by a single statement. CASPAR extends this approach, so that the data is handled entirely automatically. The advantage of this is that a standard has been set, and any future process has only to conform to this to ensure correct data flow.

When writing a program, the input and output of data has to be considered, as essentially, the function of the program is to transform one into the other. This data will be stored in memory. The operator specifies the particular routines by typing in a string of characters, which define the routines to be accessed, as shown in Figure 4.3. When the data is read from the analyser, it is stored in a one-dimensional array, without the operator having to define a memory area for this purpose. An extension of this is then to have similar arrays for storing the data within each routine for processing it. This will require large amounts of memory. It is an improved solution, thus, to hold the data in just one single storage area, and allow every routine to have access to this area, as shown in Figure 4.4. The

37

savings made by such a move are not only in storage space, but also in execution time, as it is no longer necessary to actually transfer the data between routines. The disadvantage of this approach is that the original data will be lost. This, however is of little consequence in a processing regime which is formed of a string of routines, one passing its result as the data for the next. If it is desired to keep the original data, a separate routine is provided to transfer the data from the common area to one of five identical, but protected areas, as shown in Figure 4.5. In addition, spectra can be stored on a magnetic medium. The data is then permanently recorded. This was useful for maintaining records throughout the project. Access to these, via the CASPAR program is protected; once a spectrum has been committed to disc, it cannot be erased or overwritten from the program. Each disc can accommodate 280 spectra, as shown in Figure 4.6. The drives, however, are not fixed, so that a library of discs may be created. Using this facility, approximately 850 spectra have been archived.

The program, then, has a modular basis. This simplifies the inclusion of extra processing routines, as they are developed. A new routine is assigned a letter for identification, and this is placed in a table, along with the routine's location. As shown in Figure 4.7, access has then to be specified to the common memory area, and the unit is fully operational.

4.5   Operator Input Handling.

It is the main feature of a "menu driven" program, from the operator's viewpoint, that the function of a particular process is chosen from a list, or "menu" which is provided by the program itself, or in the instruction manuals. This allows an operator to configure a complex signal process procedure from a number of sequential processing kernels.

In the field of machine monitoring, it is the combinations of different routines which is of interest. To allow for this, each routine is identified by a unique letter. A series of such letters, henceforth referred to as a "command string", can be set up to control the selection and sequencing of a particular set of routines. For example:

AW

This command string will read a spectrum from the analyser (A), and write it to disc. A serial number will be allocated to it, so that this particular spectrum may be recalled.

VUCD

This command string recovers a spectrum from disc (V), prompting for the serial number of the desired recoring. It then performs a Cepstrum analysis of the signal (U), selects the display function of the analyser (C) and writes the processed data to the analyser for viewing.

This reads a spectrum from the analyser and stores it in memory area number 1 (Y1). The "&" character instructs the program to hold all data valid, rather than clearing all of the processing areas at the start of each command loop, and allows spectra to be held in the memories, for reference purposes.

The command string may also contain digits, as some routines may need numerical input. Any routine which needs numerical parameters is given default values. These may not fullfil the operator's requirements, and so, new values may be entered by typing them in the input string, after the letter identifying the routine in question. The command string is read by CASPAR, and separated into classes, as shown in Figure 4.8. Valid letters for identifying the routines to be selected are removed, as are any parameters for these routines. All other characters are ignored. An exception to this occurs, should any illegal characters be encountered in the line. These would be control characters, dollar signs, quotation marks etcetera. If any of these is found, then the whole line is rejected, and a message given to identify the character at fault. Rejection of the whole line gives the advantage of avoiding confusion, as could arise when a command line has several sets of similar routines in it. The charatcter could have been found in any of these, so that its exact position, and the action to be taken would be unclear.

It may be required to repeat a given process — eg. to re-apply the same processing on a variety of signals. For this to be achieved, the command string must be stored. In CASPAR,

this is done in two separate arrays, as shown in Figure 4.9. Parameters are easily removed from the command string, as the string is stored as characters, in ASCII format - the numerals are then in a different range to the letters. They are then stored in a separate array. The function of this is to simplify the process of executing a given routine with the correct parameters - either the defaults, or those entered in the input string. The array that contains the letters of the string is then within a known number range, since the letters, stored as ASCII codes, occupy the range 65 to 142. As the array now consists exclusively of letters, the numbers 0 - 64 will be unused, as they can never appear. It is possible, thus, to use these as pointers to the parameters, held in a separate array. This approach is used, as the parameters must be allowed to be in any numerical range. As the letter array is stepped through by the program, any value less than 65 is obvious, and easily detected. It is then used as a pointer to the location in the parameter array, of any numbers that followed the particular letter.

A further requirement of this area of the program now becomes apparent. It is foreseeable that the number of parameters called for by the many routines will differ, so that the number of numerical inputs will vary. This is easily handled by the system decribed, by having not one, but two pointers in the letter array. These consist of the location of the first parameter, and also that of the last. It thus becomes a process of reading through the parameter array until all of the numbers entered as being associated with a particular letter are found.

Also, it then becomes feasible to enter more or fewer parameters than may be required for a particular routine. If fewer are entered, the defaults can be used for the missing information, and any extra can be ignored and safely left in the parameter array. To do this without the double pointer system could mean that excess parameters from one routine would be used as parameters for the next. Since the succeeding routine will have its own pointers to its specific input, no problems will occur.

4.6   Data Handling.

As each new choice is entered, marked by re-entering the command level loop, all previous data is lost (unless recorded on disc). This was implemented as a failsafe mechanism, as it gives a fixed condition at the start of every process. This also allows a certain amount of error checking to be carried out. The most useful of these is to check whether or not a spectrum is resident in the system. If this is found to be the case, then the process continues as entered. If, on the other hand, no new spectrum has been fetched, either from the analyser or from disc, then the program automatically reads one from the analyser. It is then possible to (say) plot a spectrum by typing the plotting choice as the input line. A spectrum will be read and then plotted with no further operator intervention. It may be required, however, to store the data from one process for comparison with that of a later one. This would not be possible if the above were the only regime available. It is posible, however, by entering an ampersand (&) in the choice line; this gives a "continuation" facility, whereby all past data is held

42

valid, until it is explicitly overwritten by the operator.

4.7   CONCLUSIONS.

As there is a need for a general-purpose research tool, some time has been spent on the development of such. The end product performs the tasks of data handling, processing and recording, and all operator requirements. This entails that a certain amount of programming time be spent on the interactions with the operator, as distinct from that spent on actually processing the data. The rewards for this approach, however are in the speed of process development, and of adding new routines to a given set, with the minimum of extra overheads in complex protocols.
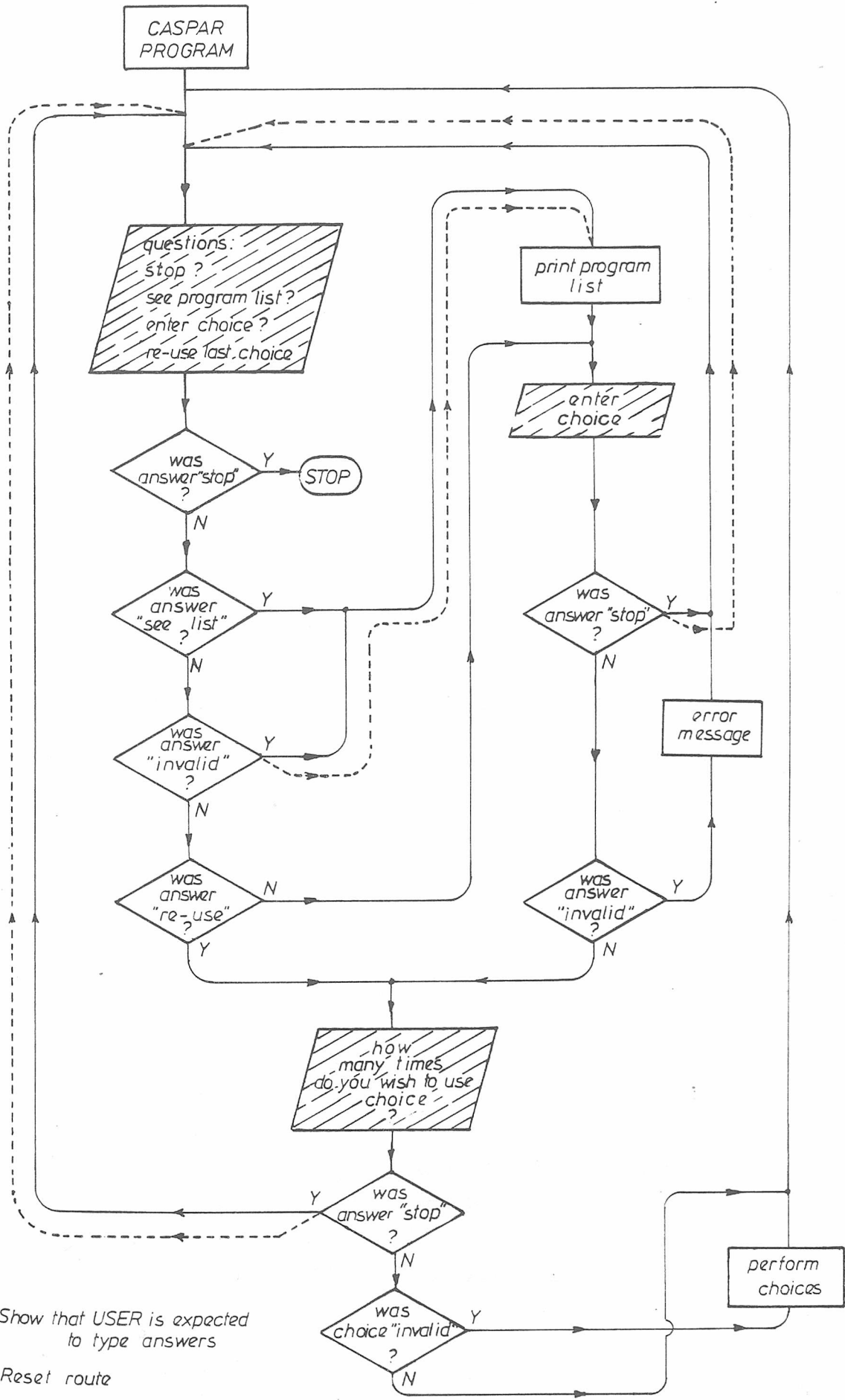
Figure 4·1   CASPAR: command level loop

START

repeat last choice — Y → was a "last choice" entered ? — N → second level repeat

N

enter new choice

Y

how many times to repeat choice — first level repeat

perform choices

all done ? — Y / N
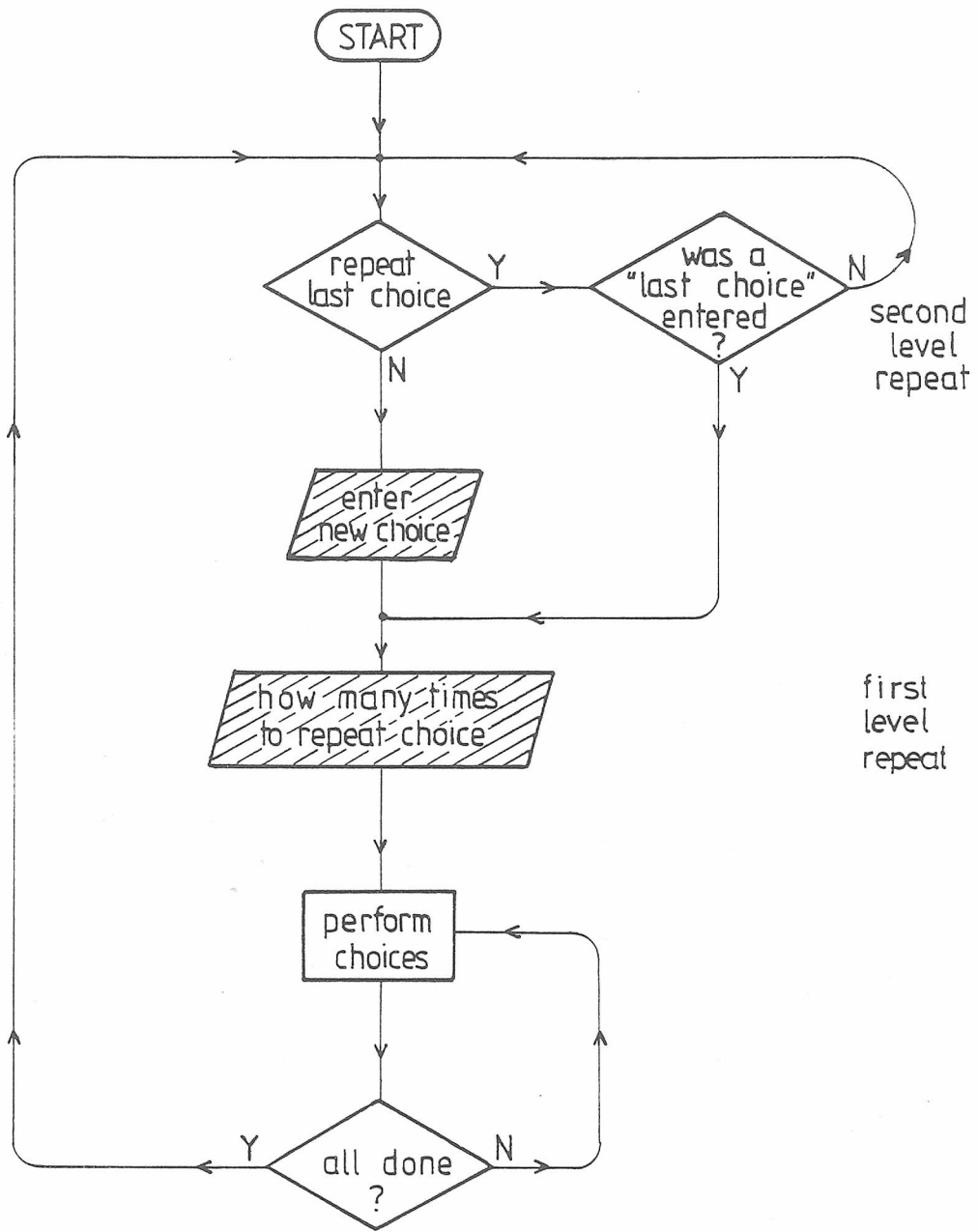
A given choice may be repeated at either (or both)
of two levels

show that USER is expected to type
answers

Figure 4·2
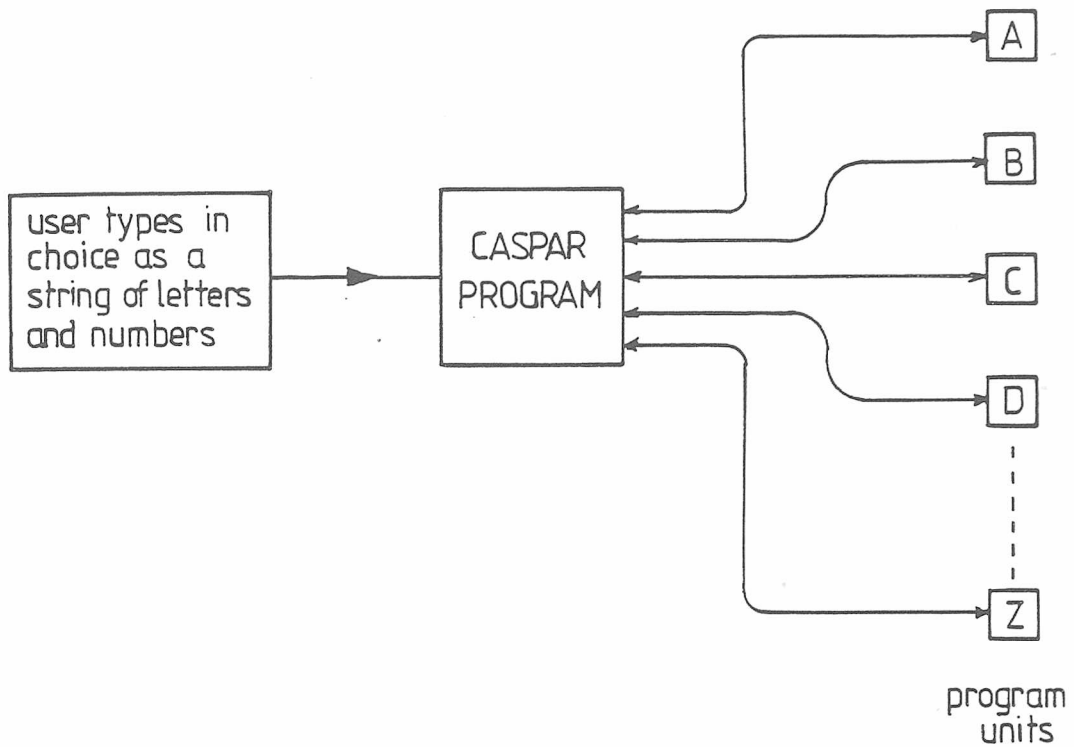
Figure 4.3   Caspar program gives simple access to
the program units
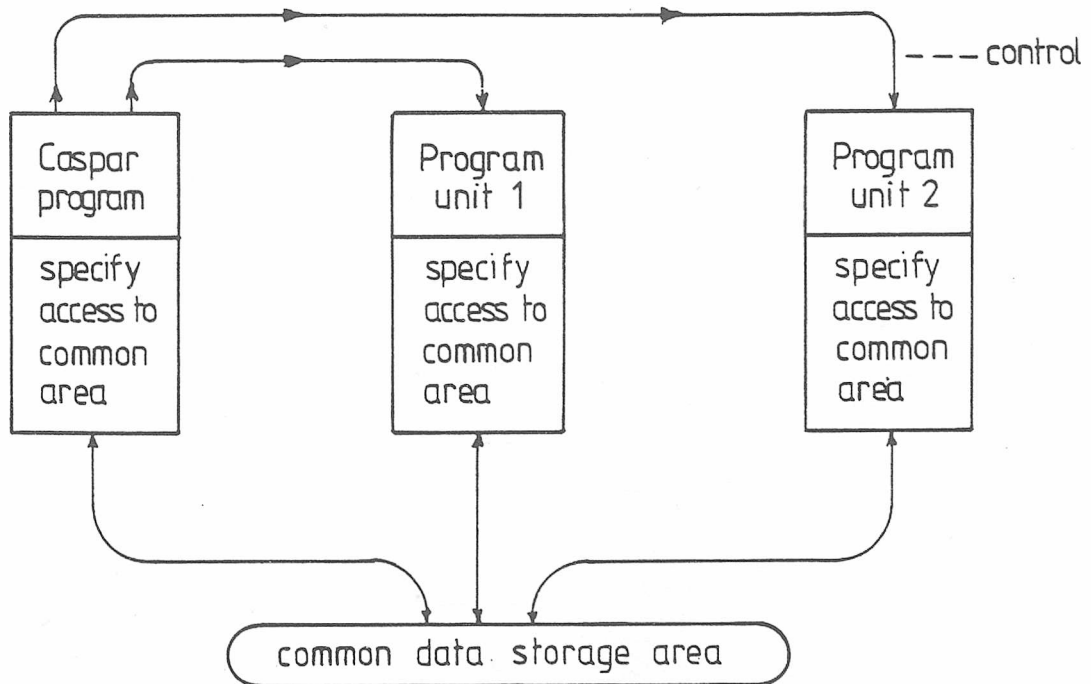
Figure 4.4 Data handling by use of "common" store
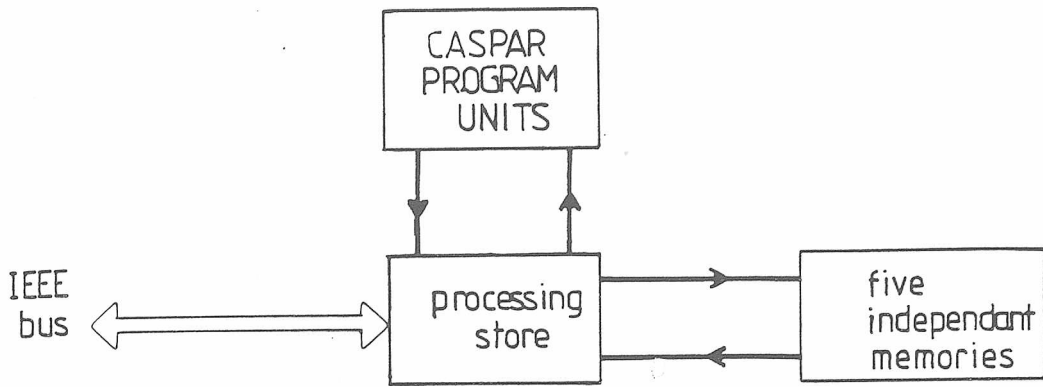
all processing and data IN/OUT is done
in a single area of memory

Figure 4.5
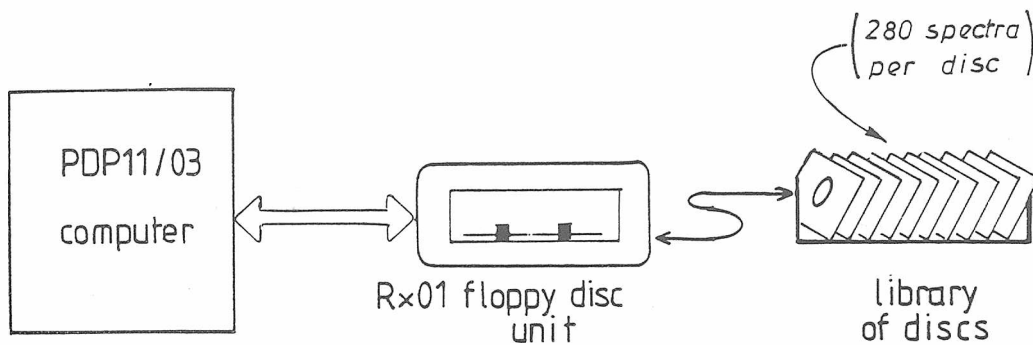
floppy disc unit can be used to provide
unlimited storage

Figure 4.6
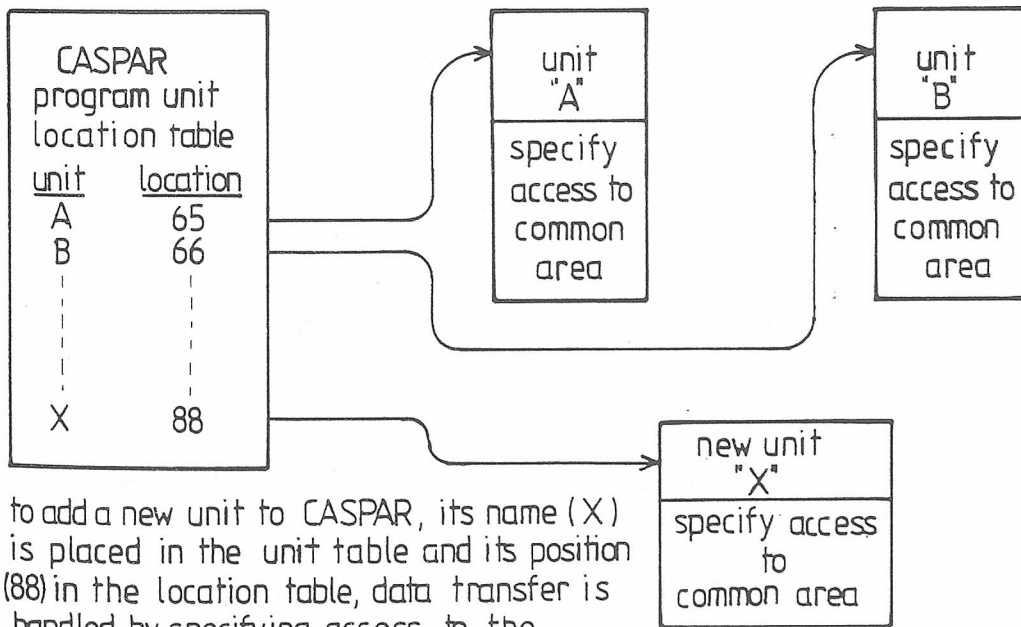
to add a new unit to CASPAR, its name (X)
is placed in the unit table and its position
(88) in the location table, data transfer is
handled by specifying access to the
common storage area.

Figure 4.7
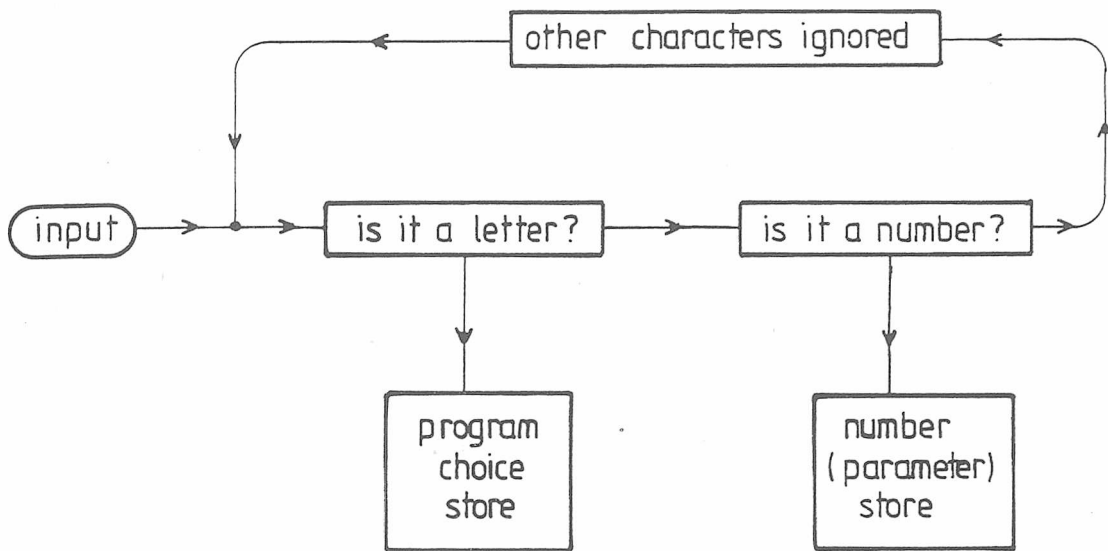
Input string is seperated into Program choices and parameters

Figure 4.8
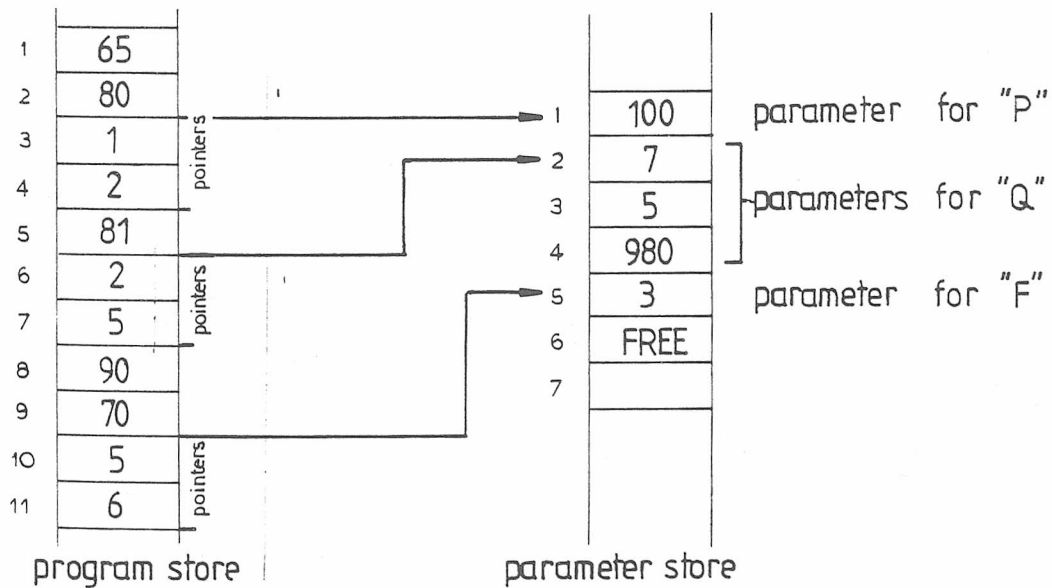
Examples of input string, as stored by CASPAR.

Figure 4.9

CHAPTER 5.

CONDITION MONITORING TEST RESULTS.

5.1   Introduction.

The preceeding chapters have discussed the characteristics
of the induction machines and the direction to be followed for
condition monitoring of them. This chapter describes the testing
facilities used, and presents the results of the signal
processing. It is shown that the approach taken is very powerful
in diagnosing single and multiple fault conditions.

5.2   Machine Testing Facilities.

Having developed various signal processing systems for the
purpose of condition monitoring of electrical machines, some
means must be available to test them. The route for this may
take several directions. The "expected" data may be modelled on
a computer. This will only give reliable results if the exact
nature of the problems is known in detail, and as such is not the
case here, this route cannot be followed. Previous work, as
discussed in the Conference papers, (see the Appendix) has been
done with the aid of special purpose motors, which have been
modified, constructed or designed from the start as research
vehicles. This does not give a true representation of an
industrial situation, within which a condition monitoring
instrument would be used.

In order to overcome these problems here, a special test rig has been designed and constructed [44]. The purpose of this is to allow control of the operating condition of the motor which is being tested. The most important feature of this test rig is that the drive unit is a standard industrial drive — it will thereby reflect the actual conditions under which a test procedure would be used, rather than some modified set of machine characteristics.

The motor is provided with a number of small studs, onto which a standard accelerometer may be placed, to sample the case vibration. This transducer may be placed in a position which will show the vibration at points of interest, such as on the bearing pedestals, or in the centre of the length of the stator core. In addition to this, a small air-cored coil may be placed at any position around the outside of the machine case. This is normally positioned near the end casings, where it will sample the magnetic flux which strays from the end of the stator windings. These transducers may be attached with a minimum of modification, to any motor, and so allow non-invasive testing to be carried out.

The signals from these transducers, along with those from an air-cored and thus linear current transformer around any of the supply lines, and from a coil placed around the drive shaft to sample the axial flux, are fed into the signal processing equipment. This consists of a commercial audio-frequency spectrum analyser which is part of a mini-computer based system. This consists of a PDP 11/03 computer running the CASPAR program, the spectrum analyser, a graphics plotter and a high-quality

45

instrumentation tape recorder. The whole test system is shown in Figure 5.1.

5.3   Test on a Machine in "Good" condition.

In order to perform condition monitoring, various transducers may be placed on the machine, and changes in the resulting signals detected. This entails a knowledge of the form of these signals in a "good" or fault free machine, so that any changes may be evaluated. In this section, the frequency spectra from a good machine are presented. The signals used for this investigation are vibration from the bearing pedestals, and the centre of the machine casing (for stator vibration), stray and axial flux and supply current. Typical spectra are presented in Figures 5.2 to 5.7.

It will be seen from these that, in general, the signals change with load, the stator vibration signal contains more information than the bearing pedestal vibration signals, and there is a similarity between the flux and current signals.

Consider the vibration signals. These may be expected to show certain characteristics, depending on where the transducer has been mounted. Those on the bearing pedestals will contain a larger proportion of the bearing vibration than will the centre measurement, whilst this latter signal will show more of the stator vibration, due to the proximity to these sources. The signal from the drive-end bearing pedestal is also nearest to the load. This implies that it is the most likely to be contaminated by load vibrations, and is thus of less interest as a source of

46

information on the motor itself. The overall information content of the stator vibration signal also can be seen to be greater, as the bearing vibration signals have a smoother form.

Whilst the vibration can be considered to give an overall picture of the motor state, the electrical conditions are of prime interest. To enable these to be monitored, three signals are used, which reflect purely the electrical phenomena. These are the stray and axial flux, and the supply current. As the current sets up the flux, and the flux then cuts those coils through which the current flows, all three signals may be expected to be similar. Comparing Figures 5.5, 5.6 and 5.7 this is seen to be the case. Further to this, the current will be composed mostly of a 50Hz. component and harmonics thereof, as the supply current is larger than any secondary effects caused by the conditions within the motor. Again, the spectra clearly show that the current signal contains less information than the flux signals.

5.4   Choice of Analysis Parameters.

Six signals from the machine test-set have been investigated. It is clear that the vibration signal contains the most information, from more sources than any of the other five, so making it a first choice for analysis. Three measures of the vibration have been used. As it is desired to look at electrical faults, all of the analysis should be biased towards this, so pointing to the accelerometer being placed in the centre of the case, where it will contain information which is coupled through from the stator core. This will then contain the required

47

information, with a larger content of electrically and magnetically induced vibration, than will the positions above the bearings.

The vibration signal, however, is easily "contaminated" by sources outwith the machine being monitored. On an oil production platform, for instance, the whole structure will be vibrating. To give a good indication that any fault detected is actually in one particular machine, more signals must be employed. Of the three other signals considered, the current is the least attractive. This is due in part to its content being mainly supply-frequency related, but mostly because it cannot be monitored as a non-invasive test. To sample the current, a transformer must be placed around at least one supply line. These may be enclosed in a conduit and so be inaccessilbe, and the transformer would be difficult to install. This directs attention towards the flux sensing coils. Those used on the test rig consisted of air cored coils wound on a small plastic bobin. These are insensitive to fields, except ones which are produced close to them, and so are not as easily contaminated as the vibration signal. This narrows the choice to two signals. The need for non-invasive test procedures dictates which of these is used, as the axial flux is sampled by a coil which is placed around the drive shaft. This requires a modification of the motor / load system, as space must be allowed for it. The stray flux on the other hand, is sampled by a small coil which may be placed on the outside of the machine, just above the ends of the stator windings. In this position, it sees the flux from the windings along with leakage from the airgap, which is exactly the

required information. It may be held in place by any means which is convenient, and is therefore a much more attractive proposition than a coil placed around the shaft.

Two test signals, namely stator vibration and stray flux have been selected. These must now be analysed in the most ecconomical and meaningful way. For the two faults to be considered, viz. broken rotor bars and supply failure, the fundamental mechanisms were discused in Chapter 2. This showed that supply failure will be reflected as a large increase in the twice-supply component of the vibration, and that the broken bar will be seen as a frequency modulation at twice the slip frequency. The modulation appears as equally spaced sidebands, as discussed in Chapter 3. For sidebands at twice slip frequency, the minimum resolution will have to be half of this, ie 1Hz. for the 28 slot rotor, with full load speed of 1470 rpm. This requirement comes from the need to perform Cepstrum analysis to evaluate the sideband content — so that the spectrum must itself be sampled. Applying Shannon's theorem, this must be at twice the frequency of interest. As discrete Fourier transforms are to be carried out on the signal, the output of the transforms will also be discrete. The sampling for the second transform cannot, then, be done at a "rate" which is "higher" than the resolution of the first transform. These criteria, together, dictate the size (resolution) and bandwidth of the first Fourier transform. Since it is the combination of these two parameters which is of importance, a third criterion is necessary to fix the solution. To this end, the 100Hz. component (supply induced vibration) is chosen to be at half the full scale bandwidth, so

giving rise to a 200Hz. bandwidth for the first transform. If a wider bandwidth were chosen, then the "sample rate" in the frequency domain, for performing the second transform, would be lower. This then leads to the cepstrum bandwidth being decreased. This may not be a problem, as it can be overcome by using a larger sample for the transforms, which effectively increases the sampling rate in the frequency domain. However, these extra samples have to be stored, they will take longer to acquire and longer to process.

Thus a compromise is reached between size and bandwidth. The result of this is a 200Hz. bandwith with 1024 samples. This gives a frequency spectrum with 512 points, as the Real and Imaginary points are combined to give a "Power" spectrum. When the second transform is performed, the result is 256 points. Choosing the bandwidth and sample size as described then places the quefrency of interest (corresponding to 2Hz.) in the upper region of the cepstrum. This gives a good deal of noise immunity, as the noise, as discussed in Chapter 3, will be concentrated in the lower region, which is compressed, due to the inverse frequency scaling of a cepstrum. The calibration of the "X" scale of the cepstrum is in time, or by an inverse law, in frequency. The frequency represented by any line is given by a simple formula. This also takes into account the fact that these tests are carried out with the aid of a commercial spectrum analyser. This produces its results by way of a 1024 point transform, giving 512 results. Only 400 of these are used, however, as an aid to anti-aliasing, since the rejection of the top 112 points acts as an additional low-pass filter. Thus a

factor of 400/512 comes into the cepstrum calibration, as the 400 results must be padded with 112 zeros, before the second transform can be done. The calibration from cepstrum line number to modulation frequency is thus given by:

$$\frac{B.W. * 512}{Line\ L.N. * 400} = Modulation\ Frequency.$$

Where B.W. is the bandwidth of the first transform, and L.N. is the number of a line in the cepstrum.

This means that for the 51 slot rotor, with a full load speed of 1430 rpm. and thus a slip frequency of 4.67 Hz., will give a peak at line 55 in the cepstrum.

5.5   <u>Broken Rotor Bar Test Results</u>.

Having chosen the parameters for the analysis, ie stray flux and stator vibration, analysed with a 200Hz. bandwith over 1024 sample points, the case of a rotor with broken bars may be considered. Previous chapters have discused the effects that such a fault would be expected to have on the spectra. These effects are borne out by the results.

As it is anticipated that the spectra will be frequency modulated, Cepstrum analysis has been applied. This will assess the side-band content of the spectra, and thereby give an indication of the severity of such a fault. These results are presented below as a spectrum and its associated cepstrum, on the same page, for ease of comparison. Full and no load tests are reported, in both good and bad condition.

Comparison of the various spectra does indeed show that the rotor with a broken bar exhibits a modulated nature, with sidebands at twice the slip frequency. Turning then to the cepstra, and looking at the area around this frequency, a very significant change is seen. As the load increases, so will the rotor current. This would imply that the amplitude of the modulation, and thus the size of the peak in the cepstrum should also increase with load. Comparing the vibration spectra in Figures 5.8 and 5.9 or 5.12 and 5.13 this is the case. However, considering the change in level between the cepstrum in Figure 5.9 with that in Figure 5.13, the change is less than would be anticipated. This effect is discussed later.

It has been demonstrated that performing a cepstrum analysis on the vibration signal is a powerful technique for detecting broken rotor bars. The change in the component at twice slip frequency is significant and thereby easily detected by a threshold based on the "new" value, measured when the motor is installed. This is important, as each machine is an individual case, and some may exhibit the characteristic sidebands even when running normally.

This is the explanation for the small change between Figures 5.9 and 5.13. This particular rotor has several of the bars broken, and a connector made in their ends. This allows them to be "made" or "broken" at will, to enable these test to be carried out. However, this has the unfortunate side-effect of high resistance at these joints. This disturbs the flux distribution around the rotor, as does the fault in question. The basic nature of this test, then, is to assess the effect of the

resistance in the rotor bars — a broken bar merely being an extreme case of this generality.

A model of the two types of joint — one via the connector and one soldered showed that the "connector" joints do exhibit a high resistance, so accounting for the results of these tests. The high resistance of these joints shows up in the tests as would a breaking bar. This shows that condition monitoring for this fault does have to be done in relation to the "new" state of the machine, and the diagnosis based on trend analysis or a threshold, added to the original value.

A test procedure is thus established and proven for broken rotor bars. This is performed by a non-invasive test of the case vibration, and results in a single "confidence factor" for the fault. The vibration signal, although a good source of information is easily contaminated, and so a second source is used. For this, the stray flux is analysed, and these results are presented along with those for the vibration. The effects are exactly the same.

To test the procedure's ability to determine the severity of the fault, a full load test was done on a rotor with five broken bars, and the spectra and cepstra of these are given in Figures 5.16 and 5.17.

To prove that the major peak in the cepstrum is related to twice the slip frequency, a second rotor was tested. This consisted of a standard production type, and the fault in this case was a broken end-ring. The effect is to unbalance the rotor field in the same way as does a broken bar, as the current and

53

thus the flux distribution is altered. The full load speed for this rotor (in the same stator) is 1470 rpm. This gives rise to a peak at line 128 in the cepstrum. The results for these tests, corresponding to those on the 51 slot rotor, are given in Figures 5.18 to 5.25.

As this rotor, in good condition, had not been modified in any way, there were no high resistance joints to upset the process, and so a very good distinction is seen between the "good" and "bad" condition. The characteristic sidebands are again seen in the spectra, and a peak appears in the cepstrum at the predicted line number, so proving that the technique is applicable to more than one motor. This is the desired case, and the processing has been based on the fundamentals of the machine in order to achieve this end.

5.6   Table of Broken Bar Results.

In order that the results of the broken bar tests can be compared easily, the levels of the peaks in the cepstra have been measured form the Figures, and are now presented as a table of results.

51 slot rotor, full load.

Vibration	Stray flux.	
46 dB.	13dB.	Good.
48 dB.	45dB.	1 Bar broken.
52dB.	65dB.	5 Bars broken.

<u>51 slot rotor, no load</u>.

Vibration	Stray flux.	
28dB.	8dB.	Good.
28dB.	13dB.	1 Bar broken.

<u>28 slot rotor, full load</u>.

Vibration	Stray flux.	
8dB.	11dB.	Good.
23dB.	42dB.	1 Bar broken.

<u>28 slot rotor, no load</u>.

5dB.	2dB.	Good.
17dB.	6dB.	1 Bar broken.

This clearly shows that the test is effective, and is more so with increasing load. As most motors to which condition monitoring would be applied will be running at full load, this is an advantage of the procedure.

5.7   <u>Single Phasing tests</u>.

The remainder of the test results refer to a supply failure. This results in an unbalanced magnetic field, with a large increase expected in the supply induced components. The spectra in Figures 5.27 − 5.29, show that this is the case, and this fault can again be detected by a threshold set above the "new" level.

These Figures also show Cepstra of the fault spectra, which indicate no significant change. Thus the two tests are independent — the faults may be diagnosed separately, or together.

5.8   Conclusions.

The results of the signal processing which was developed for condition monitoring have been given. It has been demonstrated that electrically based faults can be reliably detected, singly or in combinations. The processing, based on machine fundamentals, has thus been proven to perform the required monitoring and diagnosis.
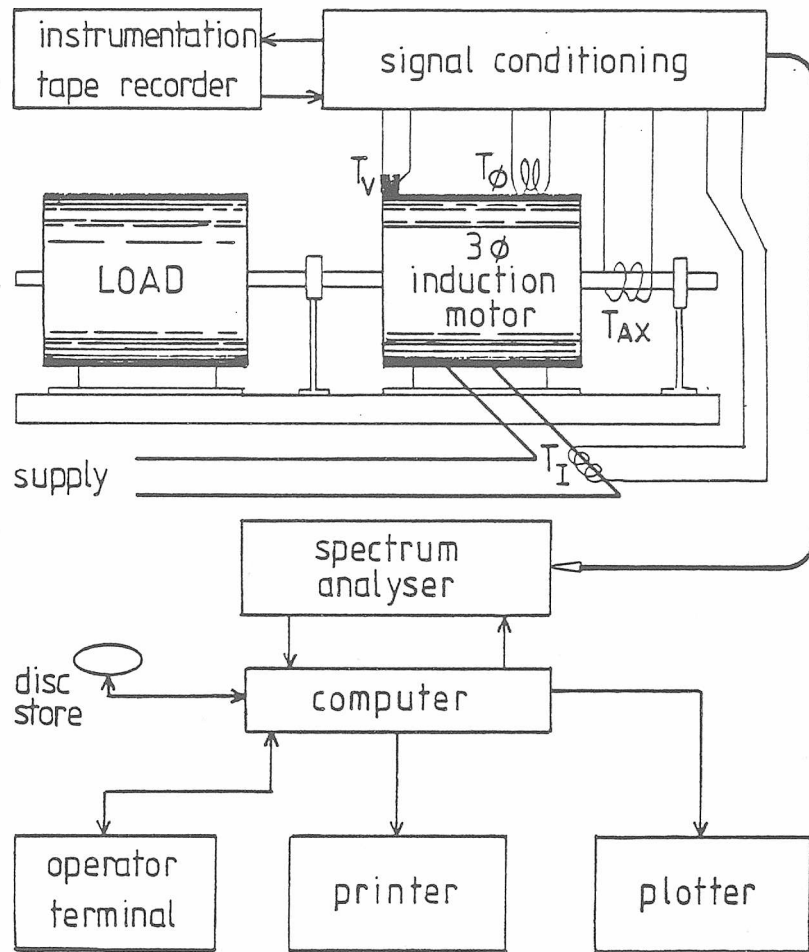
TEST RIG, DATA ACQUISITION AND PROCESSING EQUIPMENT

Figure   5.1

condition: GOOD

NO load

FULL load

1116.35

1316.35
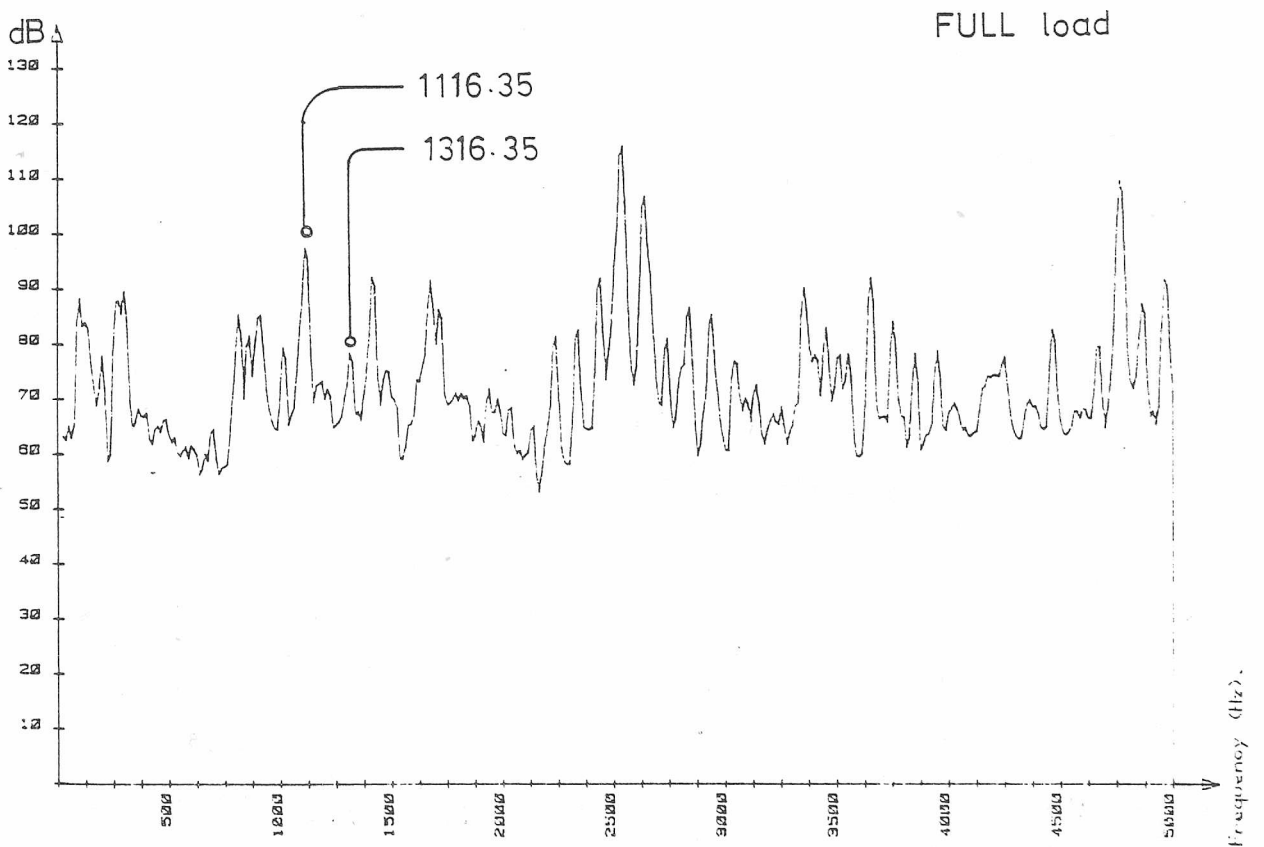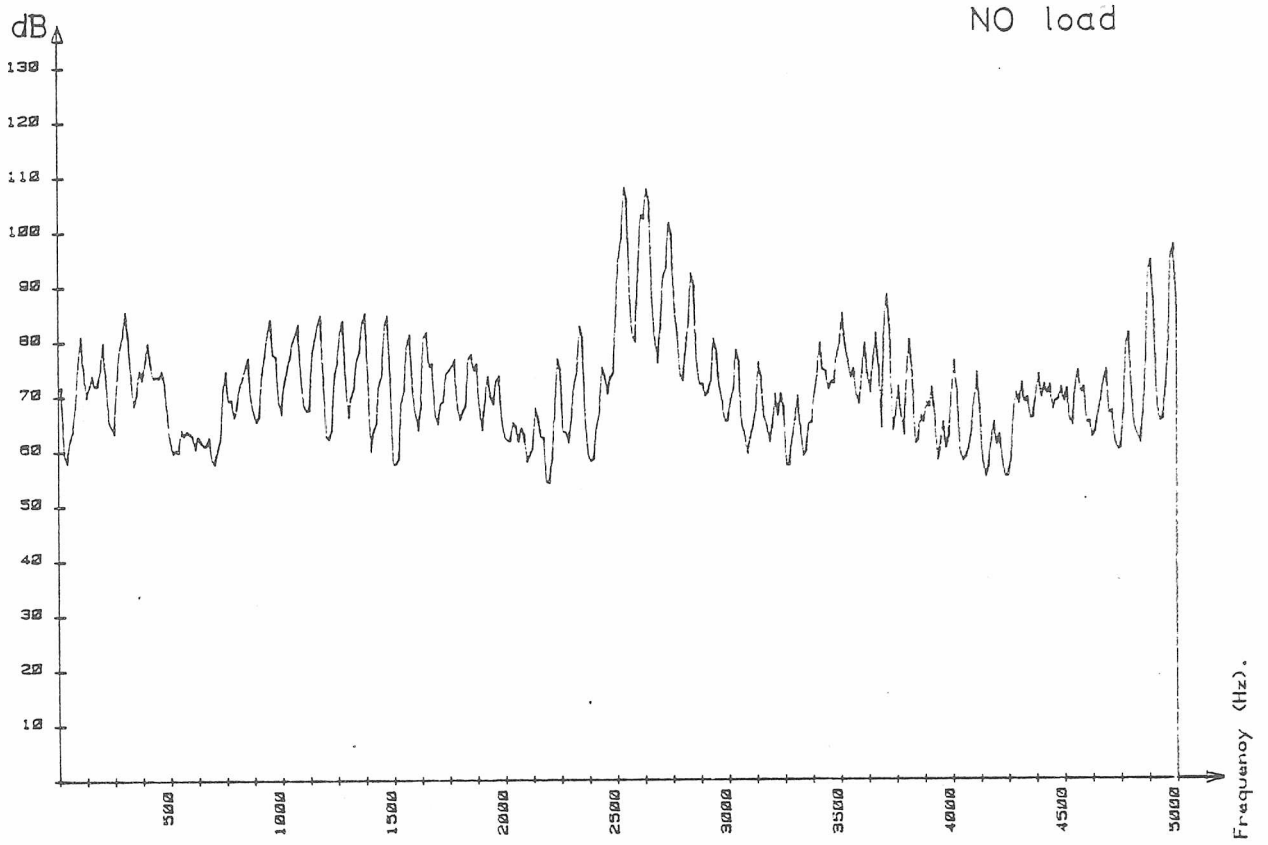
Figure 5.2   Vibration - stator core

condition: GOOD

dB   NO load

dB FULL load
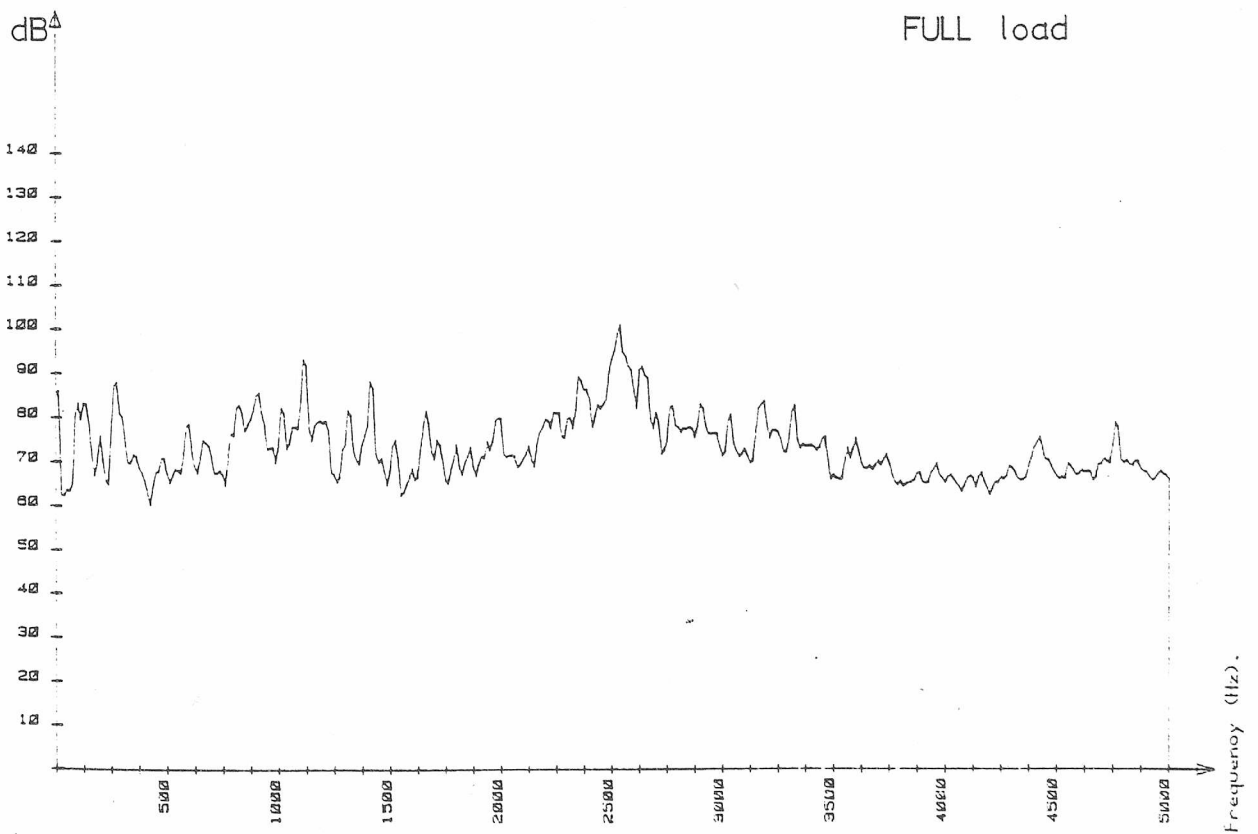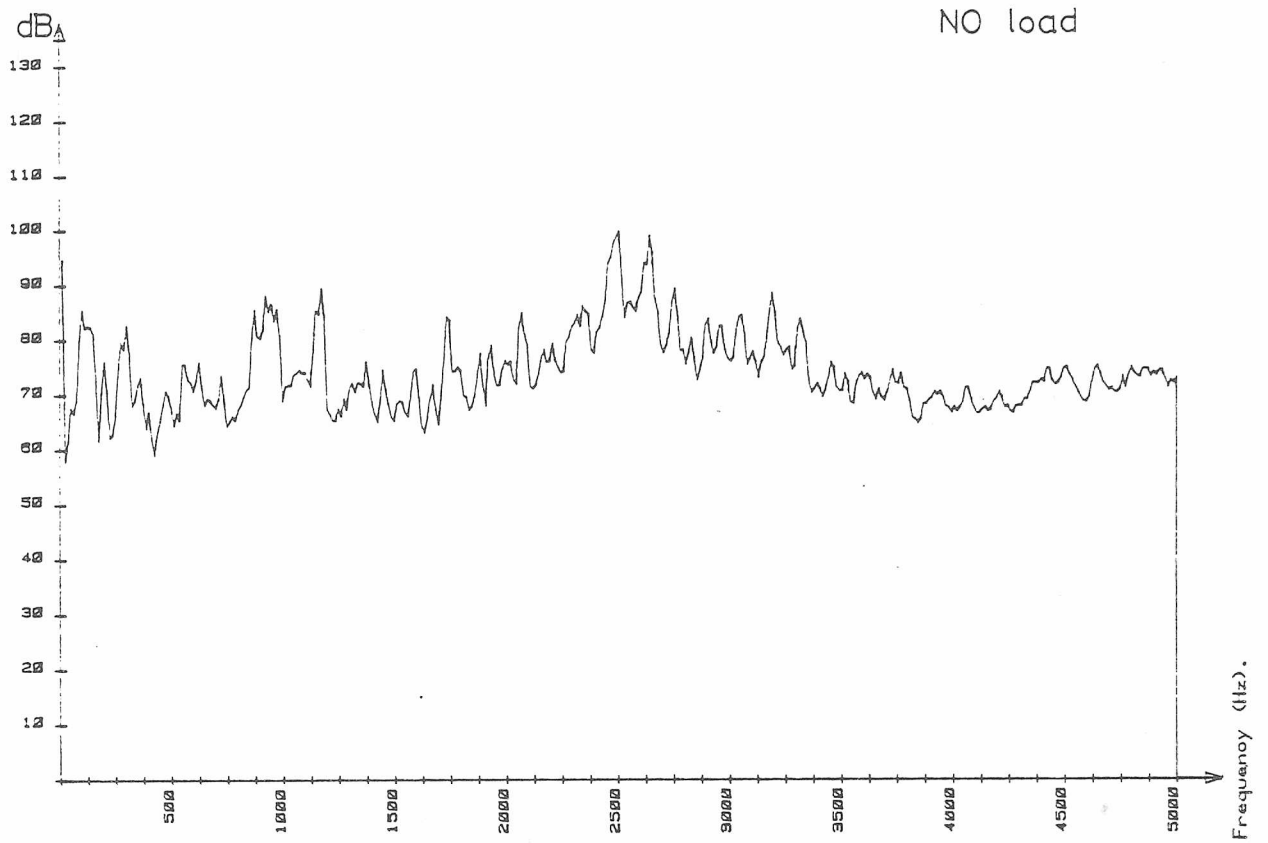
Figure 5.3   Vibration – free end bearing pedestal

condition: GOOD

NO load

FULL load
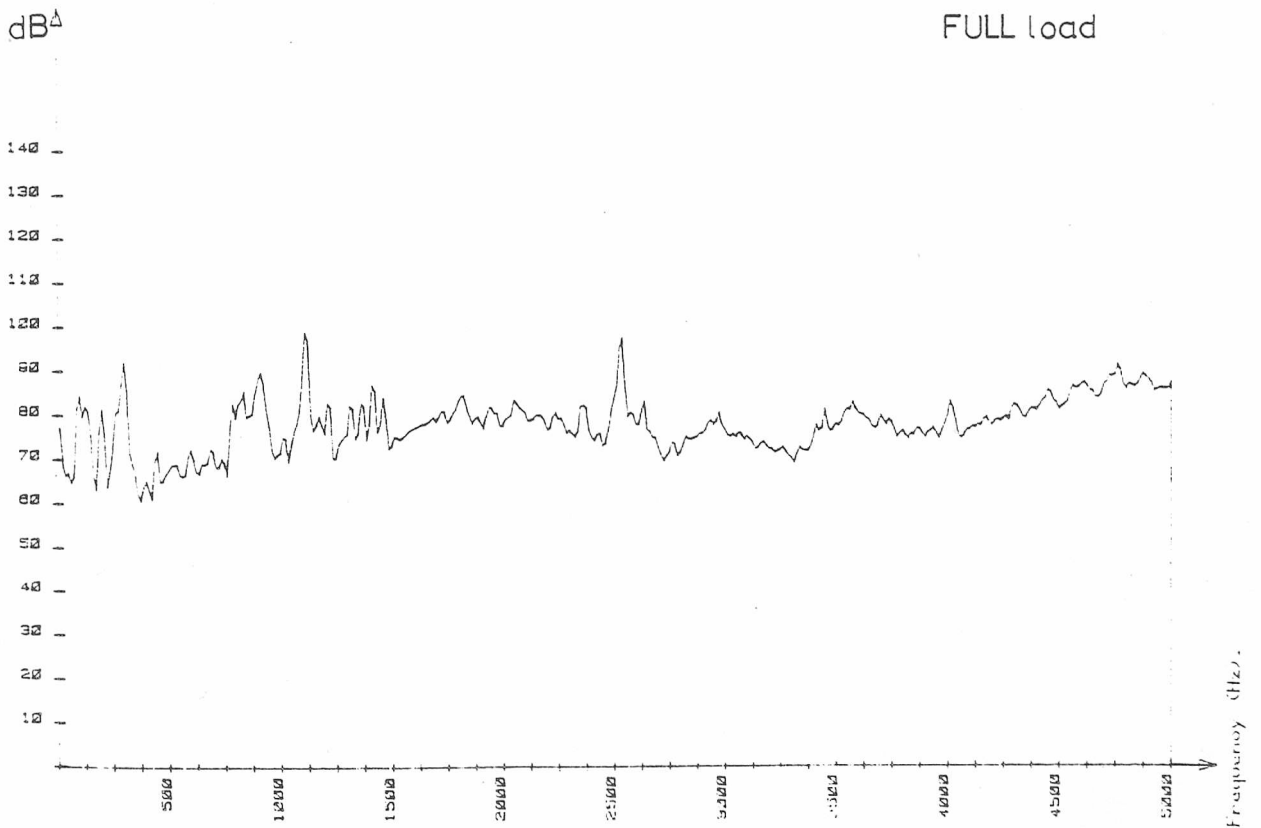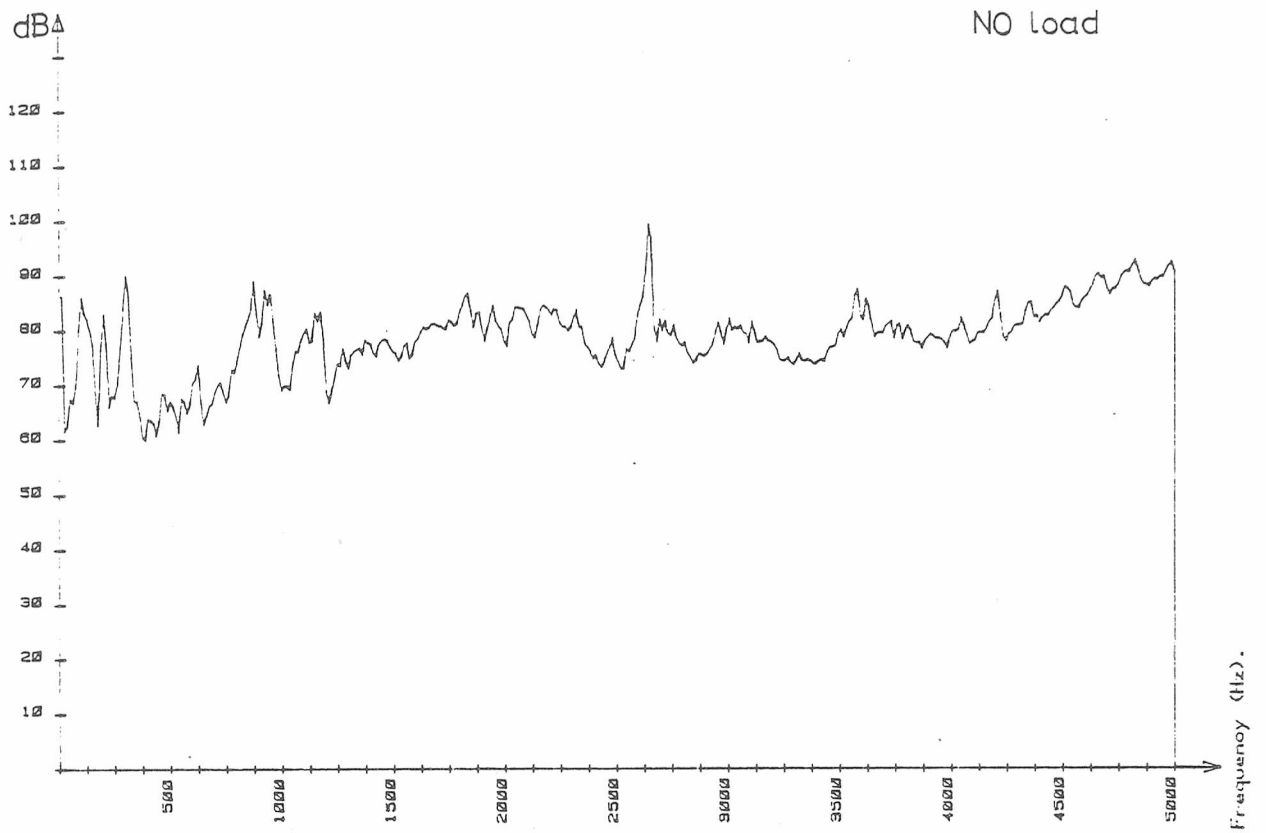
Figure 5.4   Vibration – drive end bearing pedestal

condition: GOOD

dBA   NO load.
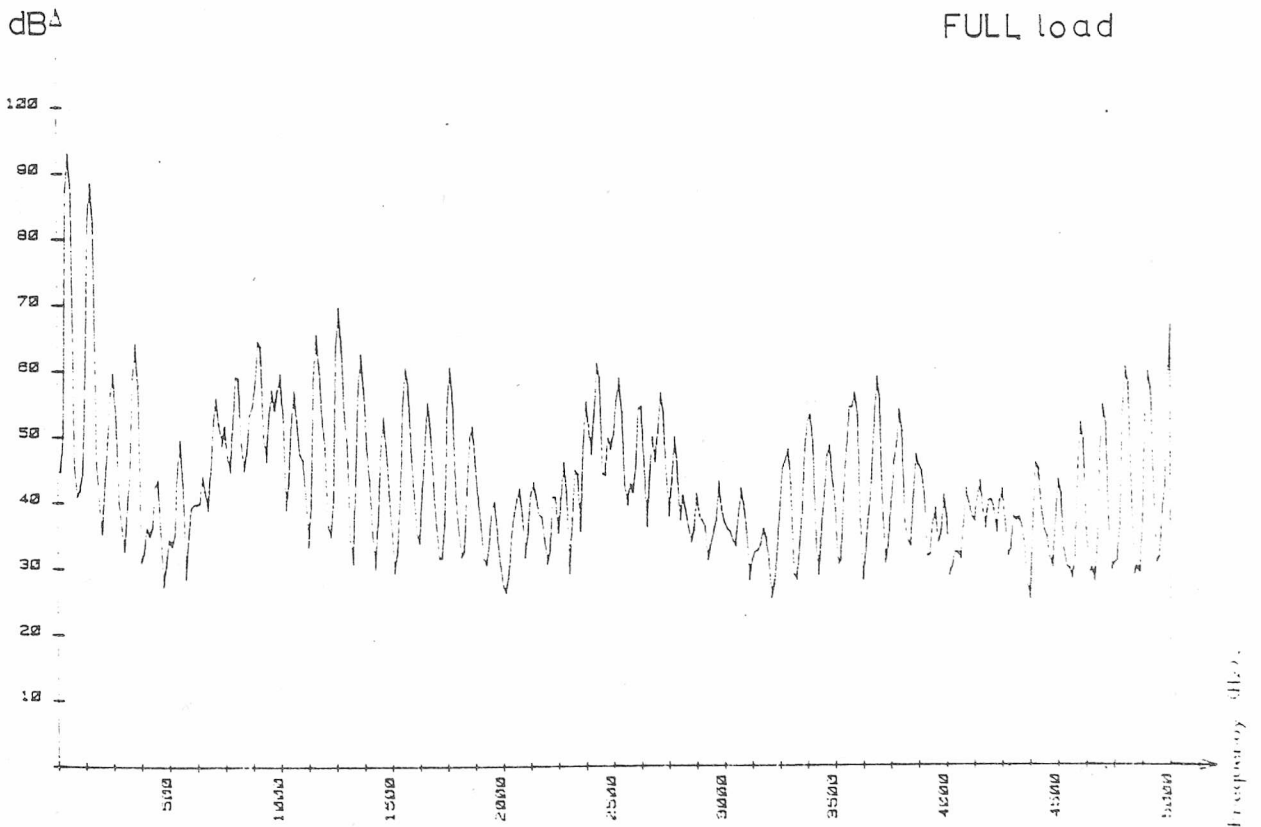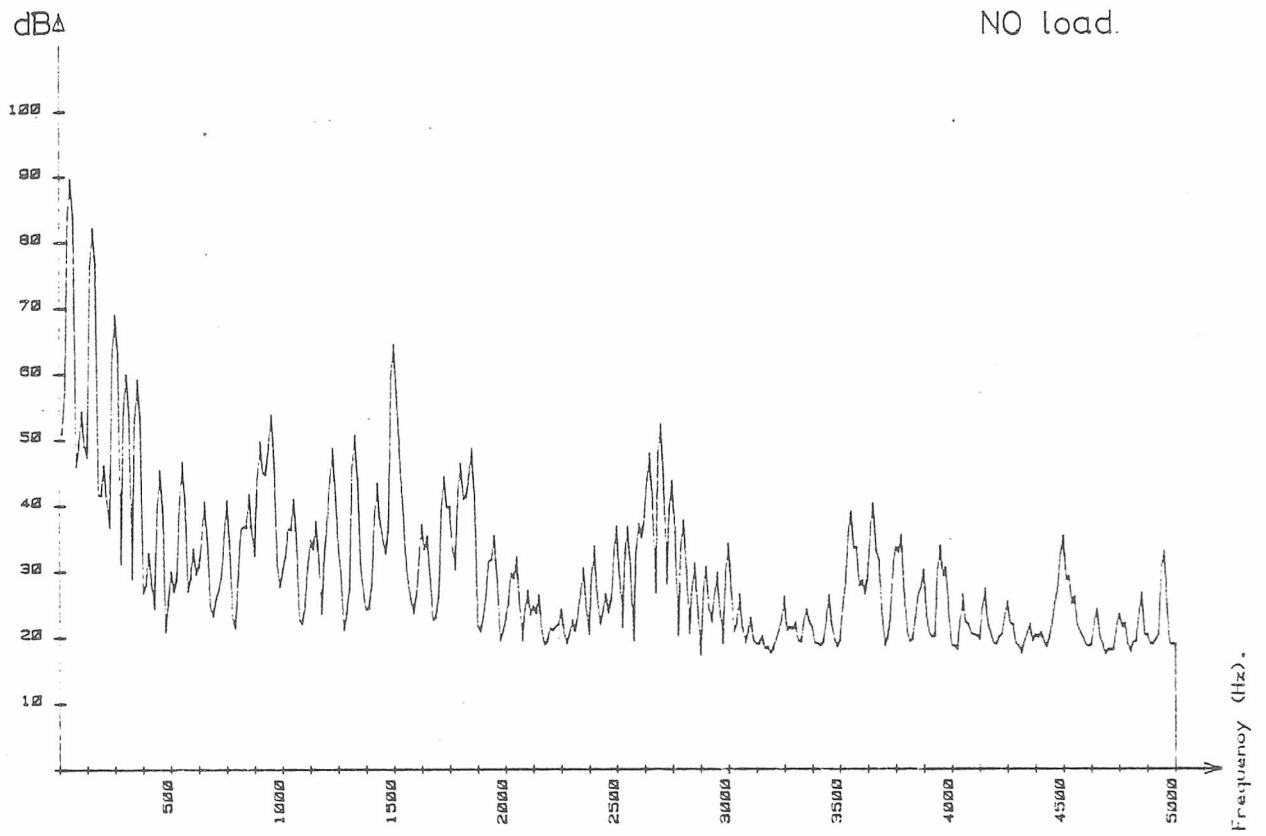
dBA   FULL load

Figure 5·5   Axial flux

condition: GOOD

dB

NO load

dB
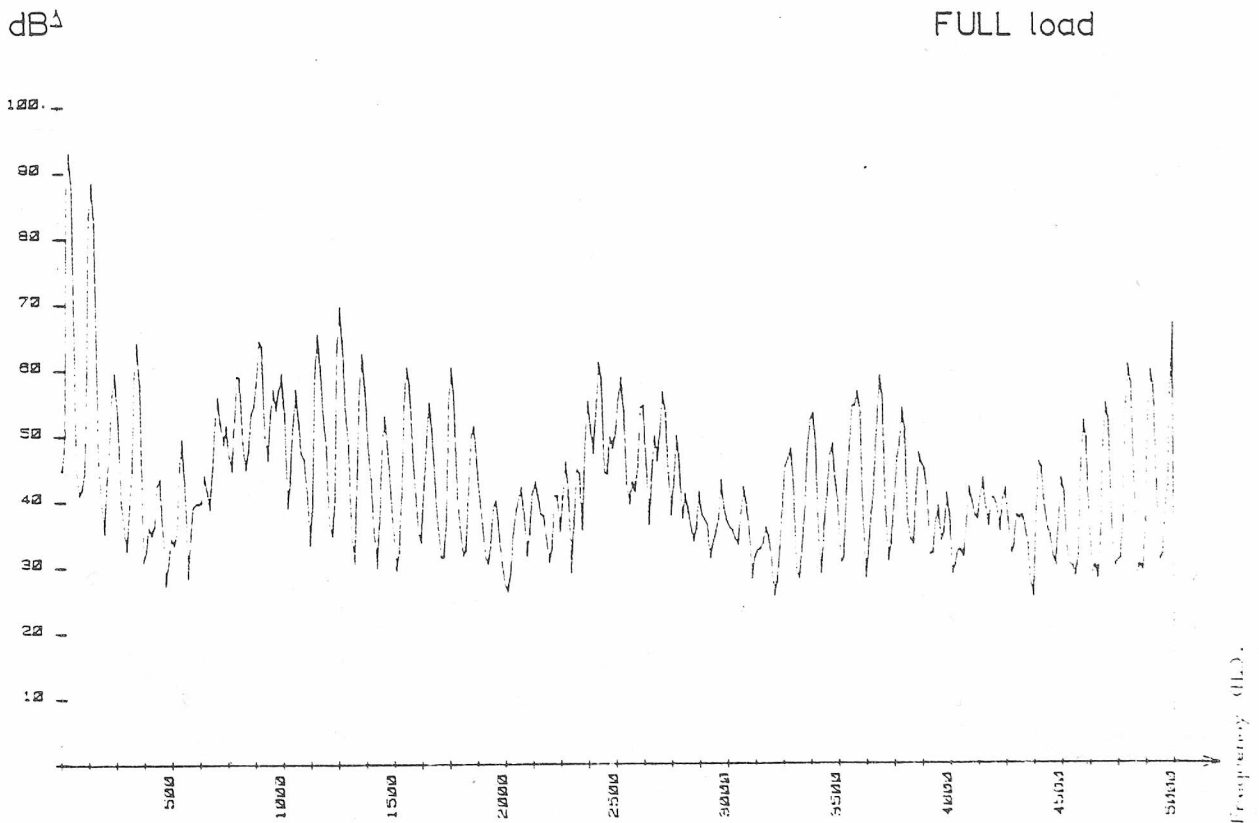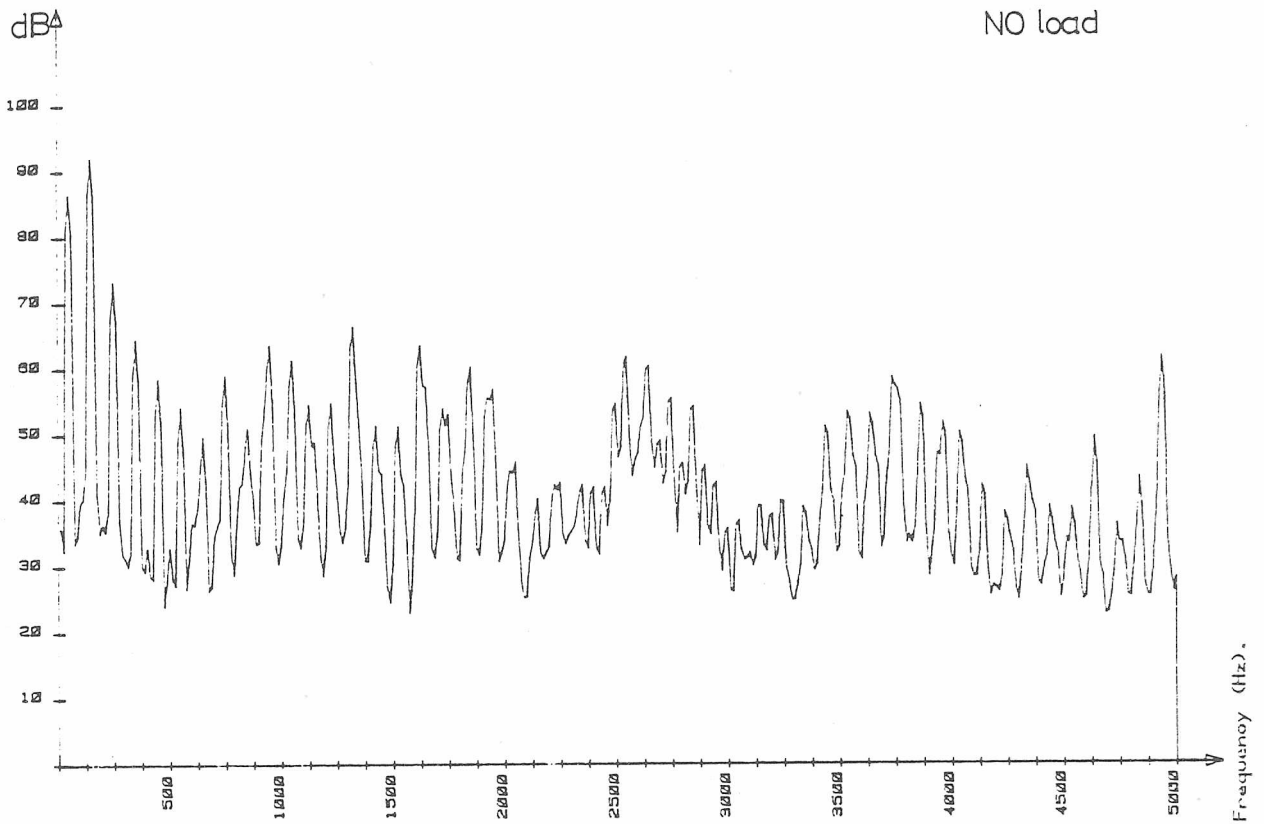
FULL load

Figure 5.6 Stray flux

condition : GOOD
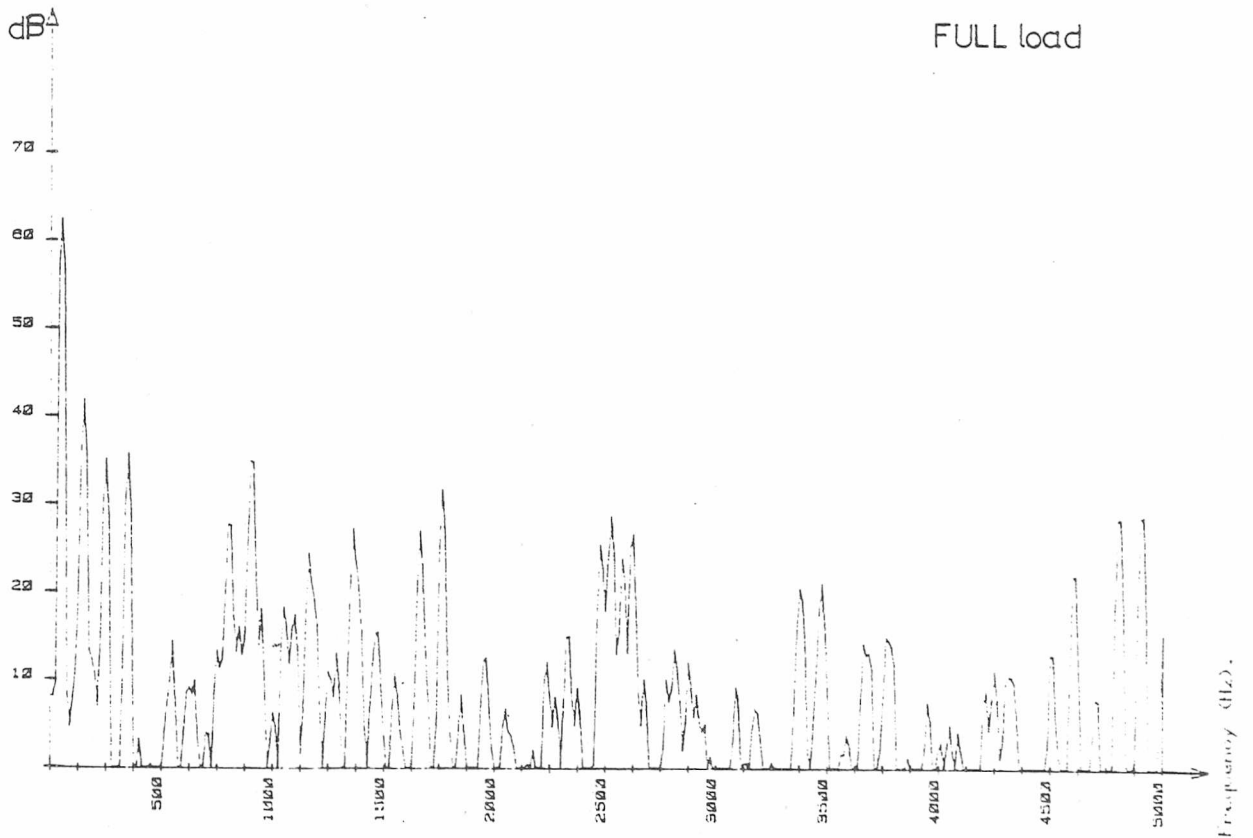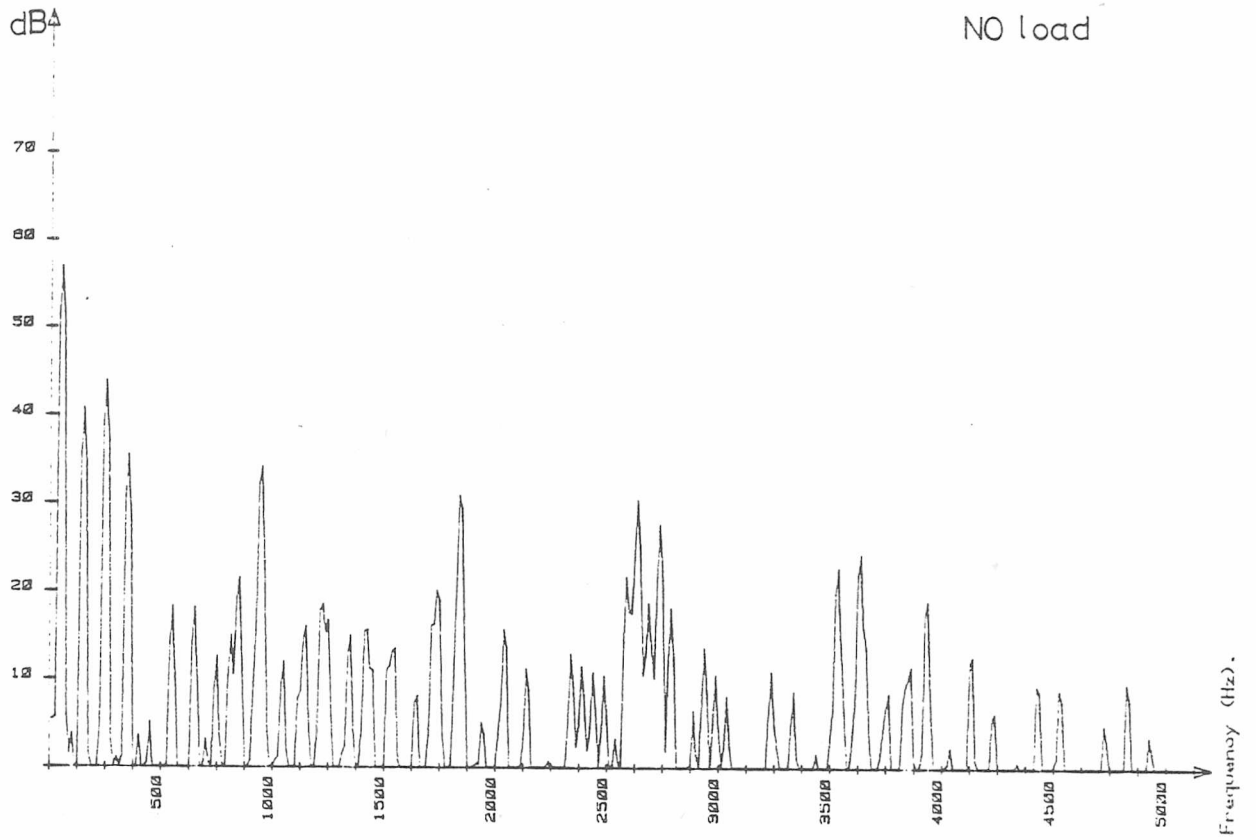
NO load

FULL load

Figure 5.7 Supply current

51 slot rotor, condition: GOOD
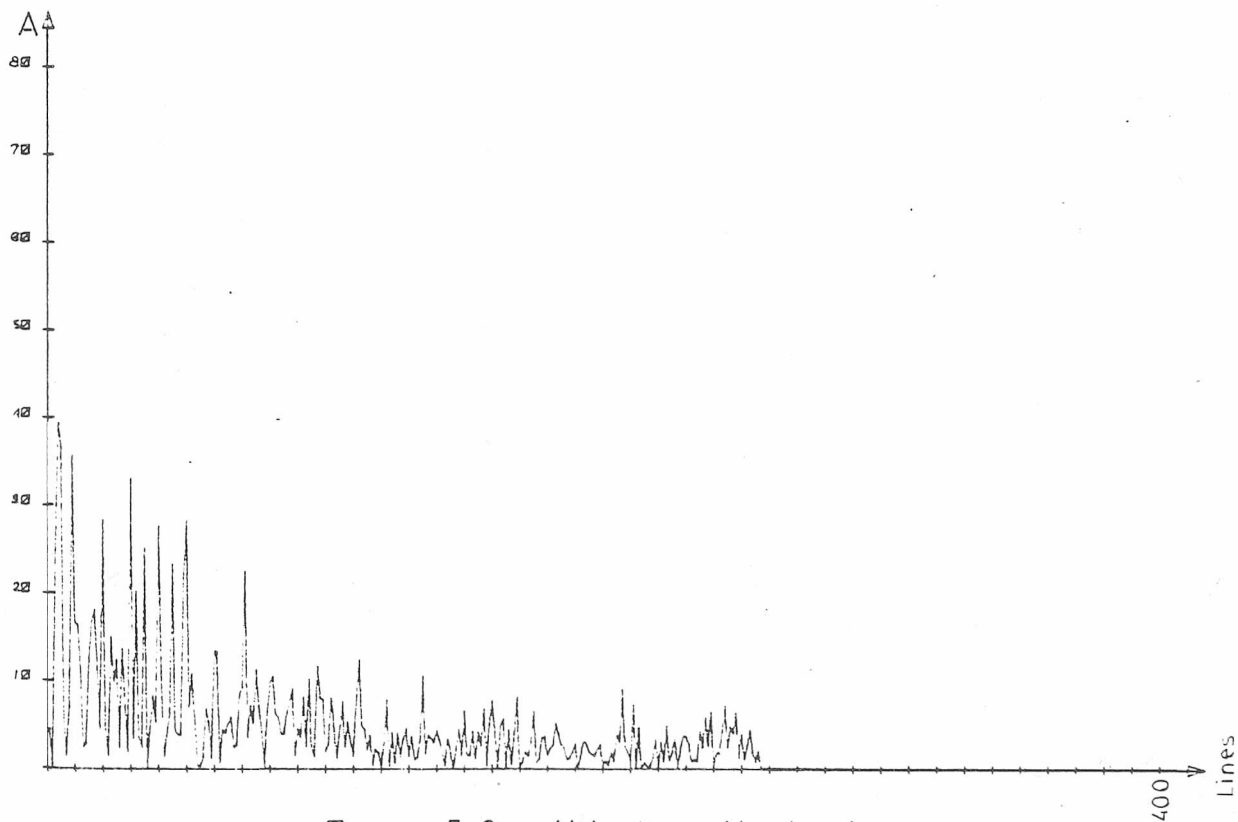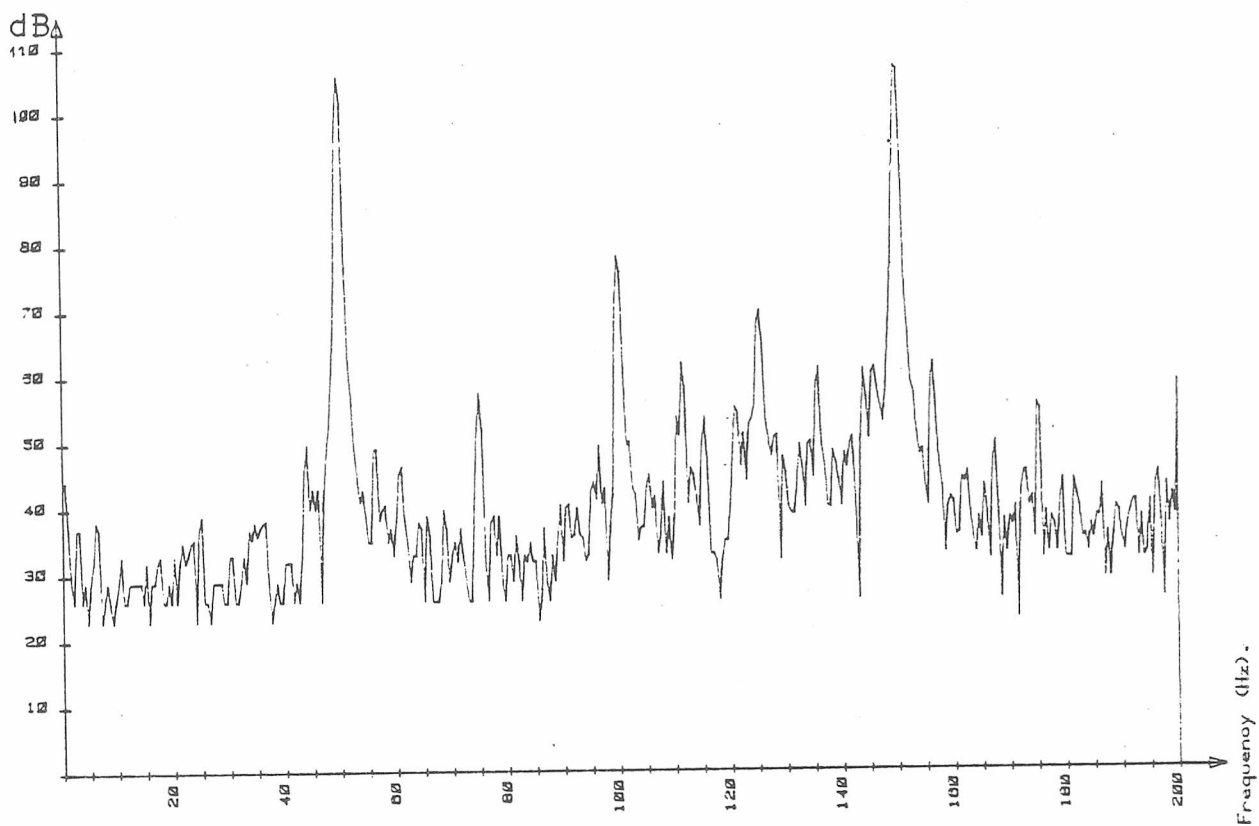
Figure 5.8   Vibration, No load

51 slot rotor, condition: GOOD
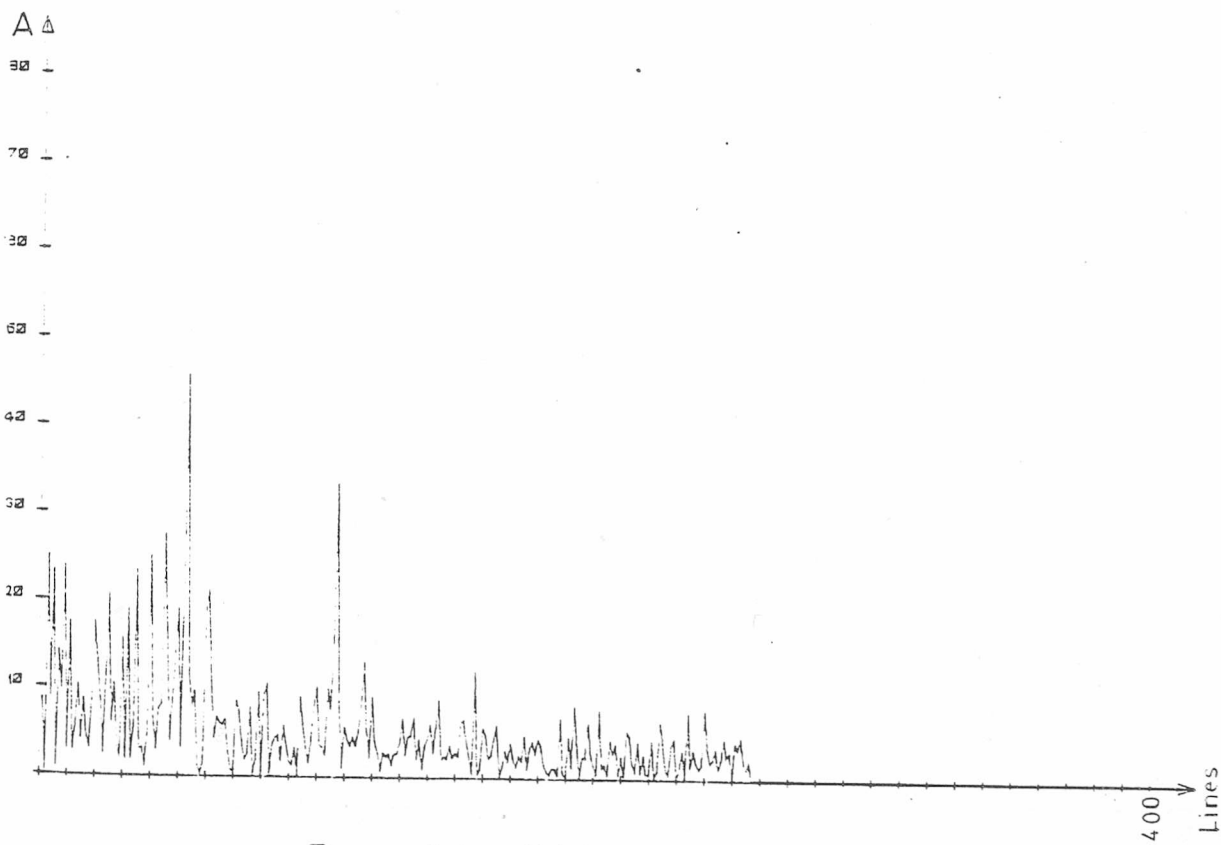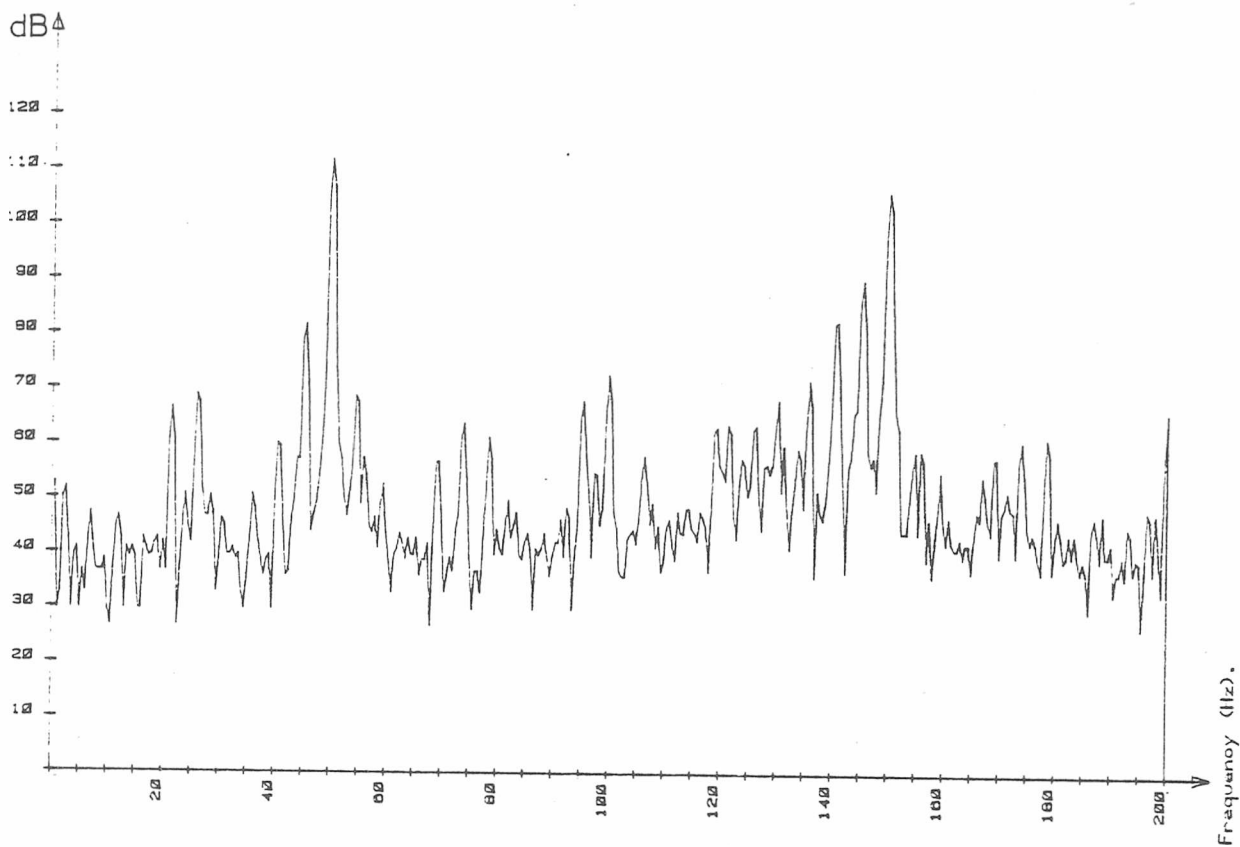
Figure 5.9   Vibrations, Full load

51 slot rotor, condition: GOOD
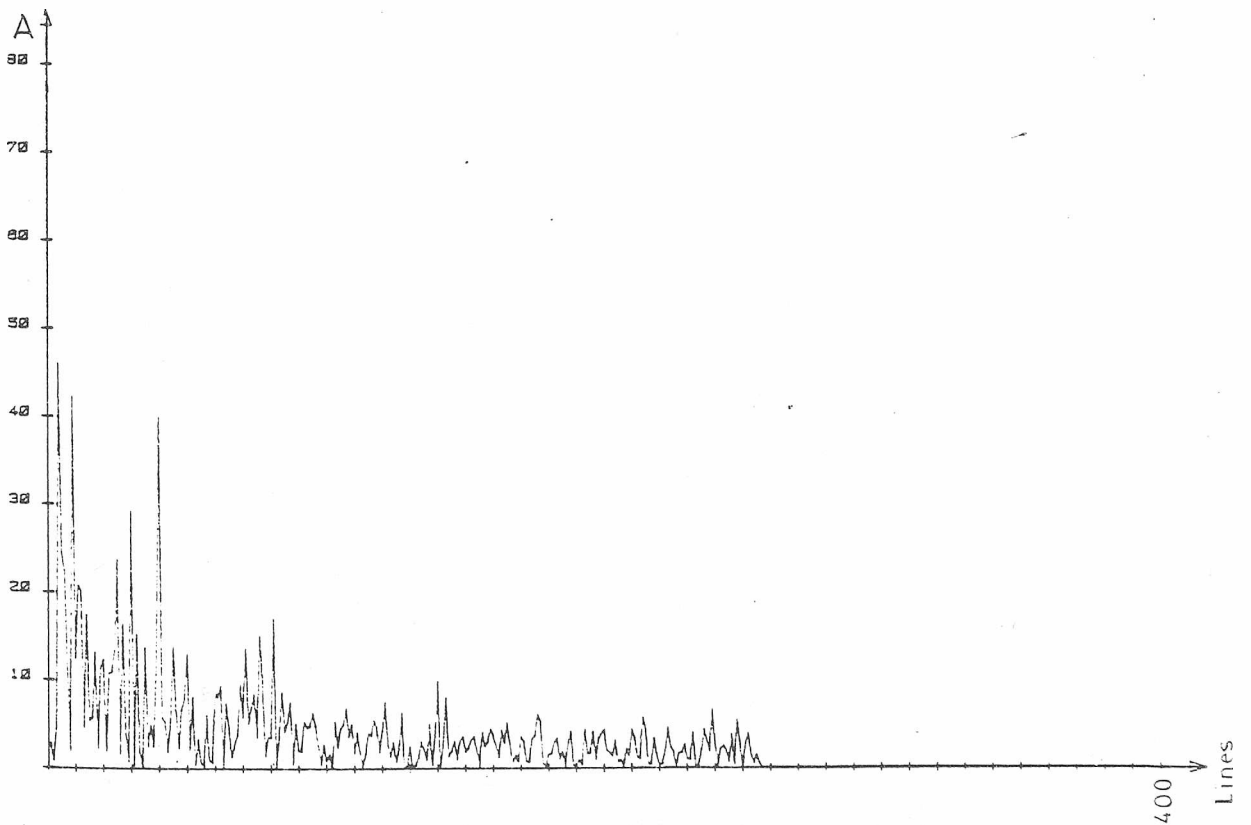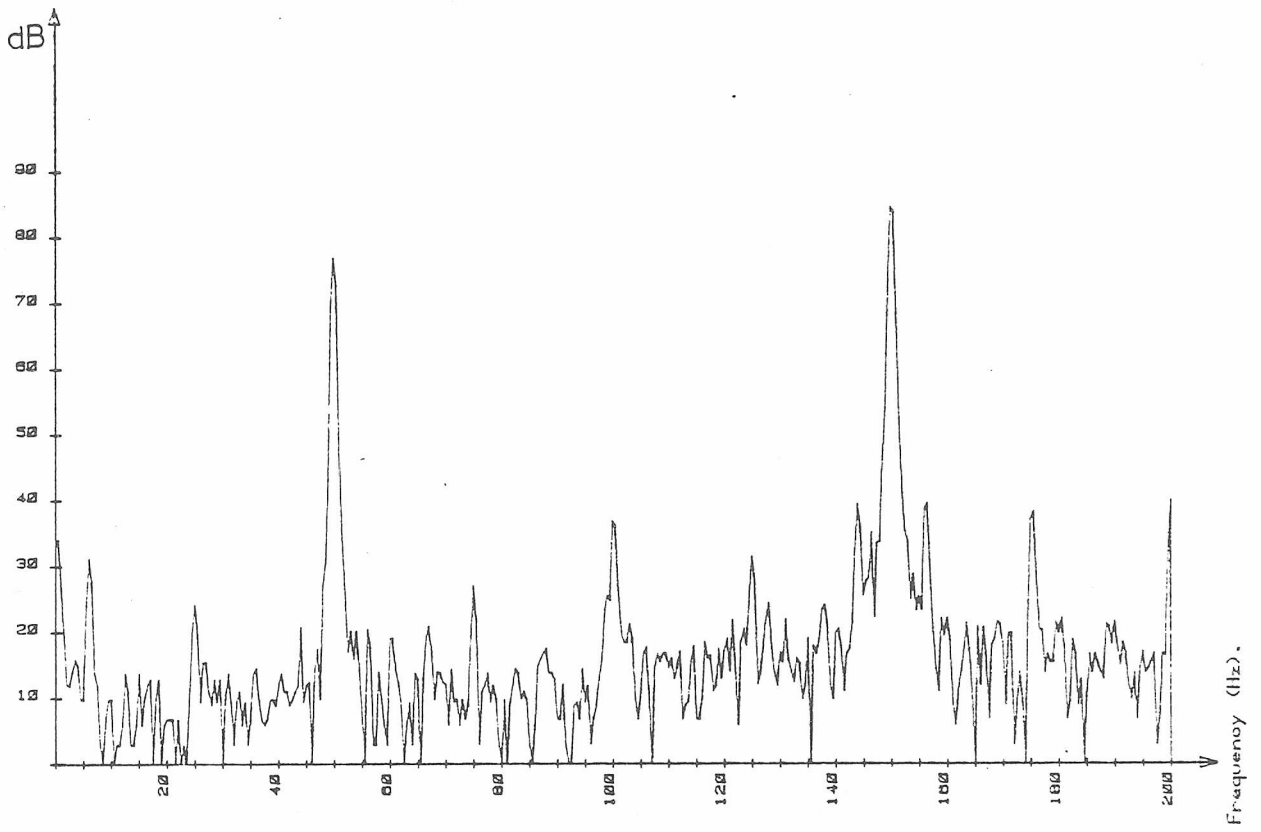
Figure 5·10 Stray flux, No load

51 slot rotor, condition: GOOD
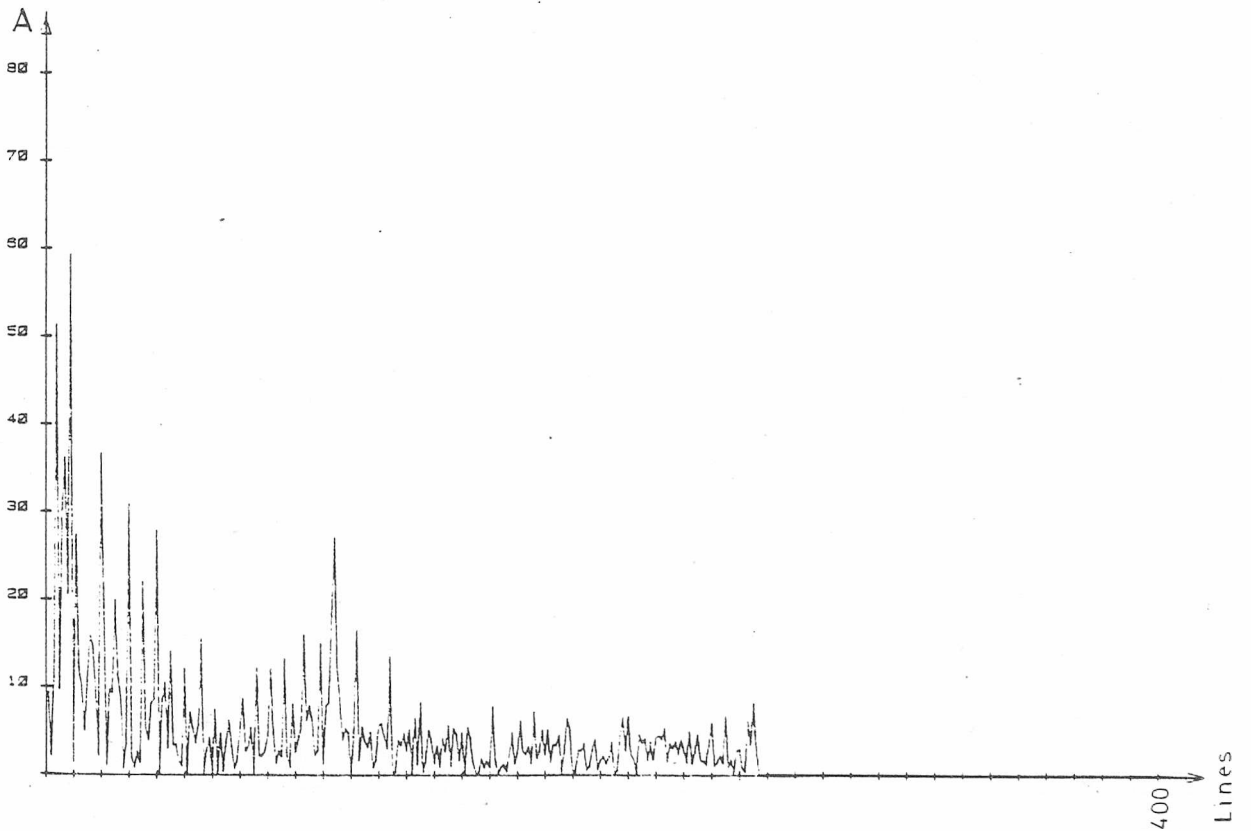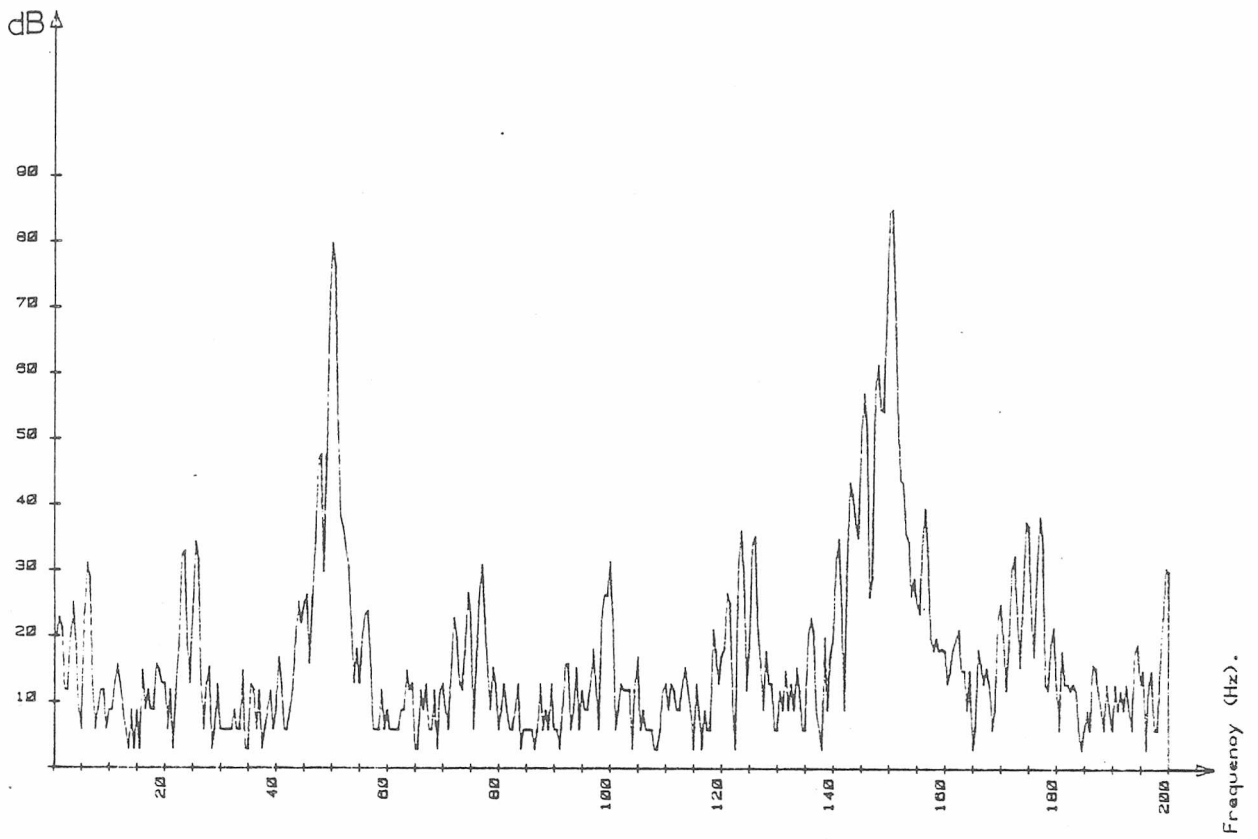
Figure 5.11 Stray flux, Full load

51 slot rotor, condition: 1 BAR BROKEN
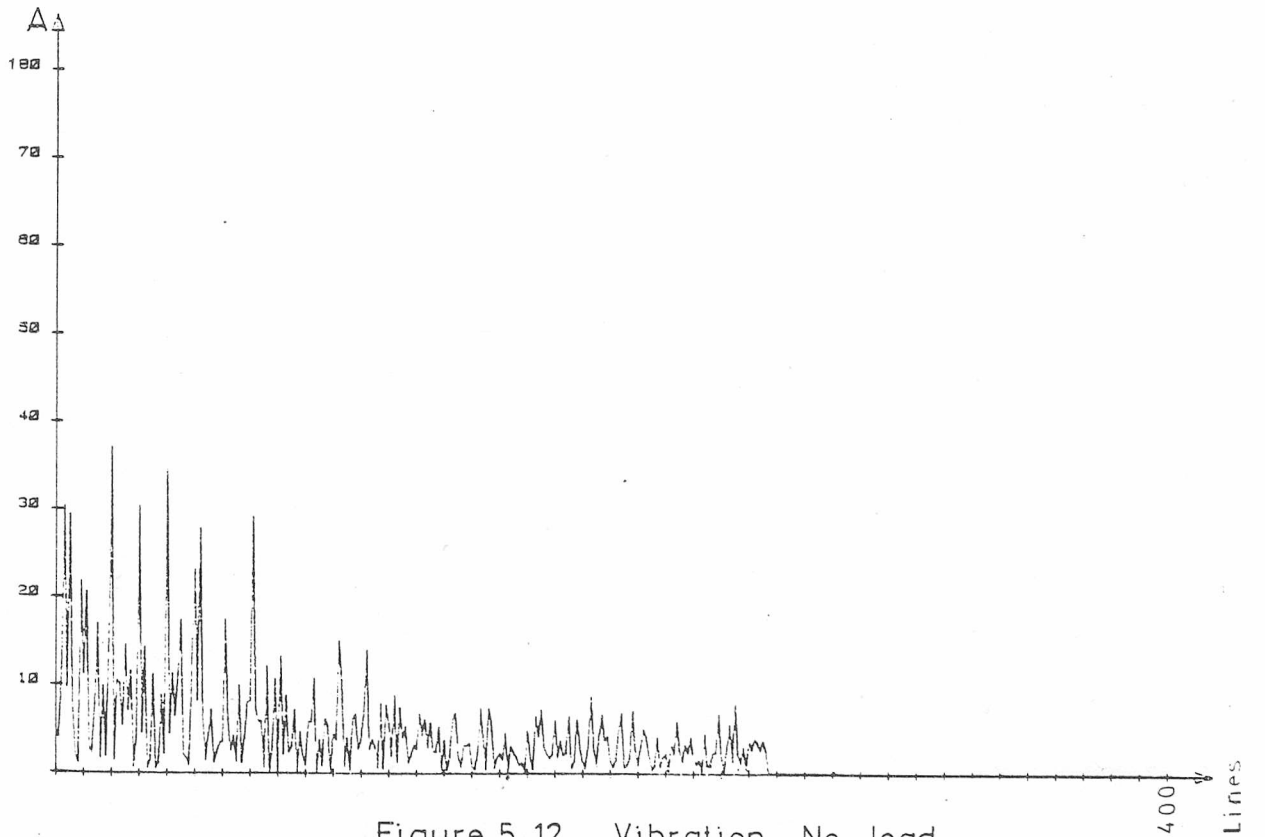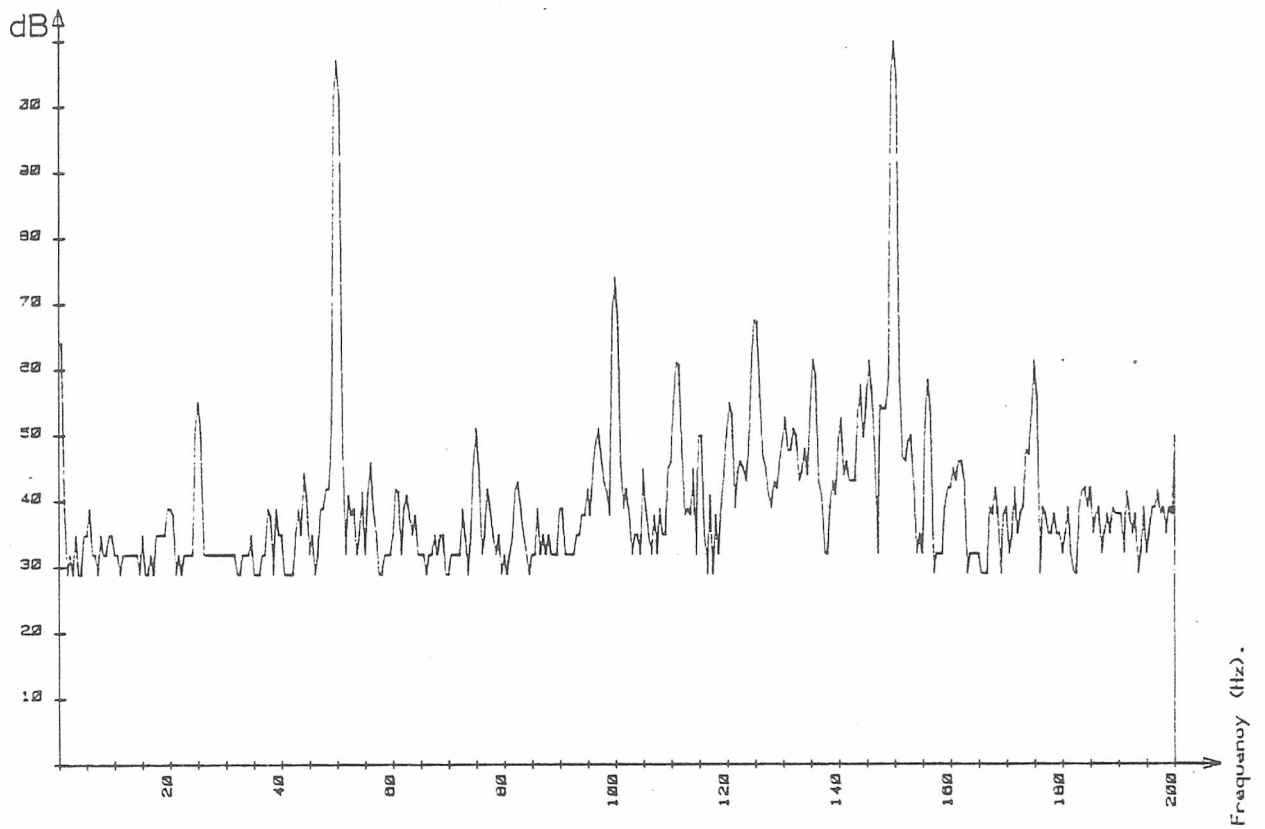
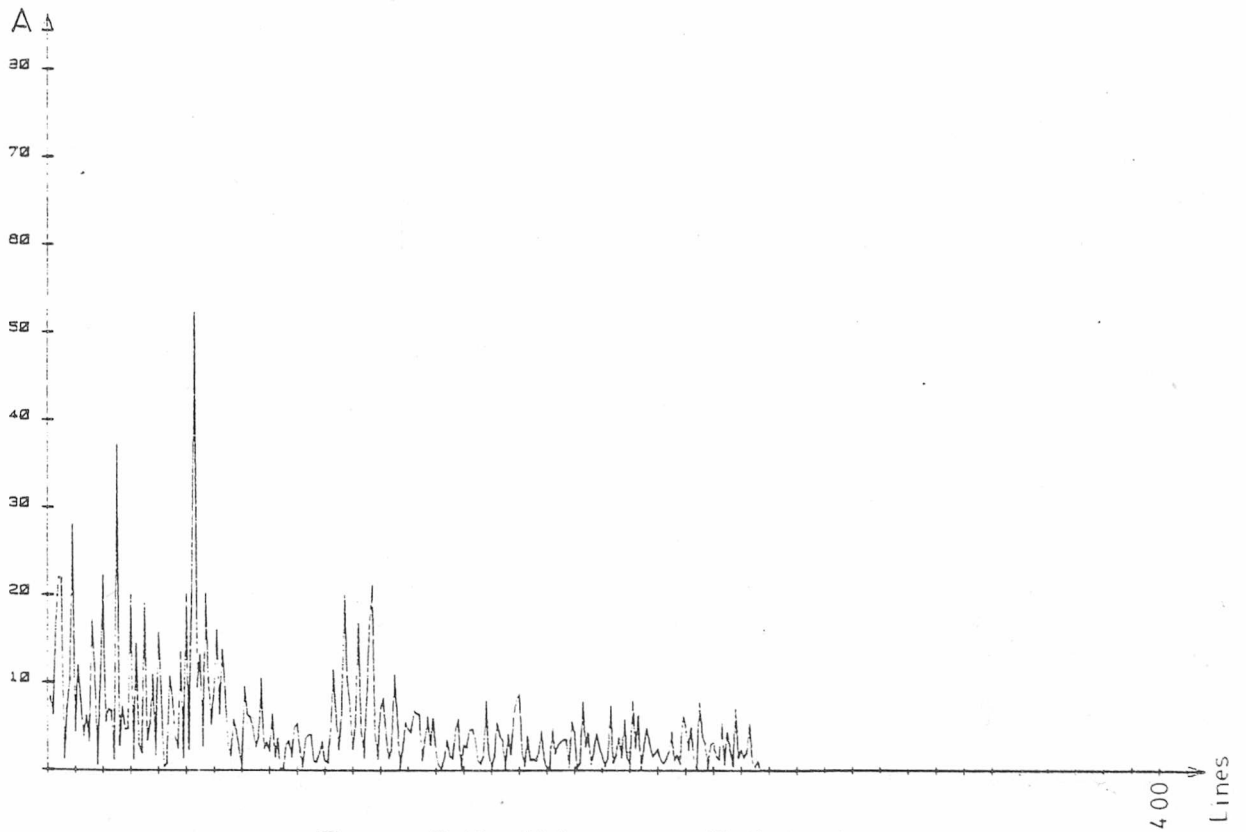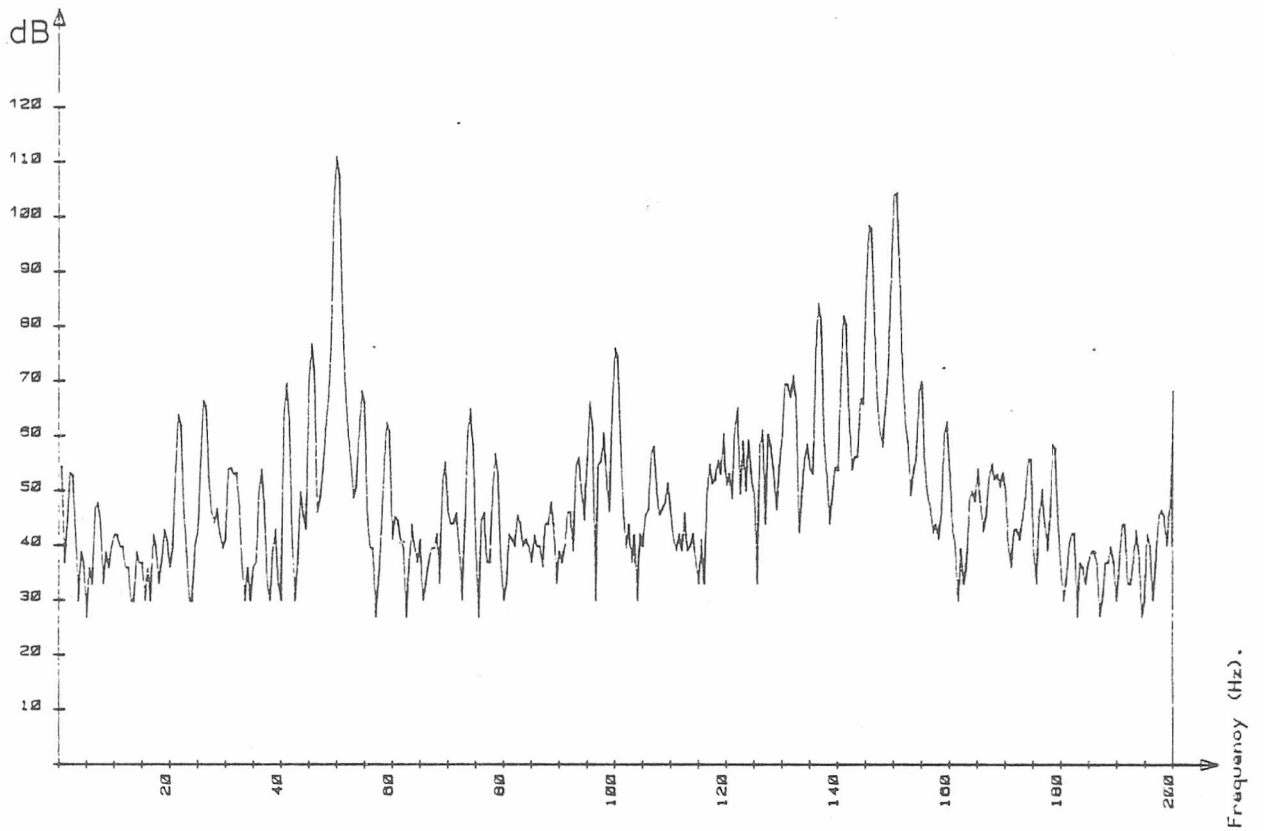Figure 5.12   Vibration, No load

51 slot rotor, condition: 1 BAR BROKEN

dB

120
110
100
90
80
70
60
50
40
30
20
10

20 40 60 80 100 120 140 160 180 200

Frequency (Hz).

A

90
70
80
50
40
30
20
10

400 Lines
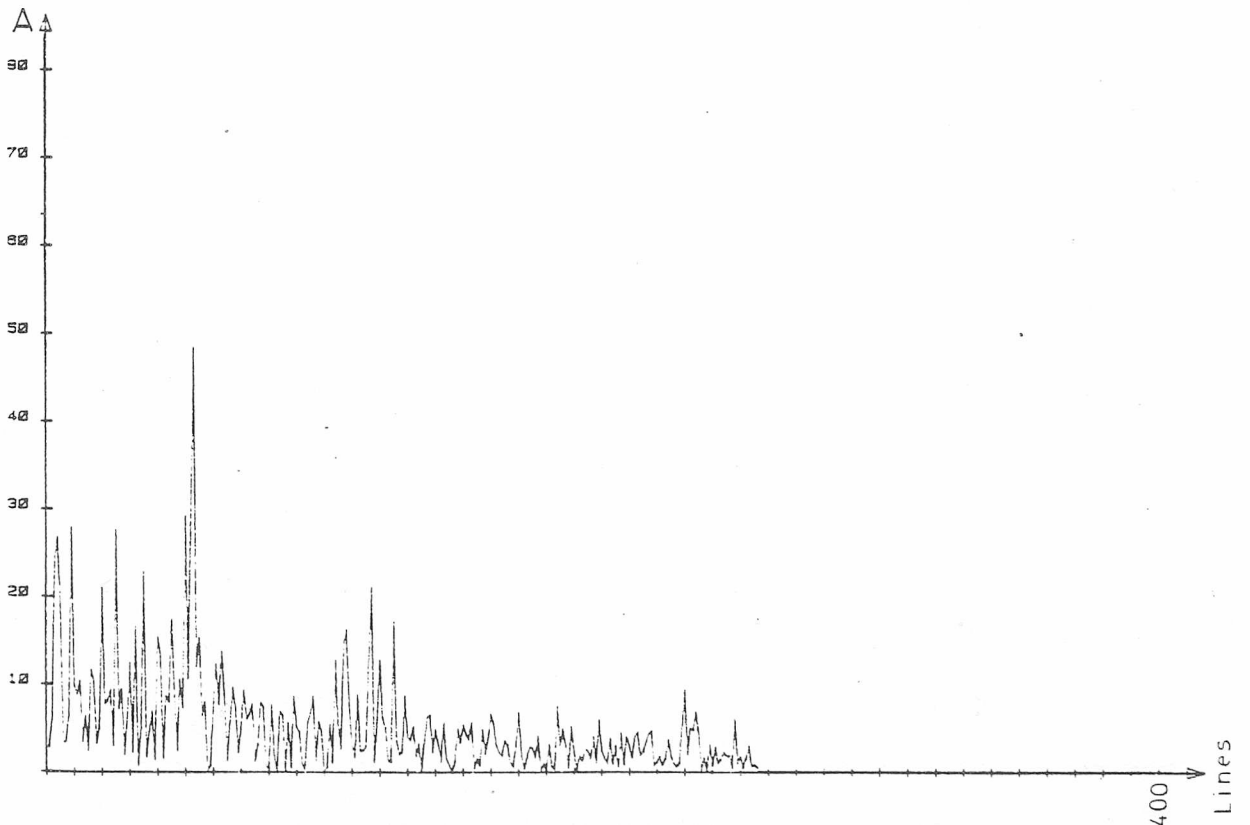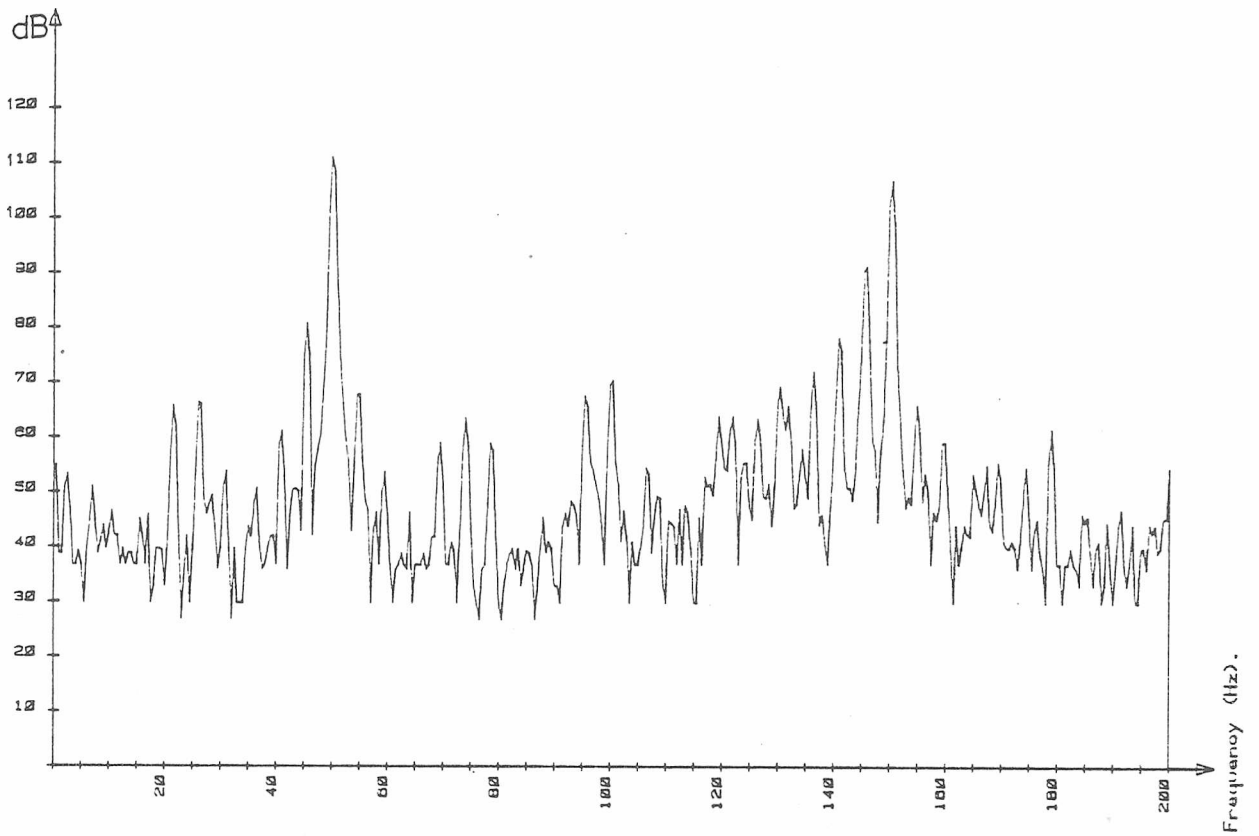
Figure 5·13 Vibration, Full load

51 slot rotor, condition: 1 BAR BROKEN
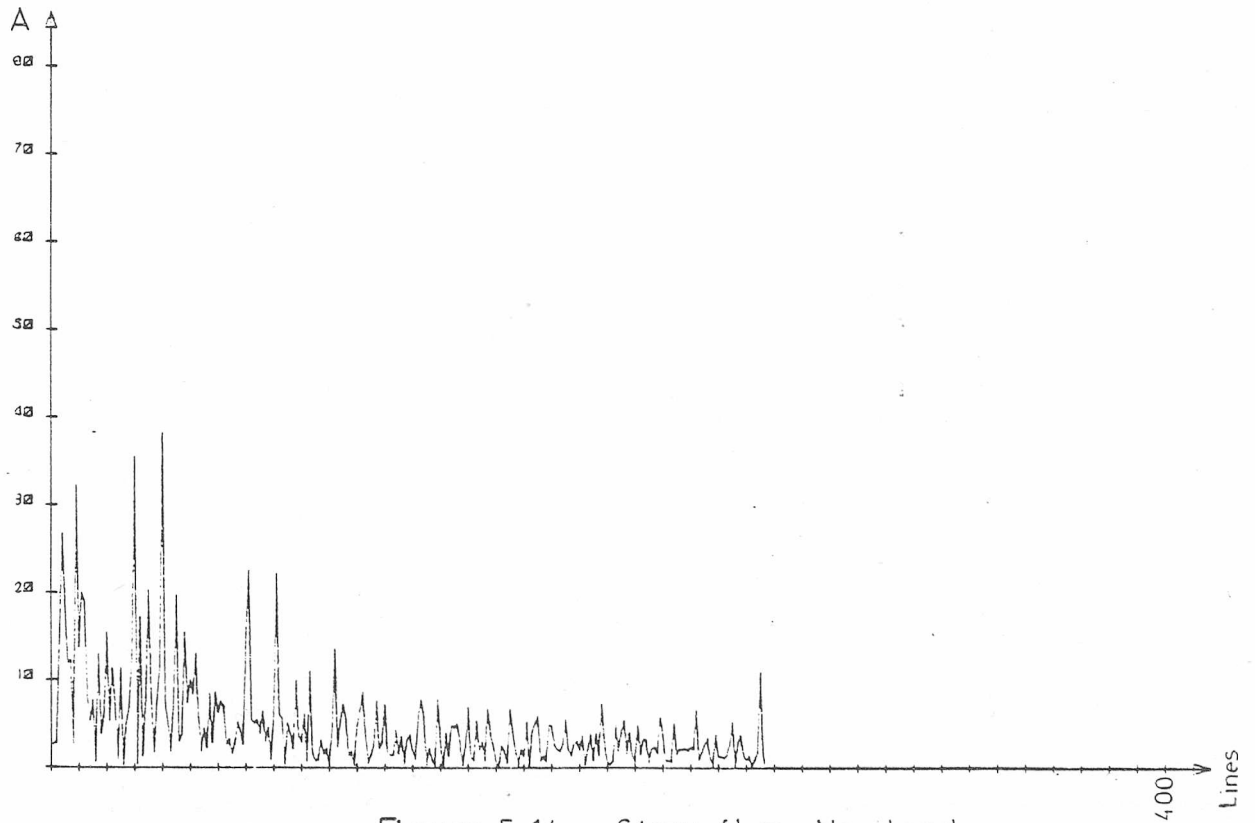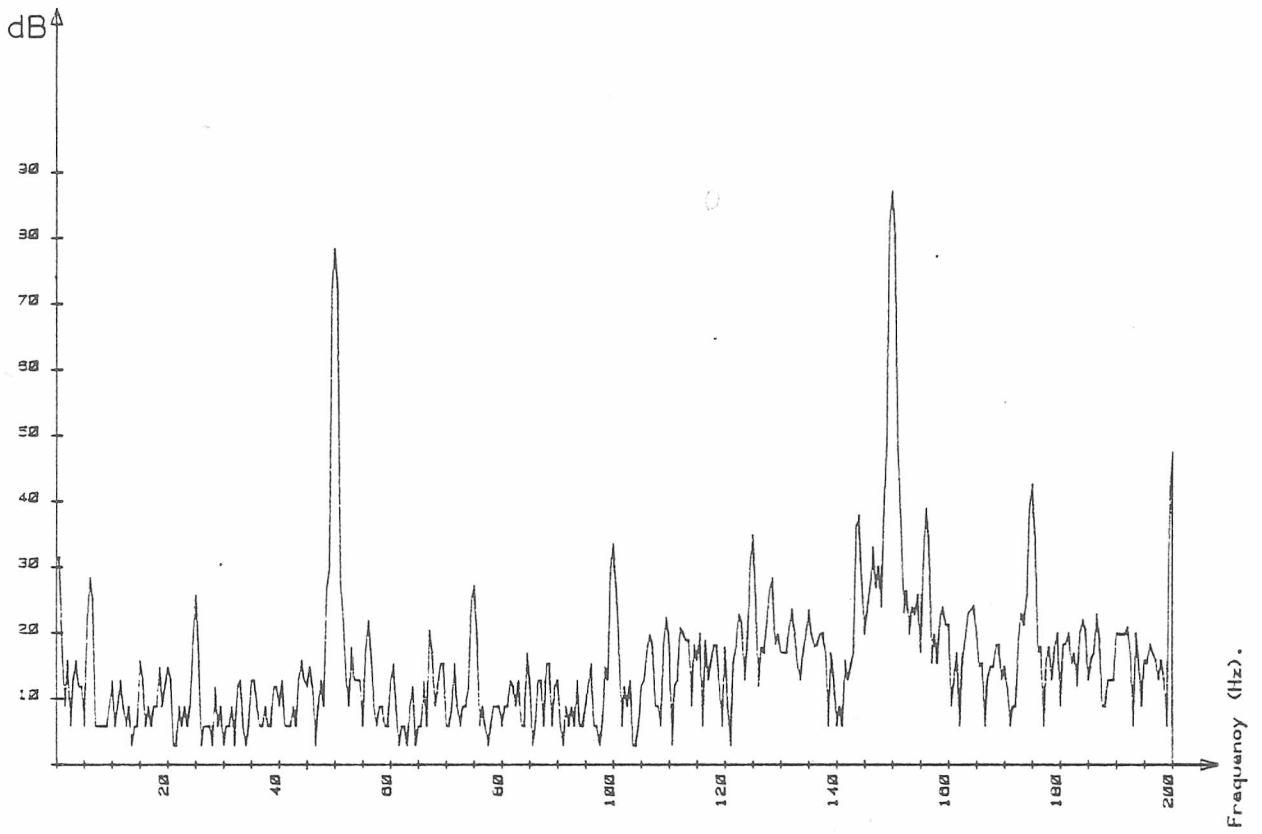
Figure 5.14   Stray flux, No load

51 slot rotor, condition: 1 BAR BROKEN
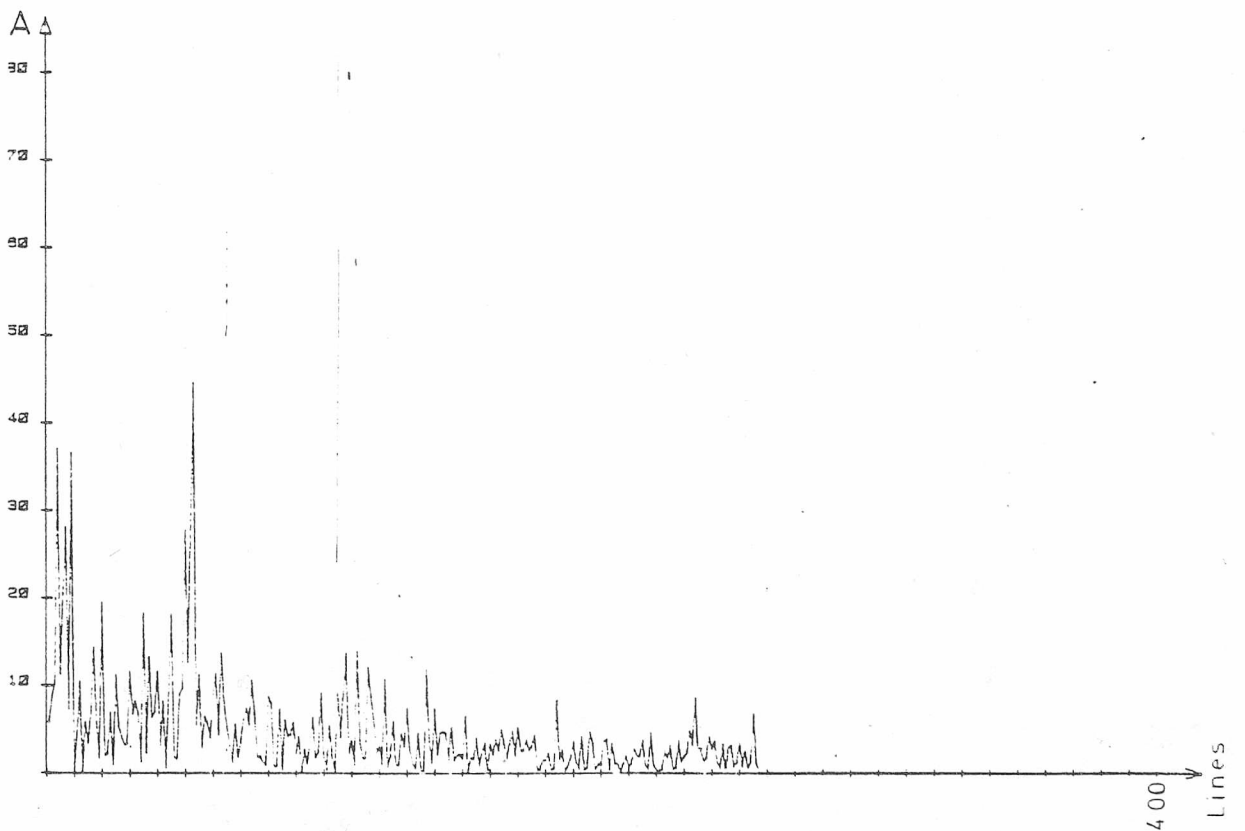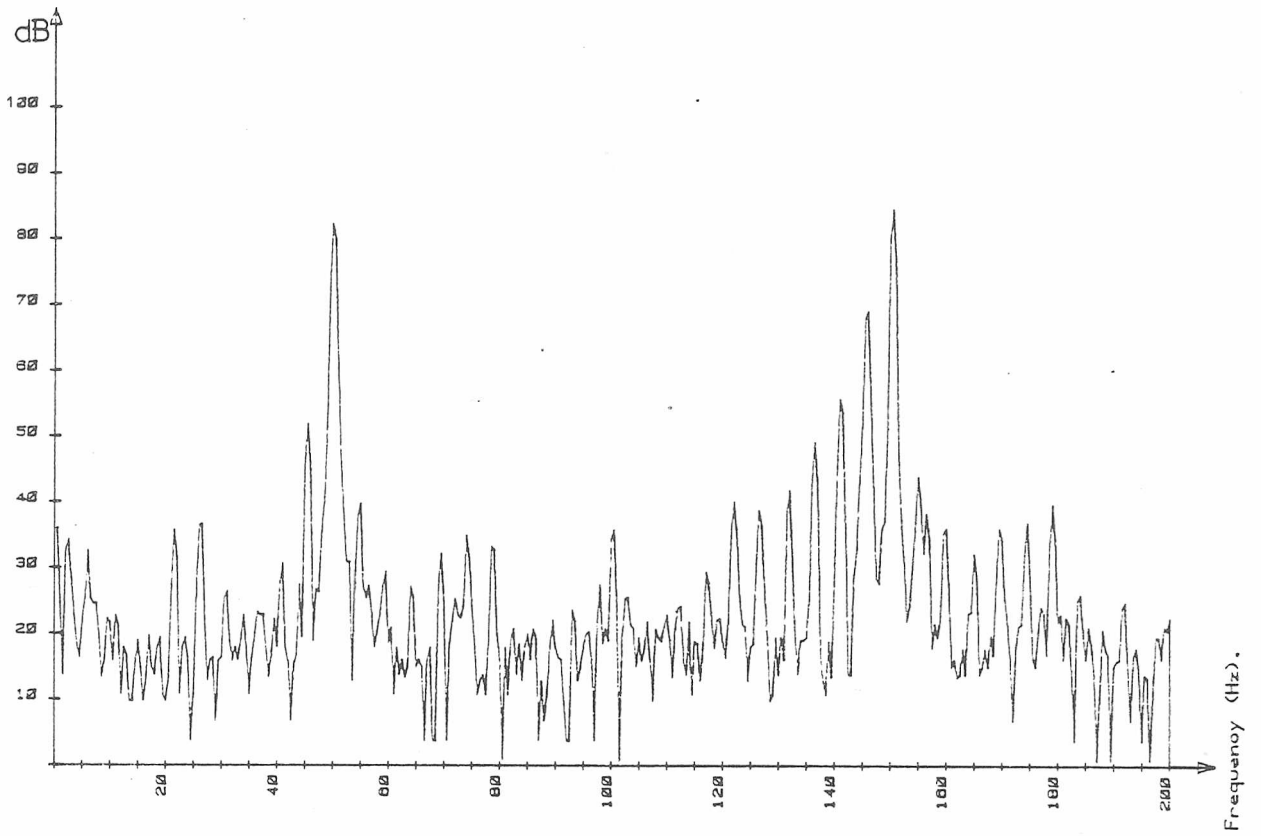
Figure 5.15   Stray flux, Full load

51 slot rotor, condition: 5 BARS BROKEN

Figure 5.16 Vibration, Full load
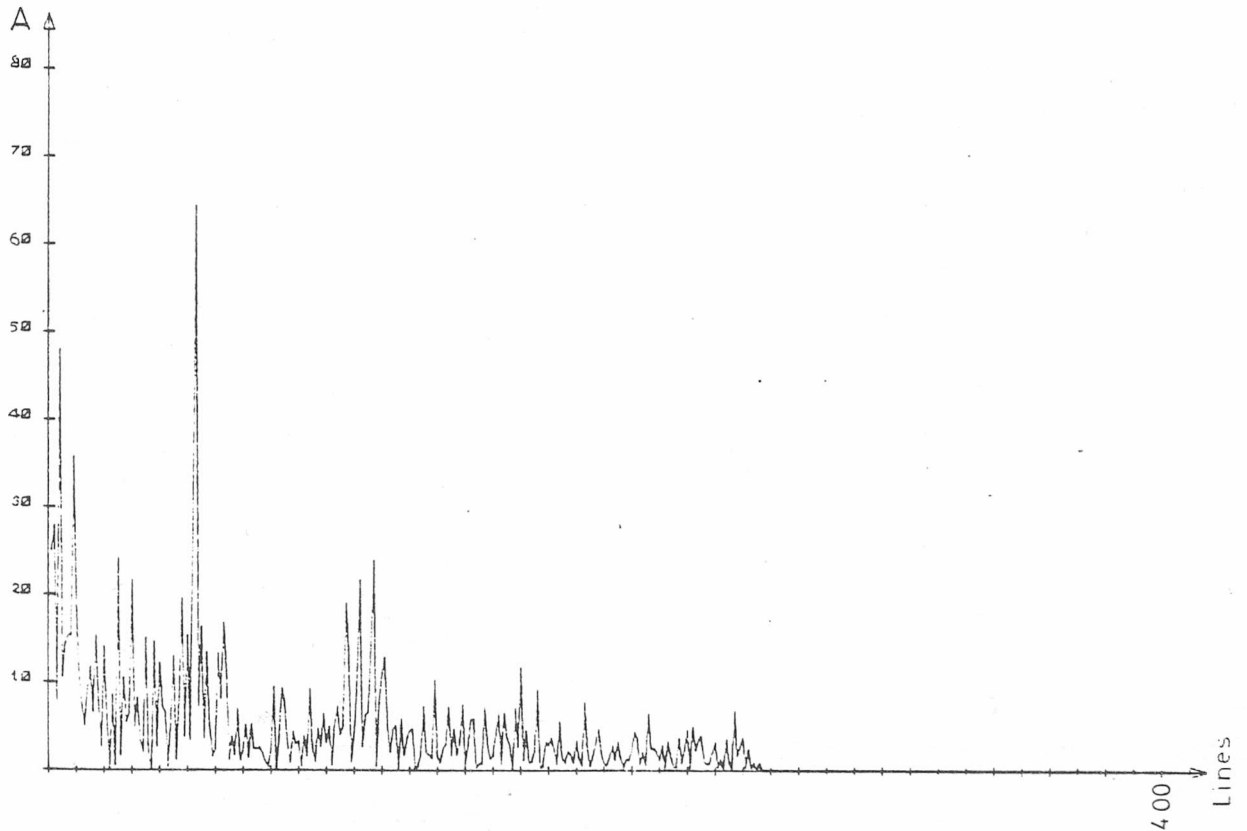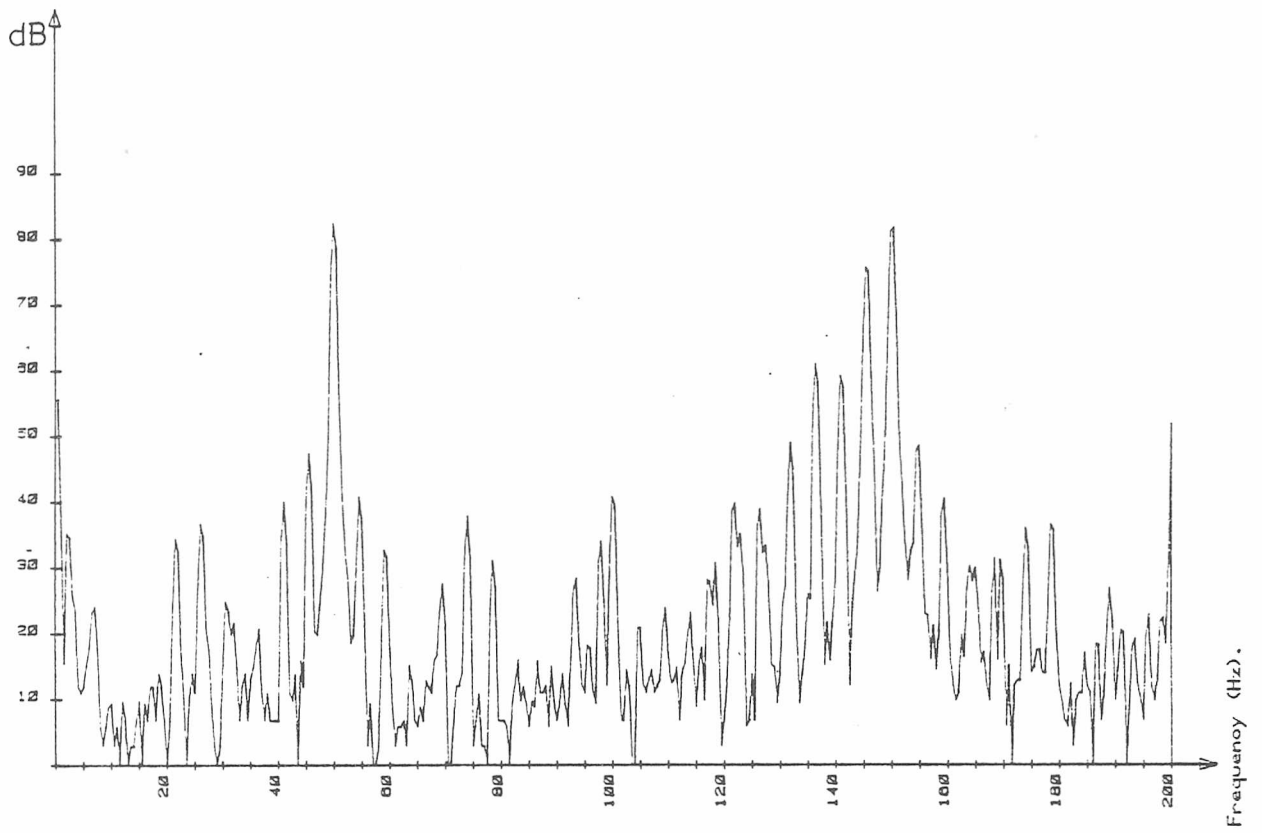
51 slot rotor, condition: 5 BARS BROKEN

Figure 5·17 Stray flux, Full load
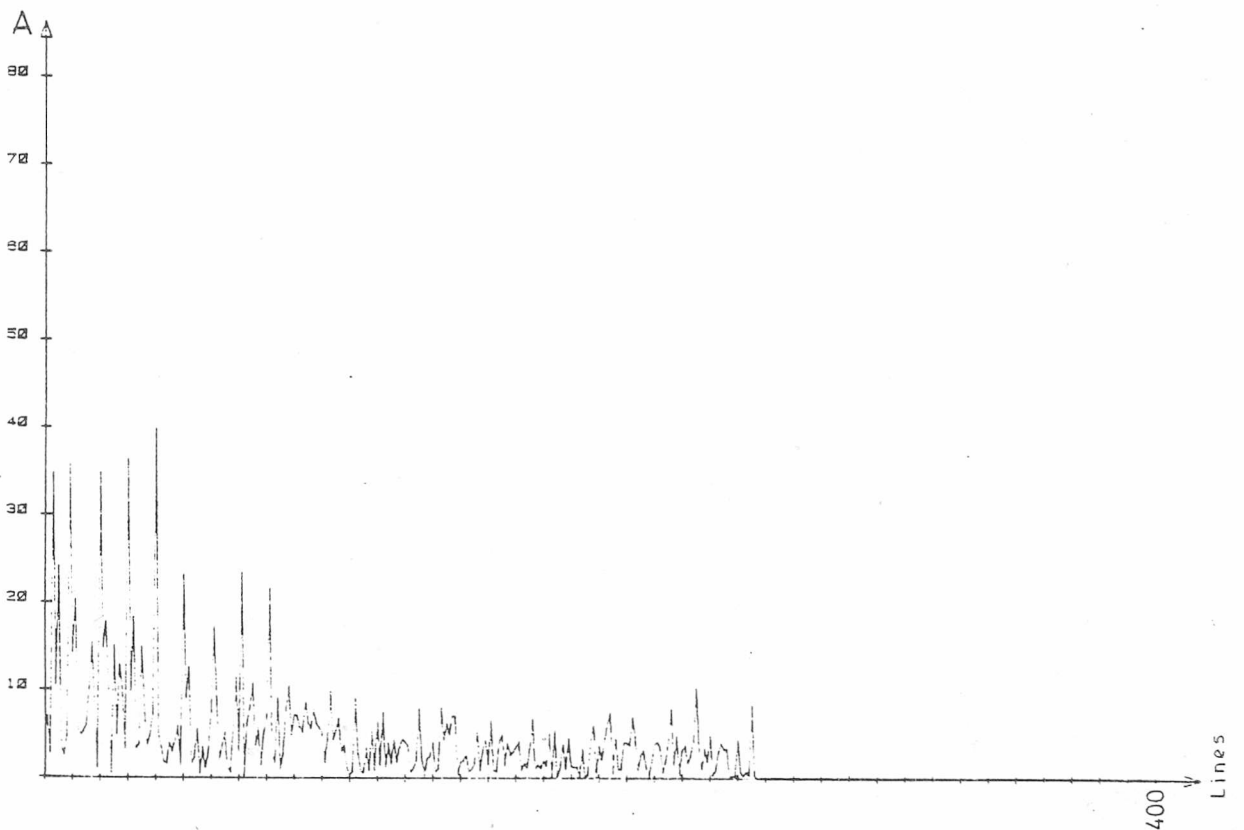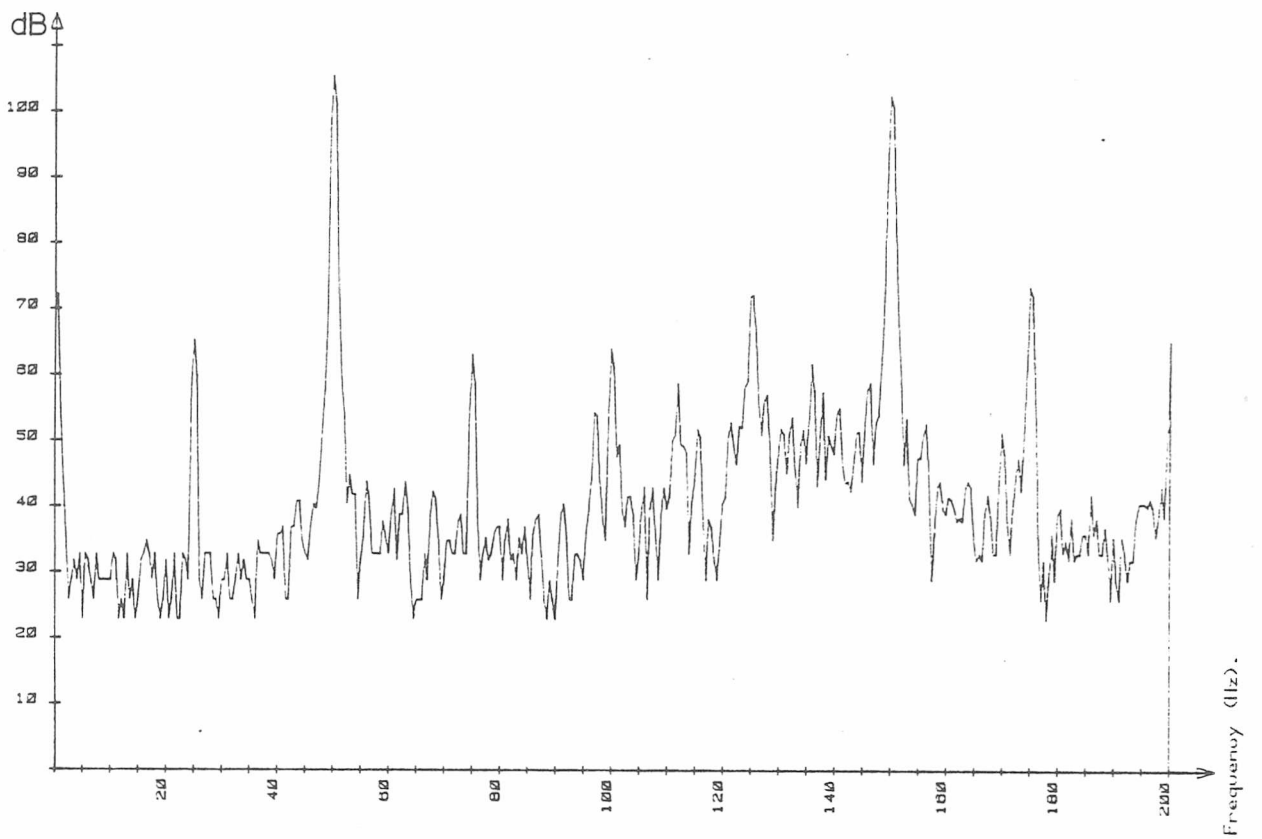
28 slot Rotor, good condition

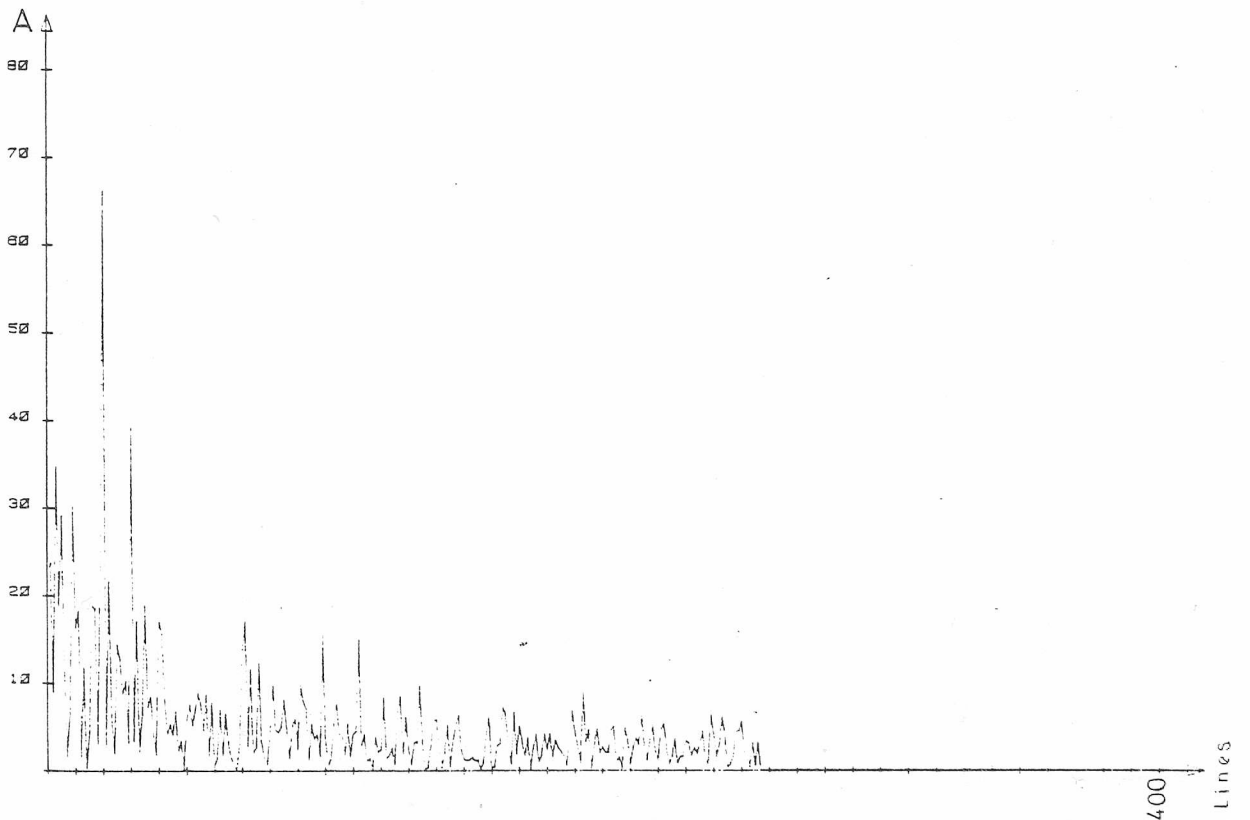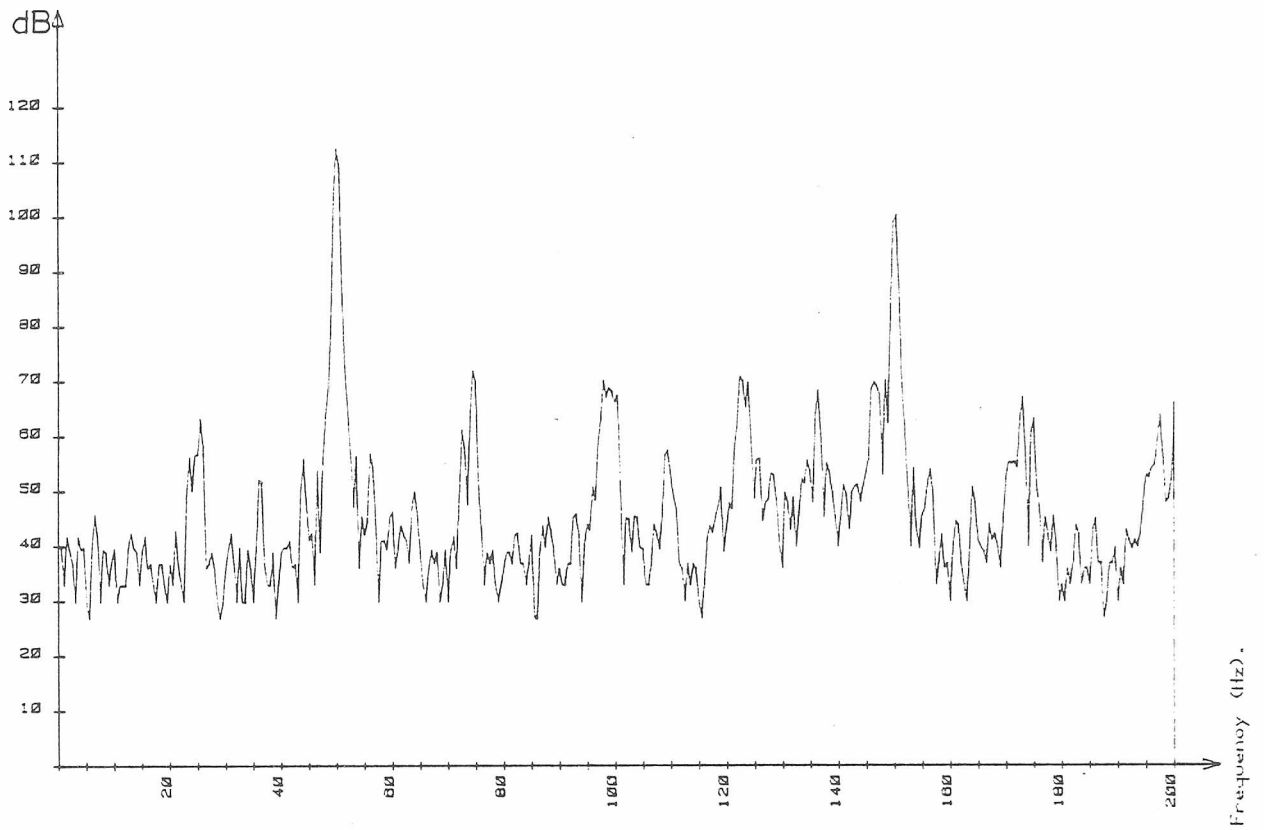Figure 5.18   Vibration,   No load

28 slot Rotor, good condition

Figure 5·19   Vibration, Full load

28 slot Rotor, good condition
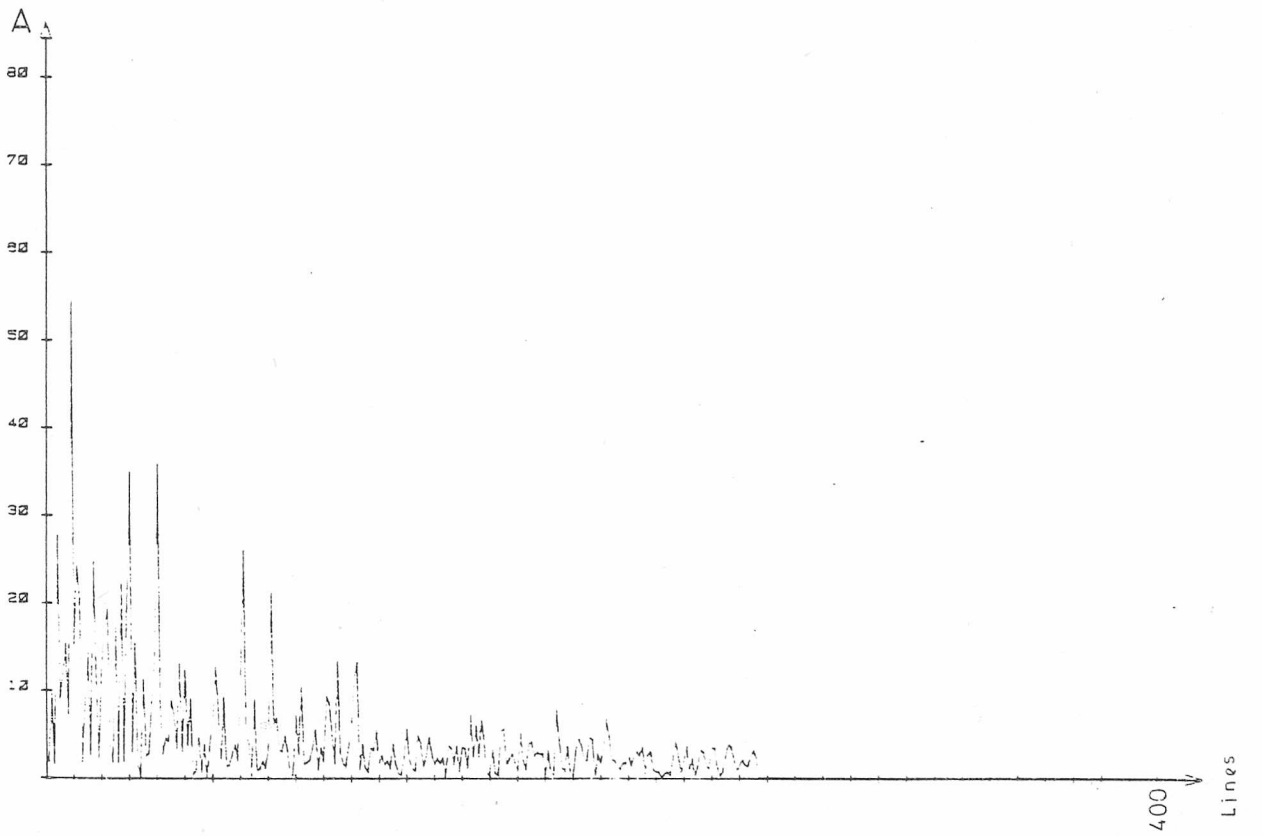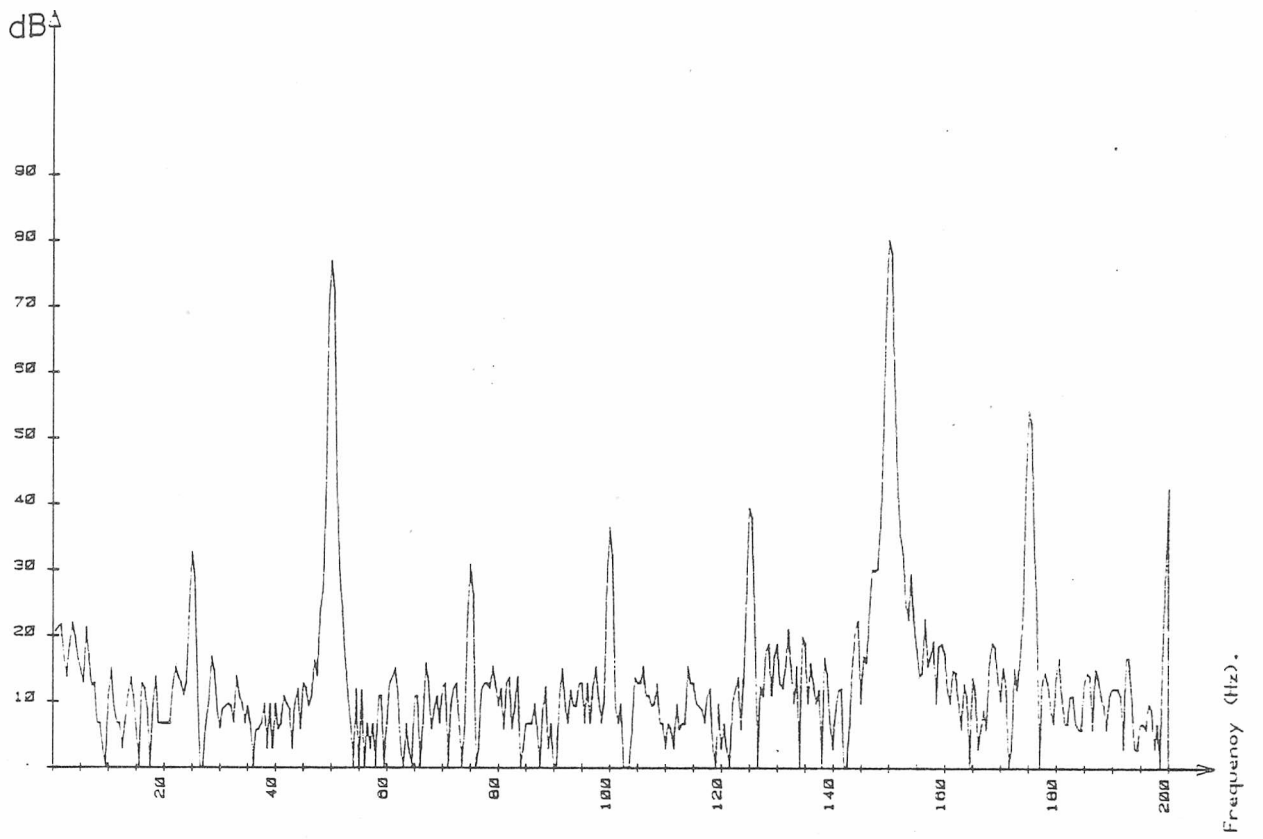

Figure 5·20   Stray flux, No load

28 slot Rotor, good condition
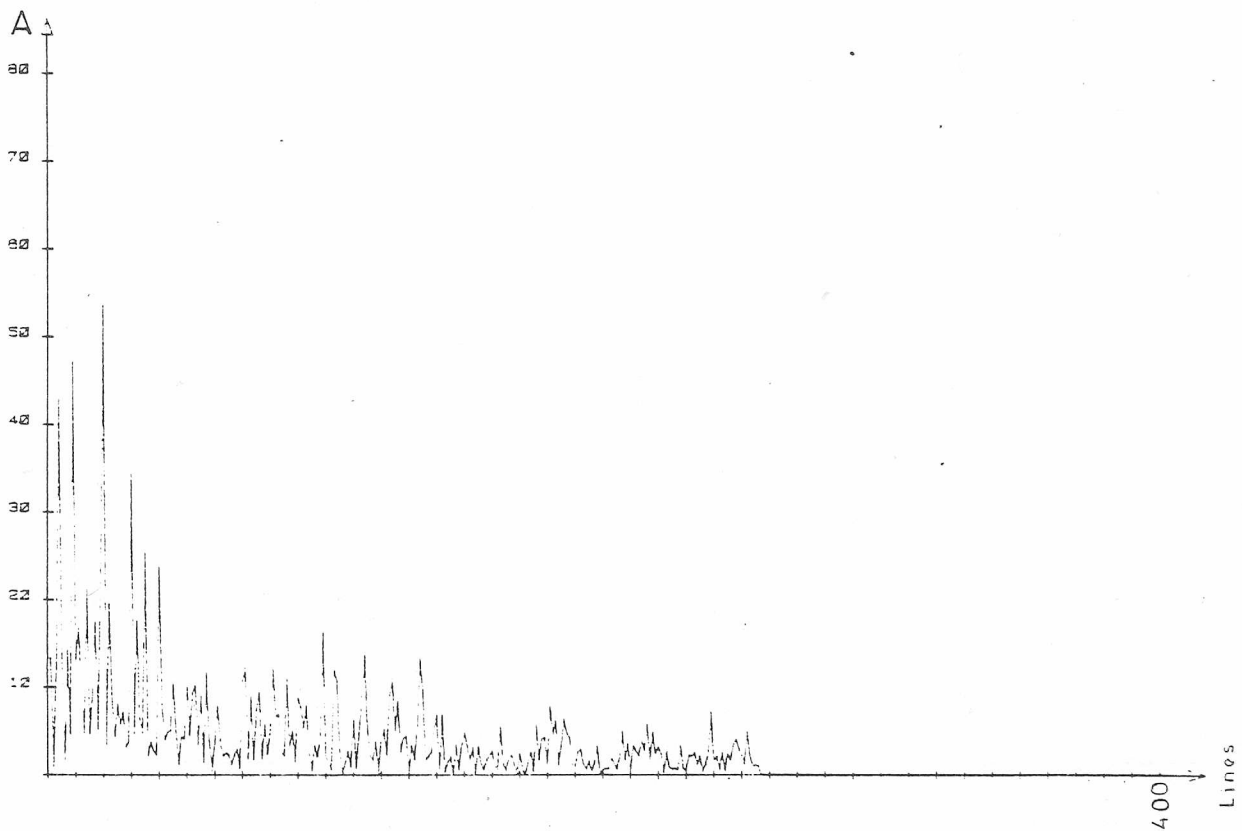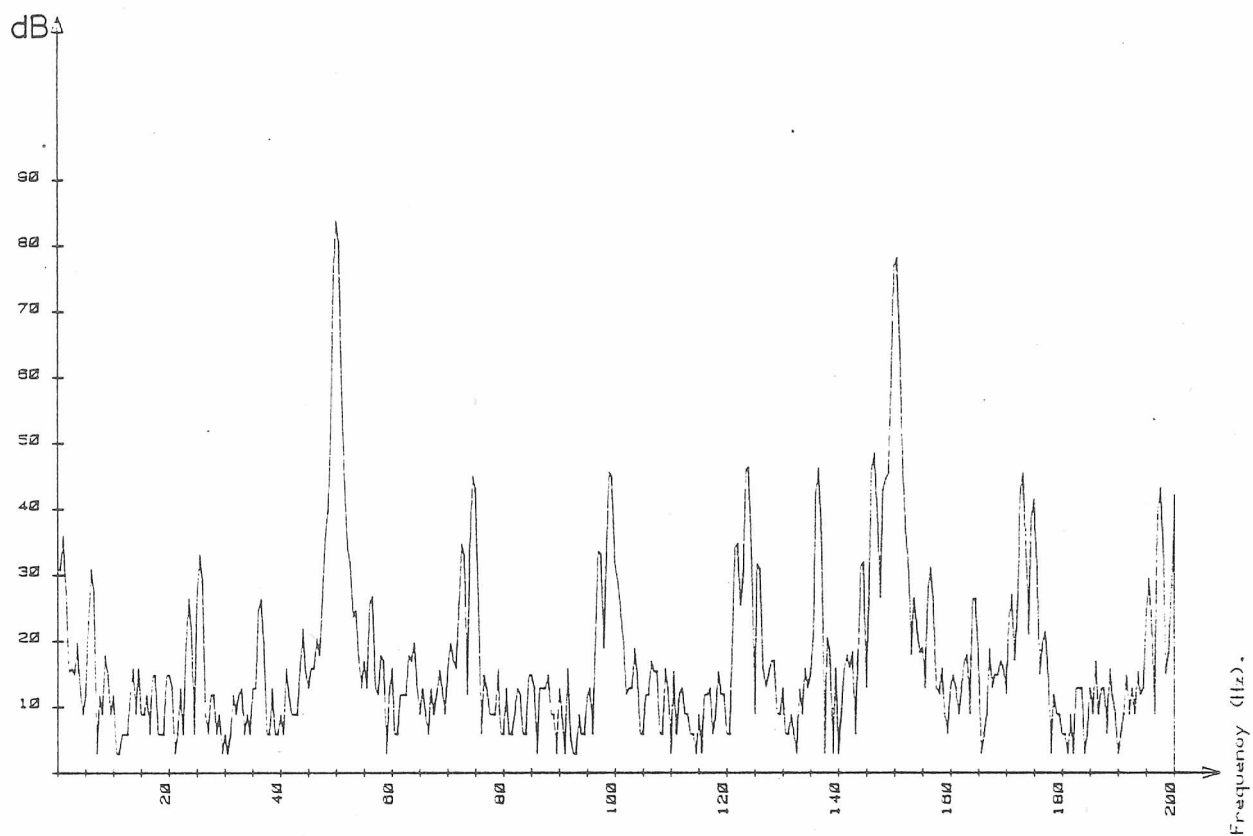
Figure 5·21   Stray flux, Full load

28 slot Rotor, broken end ring
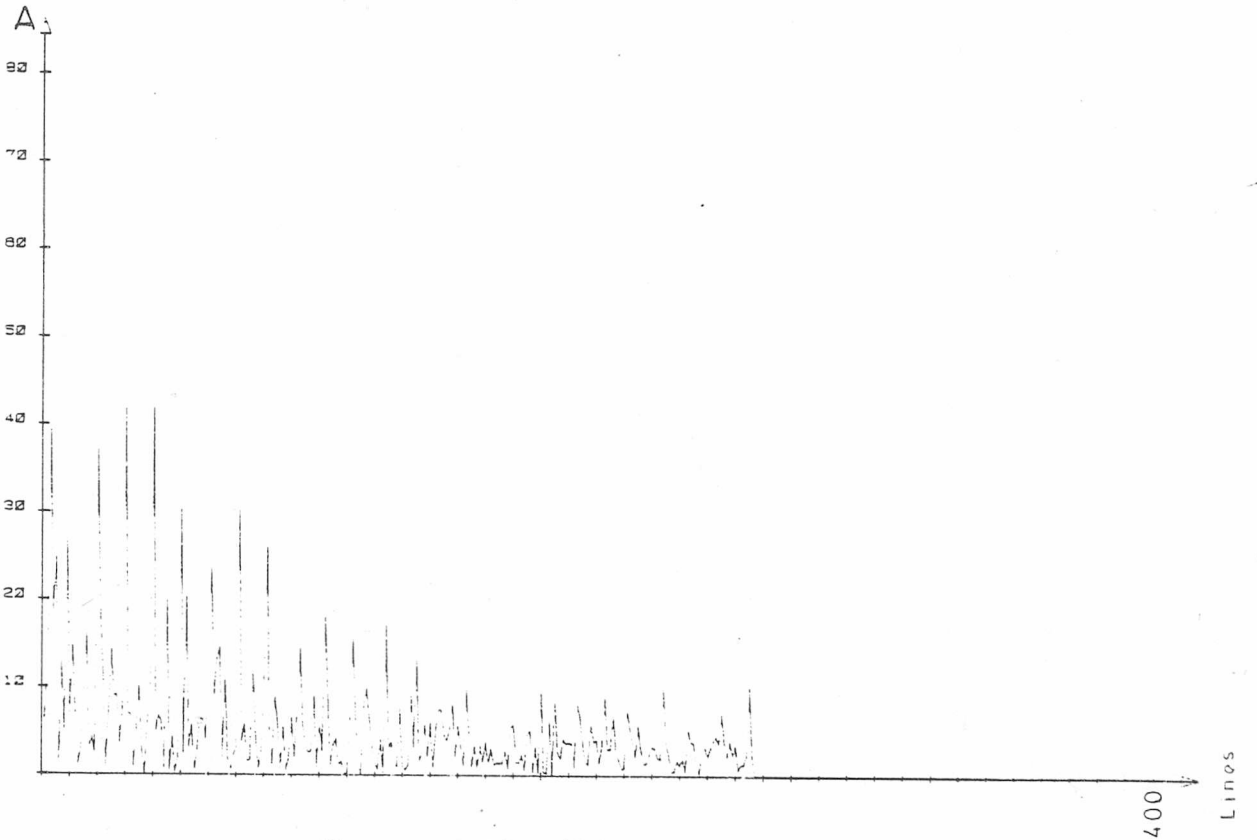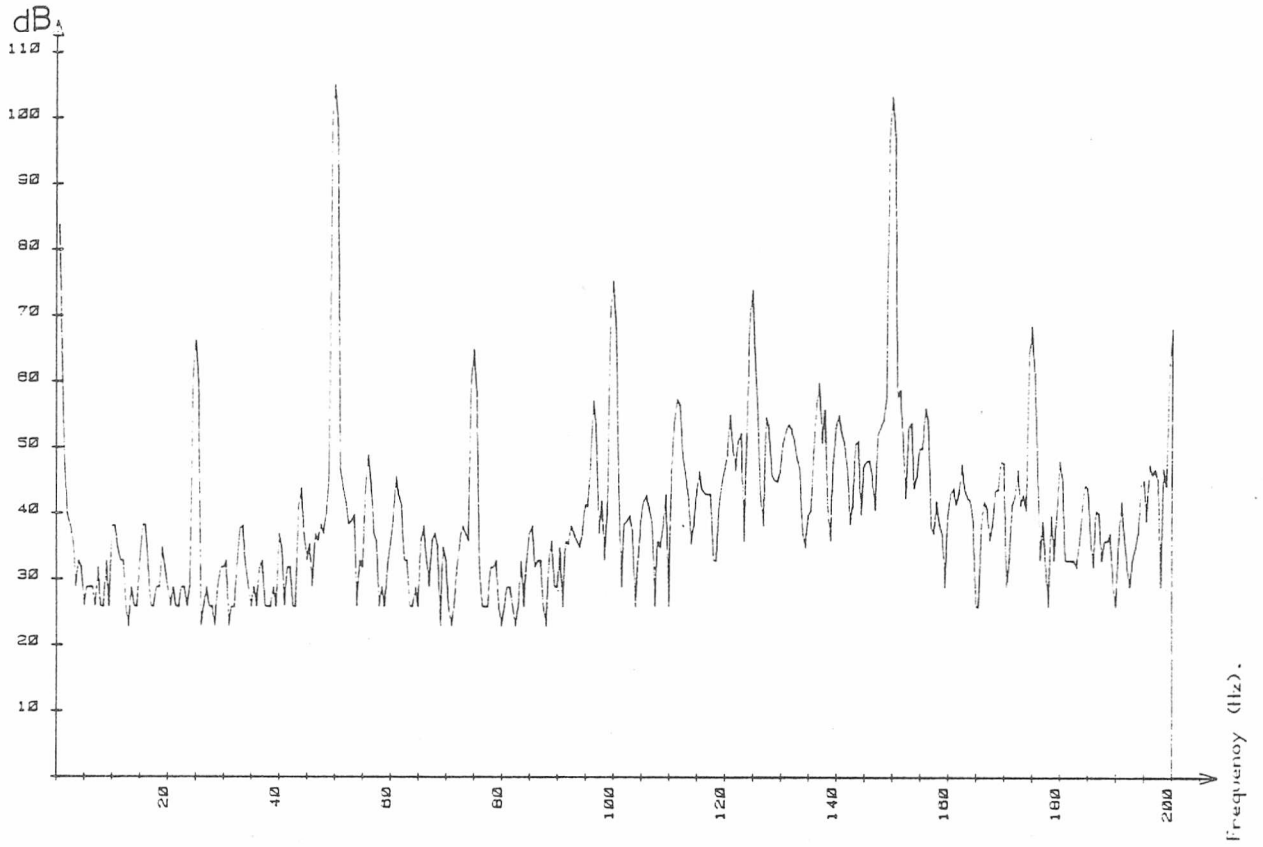
Figure 5.22   Vibration,   No load

28 slot Rotor, broken end ring
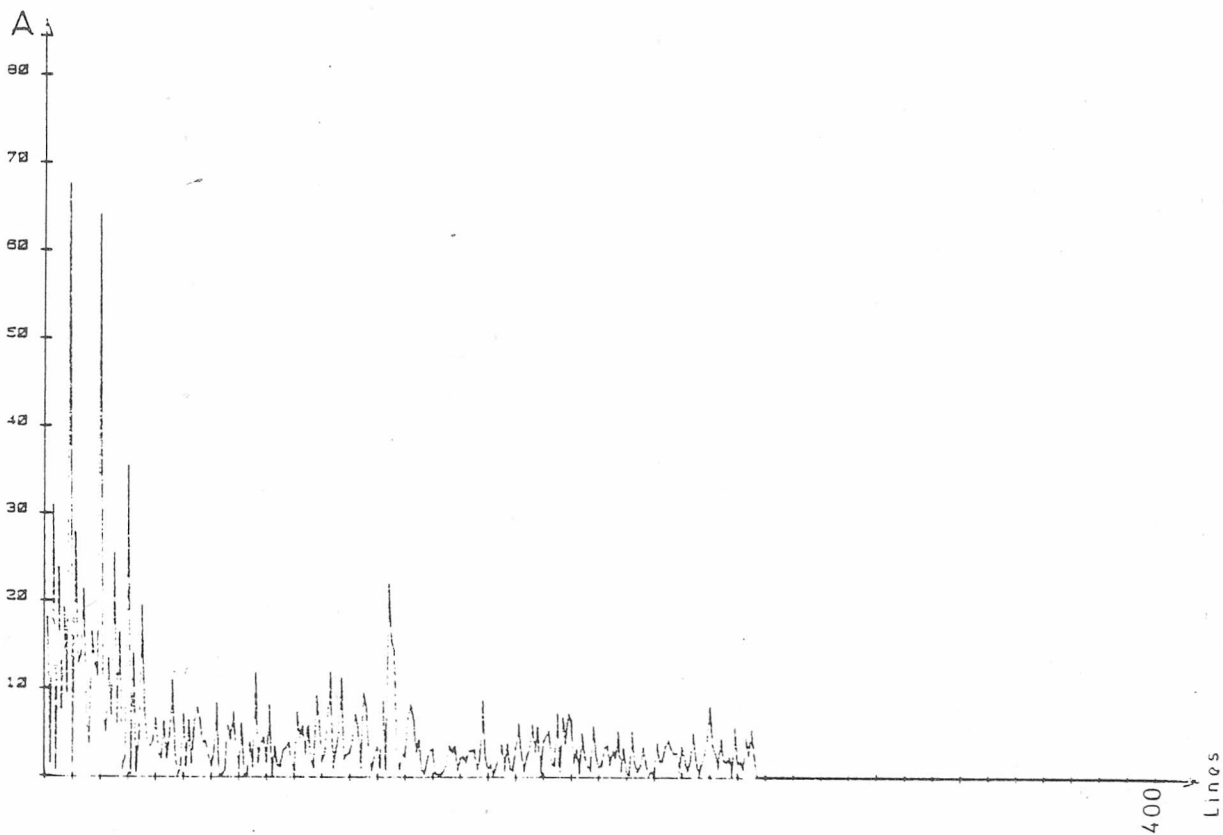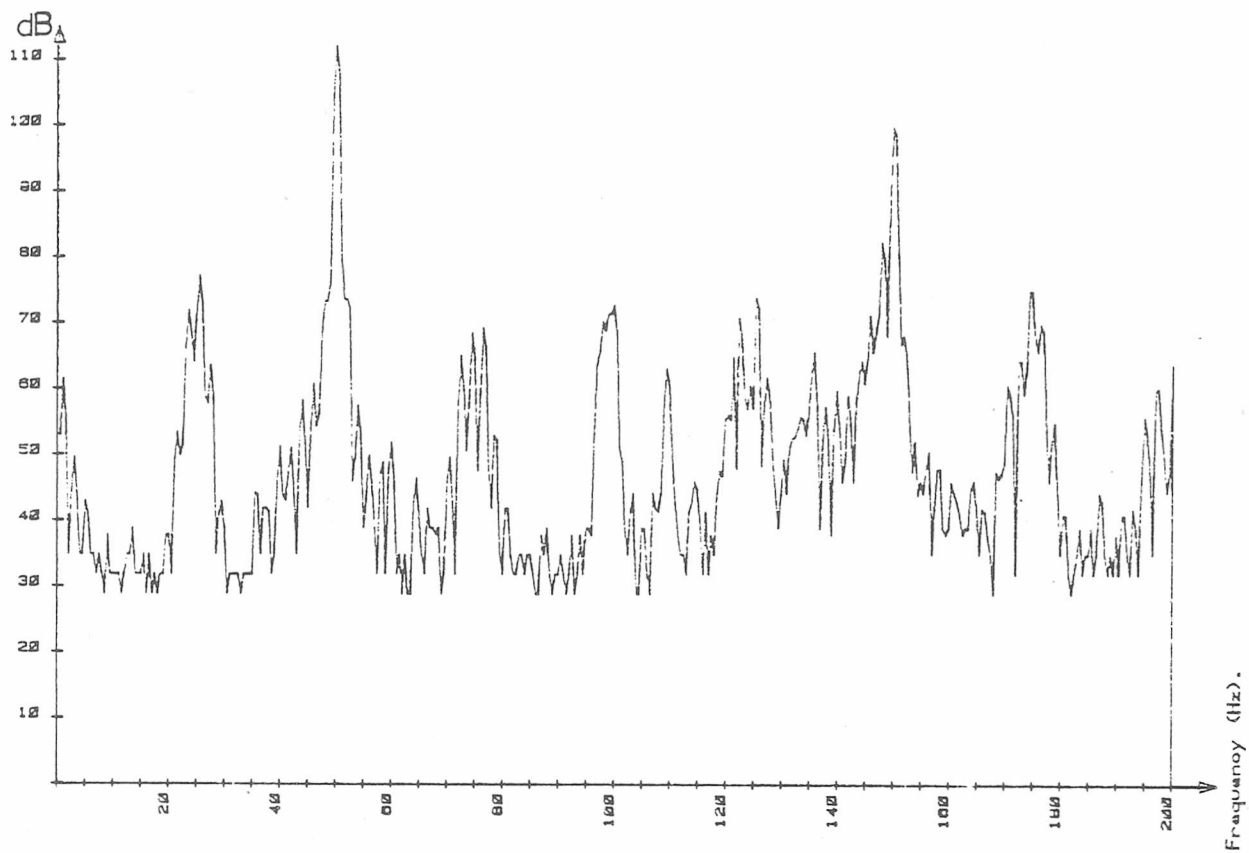
Figure 5.23 Vibration, Full load

28 slot Rotor, broken end ring
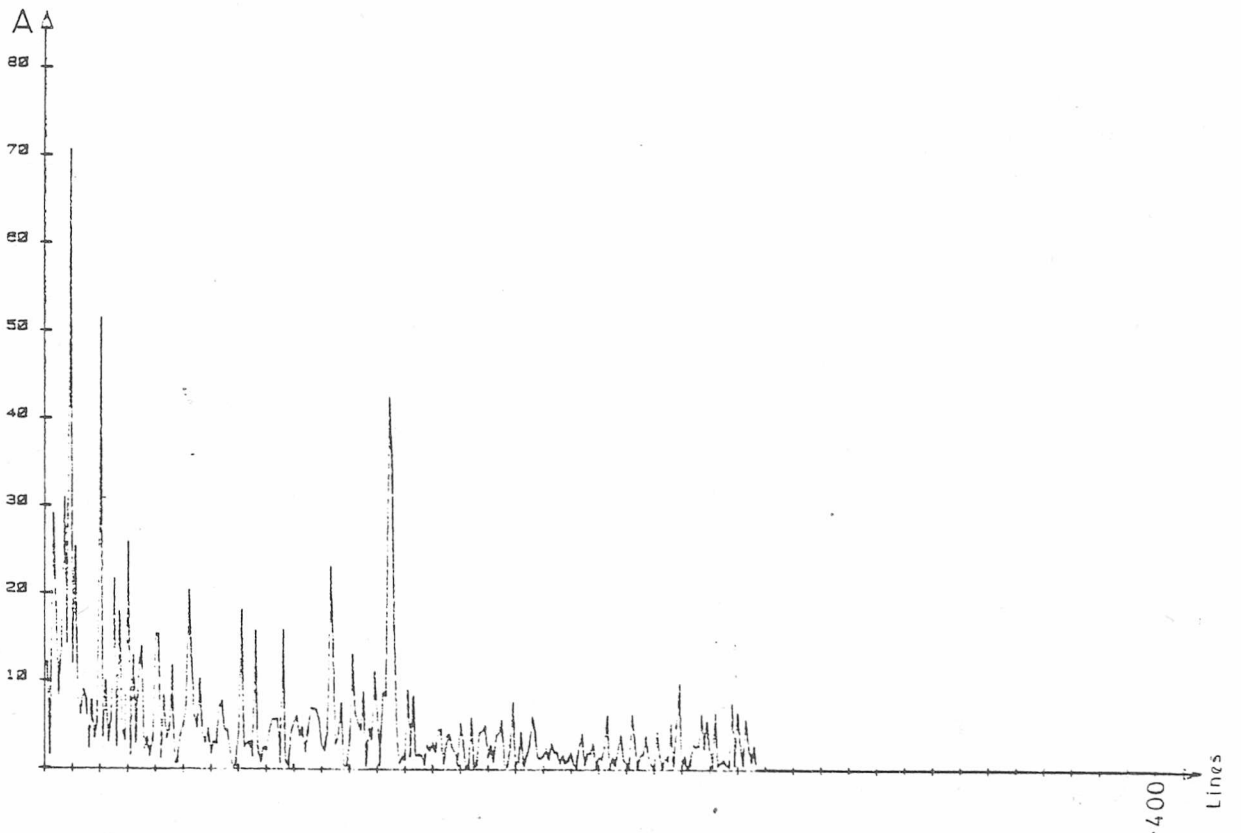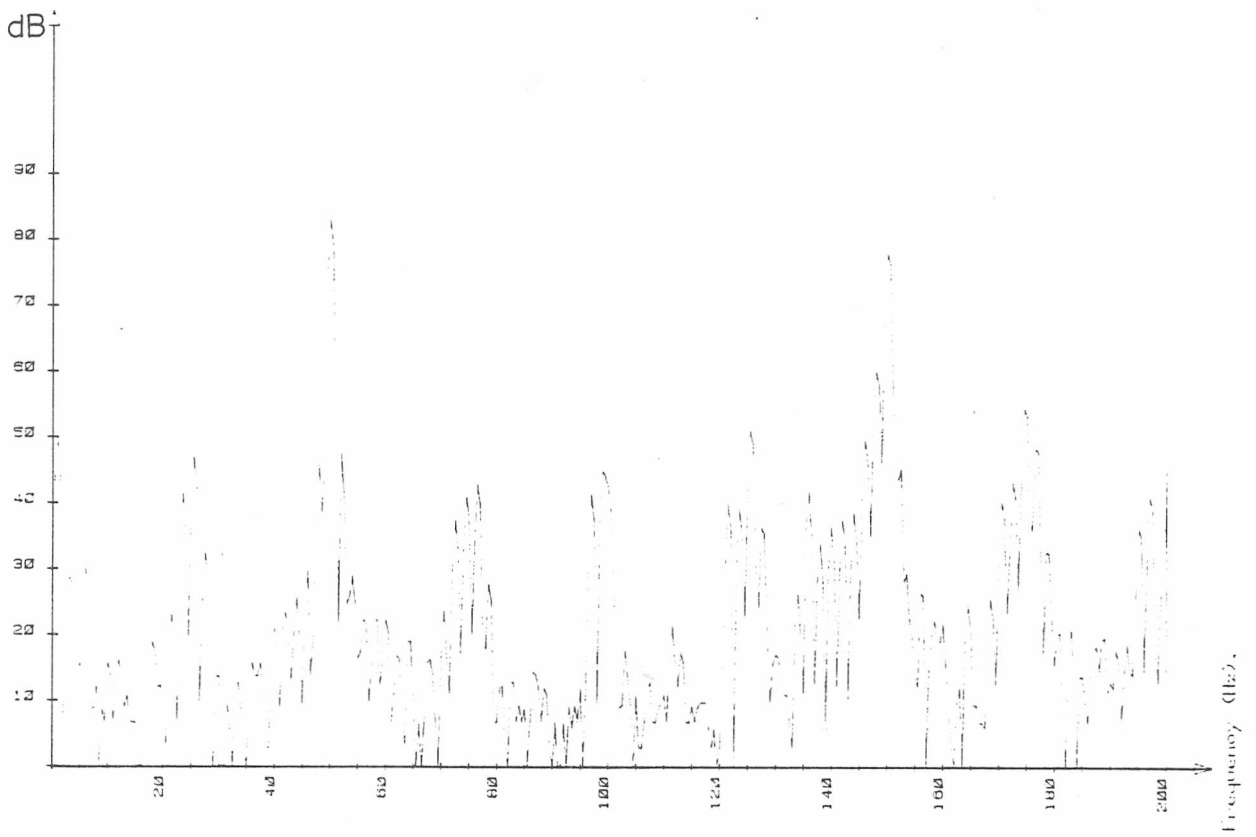
Figure 5.24   Stray flux, Full load

28 slot Rotor, broken end ring
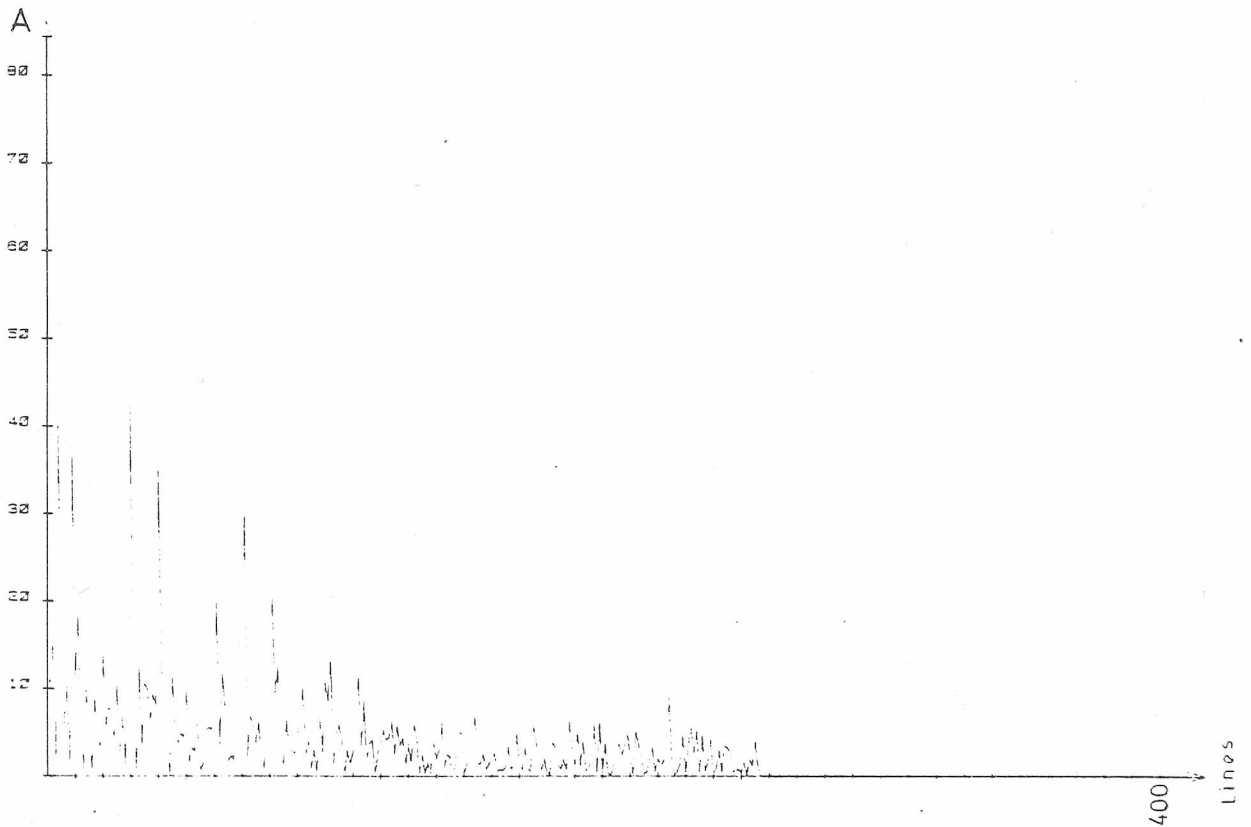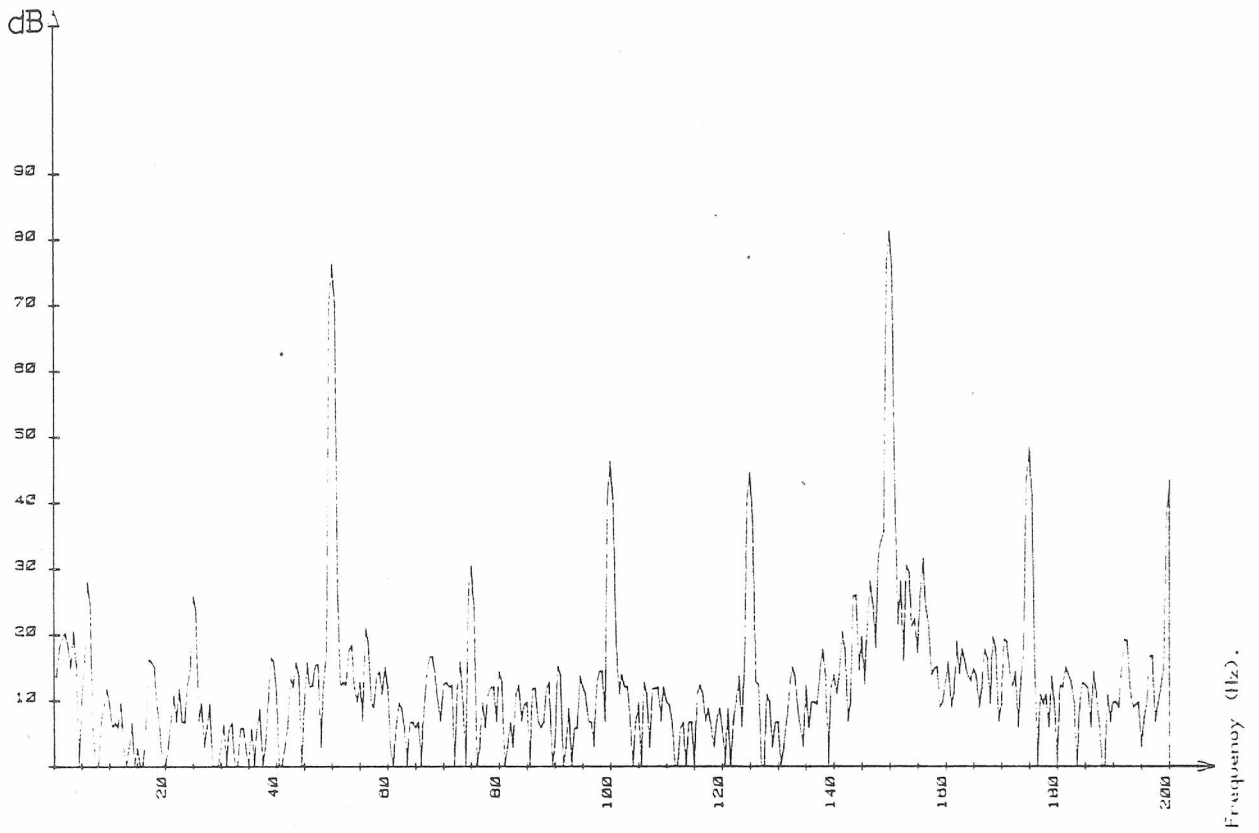
Figure 5.25 Stray flux, No load

condition : BROKEN ROTOR BAR
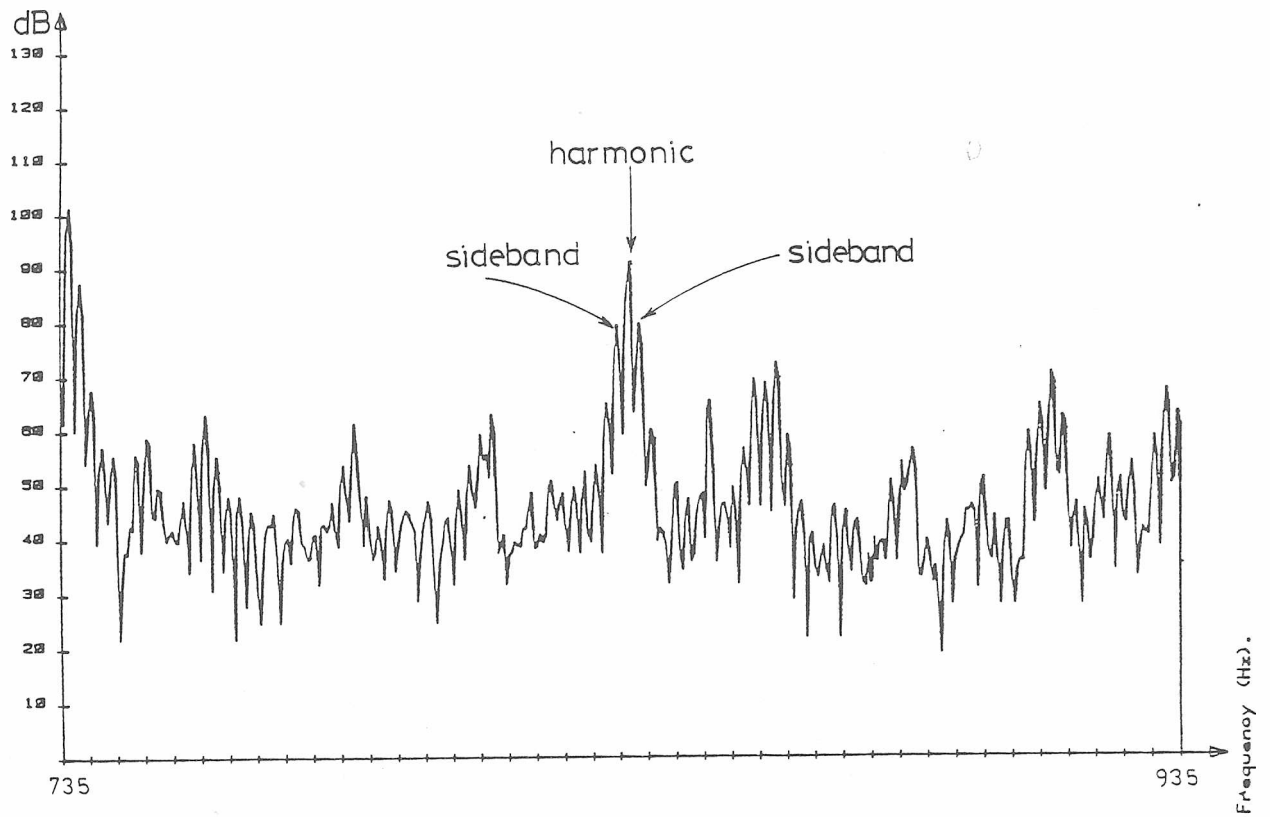
Figure 5.26   Sidebands appear around a Slot harmonic

condition: FULL LOAD
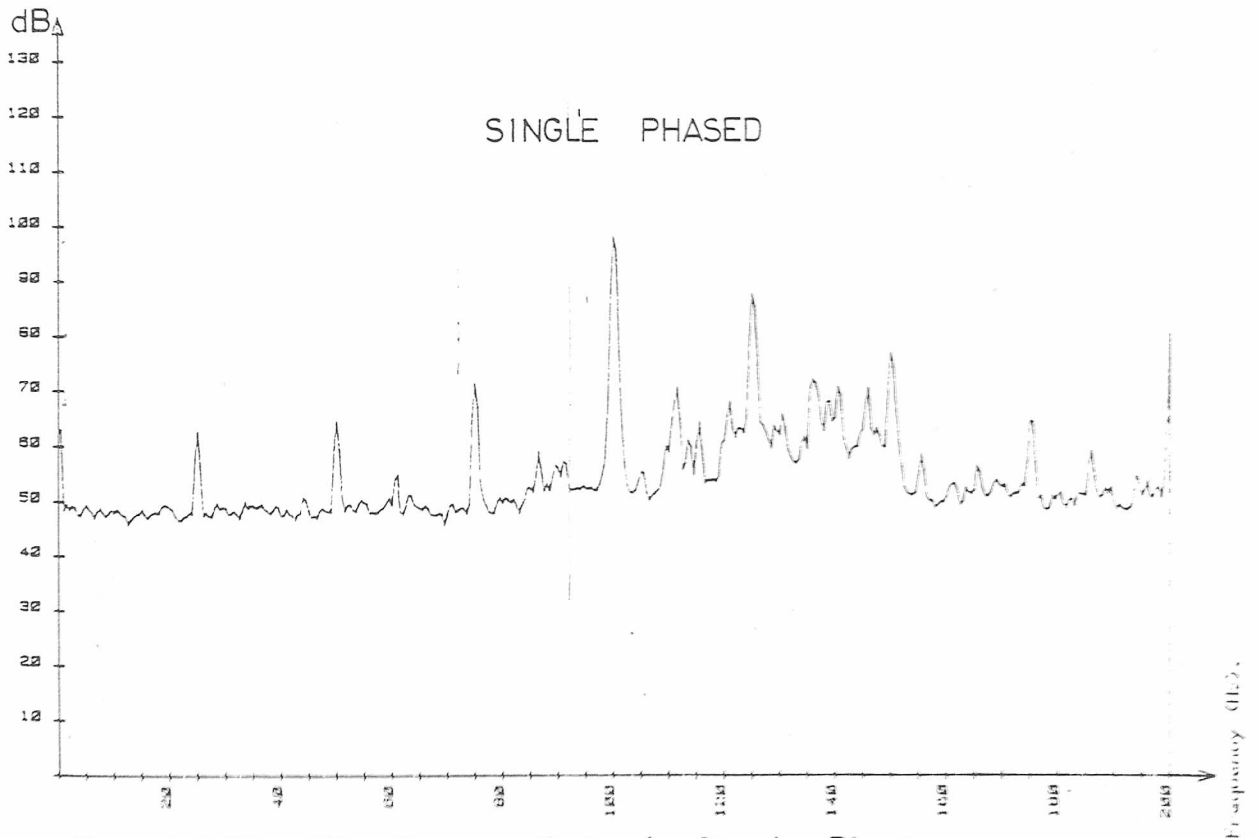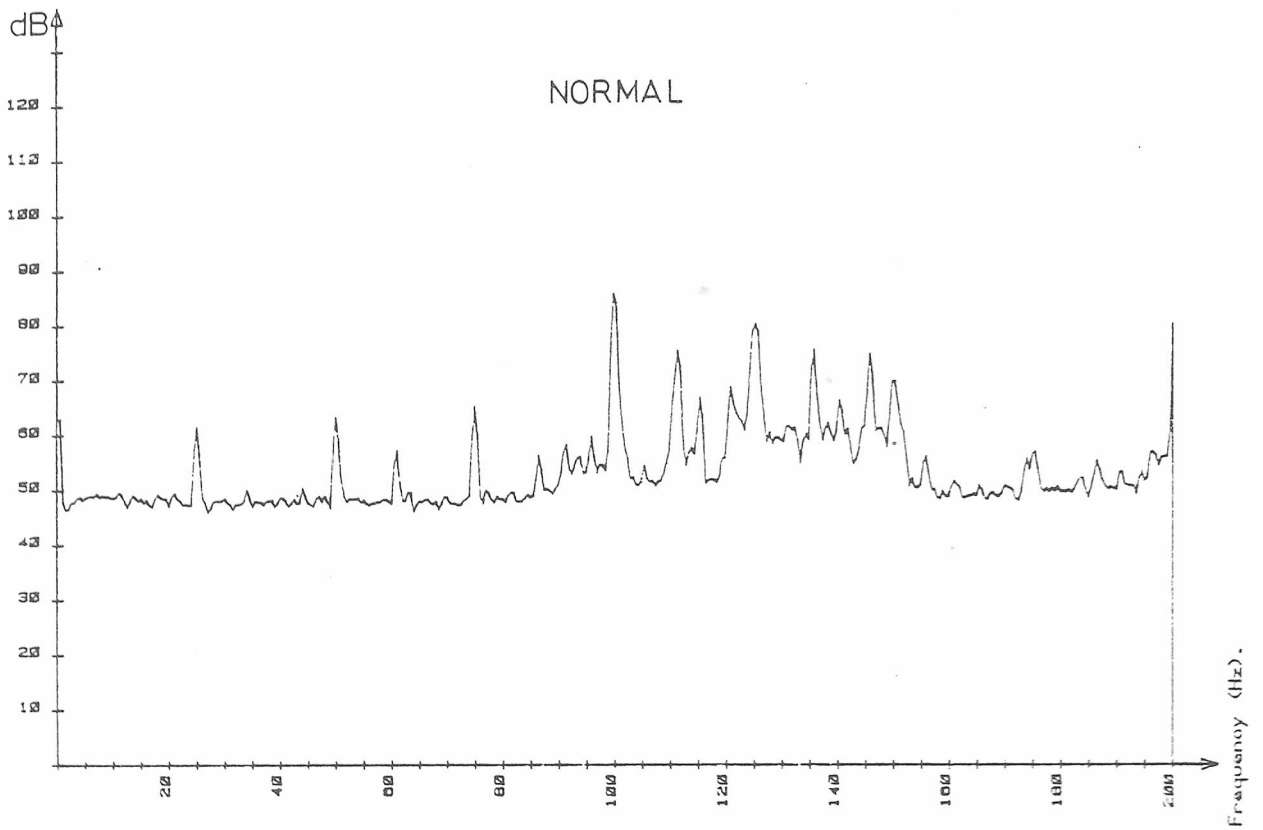
Figure 5.27   Vibration – effect of Single Phasing

condition : NORMAL
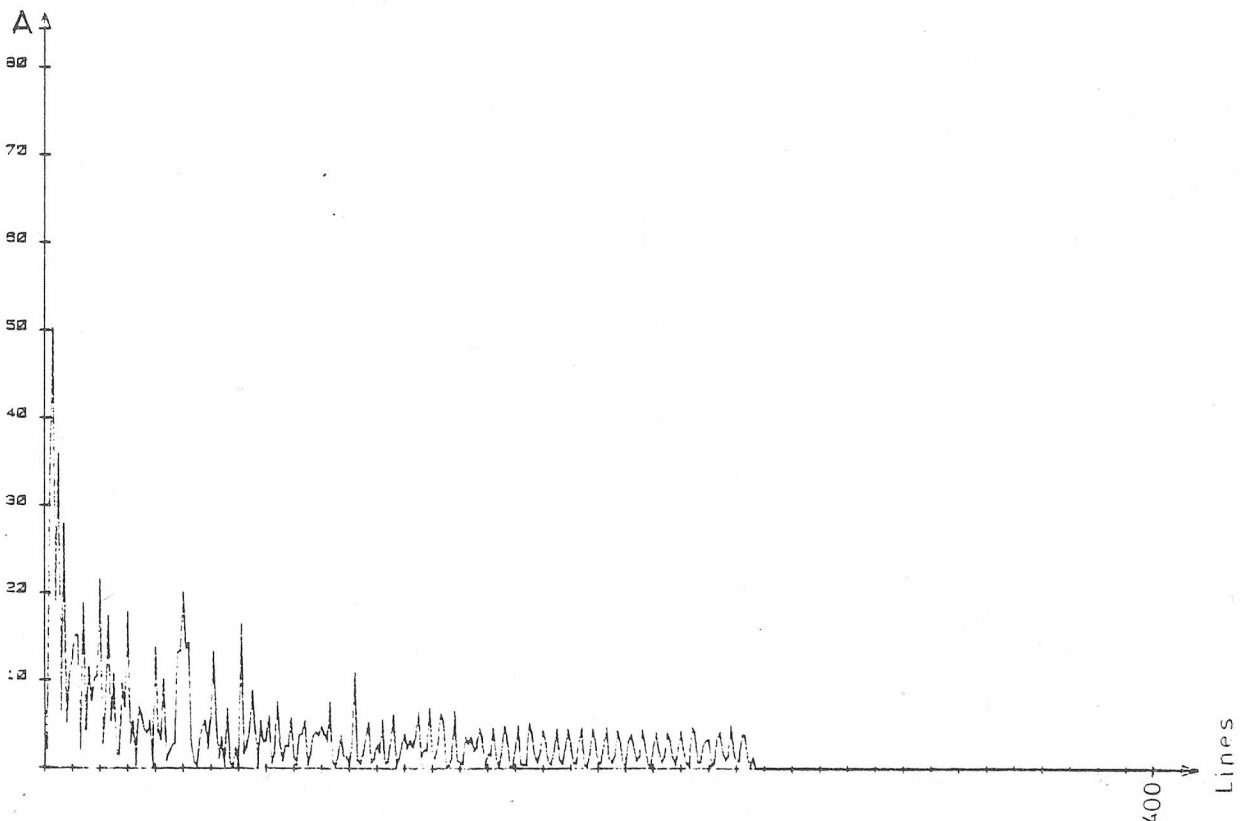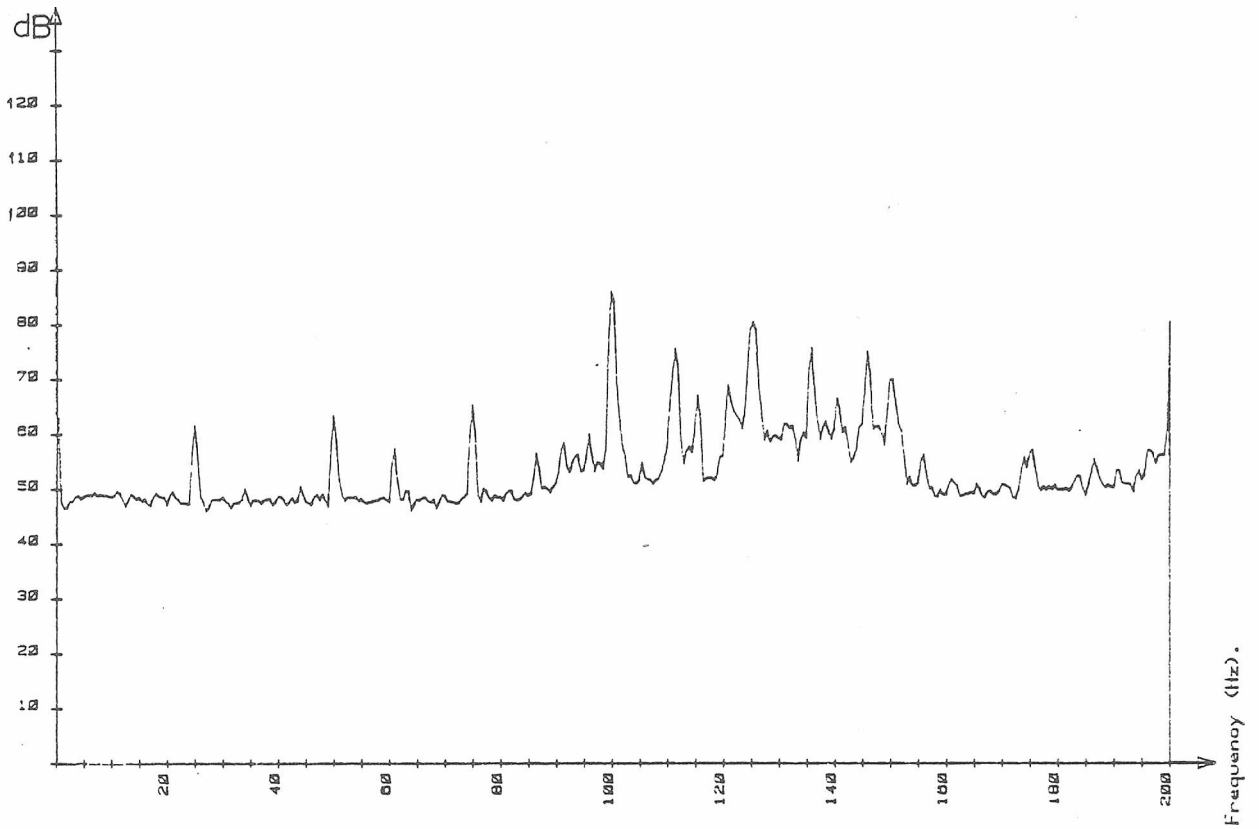
Figure 5.28 Vibration, No load, good 51 slot Rotor

condition: SINGLE PHASED
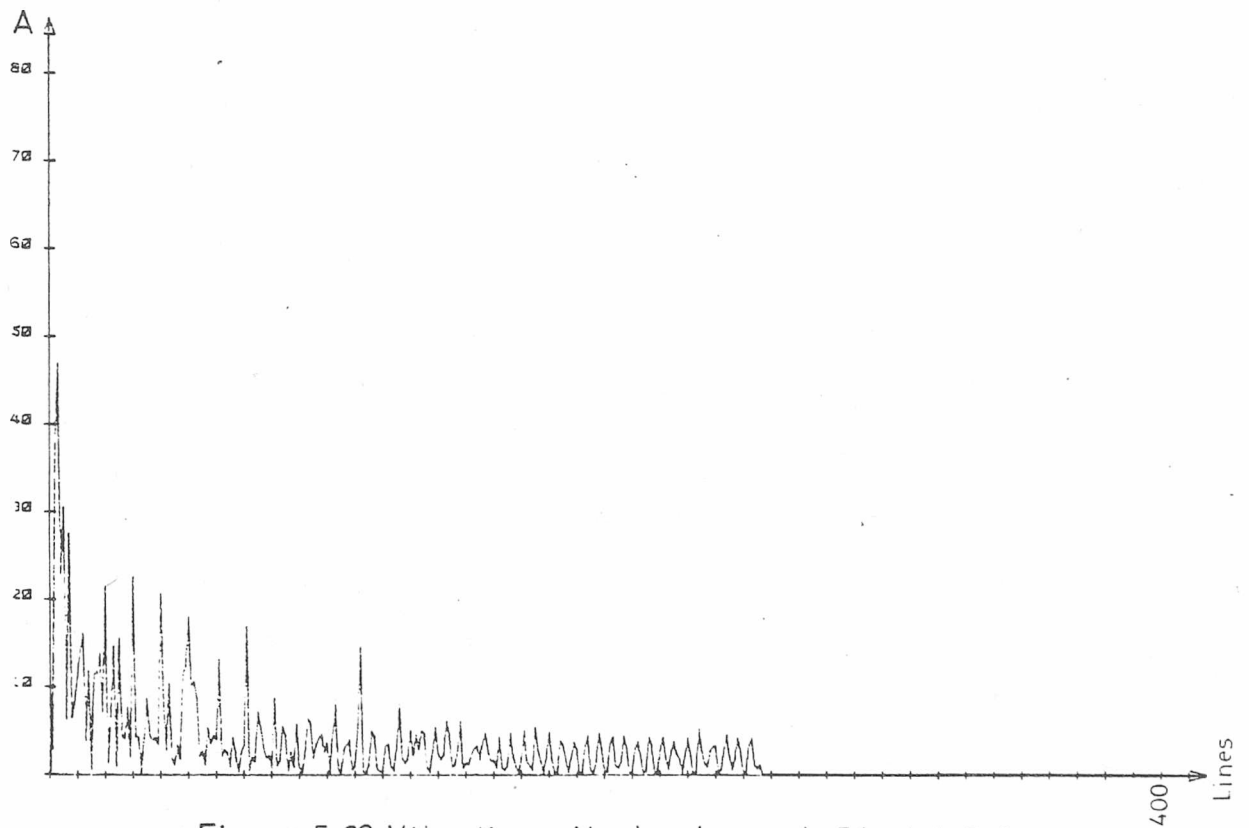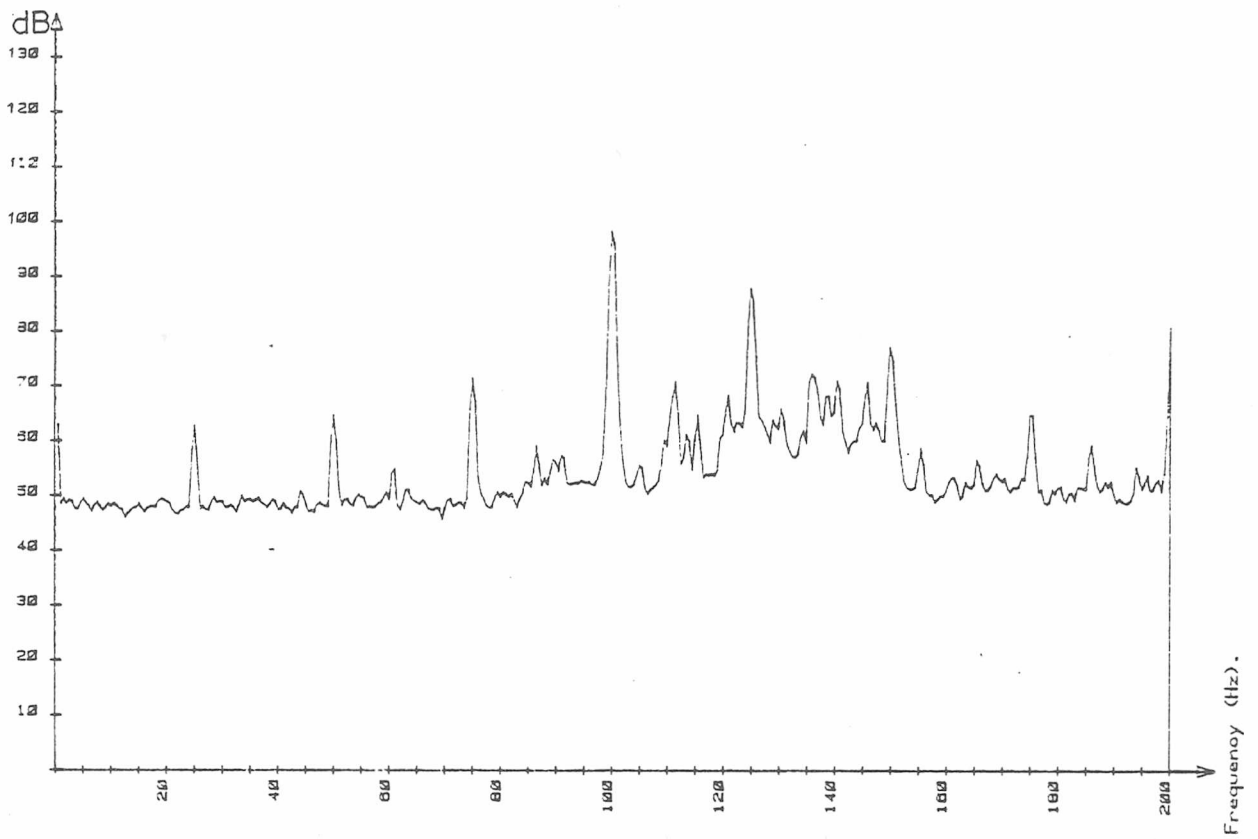
Figure 5.29 Vibration, No load, good 51 slot Rotor

CHAPTER 6.

A DEDICATED MICROPROSSESOR INSTRUMENT.

6.1   Introduction.

Although the system developed so far has many virtues, it also has major drawbacks. These essentially are its size and cost. A simpler system is required, for the implementation of the final instrument. The chosen route to this solution is to use industrial microprocessor technology. This allows the development of equipment which is cheaper and smaller, but which still possesses the ability to diagnose machine faults.

6.2   Instrument Architecture.

Having developed the necessary signal processing regimes on a general purpose instrumention system, attention was diverted towards a self-contained micro-processor based instrument to automatically carry out condition monitoring. As there are a great number of involved processes to be carried out, there are several possible solutions.

A multi-processor system may be used. Such a system was described by Penman et al [45], but for the present task, it has considerable disadvantages. Because it uses three processors, there will inevitably be times when they may conflict with each other for the hardware resources of the system, such as the memory. To overcome this, complex protocols have to be devised and implemented, which takes some time, both in the development and the run-time environment. In the system described in [45],

57

one processor is solely dedicated to handling protocols.

This approach has further disadvantages in the development stages. Each subsystem has to be designed, constructed and commisioned, with reference to the others, so that the whole system is homogeneous. When the subsystems use different type of microprocessor, these problems become even greater.

A much simpler approach is to adopt a single processor solution, as shown in Figure 6.1. Whilst it is true to say that a multi-processor system can, when used efficiently, provide a greater throughput than a single processor, it will now be shown that for the diagnostic processing involved here, the extra speed would be wasted, and thus the effort in developing a more complex system is not justified.

One of the first advantages of a single processor system is in that it forms one contiguous unit, and as only a single microprocessor is in use, the development stages will be similar for all sections. In addition, with only one processor, there cannot be any conflict for the hardware. This normally forces the condition of serial working, as only one task can be carried out at any one time. If, on the other hand, the hardware is designed so that it can operate to some extent independently to the processor, the disadvantage is reduced. In the system developed here, this is the case in the most important area. It was shown earlier that the incoming signals need only be sampled at 400 samples per second. In terms of the time taken to perform the mathematical analysis, this is a very slow rate. If the processor had to directly oversee the sampling process, the

58

analysis would be very slow indeed.

In order to overcome this, two pieces of specialist hardware are utilised. Firstly, the sampling must be timed. This could be done by a counter on the processor, but a better approach is to use an external timer. This then gives a pulse every 1/400 seconds, regardless of the processor state. These are used to initiate fresh samples of the signals, which are taken by the second part of this hardware. This device produces a new sample, after a delay of approximately 33 microseconds. Having done this, the processor is interrupted and the sample stored. In the mean time, the analysis will have progressed without any hinderance from the reading of fresh data.

To fully utilize the processor, two data buffer areas are used. While one area is being processed, the other is filled with new data samples, interrupting the processor only when the sample is ready to be stored. This has little effect on the processing speed, as the work involved in storing the data is insignificant beside the Fourier Transform mathematics, and the time involved in sampling the signals at the correct rate is invisible to the processor. This is the point at which any extra speed obtained from the multi-processor approach is seen to be wasted. Since the analysis is dependent on new data being available, it cannot, in overall terms, progress any faster than the sampling rate. As the Fourier Transforms run in less time than the sampling, no advantage is to be gained.

6.3   Processor Choice.

The choice of the particular microprocessor to be used is based on several factors. The main of these are:

- Word length,

- Execution speed,

- Special hardware features, eg hardware multiplication and division,

- Input/output facilities,

- Supporting hardware.

The prime factor for a condition monitoring instrument, other than accuracy of diagnosis, is speed. Knowledge of the number of operations involved in a single diagnosis, along with the time taken to acquire a complete set of data samples can be used to determine the required execution speeds of the processor to be utilized. For a complete set of samples, a time of 1024/400 (number of samples divided by the sampling rate) will be required. It is desirable that the processing is carried out within this period, such that each multiplication should be executed in less than 128 microseconds, since the Fourier Transforms perform approximately 20,000 such operations for a 1024 point transform.

Considerating these facts, a decision was taken to use an INTEL 8086 microprocessor. This is a 16-bit processor, and is capable of executing a multiplication instruction, in hardware, in around 100 microseconds, for a clock frequency of 5 MHz. This processor also has advanced addressing facilities which make the handling of data arrays more efficient, and are used to improve

the speed of the Fourier Transforms, as discued in Section 6.5. Devices are readily available for this processor, as it uses all of the standard INTEL peripheral integrated circuits, without the need for specially designed 16-bit devices, so making system development easier. The facilities which are inbuilt makes it eminently suitable to a task which involves a large amount of complex mathematical manipulations on large amounts of data. Supporting the advanced architecture of the device are other large-scale integrated circuits are available to support it, further expanding its capabilities, eg to allow automatic generation of functions such as sine and cosine, exponentials and logarithms.

These devices, however, are not utilized here. This is due to the desire for as small an execution time for the program as is possible. Although these special support devices are much faster than direct software generation for, say, sines and cosines, they are not as fast as a look-up table approach. Here, all the neccessary values are stored in memory, so that the generation of the value is no more time consuming that a single memory read operation. This however requires additional memory, and is yet another example of the inevitable trade-offs between various program parameters - here, speed and memory size.

6.4   Analogue to Digital Converter Choice.

The selection of the analogue to digital converter (ADC) is partly determined by the accuracy of representation required of the signal processing. The data here are the electrical signals derived from transducers on the periphery of the machine

under test. These must be converted, by some means, into numerical values which the microprocessor can then manipulate, as shown in Figure 6.2. In this choice, the actual level of these signals need not be considered - an amplifier will allow signals of any desired level to be handled. It is the difference between the smallest and largest possible signal - its dynamic range - which is of concern.

If this is known, then a device which can look at the level of the signal and produce a numerical representation of it can be selected. The difference between the various types of converter available are in their speed of conversion, internal accuracy, and in the overall accuracy of them. For this application, 12 bits are used, giving a dynamic range of 72 dB. This decision is based partly on the fact that a 12 bit converter is used in the commercial spectrum analyser used to develop the processing, partly on the fact that a 16-bit processor is being used, and so can use the extra range from this convertor, and also from observation of the signals from the machine. The sidebands which are to be detected may have little energy themselves, and so be difficult to detect alongside the main spectral components. The higher accuracy of a 12 bit converter is necessary to allow their separation.

If the data is then considered to have a 12-bit resolution throughout, the effects of truncation within the mathematics performed by the processor can be limited to insignificant proportions by the use, as described earlier, of a 16-bit microprocessor. By performing all of the processing to this degree of accuracy, a further 24dB is added to the overall range,

so that in essence, any noise produced by truncation will be at least 24dB down on the signal, in a range of 72dB.

As a finite time is taken for the ADC to convert a signal sample, errors may occur, due to the signal amplitude changing during the sampling time, as shown in Figure 6.3. Because of this, the signal must be held constant during this period by a "sample and hold" circuit. If, however, the present situation is examined, its use is seen to be unnecessary. The signal is band limited to 200Hz. by an analogue anti- aliasing filter. This is a requirement of the Fourier transform. Its effect is to prevent unwanted higher frequencies degrading the performance of the transform. If it is then considered that the ADC in use will perform a full 12-bit conversion in a maximum of 33 microseconds, the signal change during the conversion may be determined. A cosine wave will have its maximum slope at the zero crossing point. For a signal which is band limited to 200Hz., the maximum change during the sample period may be calculated as:

$$COS \quad \frac{2*PI*33 \text{ microseconds}}{5 \text{ millisconds}} \quad = 2\%.$$

The fact that this is only two percent shows that a sample and hold circuit will not be needed, as the changes in the signal, reported in Chapter 5 for the difference between "good" and "fault" conditions is of the order of hundereds of percent. The error due to conversion times is thus minimal.

6.5   The Fourier Transform.

Having sampled and digitised the signal, a table of its values is available. In order that frequency domain analysis may be carried out on this signal, it must be transformed into the frequency domain. This is the function of the Fourier Transform. It was noted earlier, that this is based on sine and cosine functions. Accordingly, values of these are tabulated within the program. These are stored in a form which allows maximum use of the processor's 16-bit resolution, but in one 16 bit store (or word) only. This representation is used throughout the processing, and is thus referred to as "integer" representation, since only integer values are considered, stored in two's complement form.

The reason for performing integer arithmetic in the processing is one purely of speed. If the instrument is to be of any great use, it cannot spend lengthy periods of time in analysing the signals, without producing any results. Thus, for this area of the analysis especially, speed is of prime importance. To produce a single 1024 point transform, requires of the order of 20,000 multiplications. It is this operation which is used as a guide to computation time, since it itself uses the most time for its execution. There are several methods of producing a frequency spectrum, as discussed in references [18 - 26, 28]. These include special purpose hardware implementations [23, 25, 26]. As a flexible approach is required, in order to develop a complete system, an FFT algorithm was chosen in this application, to run on a general purpose microprocessor. The algorithm which performs the Fourier

64

transform is then standard, and is known as the "fast Fourier transform", or FFT, described by Brigham [46]. This algorithm was first described in 1942 [21]. It enables great savings in computation time to be made, due to the use of a factorisation of a matrix which may be used to represent the transform, and thus dramatically reduce the number of multiplications. This performs a large transform by operating on a combination of smaller ones. This process, known as decimation [46] may be carried through until the smallest unit - called a "Butterfly", as shown in Figure 6.4 - is reached. The overall transform consists of groups of butterflies. A simplified version of this process, for a four point transform is shown in Figure 6.5. If this separation into smaller units is carried out on the time series data, the method is known as "Time Decimation" transformation. If the time series is taken as two units, and these then processed in succesively smaller units, the term used is "Frequency Decimation" transformation, and this form is used here.

As the time series data has thus to be accessed in units of varying size, the advanced addressing facilities of the 8086 microprocessor can be utilised to improve the speed performance of the transform.

The algorithm used here, from Eckhouse and Morris [47], uses two separate data arrays - one for the Real and one for the Imaginary components of the signal. This requires the use of four data pointers. One pointer has to be set at half the total number of data points, and decreased by a factor of two after each stage of the transform. This is because of the decimation

of the data. Further to this, a pointer has to be added to this to allow access to the individual data points within each section of the transform. Both of these pointers are required for each of the arrays. A better approach, made possible by the architecture of the 8086, is to store the data in a single array, and to use an extra "offset", or fixed-value pointer to fetch the Real or Imaginary data. If these two quantities are stored in successive locations for each point, (as shown in Figure 6.18(a)), then this offset is zero for the Real points, and two for the Imaginary ones, since they are one word, or two bytes further into the array. The problem of the remaining two pointers is then solved by using two registers within the processor as further offsets. The data is then fetched from an address defined by the addition of these two registers to the constant zero or two, for each point. The number of pointers has thus been reduced, saving the time otherwise needed to set up their values and also freeing a register in the processor, as there is no longer any need to point to a separate data array for the Real and Imaginary points.

In order to achieve high processing rates, efficient programming methods are necessary, and this predetermines the language to be used — every part of the transform must be written in assembly language. This allows the programmer to control exactly the operation of the processor, and to eliminate all unnecessary work from its task.

This choice makes the development of the program generally slower and more difficult. A further increase in speed is possible by choosing the correct format for the algorithm. Due to the nature of the FFT, the actual mathematics can be broken down into six types of butterflies. This caters for the special cases where the value of the sine and cosine functions have a particular values. Obvious savings can be made where these values are unity or zero, as the multiplications can be removed. In other cases, the value can be stored "in line" with the program code, thus saving on time spent fetching it from further afield. Having split up the program into these units, they must be used in the correct order. This could be achieved by a secondary program, working out which butterfly to use and then calling it as a subroutine. To call them as subroutines is inefficient, since certain operations must be carried out on each subroutine call, operations that have nothing to do with the data - the so called "data independent" operations. These operations are removed from the time involved in the transform by calculating and storing them beforehand. The program has then only to look at a list to see which operation to perform next. This list also contains the address of the data to be used, as well as the entry ponits of the butterflies. Further to this, it contains markers, zeros in this case, which are known never to appear otherwise, as shown in Figure 6.6.

Since the action of calling the butterflies as subroutines is so time consuming, a different approach is used. The list of the addresses described above is called a "Thread", as the program threads its way along a pre-defined list of operations.

The program is so arranged that the butterflies are used on several successive occasions, so that to call one, return from it and find that it is to be called again would waste even more time in a subroutine version. This is an advantage where the program is written in threaded code. The thread tells the processor which butterfly to use. Once it has performed this task, it looks again at the thread. It is expecting to find the address for the next data point, as the butterflies are used on groups of data. The thread, then, will contain a pointer to this next data point, and the butterfly loops round on itself to process this point. It was stated earlier, however, that special pointers are also included in the thread. If one of these is encountered, a new butterfly is to be executed. The test for this is one of the fastest available on a microprocessor - a test for zero, and branching or not, on the result, as shown in Figure 6.7. The processes involved in calling the butterflies as subroutines have thus been reduced to a single test-and-jump, which is much faster, and all of the data-independent calculation of deciding which butterfly to execute has been removed to the program development, rather than execution phase.

Having placed these special pointers in the thread, it becomes what is known as "knotted code". This is due to the fact that the thread loops round on itself - executing the same butterfly on successive data - before continuing. This is said to have "tied knots" in the thread, and hence the term for the program form.

Its use here is well justified, and the approximately 20,000 complex multiplications required for the transform are executed at a rate in excess of 5 points per millisecond. This is less than the time which could be predicted by adding the execution times of the operations involved, again due to the architecture of the 8086. Instructions are fetched ahead of the need to execute them, allowing a "pipeline" effect to reduce the overall execution time. A table of the execution speeds of the six butterflies developed here is given in Figure 6.8, run on a 5MHz. 8086. As the thread which drives the transform is a very large unit, its generation can be carried out automatically, by a further computer program. This may, however, be modified to produce other information on the transform. Based on the execution times in Figure 6.8, this program was modified to give an estimate of the execution time for a transform of any desired size. These estimates are presented in Figure 6.9. For the condition monitoring processing, the desired transform uses 1024 points, and is estimated to run in 435ms, based on the execution times of the butterflies alone.

The initial development of the microprocessor system was carried out on a small INTEL SDK86 development system. This allowed useful experience to be gained in its use, and the signal processing techniques and execution speeds to be confirmed. An enhanced 8086-based system with 128K of read/write memory and five input/output channels was used to test the full 1024 point transform. A comparison of these two systems is shown in Figure 6.10. The execution time of this, including all data transfer overheads was 890 ms. This differs markedly from the estimate of

435 ms., especially as the new   system runs on nearly twice
the clock speed. This is accounted for by the pipelining effect
of the 8086 architecture. This fetches several instructions in
advance, so that the time involved in fetching them is
parallelled with the execution time of the present instruction.
This enhances the execution speed, provided that the program does
not contain any branches, as the pipeline has then to be
re-filled on every branch. There is still a significant
improvement in speed though, as shown by considering that the
20,000 multiplications for a thousand point FFT would require 2
seconds without the pipeline, whereas the whole transform is done
in less than one second.

6.6   Anciliary functions.

    As all of the software for the condition monitoring system
is to be written in assembly language, it is common to use a
microprocessor development system to aid the writing. This
normally consists of an editor, which allows entry and
modification of a program, an assembler, which converts the
assembly language so written into machine code, and a linker,
which allows a group of sub-programs to be concatenated, to form
the final executable code. The equipment used to develop the FFT
signal processor consisted of an HP64000 system, with assembler
and linker packages for the INTEL8086.

    To transfer the program code from the HP64000 to the 8086
system a serial loader program was written. This overcame all of
the problems associated with developing software using PROM's.
Once the code had been finalised on the development system, it

was converted (by the HP64000) into an ASCII file, suitable for display on a terminal, or printer. The resulting file contained all necessary information on the code written, including the number of bytes produced, and their intended locations in the 8086 system memory. The loader program read this file.

Along with the desired information, there are also control and other unwanted characters. The loader had thus to strip these from the file as it read it - checking for errors in the data format as it did. This resulted in the ability to directly transfer the program code from the HP64000 to the 8086 by a fast and straight-forward means. Further to this, two extra advantages were gained. Since the development system produced a file which included the intended location of the code, any part of a program could be selectively modified, without the need to re-load the whole program. This was important when developing large program units, as the time involved in repeatedly re-loading the program could be large. As the loader stored the program, the storage area must implicitly be read/write memory. This meant that it was then possible to change individual locations by hand, a facility not available in a PROM based system.

The loader itself, however, resided in PROM, as its code was fixed, and was required to be available at all times, without having to be loaded itself. The larger 8086 system, does not allow any space for PROM. This led to the design and construction of a new circuit board, for this purpose. To overcome the problem of the S100 bus being an 8-bit bus, whilst the 8086 is a 16-bit processor, both the data-in (DI) and

data-out (DO) busses were used as a single 16 bit bi-directional bus.

In order to utilize this facility, the PROM area was split into a high and a low byte bank. The data from these was then routed, via buffers, to the DI bus for 8 bit transfers, and to the DI and DO busses for 16 bit transfers. These buffers were controlled by the S100 status signals, and the A0 address line, as this was used to select which bank of PROM's was to be accessed - the devices being in parallel. A block diagram of this board is shown in Figure 6.11.

It is a property of Fourier Transforms, that the data is assumed to be exactly periodic within the sampling time. This is a condition which is rarely satisfied in real systems, as shown in Figure 6.12, so that steps must be taken to modify the sampled data to make it appear to be so. This is performed by the use of a windowing function, two of which are shown in Figure 6.13. Since the data is produced by sampling a signal at known intervals, for a fixed period, it is already windowed, by the rectangular or "box car" function. The process of modifying the data in this way also modifies the frequency domain representation of the signal, as it affects the bandwidth of the filters, of which the Fourier transform can be assumed to consist. The equivalent bandwidths for a rectangular and a Hanning window are shown in Figure 6.14. This shows that although the Hanning window has a shallower initial cut-off than the rectangular window, its sidelobes are of a lower amplitude and decay at a faster rate. The use of this window is common for steady state signals, as it greatly reduces the effects of a

72

signal being non-periodic within the sample time, whilst its smooth form does not unduly complicate the resulting spectrum. The effects of a Hanning window may be seen by comparing the transform shown in Figure 6.16 with those in Chapter 5. This is the spectrum of a 100Hz. sine wave, with a rectangular window, whereas all those in Chapter 5 use the Hanning window. The Hanning window utilises a cosine squared function, making the end points small and the centre points large, by comparison with the simple rectangular function. The resulting envelope of this windowing process is shown in Figure 6.16.

As the necessary values for the cosine function are already stored, for use by the Fourier Transform, the implementation of a Hanning window requires little extra program space.

As it is intended to perform cepstrum analysis, a logarithmic function is also needed. This may be done by a series of calculations on values obtained from tables stored within the program. This not only consumes large amounts of memory space, but also large amounts of time are required for the calculations. It was decided, therefore, to use an algorithm which would directly calculate the logarithm of any number.

In the normal definition of a cepstrum, it is a logarithm to base ten which is used. This is convenient, since the first transform may then be scaled in decibels. The algorithm used is due to Knuth [48], and directly generates the logarithm of any number for which a logarithm exists. Since it is the properties of a logarithm which are desired, it matters little which base is used, and in any case a conversion from one base to another needs

only a simple scaling operation. This allows the logarithms to be generated to base two, thus reducing the problems of truncation which would otherwise result from decimal representation in a finite word length.

When a number is squared, its logarithm is correspondingly doubled. Functions involving factors of two - doubling and halving - are easily handled in a binary system, by shifting the number one place left or right. Also a property of logarithms is that multiplying by the base will add one to the logarithm, whilst dividing by it subtracts one. These factors may be combined, and are used as the basis of the logarithm routine.

Two storage locations are required, as shown in Figure 6.18. The required number is placed in the first of these, and shifted so that it is less than the base - in this case, divided by two until in the range of zero to two. The number of shifts needed to get it with in the desired range is recorded for later use. It is then squared and compared with the base. If it is larger than the base, a bit in the second number is set, and the square is then divided by the base. If it is smaller, the same bit in the second number is cleared. This is the kernel of the algorithm, as shown in Figure 6.17. Squaring one side of the equation gives a factor of two on the other side. The doubling is carried out by setting or clearing the next least significant bit of the result at each test. It is the next least significant bit which is set or cleared, rather than the next most significant, because it is the next fractional part of the number which is calculated, so that the result at each stage represents a half, a quarter, an eighth and so forth, until a given

74

accuracy, in terms of the number of bits in the fraction is achieved. This gives the fractional part of the logarithm, and the number of shifts needed to bring the number in range is now added, to find the final value of its logarithm.

To clarify this, an example is now given. If 8 bits are assigned to the fractional part, then the logarithm of 123, in decimal form may be calculated by:

123 is greater than the base (10) so divide to get 12.3

this is still greater, so divide again, to get 1.23.

Storing the number of divisions (2), the algorithm proceeds as follows:

1.23 * 1.23 = 1.51. Less than 10, so clear MSB of result

1.51 * 1.51 = 2.28. Less then 10, so clear 2nd MSB.

2.28 * 2.28 = 5.24. Less than 10, so clear 3rd MSB.

5.24 * 5.14 = 27.44. Greater than ten so set 4th MSB,

27.44 / 10 = 2.74.

2.74 * 2.74 = 7.53. Less than 10, so clear 5th MSB.

7.53 * 7.53 = 56.74. Greater than 10, so set 6th MSB,

56.74 / 10 = 5.67.

5.67 * 5.67 = 32.19. Greater than 10, so set 7th MSB,

32.19 / 10 = 3.22.

3.22 * 3.22 = 10.36. Greater than 10, so set 8th MSB.

The desired accuracy of 8 binary places has now been achieved, and the result is 2, for the number of shifts, and 00010111 binary, as the fractional part of the logarithm. Taking this binary number into decimal form, with each bit representing half the value of its left hand neighbour and the MSB having one

75

half as its value, the final result is given by:

2 + 1/16 + 1/64 + 1/128 + 1/256 = 2.0898.

The logarithm to base ten of 123, given by tables is 2.089. The algorithm yields results sufficiently accurate for the processing being carried out.

This routine could be modified to directly calculate logarithms to any base, by changing the division factor to the base concerned. The algorithm itself is independent of the base.

As the logarithm is a non-integer quantity, some bits of the original and result numbers have to be assigned to be integer, and the rest to be fractional - in other words, the binary point must be defined.

The position of the binary place is open to the user of the algorithm. Since twelve bit quantities are being handled, it is logical to put the binary place between the fifth and sixth bits, so that equal range is assigned to the integer and fractional parts, in order that the algorithm may be tested. The ADC has a dynamic range of 72dB. As the result of this algorithm is the logarithm, the integer part of the result should be chosen to match this, ie 72. This may be represented in 7 bits, but using 6 bits does not truncate the range to a great extent, whilst giving an extra bit, and thus greater accuracy to the fractional part of the logarithm.

6.7   Two Channel Fourier Transforms.

In condition monitoring , all the signals are real, so that the sampled data will consist only of a real part. Since the Fourier Transform makes no definition between real and complex signals for its input, this implies that the input data is half filled with the sampled data, and the remaining half with zero, representing the imaginary components, as shown in Figure 6.18(a). This is wasteful of space, and of calculation time. To overcome this, two signals may be transformed at the same time. This is achieved by taking one signal and storing it in the real values, the other signal being stored in the imaginary values. A complex signal has thus been formed, as shown in Figure 6.18(b).

This new signal is then transformed as normal. The output must now be re-arranged so that tha original two transforms may be recovered [49], as shown in Figure 6.19. Each point in the composite transform has a real and imaginary part. The points in the first half of the transform are taken, and their complex conjugates formed. The corresponding point, from the opposite end is then added is and subtracted from the conjugates of the first points. The two new values formed are the transform values for the signal in the real and imaginary parts of the composite complex signal.

As the magnitude of the transforms is required, rather than the complex representation, the real and imaginery parts of the transform values may be squared and added. The square root need not be taken, since it is the comparison of components within a single transform which are to be compared, so that a scale factor

is the only result of not taking the root, remembering that a logarithmic transform is also performed. Squaring the terms of each final point, it becomes clear that a number of values are common to both points. This allows factorisation to be used to reduce the number of calculations needed at each point. This is similar to the method used to reduce the computational work involved in the transform itself.

The result then is two transforms performed within the space, and very nearly within the time, of one.

The program code for the FFT is a large unit, as is shown in Figure 6.20, and thus is obviously going to be relatively slow to execute. To avoid the further time delay of waiting for a complete set of new data samples to be taken before the start of each transform, the sampling is done at the same time as an FFT. The ADC is controlled by a clock generator which exists as external hardware to the processor as discussed earlier.

To facilitate this, two data buffer areas are used. One of these may be processed, whilst the other is filled with the new samples, so that the two operations can run in parallel. At the end of each cycle, the channels are swapped, so that the new data is processed, and the old overwritten with the next set of samples. This change-over can be implemented in three microprocessor instructions as the 8086 uses an extra set of special-purpose or "Segment" registers to access the memory. This technique enables four areas of 64K bytes to be addressed independently. Using this, the FFT fetches and stores its data with reference to one register, and the samples are stored with

reference to another, as shown in Figure 6.21. To change channels, the contents of these registers are swapped. The program code needs no modification, and there is no speed difference between the two chanels. Since the transform is capable of handling two signals at the same time, both arrays could be stored and transformed together. This would be wasteful of time, since both channels would need to be filled with fresh samples before transforming could take place, and no time overlap would be possible.

Instead of this, one channel is transformed, whilst the other is filled. It is then possible to take the output of this first transform and produce the first cepstrum from it. If this were done in the imaginary sample space of the first data array, the cepstrum would always be one transform behind. If, on the other hand, the result of the first transform is placed in the imaginary sample space of the second channel array, the cepstrum is available sooner. This is another feature of the software which is made possible by the architecture of the 8086. It is used to good effect, since the transforming takes approximately one second, whereas the sampling takes over two seconds. Had the cepstrum been performed by its own channel, it would be necessary to wait for this to fill again, which would need, overall, more than six seconds. When the channels are interleaved, however, the first cpestrum is produced after 5 seconds, and subsequent ones after only three.

6.8   Conclusion.

For condition monitoring to be practical on a large scale, the cost of individual parts of any monitoring system must be kept as low as possible. It is also an advantage if the equipment is small, as space may be at a premium in some applications.

The initial test system developed here, consisted of large and costly general-purpose equipment. Such drawbacks have been overcome by the development of a self-contained instrument. This is based on a single microprocessor, and is capable of performing all of the diagnostic functions of the larger system, but in a much smaller space.

In addition to the reduced size and cost, the microprocessor system is faster, as the algorithms used to implement the analysis of the machine signals have been developed with execution speed as a high priority. As a part of the development of this, a complete 8086 program development system has been created. This consists of a commercial editor/assembler/linker, the 8086 itself, and a loader program which allows the two to be directly linked together. This saves considerable amounts of time in the development of the software, as an effective means of performing program changes is made available. Without it, the stages of testing and improving the software would involve much time and effort being spent in the re-programming of large PROM devices.
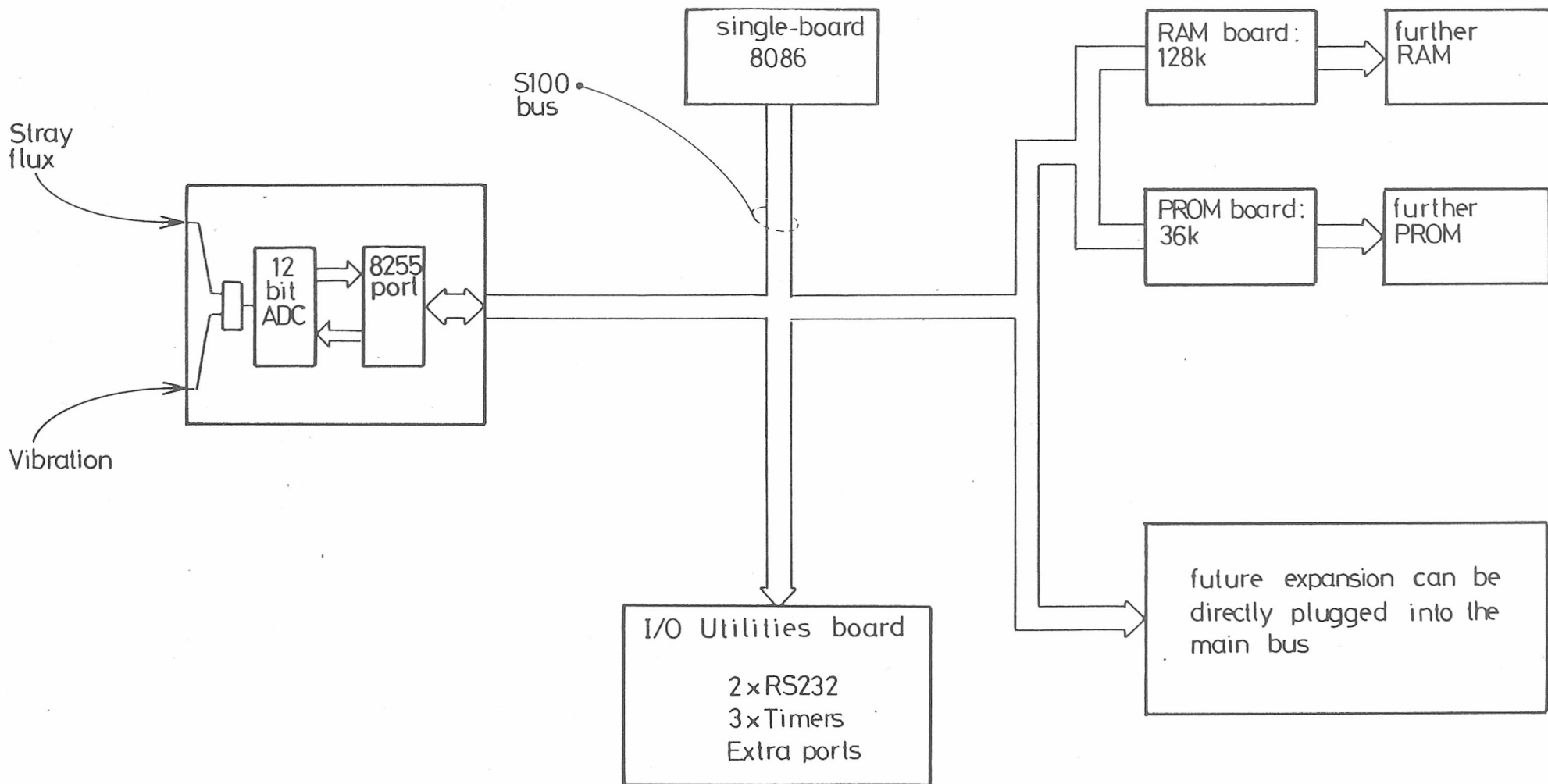
Figure 6·1   System architecture

incoming analogue signal   converter   table

A

Analogue
to
Digital
converter

0000
0012
3908
1463
0120
3369
1733

table of
numerical,
or digitised
samples

Figure 6·2

start of conversion   end of conversion

A

ERROR, due to signal
changing during the
sample time

t
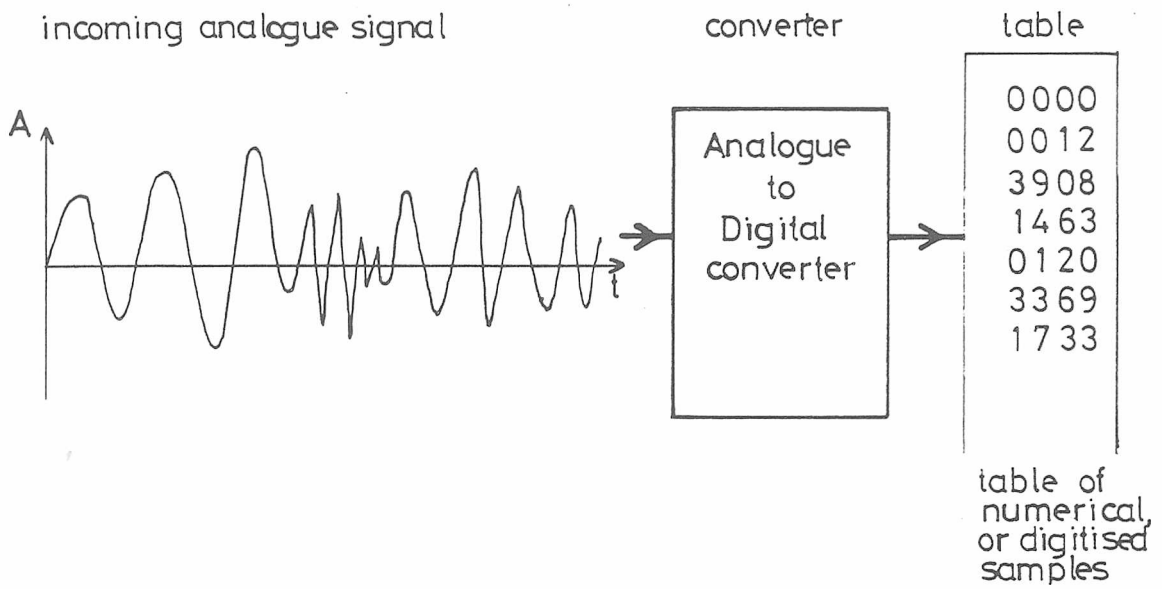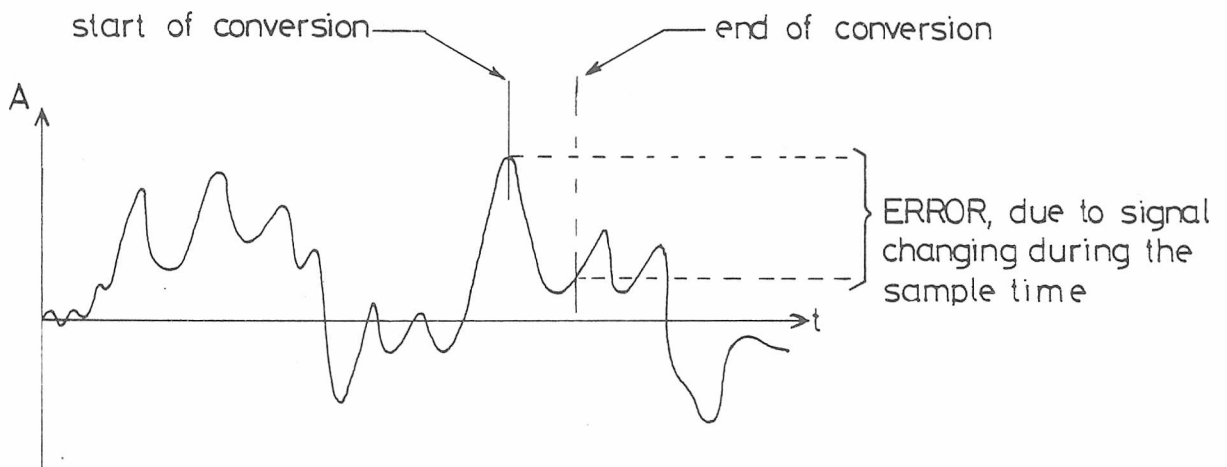
Finite time for the ADC to work can give errors

Figure 6·3
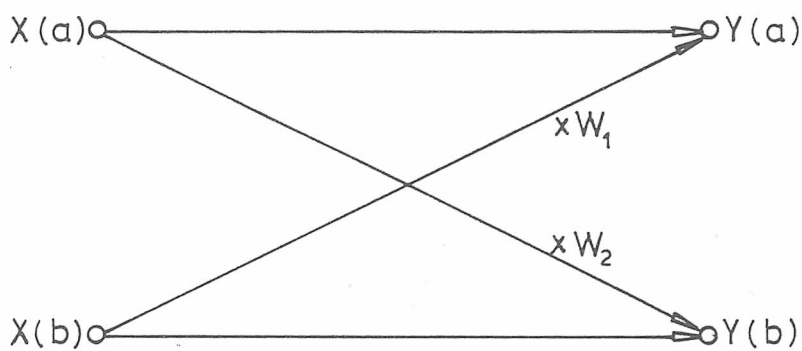
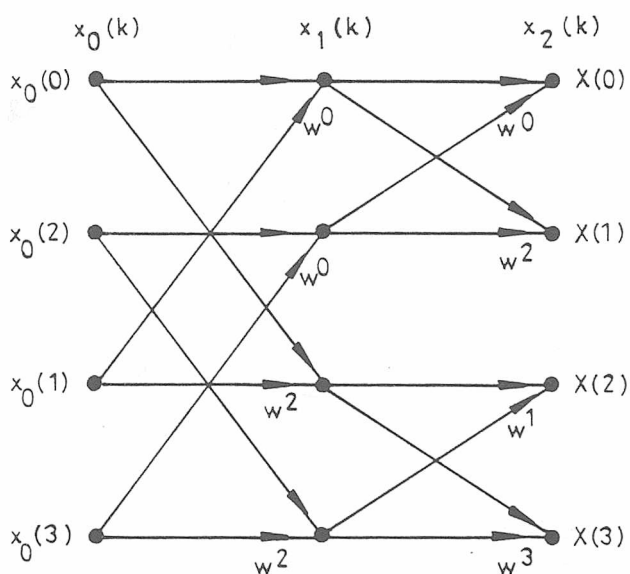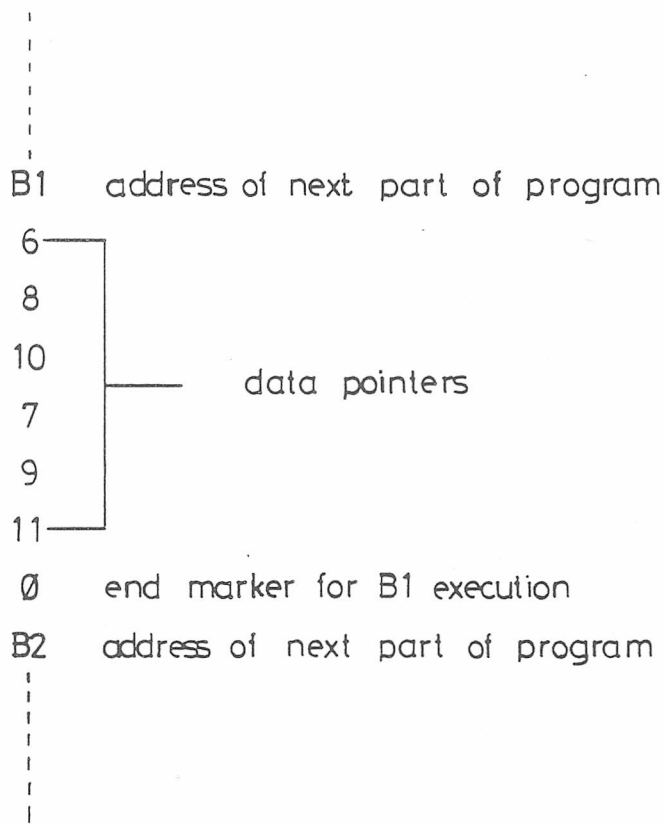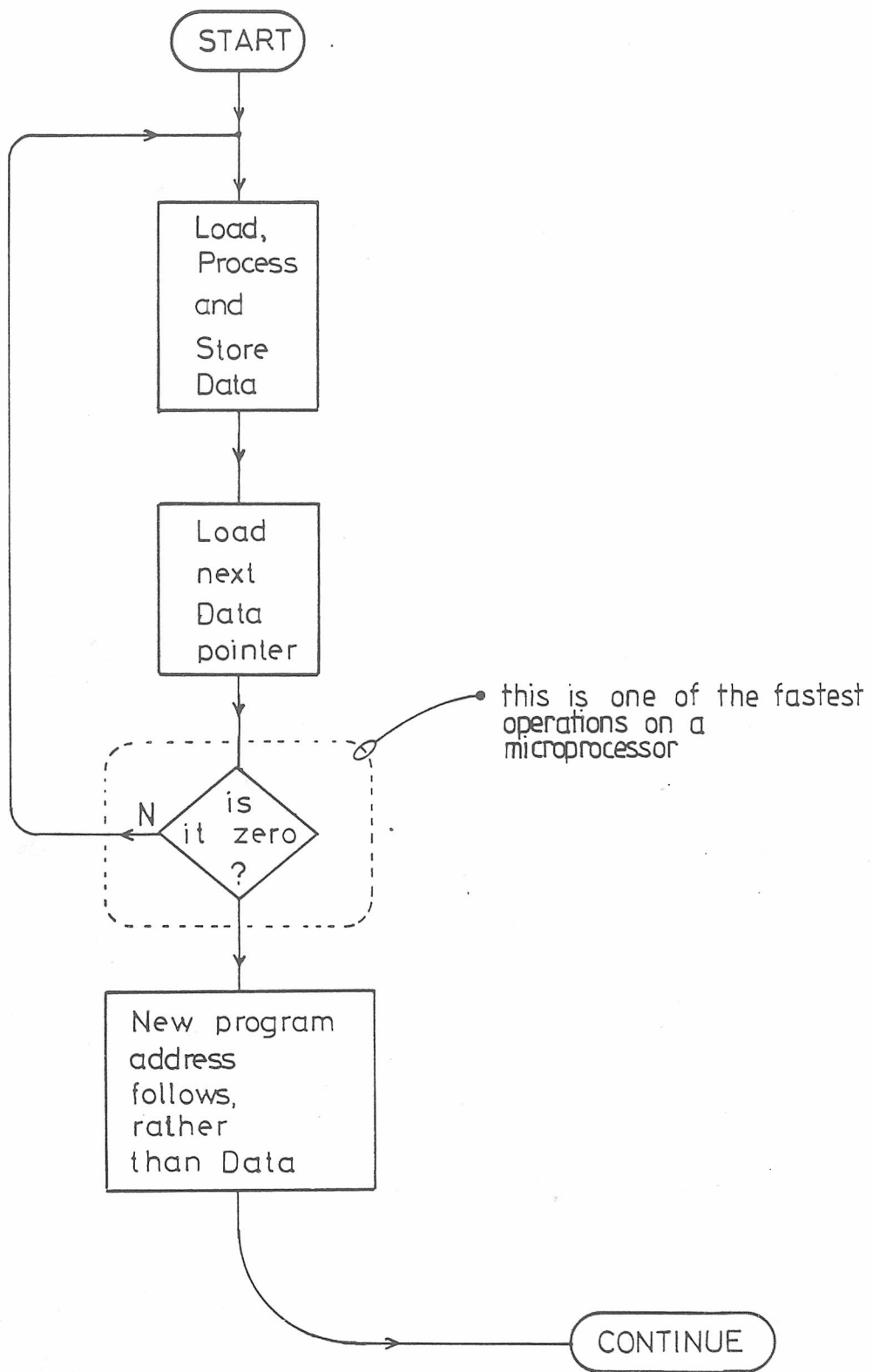where W has the form: $W_N = e^{-2\pi j/N}$

Figure 6·4 The basic unit of FFT – "the Butterfly"

Figure 6·5 Signal flow graph for four points using the Cooley-Tukey decimation in frequency algorithm

```
  ¦
  ¦
  ¦
  ¦
  ¦
B1    address of next part of program
  6┐
  8 │
 10 │
    ├──── data pointers
  7 │
  9 │
 11┘
  Ø    end marker for B1 execution
 B2    address of next part of program
  ¦
  ¦
  ¦
  ¦
  ¦
```

A section of the knotted thread

Figure 6·6

START

Load,
Process
and
Store
Data

Load
next
Data
pointer

this is one of the fastest
operations on a
microprocessor

N   is
it zero
?

New program
address
follows,
rather
than Data

CONTINUE

Internal structure of all the butterflies

Figure 6·7

Butterfly name	Number of additions and subtractions	Number of multiplications	Execution time (μS)
BUT1Ø	4	Ø	53
BUT1225	6	2	123
BUT127Ø	4	Ø	53
BUT1315	6	2	128
BUTT1	8	3	93
BUTTOV1	8	3	95

Butterfly execution times measured on a 5MHz 8086

Figure 6·8

Number of points transformed	Estimated time (mS)	Measured time (mS)
32	6	7.5 (5MHz) (8086)
64	15	
128	36	
256	85	
512	195	
1024	435	890 (8MHz) (8086)

FFT execution time estimates and measures

Figure 6.9

System 1:

memory	8086 16 bit processor	clock.
2k RAM + 8k PROM		5 MHz

System 2:

memory	8086 16 bit processor	clock
128 k RAM NO PROM		8 MHz
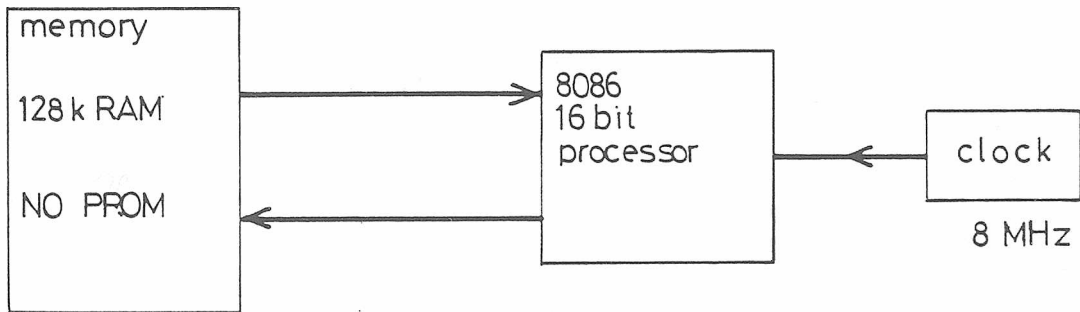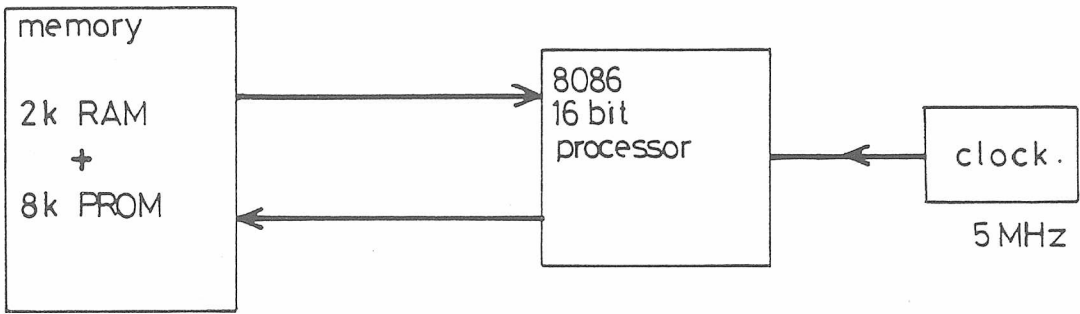
Comparison of the two systems used

Figure 6·10

DATA (Hi)

Hi - byte PROM bank

PROM   PROM   PROM

ADDRESS bus
$(A_1 - A_{20})$

Lo - byte PROM bank

PROM   PROM   PROM

DATA (Lo)

buffer A   DI

A

buffer B

B

buffer C   DO

C

S100 data busses

A_0

decode logic

S100 status bus

A
B
C
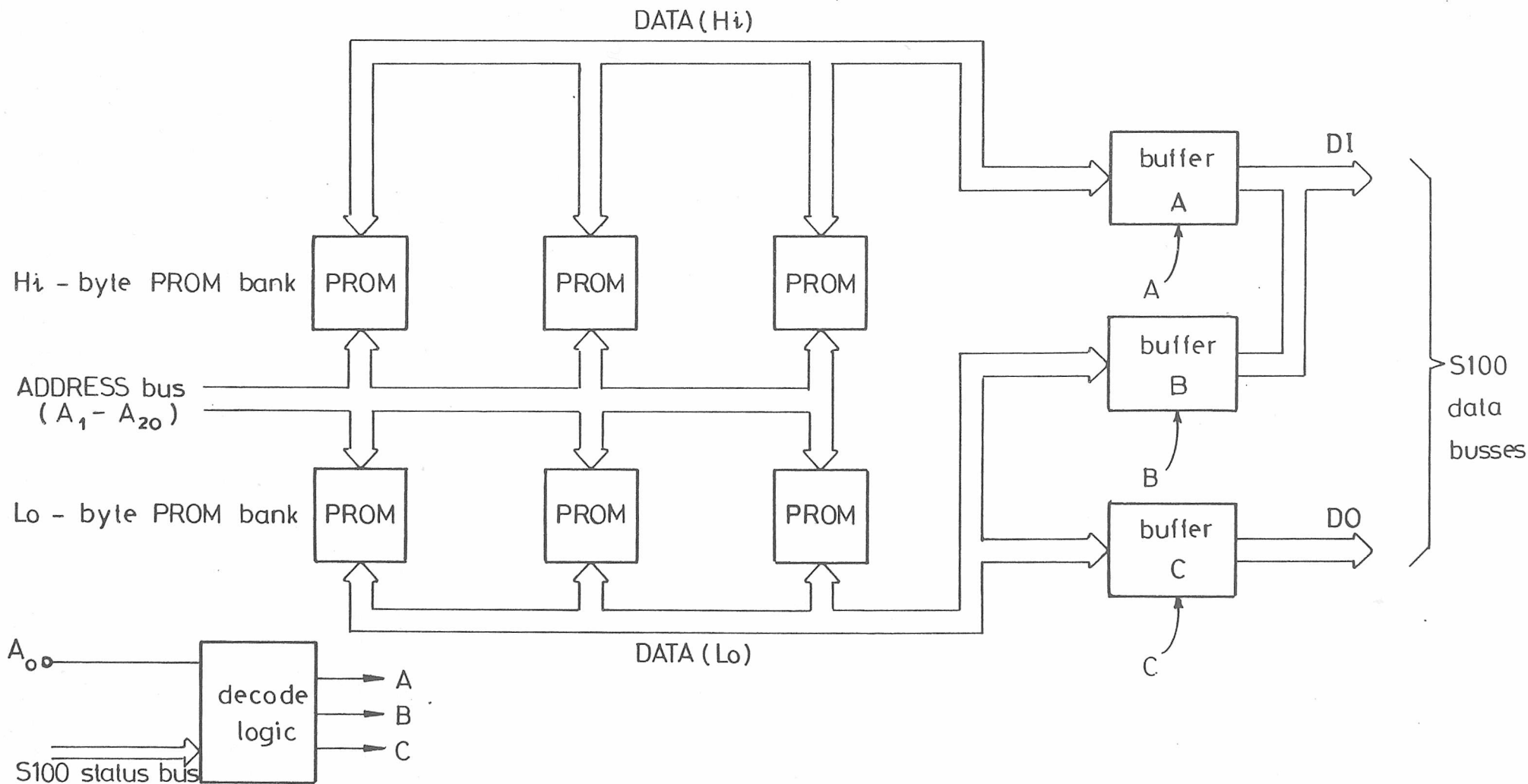
S100 bus modifications for a 16-bit PROM board using
three buffers to route the data

Figure 6·11

sampling time

Values at
either end
do not
correspond
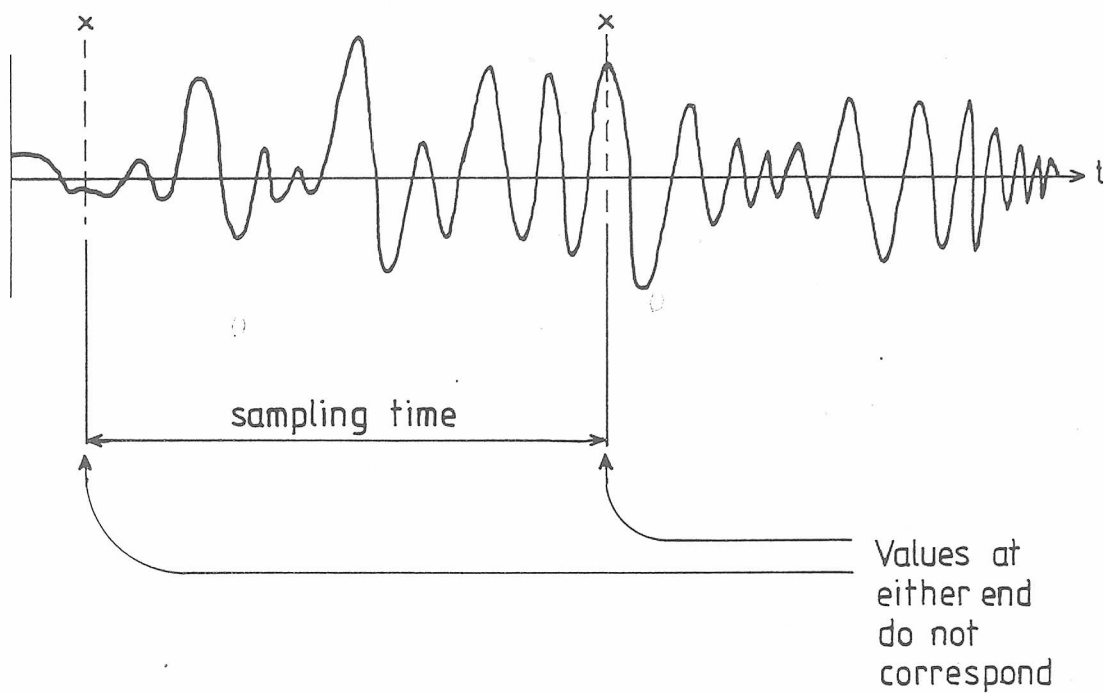
The signal must be weighted, or windowed to remove these
"end effects"

Figure 6·12

(a) Rectangular or "Box-Car"
Window

(b) Cosine^2 or "Hanning"
Window
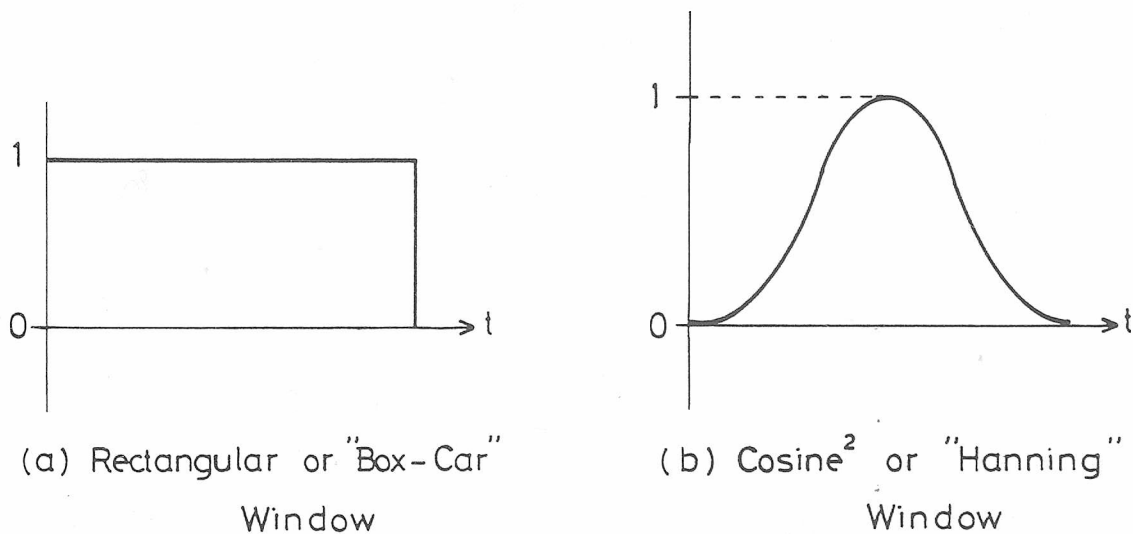
Two forms of Window most commonly
used

Figure 6·13
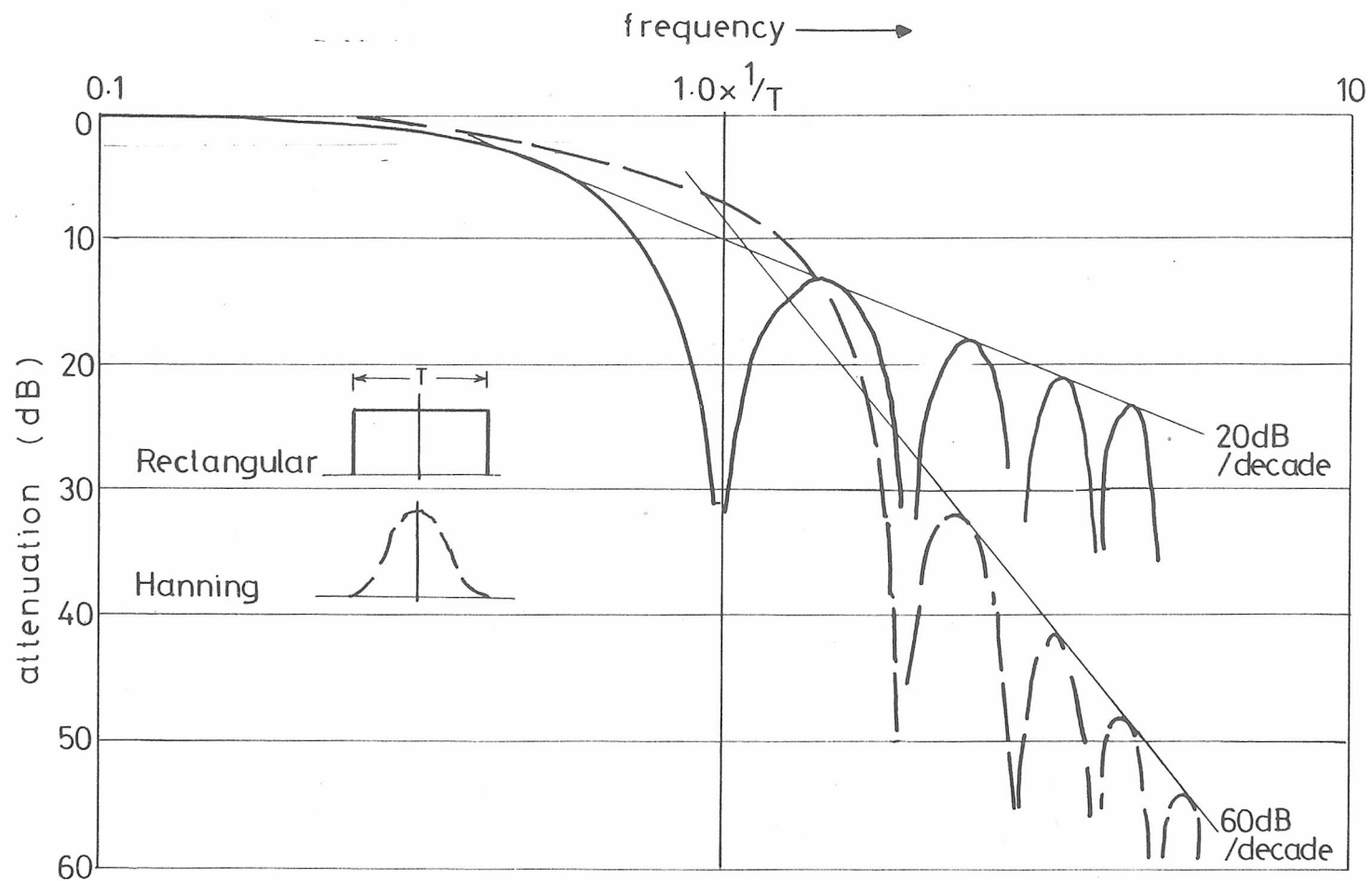
Equivalent filter bandwidths of a Rectangular and a Hanning Window function

Figure 6·14
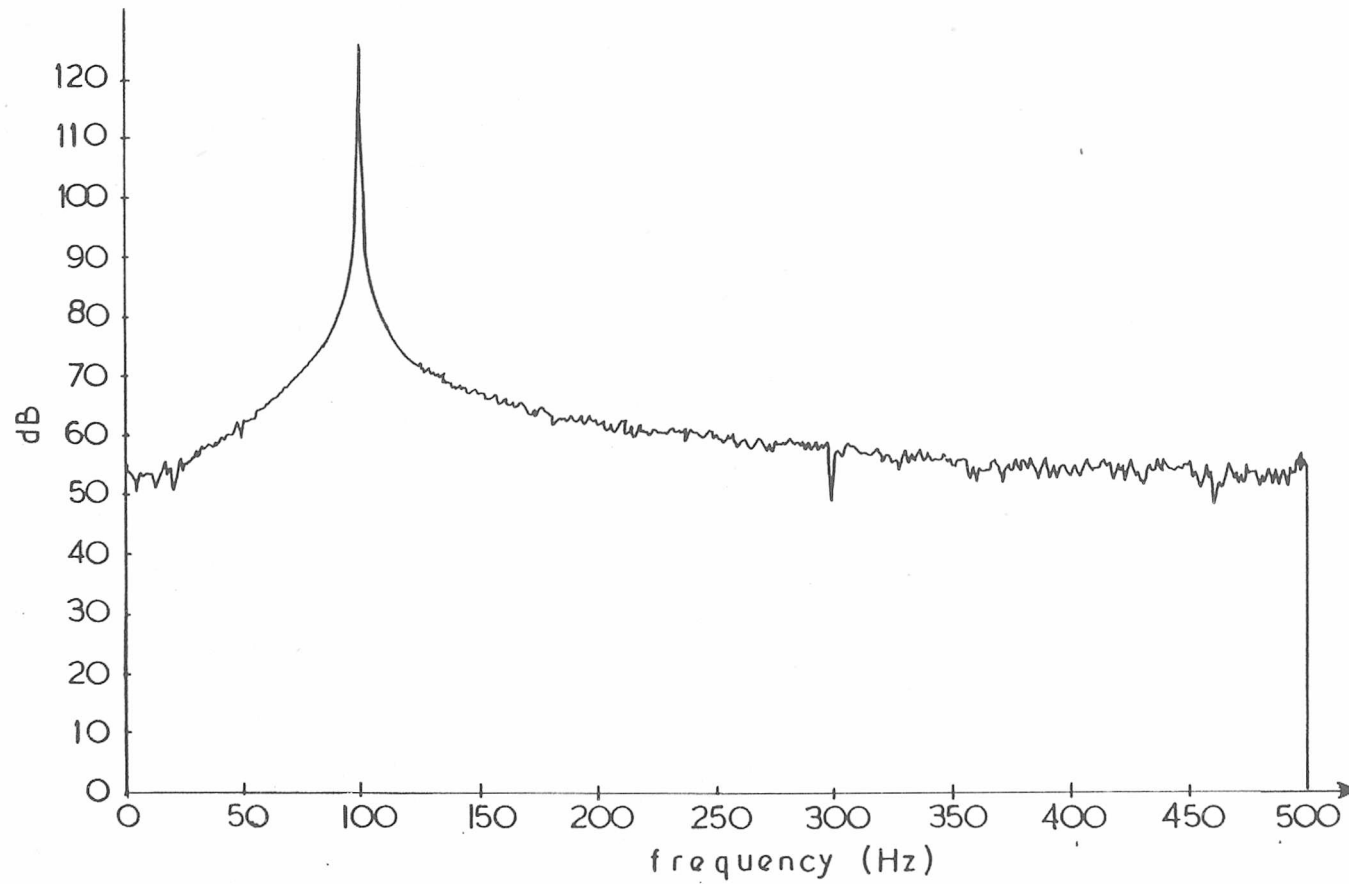
Figure 6·15 Fourier transform of a 100 Hz sinewave
with a rectangular window function
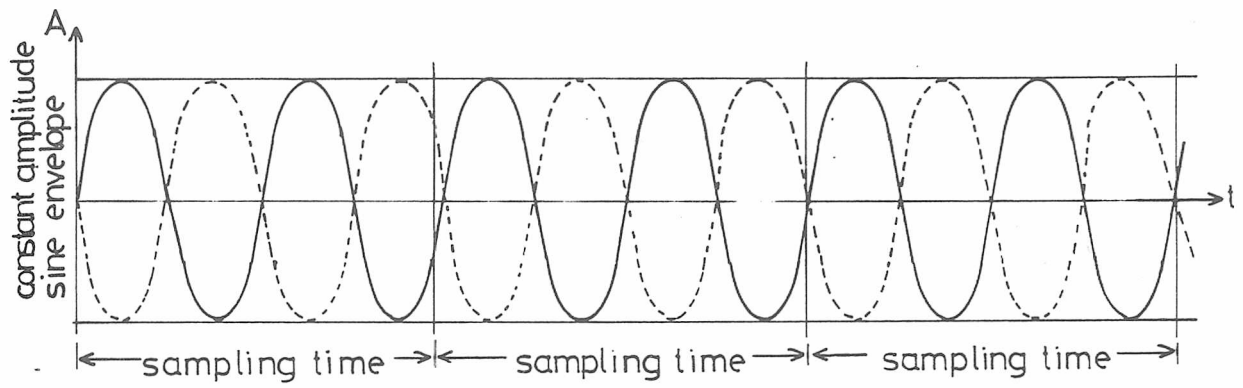
(a) signal before windowing
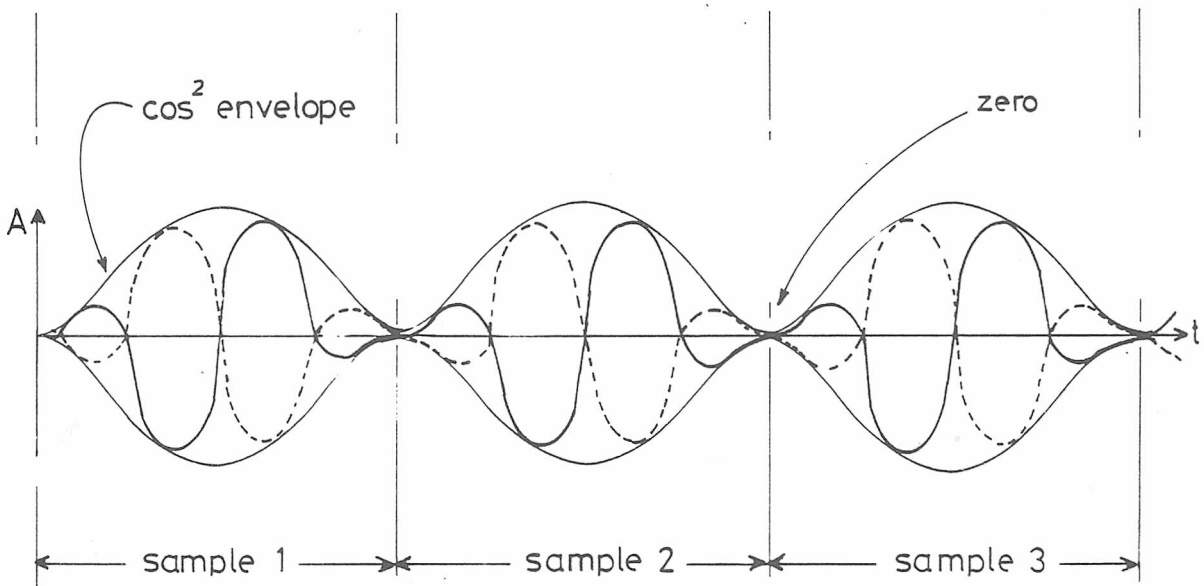
(b) after windowing, the signal is exactly periodic
within the sample time, giving a cleaner transform

Figure 6·16
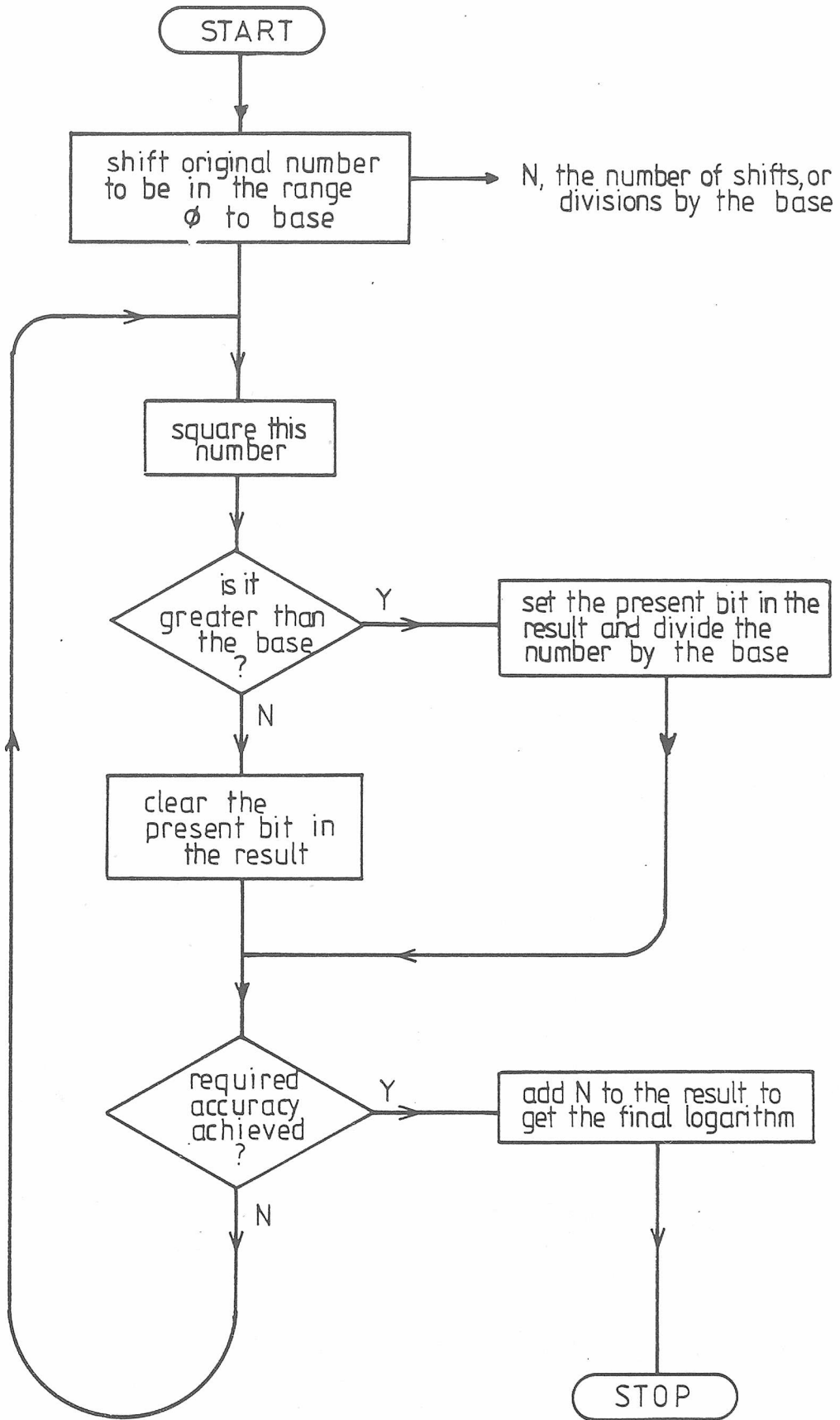
Flow chart for the logarithm transform

Figure 6·17

Re

Im

Re

Im

Re

Im

Re

Im

these samples are zero for a Real Signal
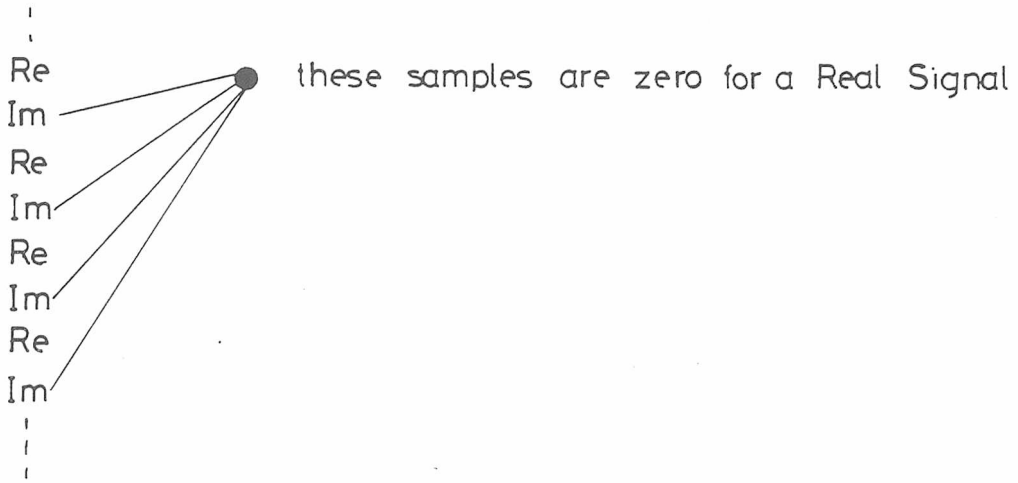
A Real Signal may be written as :

$$e(t) \;=\; Re(t) + 0j$$

(a) Storage is wasted for Real Signals

Re A

Re B

Re A

Re B

Re A

Re B

Re A

Re B

imaginery components filled with samples for the second channel.
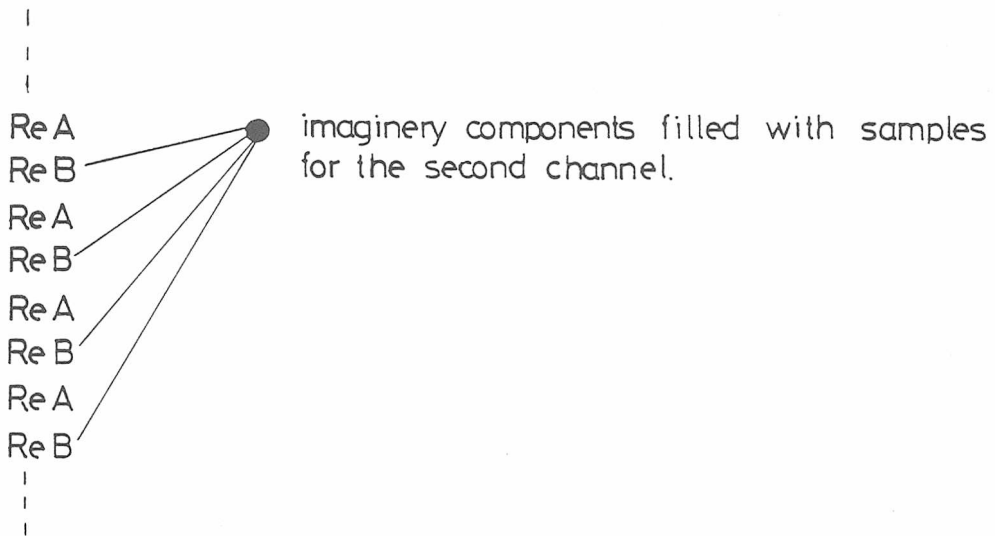
(b) A composite signal may be formed from signals A and B to give :

$$e(t) \;=\; ReA + jReB$$

Figure 6.18

the composite signal:

$$e(t) = \text{ReA} + j\text{ReB}$$

will have a Fourier transform:

$$X(f) = Z(k), \quad k = 0 - N - 1,$$
$$Z(k) \text{ is complex}$$

the two separate transforms are then recovered when:

$$A(f) = \tfrac{1}{2}\left(Z^*(N-k) + Z(k) \right)$$

$$B(f) = \tfrac{1}{2}\left(Z^*(N-k) - Z(k) \right)$$

where * means the complex conjugate

Figure 6·19

Data storage $\left(\begin{array}{c}\text{input}\\\text{and}\\\text{output}\end{array}\right)$	Program Code	Table of sine and cosine values
8K bytes	18K bytes	3K bytes
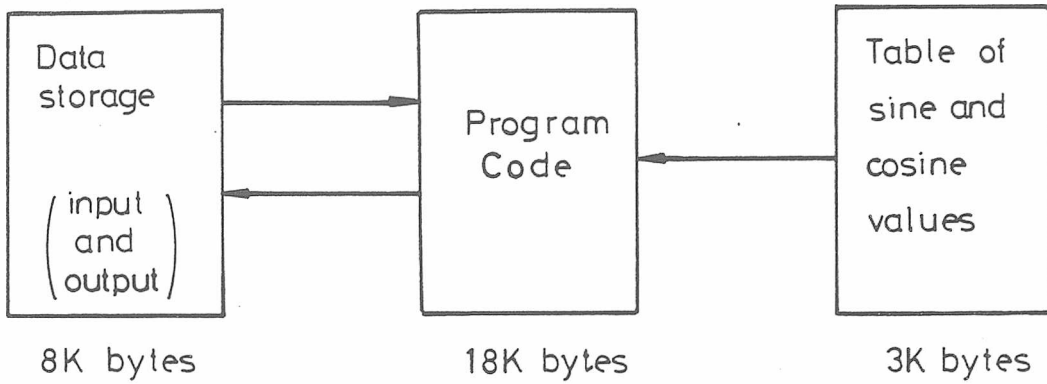
The FFT program needs three distinct memory areas

Figure 6·20

DS:⟶ Channel 1 data buffer   ES:⟶ Channel 2 data buffer
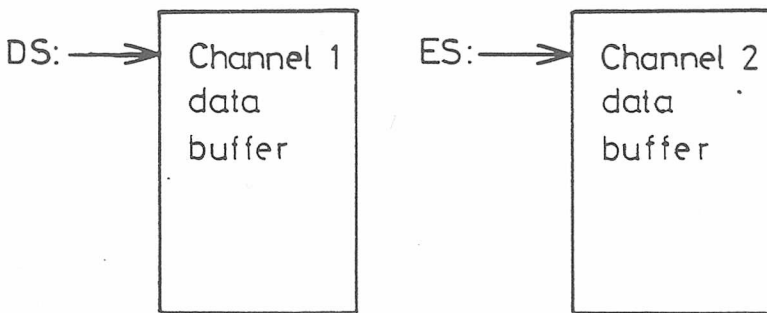
The DS: and ES: segment registers of the 8086 are used
as pointers to the two buffers, changing channels is
achieved by swopping the contents of these registers

Figure 6·21

CHAPTER 7.

7.1   Overview of Project.

This project has endeavoured to advance the application of signal processing techniques to the condition monitoring of asynchronous induction motors. Many techniques have been used successfully on the monitoring of mechanically based faults in gears and bearings, but little has appeared on the diagnosis of electrically based faults.

The underlying mechanisms in these faults have been investigated, and the effects caused by mechanical and electrical means separated. This was achieved by the use of signals which reflect different aspects of the motor – viz. vibration for the combined mechanical and electrical effects, and flux for the electrical effects. Correlation of these allows a further understanding of the mechanisms behind the faults to be gained. Having achieved this, the necessary processing, to be applied to carefully chosen signals from transducers mounted on a machine, has been developed. It has been shown that considerable information is available as to the machine's running condition, purely from external measurements. This has the advantage that the machines need not be modified in any way to allow the techniques developed here to be applied.

The signals used to develop the condition monitoring processing were derived from a test rig consisting of a real machine. This gives greater validity to the results than would a mathematical simulation of the situation, or simulation by a modified machine.

Single phasing faults - associated with severed supply lines have been catered for. The importance of detecting such failures as a part of condition monitoring is in the speed of detection. It is normal practice to protect motors by the installation of over-current circuit breakers. However, to obtain reliable service under conditions such as direct on-line starting, these may be set at too high a level. As the detection of such a fault is easily implemented within the monitoring system, its inclusion is justified.

Broken rotor bars, on the other hand are a more serious application of condition monitoring techniques. The nature of such faults - being internal, and not easily seen on visual inspection, makes them difficult to detect by conventional maintainance strategies. Their presence may not be immediately fatal to the motor, but they will reduce its performance and increase the losses, and may contribute to premature failure by overheating before the rotor itself fails. The detection of these by Cepstrum analysis of the vibration and stray flux signals from a motor is a very powerful technique - allowing a direct indication of the state of the motor in these terms, although longer term monitoring is always desirable. This is especially true when it is considered that a motor, whilst being in perfectly sound running order, may give a positive result to this test. This is based on the mechanism that is being observed, namely the resistance of the rotor bars. Some motors exhibit the characteristic sidebands even when in good condition, because the process by which the rotor was manufactured has resulted in high resistance joints in the rotor. Long term monitoring based on trend analysis is then the only reliable

82

method of detecting broken bars.

7.2   Conclusions.

The power of signal processing applied to machine condition monitoring has been demonstrated in this thesis. A standard motor has been investigated in a controlled environment, and the mechanical and electrical nature of fault mechanisms determined. This then allowed the form of a signal processing regime to detect and diagnose these faults to be developed.

Due to their basis on irrational functions, viz. sinusoids and cosinusoids, the method of Fourier Transformation from the time domain to frequency domain is not the most desirable for a digital implementation, due to the inherent presence of truncation errors. In an attempt to overcome this, a second set of orthogonal functions was investigated. The Walsh Transforms which result from these are based on the values of plus and minus unity only. This removes the problems of truncation, caused by finite word lengths in a microprocessor, and also leads to a much faster transform, as there are no multiplications, but only additions and subtractions. However, they give an output which is generally more complex than a Fourier Transform, and have other properties which do not lend themselves to condition monitoring. It is concluded that Walsh Transforms are not appropriate to this application.

The processing used to detect and diagnose the machine faults are existing ones, but have not found application to electrically based phenomena. Their use has proven to be very powerful in the field of mechanical faults, and this thesis has

83

shown that they may also be applied to electrical faults with good effect.

A system of test procedures, all of which may be performed automatically was thus developed to diagnose these faults. They are constructed in a sequential fashion, so that one test may follow directly from the previous one, using the data produced as input for further processing. This saves time in processing new data, and also improves the data reduction capabilities of the monitoring.

To this end, a single figure may be extracted from the processing for each fault investigated. These "confidence factors" may then be stored for future reference.

7.3   Future Work.

As this research has proceded, new areas for study have become apparent. This further work can be placed in three main categories:- trend analyses, investigation of further fault conditions and in the application of new signal processing devices, to condition monitoring.

Trend Analysis.

Although the "confidence factors" have been found to change significantly between "good" and "fault" conditions, a reliable means of fault diagnosis cannot rely on this alone. Many other factors can influence the signals derived from a machine in normal working conditions, other than actual faults. This means that the results from test must be recorded over a period of time, and any diagnosis based on an evaluation of the trends in

these results rather than a single test.

Other Faults.

The work here has covered two faults, ie supply failures and broken or cracked rotor bars. Whilst these are important, they are by no means the only conditions which should be considered by a general condition monitoring system eg. rotor-stator eccentricity.

New Signal Processing Hardware.

In recent years, the increase in interest in signal processing, and the rapid developments in large scale integration have opened up many possibilities. Amongst these are devices which may be configured to perform a specific signal processing task, such as Fourier Transforms, at a very high speed. This allows more powerful processing within a given time, or conversely a faster turn-round of test results.

REFERENCES.

1. CHAPMAN R.M.

    Vibration Analysis Applied to Machinery Maintainance.

    Naval Engineer's Journal, June 1967, pp 431 - 437.

2. Bowen K.A., Graham T.S.

    Noise Analysis: A Maintenace Indicator.

    Journal of Mechanical Engineering, October 1967, pp 31 - 33.

3. Banister R.L., Donato V.

    Signature Analysis of Turbomachinery.

    Journal of Sound and Vibration, September 1971 pp 14 - 21.

4. Kohler H.K., Pratt A. and Thompson A.M.

    Dynamics and Noise of Parallel-axis Gearing.

    Proceedings of the IMechE., Volume 184, part 30, pp 111 -
    121.

5. Ehrich F.F.

    Sum and Difference Frequencies in Vibration of High Speed
    Rotating Machinery.

    Journal of Engineering for Indusrty, February, 1972, pp 181 -
    184.

6. Eshelman R.L.

    The Role of Sum and Difference Frequencies in Rotating
    Mahchinery Fault Diagnosis.

    IMechE Conference Paper C272/80, 1980, pp 145 - 149.

7. Hemmings R.C. and Smith J.D.

   Information from Bearing Vibration.

   IMechE Conference Paper C177/76, 1976, pp 117 - 121.

8. Downham E.

   Vibration in Rotating Machinery: Malfunction Diagnosis - Art

   and Science.

   IMechE Conference Paper C160/76, 1976, pp 1 - 6.

9. France D. and Grainger H.

   Investigation of a DC Motor Vibration Problem.

   IMechE Conference Paper C262/80, 1980, pp 83 - 90.

10. Taylor J.I.

    Fault Diagnosis of Gears using Spectrum Analysis.

    IMechE Conference Paper C275/80, 1980, pp 163 - 168.

11. Randall R.B.

    Gearbox Fault Diagnosis using Cepstrum Analysis.

    Proceedings of the 4th. World Congress on the Theory of

    Machines and Mechanisms,

    Volume 1, IMechE, London, 1975, pp 169 - 174.

12. Randall R.B.

    Advances in the Application of Cepstrum Analysis to Gearbox

    Diagnosis.

    IMechE Conference Paper C276/80, 1980, pp 169 - 174.

13. Alger P.L.

    Induction Machines,

    Gordon and Breach, 1970.

14. Helms H.D.

    FFT Method of Computing Diffrence Equations and Simulating
    Filters.
    IEEE transactions on Audio and Electroacoustics,
    Volume AU 15, no. 2, June 1967, pp 85 - 90.

15. Otnes R.K.

    An Elementary Design Procedure for Digital Filters.
    IEEE Transactions on Audio and Electroacoustics,
    Volume AU 16, no. 3, September 1968, pp 330 - 335.

16. Helms H.D.

    Non-recursive Digital Filters: Design Methods for Achieving
    Specifications on Frequency Response.
    IEEE Transaction on Audio and Electroacoustics,
    Volume AU 16, no. 3, September 1968, pp 336 - 332.

17. Rader M. and Gold B.

    Digital Filter Design Techniques in the Frequency Domain.
    Proceedings of the IEEE, Volume 55, no. 2, 1967, pp 149 -
    171.

18. Kay S.M. and Marple S.L.

    Spectral Analysis - a Modern Perspective.
    Proceedings of the IEEE, Volume 69 no. 11, november 1981, pp
    1380 - 1419.

19. Cochran W.T. and Cooley J.W.

    What is the FFT?
    IEEE Transactions an Audio and Electroacoustics,
    Volume AU 15, no. 2, June 1967, pp 44 - 55.

20. Bingham C, Godfrey M and Tukey J.W.

    Modern Techniques of Power Spectrum Estimation.

    IEEE Transactions on Audio and Electroacoustics,

    Volume AU 15, no. 2, June 1967, pp 56 - 66.

21. Cooley J.W., Lewis P.A.W. and Welch P.D.

    Historical Notes on the Fast Fourier Transform.

    IEEE Transactions on Audio and Electroacoustics,

    Volume AU 15, no. 2, June 1967, pp 76 - 79.

22. Bergland G.D.

    Fast Fourier Transform Implementations - an Overview.

    IEEE Transactions on Audio and Electroacoustics,

    Volume AU 17, no.2, June 1969, pp 104 - 105.

23. Bergland G.D. and Wilson D.E.

    A Fast Fourier Transform Algorithm for a Global, Highly
    Parallel Processor.

    IEEE Transactions on Audio and Electroacoustics,

    Volume AU 17, no.2, June 1969, pp 125 - 127.

24. Welch P.D.

    A Direct Method of Power Spectrum Estimation.

    IBM Journal, April 1961, 141 - 156.

25. Wesley M.A.

    Associative Parallel Processing for the Fast Fourier
    Transform.

    IEEE Transactions on Audio and Electroacoustics,

    Volume AU 17, no.2, June 1969, pp 162 - 165.

26. Pease M.C.

   An Adaption of the Fast Fourier Transform Proceedure for Parallel Processing.

   Journal of the Association of Computing Machinery,

   Volume 15, no.2, April 1968, pp 252 - 264.

27. Bogert B.F., Healey J.R. and Tukey J.W.

   The Quefrency Alanysis of Time Series for Echoes: Psuedo-autocovariance Cross-cepstrum and Saphe Cracking.

   Proceedings of the Symposium on Time Series Analysis, edited by Rosenblatt M., Wiley N.Y., 1963, pp 169 - 174.

28. Cooley J.W., Lewis P.A.W. and Welch P.D.

   Application of the Fast Fourier Transform to Comparison of Fourier Integrals, Fourier Series and Convolution Integrals.

   IEEE Transactions on Audio and Electroacoustics Volume,

   AU 15, no.2, June 1967, pp 79 - 84.

29. Walsh J.L.

   A Closed Set of Orthogonal Functions.

   American Journal of Mathematics,

   Volume 55, 1923, pp 5 - 24.

30. Lackey R.B. and Meltzer P.

   A Simplified Definition of Walsh Functions.

   IEEE transactions on computers, February, 1971, pp 211 - 213.

31. Kitai R. and Siemens K.H.

   Discrete Fourier Transform via the Walsh Transform.

   IEEE transactions on Acoustics, Speech and Signal Processing,

   Volume ASSP 27, no.3, June 1979, pp 288.

32. Munniappan K. and Kitai R.

Microprocessor based Walsh Function Spectral Analyser.

IEEE Transactions on Instrumentation and Measurement,

Volume IM 28, no.4, Dec 1979, pp 295 - 299.

33. Siemens K.H. and Kitai R.

Digital Walsh-Fourier Analysis of Periodic Walsh Functions

Waveforms.

IEEE Transactions on Instrumentation and Measurement,

Volume IM 18, no.4, Dec 1979, pp 316 - 321.

34. Walmsley W.M.

Walsh Functions, Transforms and their Applicatons.

Electronic Engineering, June 1974, pp 63 - 68.

35. Blachman N.M.

Sinusoids versus Walsh Functions.

Proceedings of the IEEE, Volume 26, no.3, March 1974, pp 346
- 353.

36. Harmuth H.F.

A Generalised Concept of Frequency and some Applicatios.

IEEE Transactions on Information Theory,

Volume IT 14, no.3 May 1968, pp 375 - 382.

37. Frankel H.D.

Applications of Walsh Functions.

Foreword to the Conference on the Theory and Application of

Walsh and Other Non-sinusoidal Functions, Hatfield, England,

June 1971, pp 134 - 136.

38. Elliot A.R. and Shum Y.Y.

A Parallel Hardware Implementation of the Fast Hadamard and Walsh Transforms.

Conference on the Theory and Application of Walsh and Other Non-sinusoidal Functions, Hatfield, England, June 1972, pp 181 - 183.

39. Beauchamp K.G.

Waveform Synthesis using Fourier and Walsh Series.

Conference on the Theory and Application of Walsh and other Non-sinusoidal Functions, Hatfield, England, June 1973, pp 1 - 12.

40. Landwehr G.

A Comparison of Discrete Walsh and Fourier Transforms.

Conference on the Theory and Application of Walsh and Other Non-sinusoidal Functions, Hatfield, England, June 1973, pp 1 - 22.

41. Tadokoro Y. and Higuchi T.

Discrete Fourier Transform Computation via the Walsh Transform.

IEEE Transactions on Acoustics, Speech and Signal Processing, Volume ASSP 26, no. 3, June 1974, pp 236 - 240.

42. Noll A.M.

Cepstrum Pitch Determination.

Journal of the Acoustical Society of America, Volume 41, no. 2, 1967, pp 293 - 309.

43. Childers D.C. Skinner D.P. and Kemerait C.R.

    The Cepstrum: A Guide to Processing.

    Proceedings of the IEEE,

    Volume 65, no. 10, October 1977, pp 1428 - 1443.

44. Thomson W.T. and Low A.J.

    RGIT,

    The Design and Construction of a Special Purpose, Production

    Motor Test Rig. Private Communication.

45. Penman J., Dey M., Stronach A.F. and Hardwick J.G.

    A Microprocessor Based Machine Protection System.

    The 17th University Power Engineering Conference, Leicester,

    1980.

46. Brigham E.O.

    The Fast Fourier Transform.

    Prentice Hall, 1974, ISBN 0-13-307496-X.

47. Eckhouse R.E. and Morris L.R.

    Minicomputer systems.

    Prentice Hall, 2nd Edition, ISBN 0-13-583922-X.

48. Knuth D.E.

    The Art of Computer Programming.

    Addison-Wesley, 2nd Edition, 1973.

49. Eckhouse and Morris.

    Minicomputer Systems.

    Prentice Hall, 2nd Edition, ISBN 0-13-5883922-X, pp 337

50. Application of B&K Equipment to Frequency Analysis,

   Bruel and Kjaer, Naerum, Denmark,September 1977, pp 125.

APPENDIX: CONFERENCE PAPERS.

CONDITION MONITORING OF INDUCTION MOTORS FOR AVAILABILITY ASSESSMENT IN OFFSHORE INSTALLATIONS

W.T. Thomson, N.D. Deans, R.A. Leonard, A.J. Milne

Robert Gordon's Institute of Technology,

Aberdeen, AB9 1FR, Scotland, U.K.

Introduction

In offshore oil and gas production platforms and in onshore refinery installations the three-phase squirrel-cage induction motor (SCIM) is used to drive gas compressors, sea water injection pumps and oil exporting pumps. Consequently, the assessment of the condition of the motor and its future availability are important, since failure caused by one of a number of fault conditions is costly and potentially dangerous. This is particularly evident when oil production and refinery installations are being considered. Here the handling costs associated with plant removal and loss of production makes down-time unacceptable unless absolutely necessary. It is essential therefore that the operator knows the condition of the motor while it is in service and if possible is able to predict when a motor might fail.

It has generally been believed by many engineers responsible for plant monitoring that damage and wear in rotating machines can be detected by analysing vibration signals and by monitoring shaft motion. It is true that the vibration signal contains information relating to damage and wear but the spectrum also contains information about the normal operation of the motor. The inherent difficulty is the separation of these two aspects of signal information. This is particularly difficult with a three-phase squirrel-cage induction motor since the resulting vibration spectrum is a by-product of electromagnetic forces and the normal mechanically transmitted forces.[1] Due to the motor being a complex electromechanical device, the fault mechanisms can be electrical, mechanical or electromechanical in nature. This means that the normal on-line protection devices for sensing overload and earth leakage currents and excessive bearing, winding and core temperatures are insufficient, and additional on-line monitoring techniques are required. One approach involves time consuming analysis of vibration data coupled with an in-depth appreciation of plant behaviour

assisted by historical records of performance.[2] This leads
to a monitoring system based essentially on experience and
can be particularly difficult to operate in an offshore
installation due to such factors as the staff working shift
cycles, 'hot' work permits being required and the generally
hostile environment. A second approach and the one being
considered as the main objective of the work referred to in
this paper seeks to identify the fundamental causes of
various electromechanical faults and to develop an on-line
data processing system for detecting faults and predicting
the availability of the motor.

The initial results of the research work are presented in the
paper and are primarily concerned with providing a data base
for identifying faulty SCIMs, with a view to developing fast
and efficient processing techniques which are particularly
applicable to SCIM fault recognition. The results of a
survey carried out to determine the existing monitoring
techniques and data collection methods currently being used
for 3-phase induction motor fault recognition is presented,
and the types of failure and their frequencies of occurrence
are also reported. A brief discussion of the fault
mechanisms and the development of a fault producing test rig
is presented. The data acquisition and computer processing
system is described, a data bank of the processed signals
for 'healthy' and 'unhealthy' machines is presented and the
results discussed.

Survey of Monitoring Techniques and Failure Mechanisms of 3-phase Squirrel-cage Induction Motors

A survey of a variety of major industrial organisations using
large SCIMs in the offshore and onshore environment was
conducted to gain information about the types of failure of
SCIMs and the methods used for monitoring the condition of
the machine. A questionnaire was sent to each of the
operators and consisted of two sections. The first was
concerned with identifying what types of condition monitoring
techniques are currently being used and to also test the
operators' reaction to the concept of on-line condition
monitoring as part of an on-condition maintenance strategy.
The second section consisted of specific questions on the
types of failure to assess if there is a real need for
developing on-line diagnostic techniques for SCIM fault
recognition.

All of the industrial organisations completed Section 1 and
six out of the eleven operators provided specific information
about motor failures. The results are presented in Tables 1
and 2 respectively. A 100% response was not expected in
Section 2 because the collection and compilation of the data

required a considerable effort in terms of man hours. Since the information gives details on the types of failure and frequencies of occurrence of eighty-two SCIMs in the range from 425 kW to 6.3 MW, the results are able to provide sufficient information for deciding whether or not a problem exists in SCIM fault recognition.

The main conclusions from the survey and personal discussions with the operators are :

(a)   There can be considerable savings in maintenance procedures, outage time of plant and loss of revenue if reliable condition monitoring techniques are available as part of an On-condition maintenance strategy.

(b)   Due to the number of failures reported by the operators, there is a need for fundamental studies of various types of fault mechanisms to be undertaken, and to also develop signal processing techniques to provide a data base for classification of 'healthy' and 'unhealthy' motors.

(c)   The operators would welcome the development of a flexible microprocessor-based instrumentation system capable of performing an on-line analysis of different types of signal (e.g. vibration, current, stray flux) which could also identify the various types of fault mechanisms and assess the availability of the SCIM.

Fault Mechanisms

In response to the survey and additional discussions with other industrial users it was decided to investigate the following faults :

(a)   Inter-Turn Winding Faults

The insulation between turns of a coil can breakdown due to contamination, thermal ageing or vibrational stresses. The breakdown process causes heating in the winding and a change in the current distribution which leads to a complete failure of the motor's insulation system.

(b)   Broken Rotor Bars

This usually occurs when one of the conducting bars which forms part of the 'squirrel-cage' rotor winding breaks where it is joined to the conducting

end ring. The bars adjacent to the broken one carry extra current and overheat which in turn generally leads to additional broken bars. This results in torque pulsations, speed fluctuations and changes in the vibration spectrum and can lead to mechanical damage of the rotor, stator bore or bearing assembly.

(c)   Static Rotor-Stator Eccentricity

In this situation, the axial centres of both rotor and stator are not coincident. This results in increased vibration levels and could lead to bearing failure.

(d)   Single-Phasing

This is the term used when one of the supply lines or windings becomes open circuited. This is a severe fault condition and results in high current and vibration levels.

The results of the survey also indicate that bearing failure in SCIMs is a major problem. This is rather surprising since bearing fault detection has received considerable attention from researchers and industrial operators[3-7]. The difficulty of operating a vibration monitoring programme in a hostile environment has been mentioned and it is here that there is a need for the development of bearing monitoring techniques and instrumentation suitable for the offshore environment.

Previous investigators have tended to look at individual machine signals to determine the existence of a fault. Erlicki[8] has shown how axial flux could be used to indicate non-symmetric supply conditions. Penman[9,10] has clearly shown how inter-turn faults can be detected with axial flux but found the use of axial flux inconclusive for detecting broken rotor bars and dynamic rotor-stator eccentricity. Gaydon[11,12] has developed instrumentation techniques using shaft speed fluctuations as the signal source for the detection of broken rotor bars but has stated that "inherent asymmetries were found to give period fluctuations of the same magnitude as when one bar was deliberately open circuited." Hargis[12] has considered changes in the current and vibration spectra for detecting broken rotor bars but has only presented one set of results for a good rotor and one with three broken bars. Steele[13] has monitored current for the detection of electromechanical faults in small-power motors. His results clearly show the potential of the method but he states that "much further work is required to fully explain the current spectra and to produce a commercially viable system."

Hence the authors consider that further work is required
under controlled experimental conditions for the following
reasons :

    (i)   to evaluate the effectiveness of monitoring
             various types of signal

    (ii)   to explain fully the changes in the spectra

    (iii)   to develop signal processing techniques to
             highlight the fault conditions

    (iv)   to discriminate between the effects of high
             resistance joints, broken bars or end rings
             in squirrel-cage rotors

    (v)   to try and quantify the degree of severity of
             the different faults.

The philosophy proposed in this paper is to monitor various
interrelated motor signals such as vibration, current, end
winding leakage flux and axial flux during fault conditions
and to present a data base of spectra. It is envisaged that
an on-line monitoring system which utilizes three of four
types of signals for identifying a particular fault will
prove to be more useful than existing techniques which tend
to look for changes in only one type of signal.

Test Rig and Signal Processing Equipment

Figure 1 shows the test motor and associated processing
equipment. The test rig comprises an 11 kW SCIM loaded
by a d.c. dynamometer and has been specifically designed
for carrying out controlled experiments with the fault
mechanisms described in the previous section. A number of
transducers positioned on the test rig sense various
parameters for determining the condition of the motor, viz :

    T_I is an air-cored toroidal coil used to sense the
          electrical current in the main supply lead.

    T_ϕ is a coil situated on the exterior casing of
          the motor to sense the extent of the end
          winding leakage flux.

    T_{AX} is a coil wound on the main shaft of the
          induction motor to sense the degree of axial
          flux.

    T_V is an accelerometer positoned to respond to
          mechanical vibration of the casing or bearing
          pedestals.

The electrical signals emanating from the transducers are
pre-amplified, filtered and undergo frequency and time-domain
analysis in a high-resolution spectrum analyser. The
analyser exists as a peripheral device to a PDP11-03
minicomputer system, comprising an 11-03 processor, dual
floppy-disc storage unit, keyboard, visual-display unit,
printer and high-resolution plotter. The experimenter
controls, via the interactive terminal, the operation of the
analyser and the subsequent secondary processing of the
analysed signals. A library of data processing programs is
available to the experimenter to distil the data produced by
the analyser in such a way as to highlight particular machine
faults. Typical library programs are :

(i)   control the analyser, write and read spectral
       values to and from the analyser and provide
       automatic scaling of all data values.

(ii)   measure the energy content of the whole, or any
       part of the frequency spectrum of the signal
       emanating from any selected transducer.

(iii) determine the peak value of any frequency
       spectrum.

(iv)   compute the autocorrelation coefficient of the
       frequency spectrum for any given offset.

(v)   carry out a Fourier transform on a frequency
       spectrum, providing a Cepstrum of the original
       signal.

(vi)   control the plotting facility so that single
       and multidimensional plots of the processed
       data can be produced.

(vii) control the allocation of storage areas on the
       disc storage units so that historical records of
       experiments carried out on the induction motor
       can be accessed at a later date for inspection
       and comparison.

Test Results

There are various frequency components in each signal which
are expected from Induction machine theory.[14] For the
current, end winding leakage flux and axial flux signals
the expected frequencies are :

$$f_1 = F(Hz) \ldots \ldots \ldots \ldots \quad (1)$$

$$f_{SH} = F(R/P (1 - s) \pm n)(Hz). \ldots \quad (2)$$

and for the vibration signal :

$$f_{1V} = 2F(Hz) \quad \cdots \cdots \cdots \cdots \quad (3)$$

$$f_{SHV} = F(R/P (1 - s) \pm 2(n - 1))(Hz) \quad . \quad (4)$$

where   F   =   fundamental supply frequency (50 Hz)

R   =   number of rotor slots (28)

P   =   number of pole-pairs (2)

s   =   slip, 0.02 for full-load

n   =   1, 2, 3 . . . .

SH   =   slot harmonic

An FFT analysis was initially applied to all the transducer signals. Where it was difficult to identify the difference between signature patterns for normal and abnormal conditions, a zoom analysis was applied around specific frequency components. The frequency at which the zoom analysis is applied depends on the type of fault and signal being analysed. Equations 1 to 4 can be used for this purpose. Figures 2 to 37 show spectra of the signals for normal and fault conditions.

Preliminary observations of the results indicate that the spectra for the broken rotor bar fault contains many sidebands. These sidebands can be explained by the application of rotor asymmetry theory.[15]   A useful technique for determining the sideband content is cepstrum analysis.[16]   The main observations from the data bank of spectra are as follows :

(i)   Broken Rotor Bar

The tests were done under full-load operating conditions using two production type die-cast rotors. Both rotors have the same degree of dynamic balance but one has a broken bar. A spectrum analysis of the vibration signals is shown in Figures 2 and 3. The 0-2 kHz bandwidth spans the range of interest for detecting changes but it is difficult to observe any significant differences. However, using zoom analysis techniques, sidebands become apparent around the slot harmonic for the faulty rotor as indicated by comparing Figure 4 and 5. The same 'signature' patterns occur for the current, end winding leakage flux and axial flux signals, as shown in Figures 6 to 17. A cepstrum analysis was applied to highlight the increased sideband content, a sample of the results is

presented in Figures 39 to 46. The results clearly
demonstrate that this fault can be identified from four
signals. Based on the work so far the techniques will be
used for discriminating between the effects caused by high
resistance joints, number of broken bars or end rings.

(ii)   Inter-turn Winding Faults

A comparison between Figures 18 and 19 show that the 100 Hz,
200 Hz and 300 Hz vibration components increase when a
coil is short-circuited in the stator winding. In the axial
flux spectrum the 50 Hz, 100 Hz and 150 Hz components
increase, while in the current spectrum it is the 150 Hz
and slot harmonic frequencies which increase significantly,
as shown in Figures 20 and 21 and Figures 24 and 25
respectively. It was found that although there were changes
in the end winding leakage flux spectrum the sense (increase
or decrease) of the change was a function of transducer
position as indicated in Figures 22 and 23.

(iii)   Single-Phasing

Figures 23 to 33 indicate that the 100 Hz component has
a pronounced increase in both the vibration and axial flux
spectra. The 150 Hz component in the current spectrum is
also increased. As in (ii) the change in the end winding
leakage flux is a function of transducer position.

(iv)   Static Rotor-Stator Eccentricity

The only significant changes occurred in the slot harmonics
of the vibration spectrum as shown in Figures 34 to 37, and
that the sense of the change was a function of transducer
position around the motor's frame, as indicated in Figure 38.
Further work is required on the signal processing side to
try and detect changes in the other signals.

Conclusions

A study of the failure mechanisms of squirrel-cage induction
motors has been carried out and reported. The fault
mechanisms have been investigated under controlled
experimental conditions and a computer-based instrumentation
system has analysed signals representative of a motor's
supply current, axial flux, end winding leakage flux and
mechanical vibration. A comprehensive data bank of different
types of spectra for SCIM fault recognition has been
presented. The authors believe that this is the first time
a data bank of spectra in this form has been put into print.
The resulting data patterns reveal that different 'signatures'
exist for 'healthy' and 'unhealthy' motors. In addition,

three or four different types of signal may show a particular
pattern for one fault condition. The concept of looking for
changes in four signals as opposed to only one, has the
distinct advantage that an industrial user of SCIMs is more
likely to believe the former as an indication of a fault.
The tests have therefore been used to establish a data bank
of machine signatures for use in predictive maintenance
operations. Overall system reliability can then be improved.

Acknowledgements

References

1   Ellison, A. J., and Moore, C. J. : "Acoustic Noise and
     Vibration of Rotating Electric Machines", Proc I.E.E.,
     Vol. 115, No. 11, Nov. 1968.

2   Neale, M., and Associates. : "Guide to the Condition
     Monitoring of Machinery", HMSO, London, England, 1979,
     1SBN011 5121269.

3   Ray, A. G. : "Monitoring Rolling Contact Bearings
     under Adverse Conditions", 2nd Int. Conf. on Vibrations
     in Rotating Machinery, I. Mech. E., Conference
     Publications, 1980.

4   Downham, E. : "Vibration in Rotating Machinery :
     Malfunction Diagnosis - Art and Science", Int. Conf.
     on Vibrations in Rotating Machinery, I. Mech. E.,
     Conference Publications, 1976.

5   Hemmings, R. C., and Smith, J. D. : "Information from
     Bearing Vibration", ibid.

6   Stewart, R. M. : "Vibration Analysis as an Aid to the
     Detection and Diagnosis of Faults in Rotating Machinery"
     ibid.

7   Erskine, J. B., and Reeves, C. W. : "Vibration Problems on Rotating Machinery in the Chemical Industry", ibid.

8   Erlicki, M. S., Porat, Y., and Alexandrovitz, A. : "Leakage Field Changes of an Induction Motor as Indication of Nonsymmetric Supply", Trans. IEEE on Ind. and Gen. Appl., Vol. IGA-7, No. 6, Nov./Dec., 1971.

9   Penman, J., Hadwick, J. G., and Barker, B. : "Detection of Faults in Electrical Machines by Examination of the Axially Directed Fluxes", Third Int. Conf. on Electrical Machines, Brussels, 1978.

10   Penman, J., Hadwick, J. G., and Stronach, A. F. : "Protection Strategy Against the Occurrence of Faults in Electrical Machines", Int. Conf. on Developments in Power System Protection, IEE Publication, 1980.

11   Gaydon, B. G. : "An Instrument to Detect Induction Motor Rotor Defects by Speed Fluctuation Measurements", IEE Conf. on Electronic Test Measuring Instrumentation, Testmex 79, 1979.

12   Hargis, C., Gaydon, B. G., and Kamash, K. : "The Detection of Rotor Faults in Induction Motors", IEE Int. Conf. on Electrical Machines - Design and Applications, July, 1982.

13   Steele, M. E., Ashen, R. A., and Knight, L. G. : "An Electrical Method for Condition Monitoring of Motors", ibid.

14   Alger, P. L. : "The Nature of Induction Machines", Gordon and Breach Science Pub., 1965.

15   Jones, C. V. : "The Unified Theory of Electrical Machines", Butterworth Pub., 1967.

16   Bogert, B. P., Healy, M. J. R., and Tukey, J. W. : "Proceedings of the Symposium on Time Series Analysis", John Wiley and Sons, New York, 1963.

Monitoring Techniques & Types of Transducers	A	B	C	D	E	F	G	H	I	J	K	Percentage usage of Monitoring Techniques
Subjective look, feel and listen	Y	Y	Y	Y	Y	Y	Y	Y	Y	Y	Y	100%
Vibration monitoring as a general concept	Y	Y	Y	Y	Y	Y	Y	Y	Y	Y	Y	100%
Proximity transducers on plain bearings	Y	N	Y	Y	Y	N	Y	N	N	N	Y	54%
Accelerometers	N	N	Y	Y	Y	Y	N	Y	Y	Y	N	64%
Velocity transducers	N	Y	Y	N	Y	Y	N	Y	N	N	Y	54%
Vibration spectrum analysis	N	N	Y	Y	Y	Y	N	Y	Y	Y	Y	73%
Shock Pulse Monitoring for bearing defects	N	N	N	N	Y	N	N	Y	N	N	N	18%
Off-line computer processing of vibration signals	N	N	Y	N	Y	N	N	Y	N	N	N	27%
On-line computer based monitoring of vibration	N	N	N	N	N	N	N	N	N	N	N	0%
Winding temperature sensing	Y	N	Y	Y	Y	Y	Y	Y	N	Y	Y	82%
Stator core temperature sensing	Y	N	N	N	N	N	Y	N	N	N	N	18%
Bearing temperature sensing	Y	N	Y	Y	Y	Y	Y	Y	Y	Y	Y	91%
Megger insulation tests	Y	Y	Y	Y	Y	Y	Y	Y	Y	Y	Y	100%
Tan (δ) insulation tests	Y	N	Y*	N	Y	N	Y	Y	Y	N	Y	64%
ILA tests	Y#	N	Y*	N	N	N	Y	Y*	N	N	N	36%
Measurement of shaft voltages	Y	N	Y*	Y	Y	B	Y+	N	N	N	Y	54%
Wear debris monitoring	N	Y	N	N	N	N	Y	N	N	N	N	13%
Magnetic plugs	N	N	N	N	N	N	N	N	N	N	N	0%
Oil sample analysis	N	Y	Y#	N	N	N	Y#	N	N	N	N	27%
Squirrel-cage rotor bar monitoring	Y	N	N	N	N	N	N	Y	Y	N	N	27%
Ultrasonic discharge detector	N	N	N	N	Y	N	Y	N	N	N	N	13%
Integrated discharge test	N	N	N	N	Y	N	N	N	N	N	N	9%
Stray flux monitoring	N	N	Y*	N	N	N	N	N	N	N	N	9%

A to K : industrial operators   Y : Yes   N : No

* : occasionally   # : if special problem arise

+ : only during installation

Table 1 : Survey of Monitoring Techniques used on 3-phase Squirrel-cage Induction Motors with ratings of 500 h.p. (0.373 MW) and above.

Fault	Occurrence
Bearings	44.68%
Windings	44.68%
Cracked/Broken Rotor Bars	4.25%
Miscellaneous	6.39%

Total number of machines = 82
Power supplies vary from 2.3 kV to 13.8 kV
Number of machines with no fault = 30
Total number of failures = 94
Percentage of machines started D.O.L. = 98%

Table 2 : Survey Results on Machine Failure
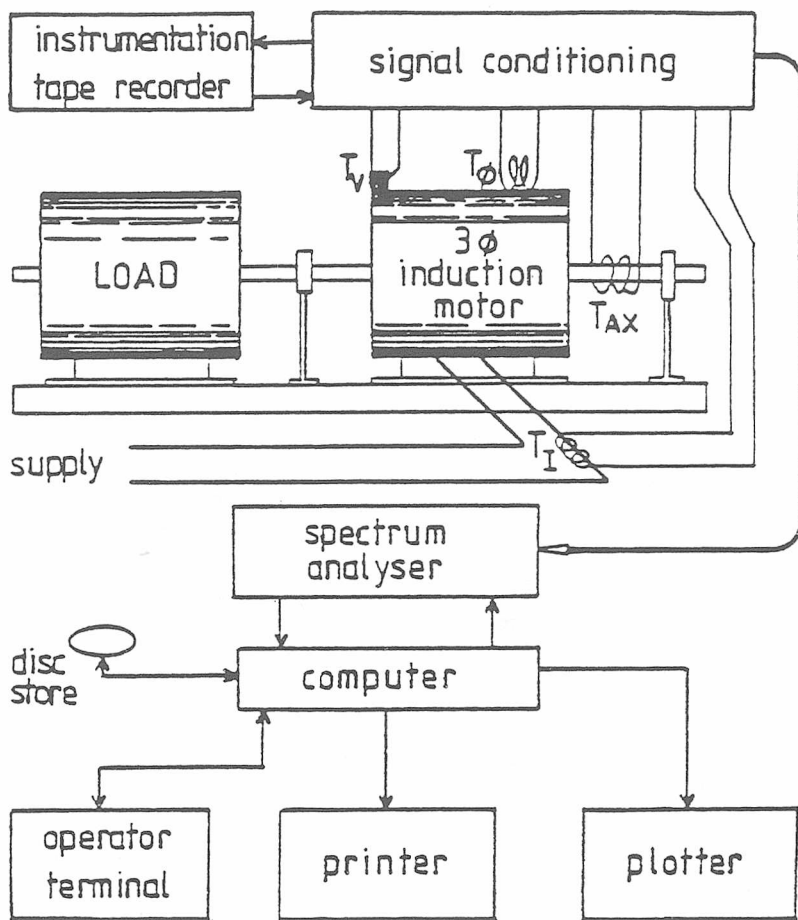
TEST RIG, DATA ACQUISITION AND PROCESSING EQUIPMENT
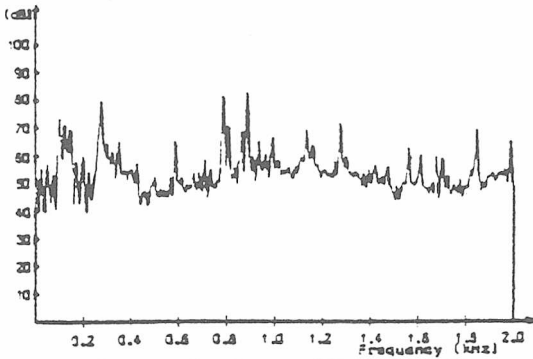
Figure 1

Figure 2 – Acceleration spectrum normal rotor
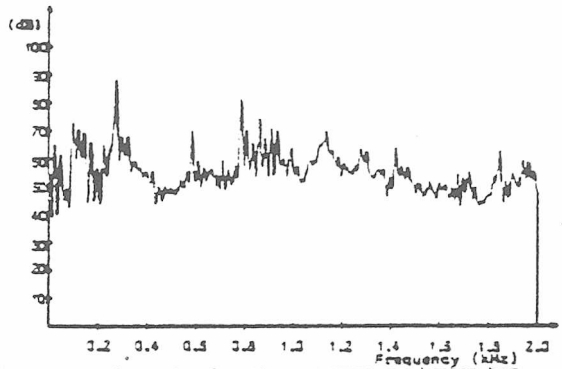
Figure 3 – Acceleration spectrum one broken bar
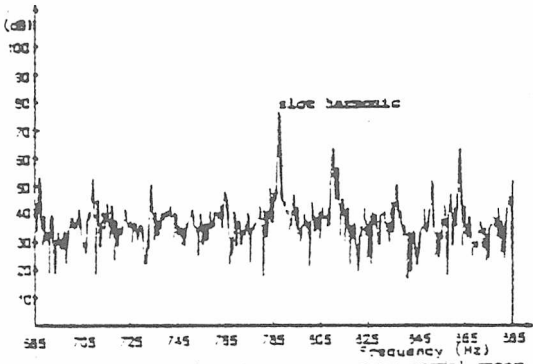
Figure 4 – Acceleration zoom spectrum normal rotor
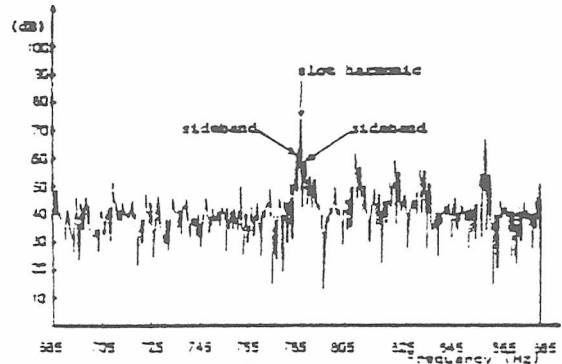
Figure 5 – Acceleration zoom spectrum one broken bar
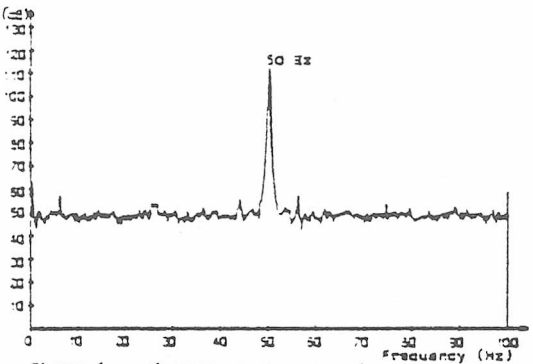
Figure 6 – Current spectrum normal rotor
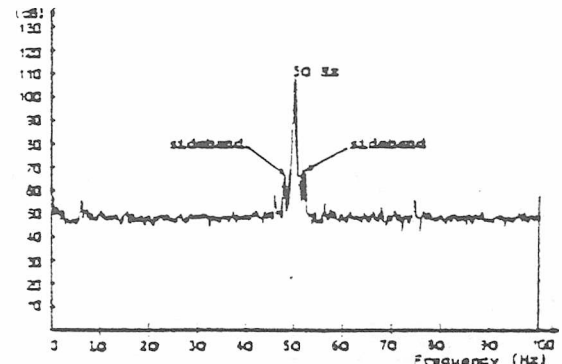
Figure 7 – Current spectrum one broken bar
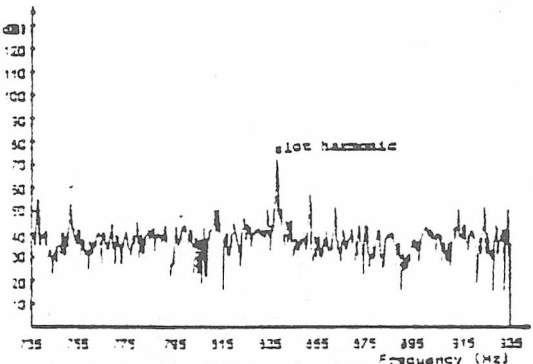
Figure 8 – Current zoom spectrum normal rotor
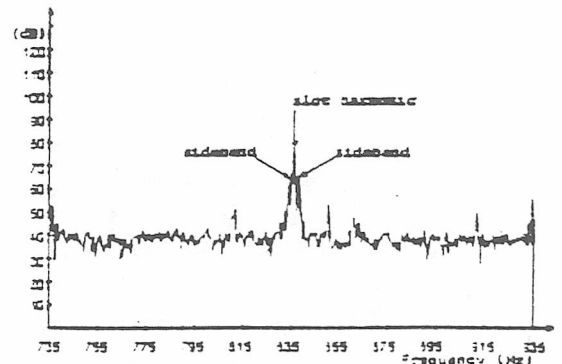
Figure 9 – Current zoom spectrum one broken bar
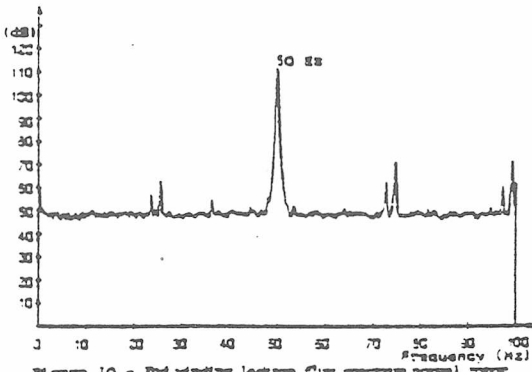
Figure 10 - End winding leakage flux spectrum normal rotor
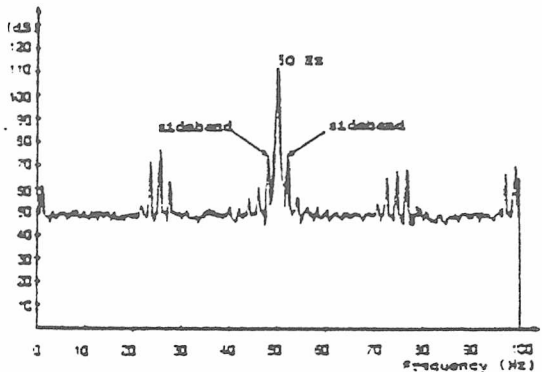
Figure 11 - End winding leakage flux spectrum one broken bar
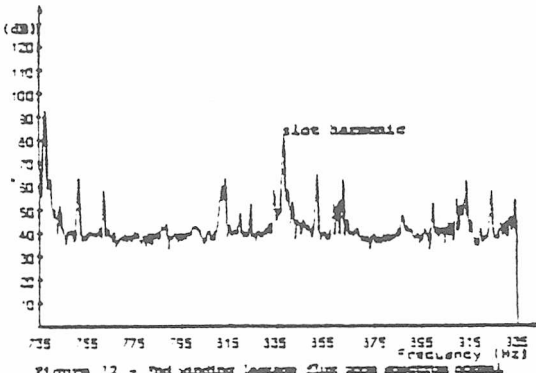
Figure 12 - End winding leakage flux zoom spectrum normal
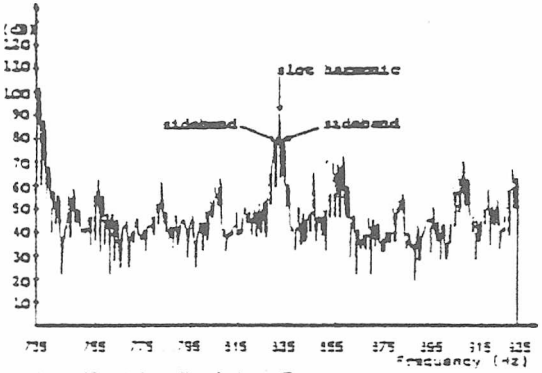
Figure 13 - End winding leakage flux zoom spectrum broken bar
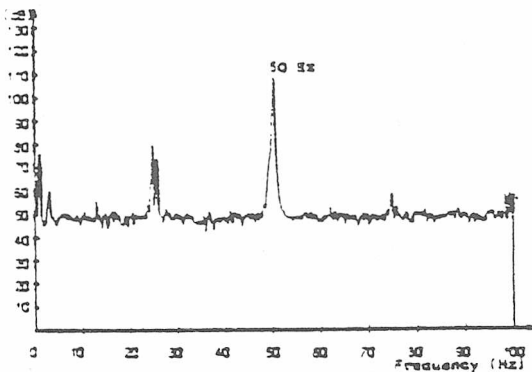
Figure 14 - Axial flux spectrum normal rotor
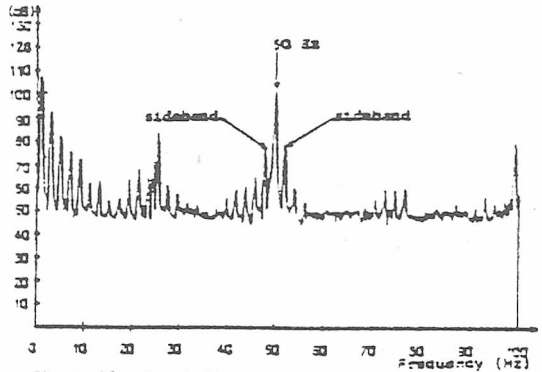
Figure 15 - Axial flux spectrum one broken bar
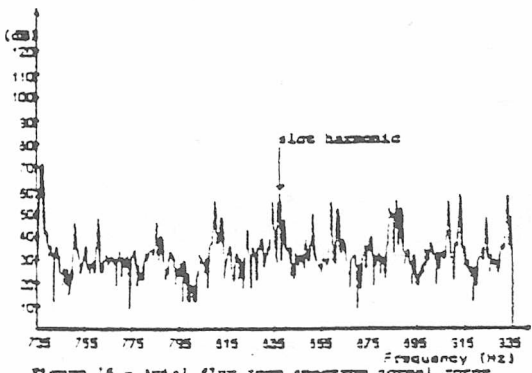
Figure 16 - Axial flux zoom spectrum normal rotor
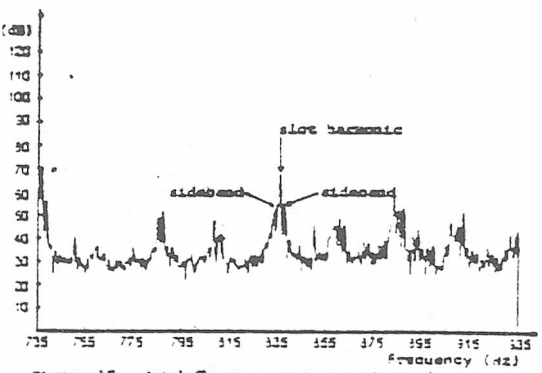
Figure 17 - Axial flux zoom spectrum one broken bar
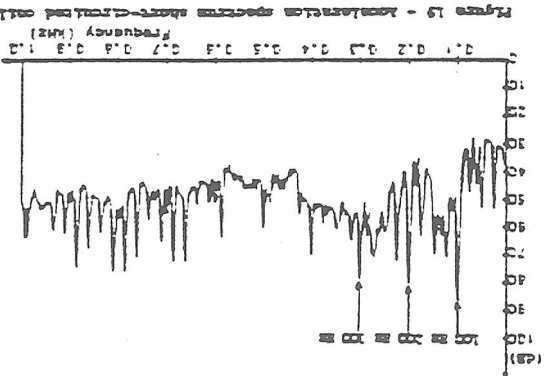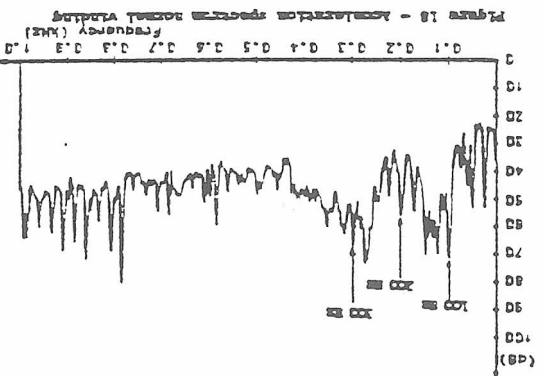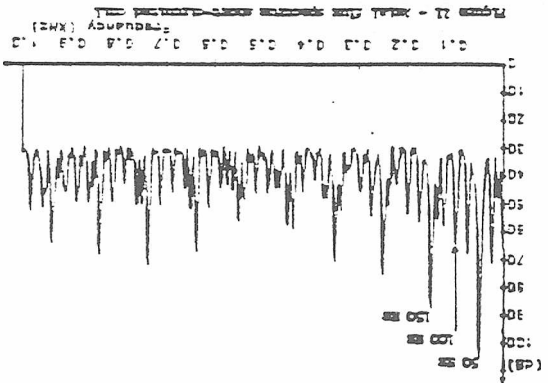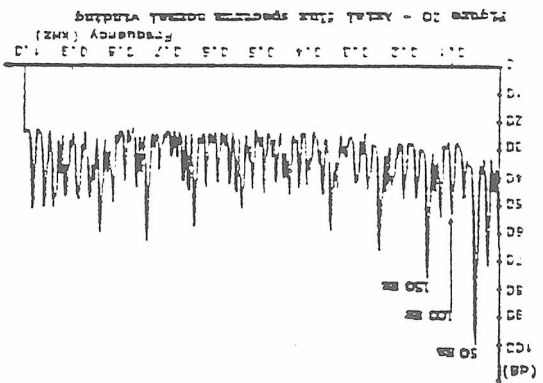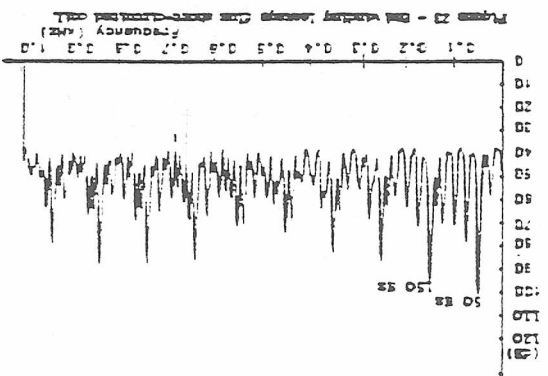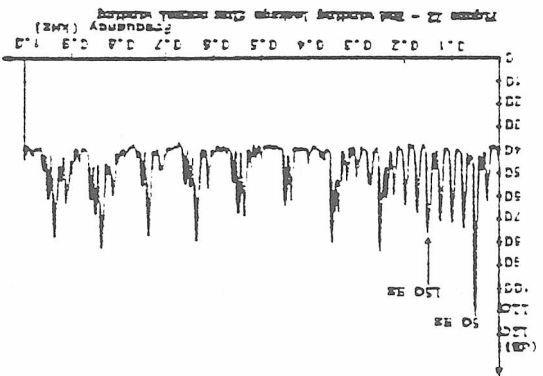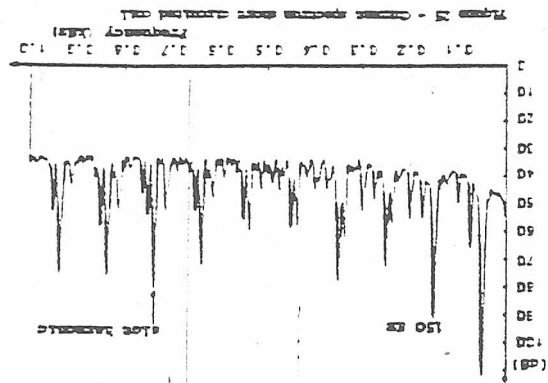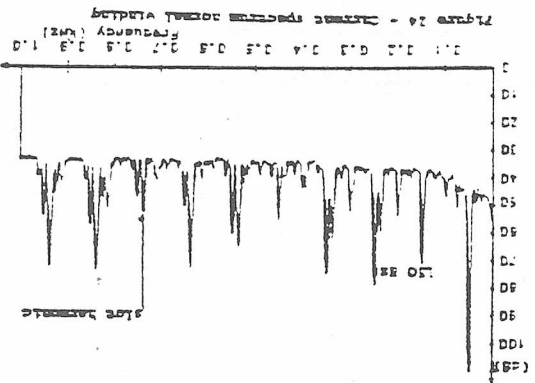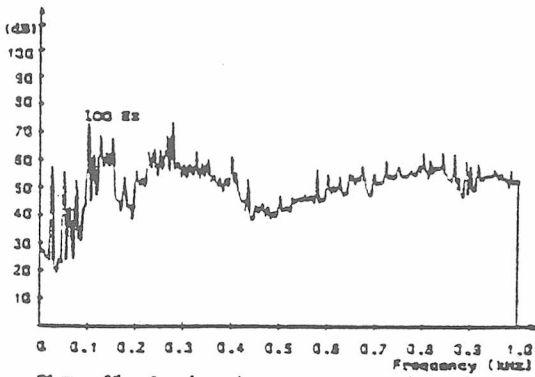
Figure 26 - Acceleration spectrum normal supply
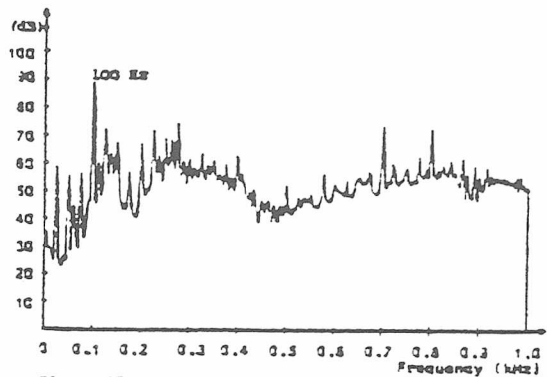
Figure 27 - Acceleration spectrum 1-phasing fault
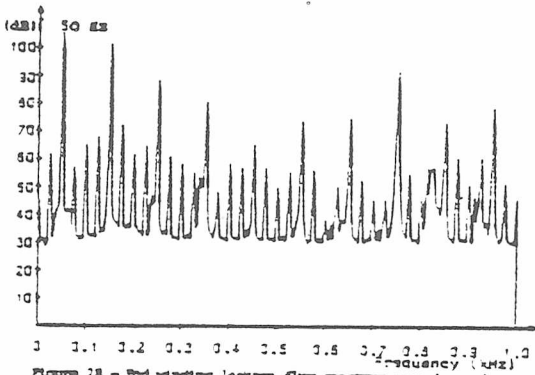
Figure 28 - End winding leakage flux spectrum normal supply
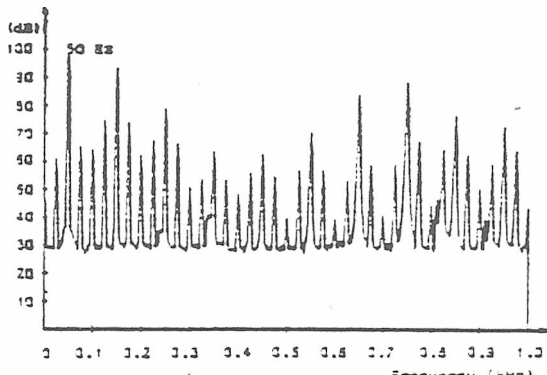
Figure 29 - End winding leakage flux spectrum 1-phasing fault
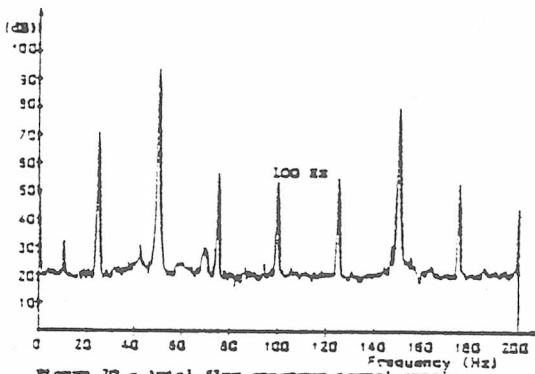
Figure 30 - Axial flux spectrum normal supply
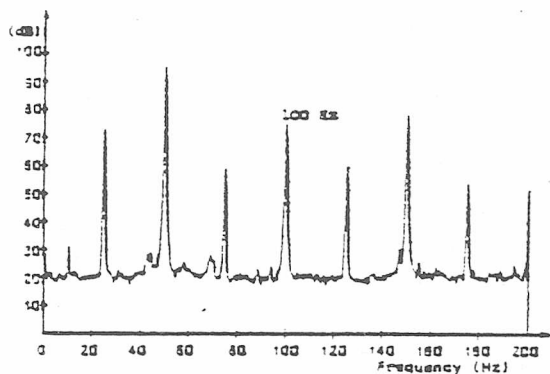
Figure 31 - Axial flux spectrum 1-phasing fault
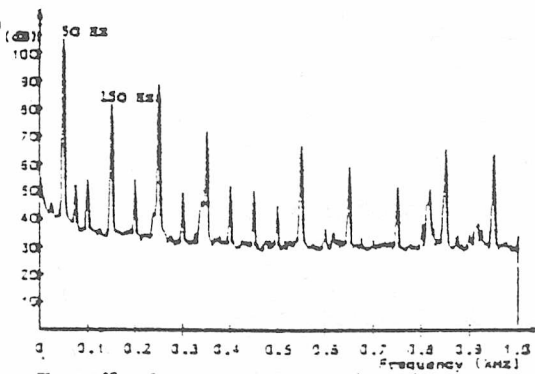
Figure 32 - Current spectrum normal supply
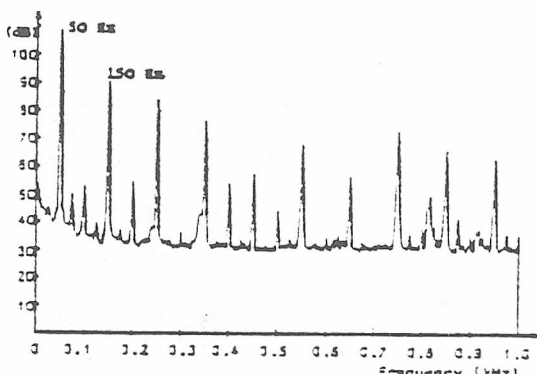
Figure 33 - Current spectrum 1-phasing fault

Figure 34 - Acceleration spectrum zero eccentricity

Figure 35 - Acceleration spectrum 6.66% eccentricity

Figure 36 - Acceleration spectrum 13.33% eccentricity

Figure 37 - Acceleration spectrum 26.66% eccentricity

• – concentric   x – 13.33% eccentricity

o – 26.66% eccentricity
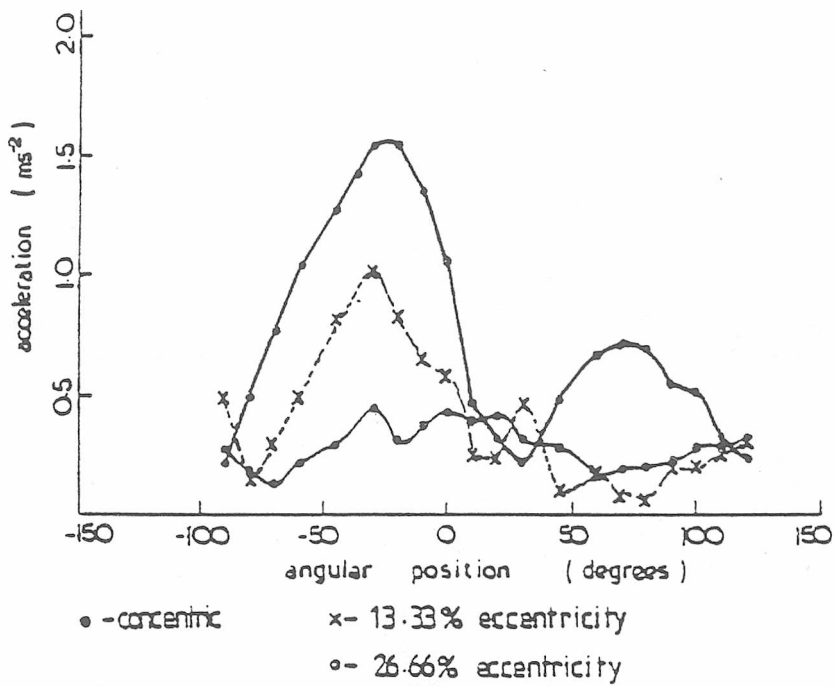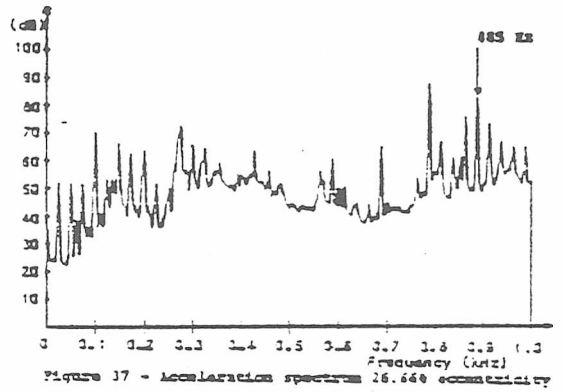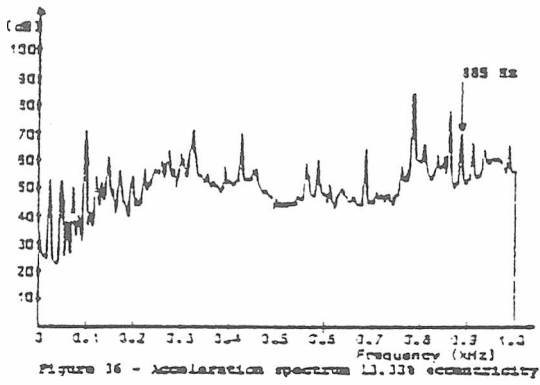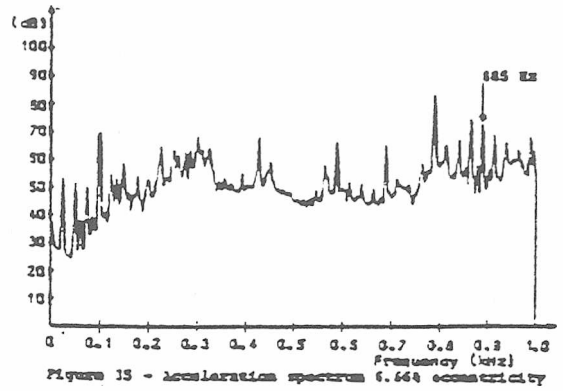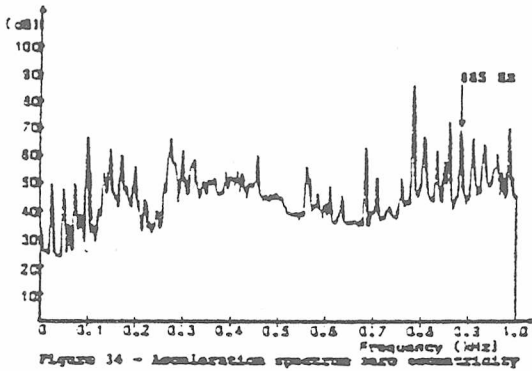
Figure 38 Acceleration versus transducer position
with varying eccentricity
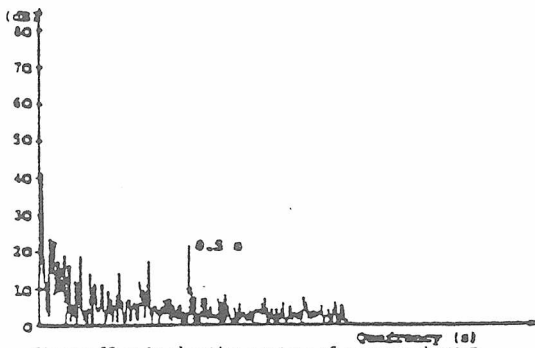
Figure 39 — Acceleration capstrum of zero normal rotor
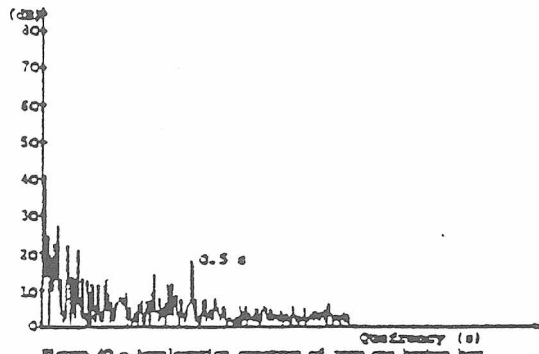
Figure 40 — Acceleration capstrum of zero one broken bar
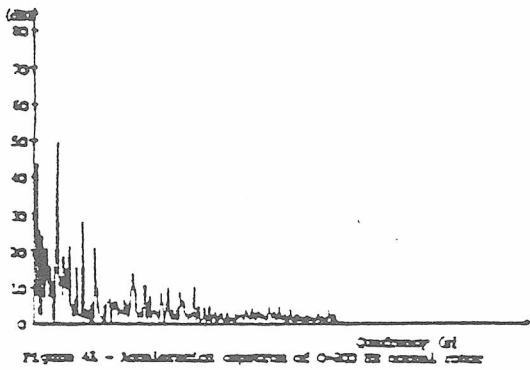
Figure 41 — Acceleration capstrum of 0-200 Hz normal rotor
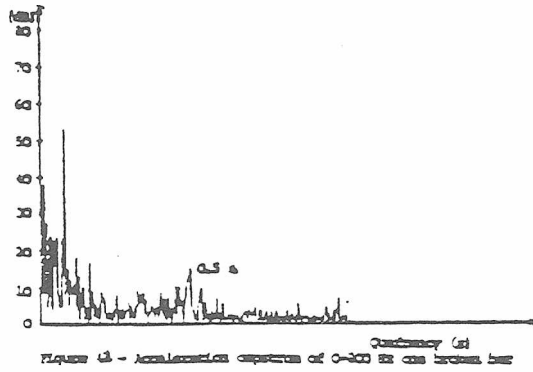
Figure 42 — Acceleration capstrum of 0-200 Hz one broken bar
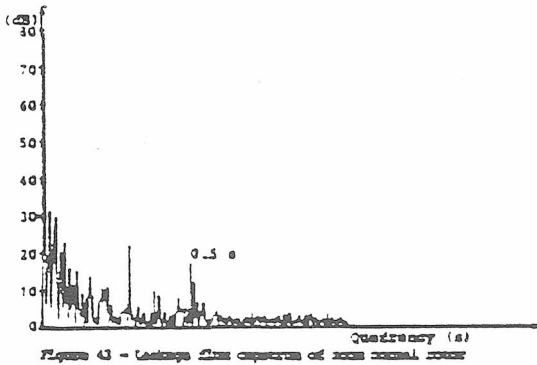
Figure 43 — Leakage flux capstrum of zero normal rotor
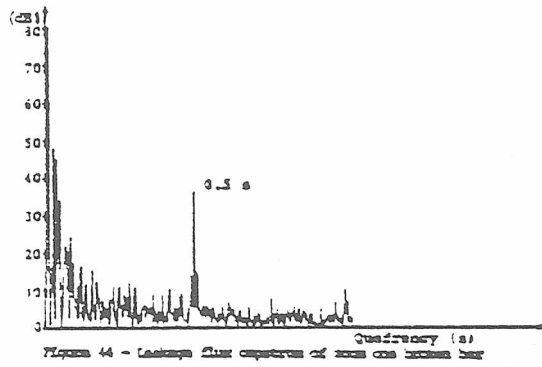
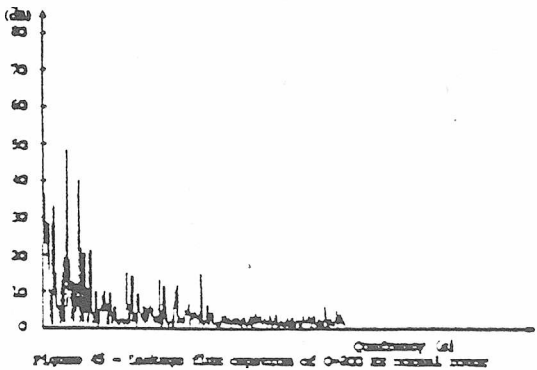Figure 44 — Leakage flux capstrum of zero one broken bar

Figure 45 — Leakage flux capstrum of 0-200 Hz normal rotor
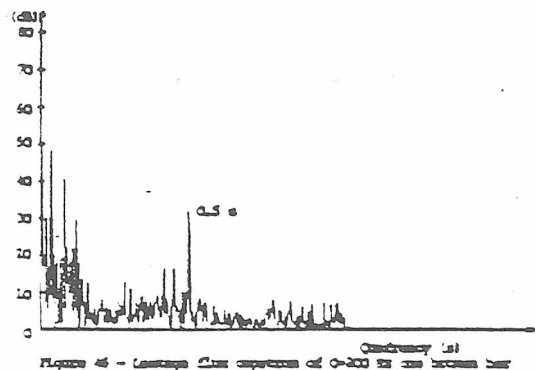
Figure 46 — Leakage flux capstrum of 0-200 Hz one broken bar

MONITORING STRATEGY FOR DISCRIMINATING BETWEEN DIFFERENT

TYPES OF ROTOR DEFECTS IN INDUCTION MOTORS

W T Thomson, N D Deans, R A Leonard, A J Milne

Robert Gordon's Institute of Technology, Aberdeen AB9 1FR

INTRODUCTION

A recent survey[1] of industrial companies using large 3-phase squirrel-cage induction motors (SCIM) in offshore and onshore installations indicated that rotor cage faults can lead to motor failures. Pulsating loads or the undesirable effects of direct-on-line starting can result in rotor bar fractures.[2,3] The fatigue mechanism causes a poor electrical/mechanical connection, arcing develops and this usually results in a broken bar. Torque pulsations, speed fluctuations and vibration changes occur and can cause rotor bearing failure[1] or stator core damage. There is a need for reliable on-line monitoring techniques for discriminating between high resistance bar to end ring joints, number of broken bars and end ring faults. It is proposed that a monitoring strategy which uses three or four interrelated types of signals for fault diagnosis is more' credible than existing instruments monitoring only one signal.

REVIEW OF PREVIOUS WORK

Gaydon[4,5] has developed instrumentation techniques for rotor fault detection based on shaft speed fluctuations but has stated that "inherent rotor asymmetries can give period fluctuations of the same magnitude as when one bar was open circuited". Hargis[4] has presented a set of spectra of vibration and current for two nominally identical motors, one with a normal rotor, and one with three broken bars but the early detection of one broken bar is important so that further degradation can be avoided. Pozanski[6] has shown that acoustic noise measurements indicated a 1 dB - 3 dB change between a motor with a good rotor and one with a single broken bar. The application of noise measurements for condition monitoring is not really suitable for offshore installations or hostile onshore situations[1]. Jones[7] has developed an equivalent circuit for modelling the effect of an open-circuited rotor phase and shows that induced e.m.f. and current signals appear at a frequency of $|1-2s|f_1$ in the stator winding. The model was verified experimentally for an open-circuited rotor phase. Vas[8] has presented a similar approach but no experimental results were given. Williamson[9] has calculated the variation in rotor bar currents when broken bars or a broken end ring exists, but the experimental motor used to verify the analysis had a high resistance cage in the stator core. The analysis was verified by experimental tests for the cases of two/three broken bars and end ring faults but the test motor was untypical of those commonly used in industry. The on-line monitoring of bar currents is of course not a practical proposition. Williamson applied his analysis to a large SCIM and predicted that it may be difficult to detect a single bar fault in terms of the $|1-2s|f_1$ component of current or the $2sf_1$ component of pulsating torque. Williamson's prediction has still to be verified by experimental tests. Penman[10] has reported that the use of axial flux monitoring was inconclusive for detecting a rotor bar fault. Steele[11] has monitored current for the detection of one broken bar in a small-power motor but did not present results for the cases of two or three broken bars. Controlled experimentation is required if rotor cage faults are to be quantified in terms of the magnitudes of specific frequency components or by using

Cepstrum analysis[11] to identify the sideband content of spectra.

PRINCIPLES

Alger[12] has shown that the air-gap flux density in a SCIM consists of five principal rotating fields. If time harmonic fluxes of the fundamental are included then a general expression for the slot harmonic frequency components is : $f_1 (\frac{R}{P} (1 - s) \pm n)$. If Jones'[7] analysis is applied to the fundamental and third harmonic time components of the stator flux then upper and lower sidebands occur at $|1 \pm 2s| f_1$ around the fundamental. The slot harmonic frequencies for a rotor with asymmetry become : $f_1(n \pm R(1 - s)/P) \pm 2s f_1$, where f_1 = fundamental frequency; s = slip; R = No. of rotor slots; P = pole pairs; n = 1, 2, 3...

These effects can be detected in the current, end winding and leakage flux spectra[1] using simple external pick up coils and spectrum analysis. Since magnetic forces are proportional to flux density squared, then sidebands occur around the principal slot harmonic vibration components. These sidebands appear in four interrelated[1] spectra and can be used as a basis for identifying various types of rotor fault.

EXPERIMENTAL EQUIPMENT AND TEST RESULTS

A test rig has been developed to investigate the effects of faults on the current, flux and vibration spectra of a machine. A 3-phase, 50 Hz, 11 kW, 4-pole SCIM, loaded by a d.c. dynamometer, has transducers attached to sense current, leakage and axial flux, and vibration. The sensed signals are amplified and filtered and subjected to spectral analysis in a high-resolution spectrum analyser acting as a peripheral device to a mini-computer. A suite of programs in the minicomputer control the analyser and present the processed data to the experimenter in graphical or numerical form. Figure 1 shows the test rig and associated processing equipment.

Tests were initially done using two 28-slot production type die-cast rotors, one as the normal reference and the other for introducing controlled rotor cage faults. For the experiments with the 28-slot rotors, the motor developed its nominal full-load torque at 1470 r.p.m. An FFT analysis was applied to the vibration, current, end winding and axial flux signals. Upper and lower sidebands appeared around various frequency components when the rotor with one broken bar was tested. An FFT zoom analysis of the vibration and end winding flux signals is presented in Figures 2-5. The spectra for the faulty rotor have a pronounced sideband content around the principal slot harmonics. A Cepstrum analysis was used to obtain a value for the sideband content. Figures 6 and 7 show that this technique can detect a single rotor bar failure. Several bars were broken adjacent to the single broken bar and the resulting Cepstra are shown in Figures 8 and 9. A similar pattern occurred for the other signals and a sample of Cepstra for the end winding flux signals is given in Figures 10 and 11.

A standard type 51-slot rotor was redesigned to investigate the effects of high resistance bar to end ring joints. A number of the bars could be broken and reconnected in situ via special bolted connections. The remaining 43 copper bars were soft soldered into the end rings. A high-resolution micro-ohmmeter was used to measure the resistances of a number of similar soft soldered joints and bolted connections on a separate rotor cage, and it was found that they were of the order of 5 to 6 $\mu\Omega$ and 21 to 22 $\mu\Omega$ respectively. The 51 slot rotor developed the motor's nominal full-load torque at a speed of 1430 r.p.m. and is typical of a standard

production model. The transducer signals were analysed when the rotor had no broken bars and sidebands appeared in the vibration, current and flux signals. This suggests that high resistance joints can be interpreted as broken bars. Figure 12 shows the pronounced sideband content. With a bar disconnected from the end ring, the changes in the current and flux signals were inconclusive. However, the sideband content in the vibration signal increased as shown in Figure 13. A further increase occurred with two broken bars.

CONCLUSIONS

A study of different rotor cage faults has been carried out under controlled experimental conditions and a set of spectra and cepstra presented. The results show that cage faults can be identified in four interrelated signals and that Cepstrum analysis can provide a single value for the relevant sideband content. Sidebands also appear in the spectra when the rotor cage has high resistance bar to end ring joints and it was observed that only the vibration signal showed a significant change when bars were subsequently broken. The concept of looking for changes in four different signals as opposed to one or two, has the distinct advantage that an industrial user of SCIMs is more likely to believe the former as an indication of a fault. This is particularly relevant in the offshore oil industry where loss of production is extremely costly. Further work is required to study the effects of decreasing/increasing the number of high resistance joints compared to broken bars, and end ring faults compared to broken bars.

ACKNOWLEDGEMENTS

REFERENCES

1. THOMSON, W. T., DEANS, N. D., LEONARD, R. A., and MILNE, A. J.: Condition monitoring of induction motors for availability assessment in offshore installations, 4th Euredata conference, Venice, Italy, March, 1983.

2. BURNS, R. L.: Rotor bar failures in large a.c. squirrel cage rotors, Electr. Eng., 1977, 54, (10), pp 11-14.

3. GAYDON, B. G., and HOPGOOD, D. J.: Faltering pulse can reveal an ailing motor, Electrical Review, Vol. 205, No. 14, Oct. 1979, pp 37-38.

4. HARGIS, C., GAYDON, B. G., and KAMASH, K.: The detection of rotor defects in induction motors, IEE International conference on Electrical Machines - Design and Applications, 1982, No. 213, pp 216-220.

5. GAYDON, B. G.: An instrument to detect induction motor rotor circuit defects by speed fluctuation measurements, electric test and measuring instrumentation - Testemex 79 conference papers, 1979, pp 5-8.

6. POZANSKI, A.: Acoustic measurement of three-phase asynchronous motors with a broken bar in the cage rotor, Zesz. Nauk. Politech. Lodz. Elektr., 1977, 60, pp 121-131.

7. JONES, C. V.: Unified theory of electrical machines, Butterworth, 1967.

8. VAS, P.: Performance of three-phase squirrel-cage induction motors with rotor asymmetries, Period. Polytech. Electr. Eng. 1975, 19, pp 309-315.

9. WILLIAMSON, S., and SMITH, A. C.: Steady-state analysis of 3-phase cage motors with rotor-bar and end-ring faults, Proc IEE, Vol. 129, PT. B, No. 3, May, 1982, pp 93-100.

10. PENMAN, J., HADWICK, J. G., and STRONACH, A. F.: Protection strategy against the occurrence of faults in electrical machines, IEE Conf. Publ. 185, 1980, pp 54-58.

11. STEELE, M. E., ASHEN, R. A., and KNIGHT, L. G.: An electrical method for condition monitoring of motors, IEE international conference on Electrical Machines - Design and Applications, 1982, No. 213, pp 231-235.

12. ALGER, P. L.: The nature of induction machines, Gordon and Breach Science Publications, 1965.

AUTHORS

W T Thomson, a graduate of the University of Strathclyde (B Sc HONS 1973, M Sc 1977) is currently a Lecturer in the School of Electronic and Electrical Engineering, RGIT, Aberdeen, U.K. His research interests are vibration and noise from electrical machines and condition monitoring of rotating machines.

N D Deans, a graduate of the Universities of Aberdeen and Heriot-Watt (B Sc ENG HONS 1966, Ph D 1973)· is currently Deputy Head of the Department of Electronic and Electrical Engineering, RGIT. His research interest is special purpose digital systems design.

R A Leonard, a graduate of RGIT (B Sc HONS, 1981) is currently a Research Assistant at RGIT. His research interests are condition monitoring of rotating machines and instrumentation development.

A J Milne, a graduate of the University of Aberdeen (B Sc ENG HONS 1980) is currently a Research Student at RGIT. His research interest is microcomputer instrumentation.

TEST RIG, DATA ACQUISITION AND PROCESSING EQUIPMENT
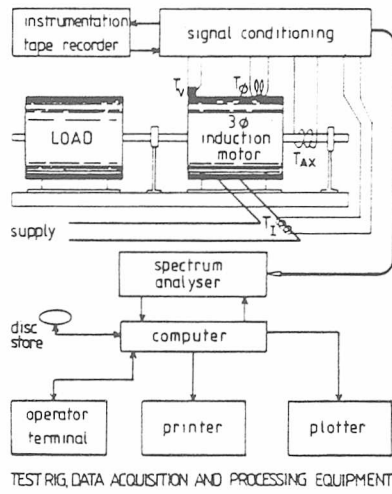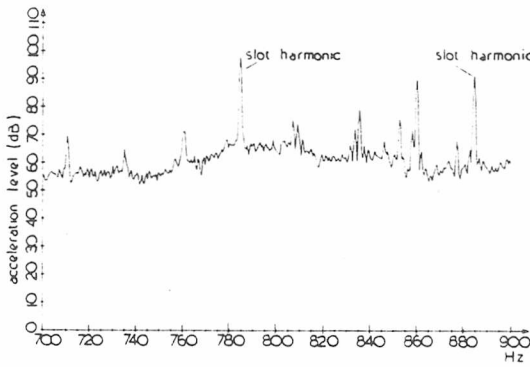
Figure 1

Figure 2

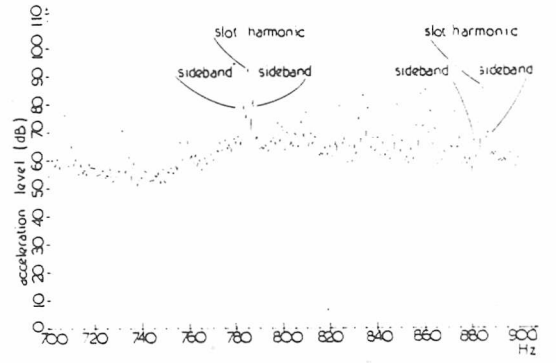acceleration zoom spectrum, normal rotor

Figure 3

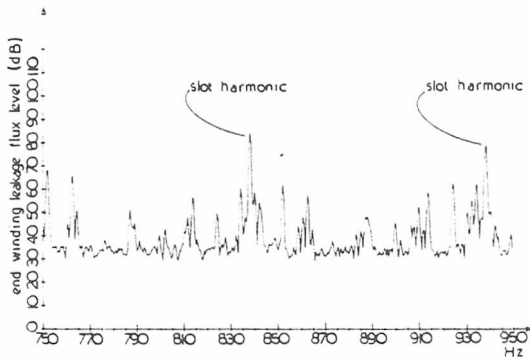acceleration zoom spectrum, one broken bar

Figure 4
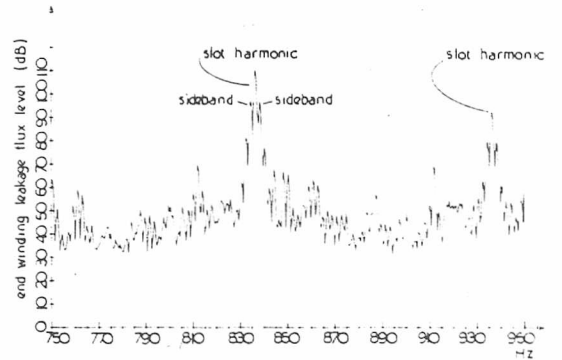
end winding leakage flux zoom spectrum normal rotor

Figure 5

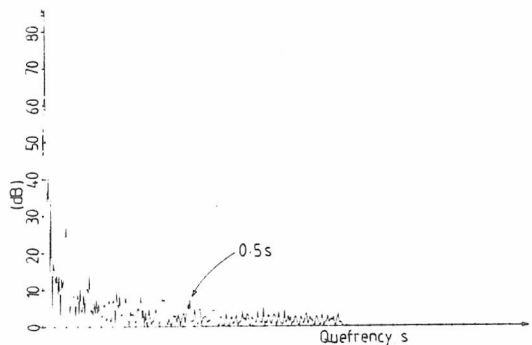end winding leakage flux zoom spectrum one broken bar

246

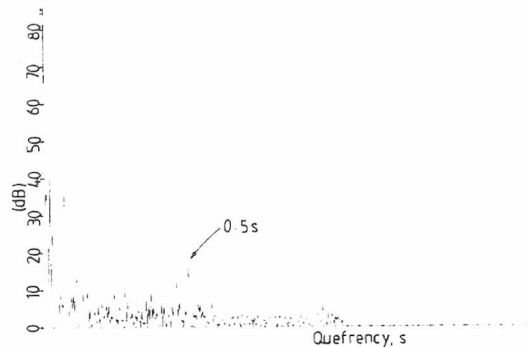Figure 6 acceleration cepstrum of zoom, normal rotor
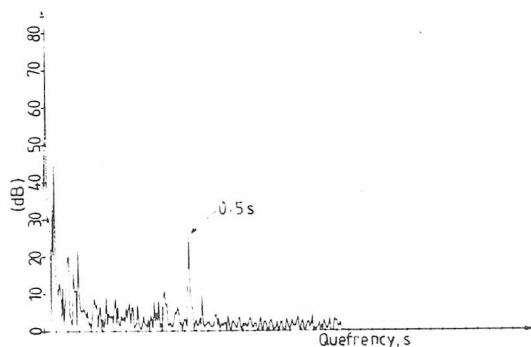

Figure 7 acceleration cepstrum of zoom, one broken bar
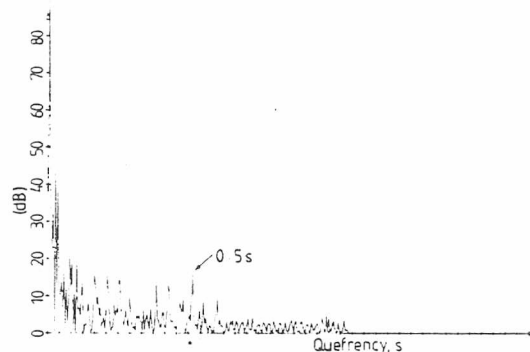

Figure 8 acceleration cepstrum of zoom, two broken bars

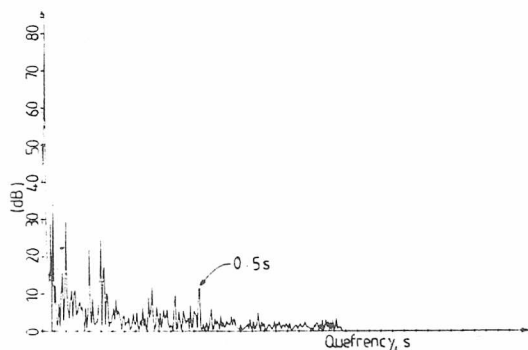Figure 9 acceleration cepstrum of zoom, three broken bars

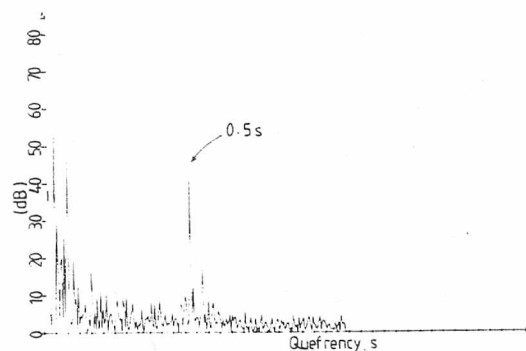Figure 10 leakage flux cepstrum of zoom, normal rotor

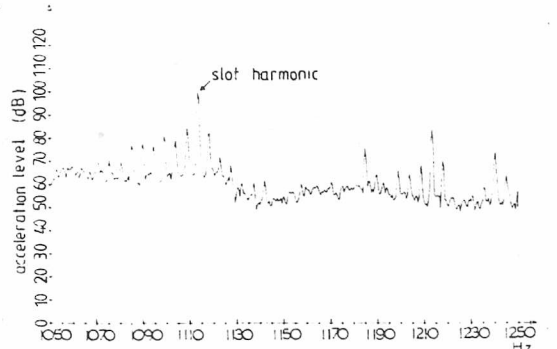Figure 11 leakage flux cepstrum of zoom, one broken bar

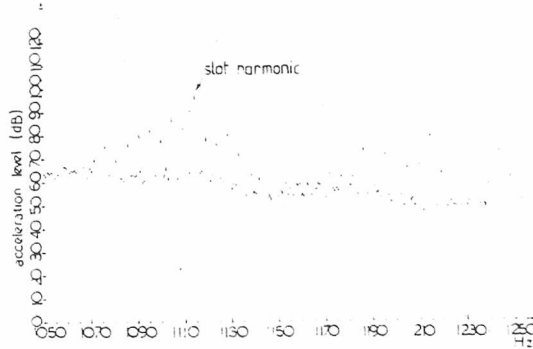Figure 12 acceleration spectrum for 51 slot rotor, high resistance joints

Figure 13 acceleration spectrum for 51 slot rotor, one broken bar

FAILURE IDENTIFICATION OF OFFSHORE INDUCTION MOTOR SYSTEMS
USING ON-CONDITION MONITORING

W.T.Thomson, R.A.Leonard, A.J.Milne   and   J.Penman
Robert Gordon's Institute of Technology,   University of Aberdeen.
Aberdeen.

This paper reports on a study carried out into the
identification of faults in 3-phase squirrel cage induction
motors. The reasons for monitoring vibration, current and
stray flux signals in a unified approach are presented and a
fault producing test rig and computer-based signal processing
system are described. The changes which occur in the signals
during single-phasing, broken rotor bar, rotor-stator eccent-
ricity and inter-turn winding fault conditions are discussed
and a sample of the signature patterns is presented. The
results show that a malfunction can be identified from various
signals and in certain instances the reliability of fault
diagnosis could be improved by the monitoring strategy
proposed in this paper.

INTRODUCTION

In offshore oil and gas production platforms the 3-phase squirrel cage induction
motor (SCIM) is used to drive gas compressors, sea water injection pumps and oil
exporting pumps. The assessment of the condition of the motor and its future
availability and reliability are important since failure caused by one of a
number of faults is costly and potentially dangerous, Thomson et al (1). It is
desirable that fault mechanisms can be detected at an early stage so that planned
outages can take place to prevent catastrophic failure. In offshore power
installations the majority of SCIMs are started direct-on-line, this results in
large starting currents and torques which can contribute to end winding, rotor
cage or bearing failures.(1) Voltage unbalance in the supply system may occur
and cause premature failure of the windings. Sea water contamination of the
stator windings has been reported as being one of the causes of insulation
failure.(1)   A recent survey has shown that the methods used for on-line fault
diagnosis tend to look at sources of information in isolation.(1)   Vibration
monitoring is traditionally done by mechanical engineers and insulation monitoring
by electrical engineers. However, the SCIM is a complex electromechanical device
and the fault mechanisms can be identified from various types of signals, Thomson
et al (2).   The motor may fail because of a faulty bearing but the fundamental
fault mechanism could be electrical, for example, bearings can fail due to
electrical bearing currents, Verma et al (3).   From the results of the survey
and discussions with the operators of SCIMs it was clear that the present
techniques used for fault diagnosis in electrical machines are not always
successful. (1,2) It is proposed that an on-line monitoring strategy which
utilises vibration, current and stray flux signals in a unified approach will
prove to be more successful than existing techniques.   This paper reports on an
experimental investigation into various fault mechanisms and the development of
data acquisition and signal processing techniques for fault identification from
non-invasive measurements of interrelated signals.

FAULT MECHANISMS

The fault conditions being considered in this paper are as follows :

Unbalanced Voltage Supply .

In offshore installations where the power supply system is relatively small, the

3-phase voltage supply could become unbalanced due to such factors as single-phasing of primary/secondary circuits or unbalanced single-phase loads, Howell and Hogwood (4). When a SCIM is fed from an unbalanced supply the motor currents are unbalanced and at full-load the current unbalance is usually six to ten times the voltage unbalance.(4) This leads to excessive heating of the windings, thermal ageing occurs and can result in insulation failure. Brighton and Ranade (5) have reported that the normal protection circuits which operate when the temperature or current increases above a pre-set level are not always reliable for protecting against failure due to unbalanced voltage supply. From a sample of 380 break-downs of standard a.c. drives up to 25 kV, Vincent (6) has reported that 12% of the total failures were due to the worst unbalanced supply condition known as single-phasing - occurs when one of the supply lines is open-circuited.

Broken Rotor Bars

This occurs when one of the conducting bars of the squirrel cage rotor winding breaks where it is joined to the conducting end ring, Burns (7). Adjacent bars carry a higher than normal current and overheat which usually leads to additional broken bars.(2) Rotor cage faults can cause torque pulsations, speed fluctuat-ions and changes in the vibration signal. Gaydon and Hopgood (8) have reported that these factors can cause mechanical damage to the rotor or stator winding.

Rotor-Stator Eccentricity

Static eccentricity exists when the axial centre of the rotor and stator are not coincident, this causes unbalanced magnetic pull (Binns and Dye (9)) and may lead to bearing damage.

Inter-turn Winding Faults

If the insulation between adjacent turns of a coil breaks down due to contami-nation or other causes, then shorting can occur and a hazardous situation results. This is because the shorted coil now lies in the main air-gap field due to the rest of the machine circuits and consequently has a voltage induced in it. The induced voltage drives current around the coil, and its magnitude is limited only by the resistance and inductance of the local circuit. The resulting currents can be very high, leading to insulation gassing with the possibility of explosion if and when sparking occurs.

The unbalance that occurs in the stator electrical circuits results in changes in the harmonic content of the air-gap flux, and this can be related to changes in the current time harmonics. One of the authors has investigated this and predicted the harmonic changes to be expected under such conditions, Penman et al (10,11). They have also shown that although such changes could be observed in the line currents of the machine, this would require the sensing of terminal quantities and the measurement of small changes with respect to the fundamental. The alternative proposed (10,11) is to monitor the axially transmitted fluxes, for such a signal effectively magnifies the effects of small unbalance in the magnetic or electric circuit of the machine, and can also provide information concerning other fault conditions such as eccentric running and phase unbalance.

TEST RIG AND PROCESSING EQUIPMENT

The fault producing test motor and associated processing equipment are shown in "Figure (1)". The test motor is a standard 11 kW, SCIM, which has been redesigned to carry out controlled experiments with the fault mechanisms described in the previous section. A number of transducers positioned on the test rig sense various signals for on-line analysis and fault diagnosis, namely :

T_i - is an air-cored toroidal coil used to sense electrical current in any of the main supply lines

$T_{e\phi}$ - is a coil situated on the exterior casing of the motor in an appropriate position to sense the end winding leakage flux

$T_{a\phi}$ - is a coil wound on the main shaft of the motor to sense the axial flux

T_v - is an accelerometer positioned to sense the vibration on the casing or bearing pedestals

The transducer signals are pre-amplified and then subjected to spectral analysis in a high resolution spectrum analyser acting as a peripheral device to a minicomputer. A suite of programs in the minicomputer control the analyser and present the processed data to the experimenter in graphical or numerical form. The system can control the allocation of storage areas on the disc storage units, so that historical records of experiments carried out on the induction motor can be accessed at a later date for inspection and comparison.

TEST RESULTS AND DISCUSSION

Alger (12) has shown that the air-gap flux density in a SCIM consists of five principal rotating fields.   If time harmonics of the fundamental flux are included then the basic equations are as follows :

$$f_1 \quad = \quad \text{supply frequency} \dots\dots\dots\dots\dots\dots\dots\dots\dots \quad (1)$$

$$f_{sh1} \quad = \quad f_1 \left(\frac{R}{p} (1 - s) \pm n\right) \text{ (Hz)} \dots\dots\dots\dots\dots\dots \quad (2)$$

These frequency components can be detected in the current and stray flux signals. Since magnetic forces are proportional to flux density squared, then the following components appear in the vibration spectrum :

$$f_{1v} \quad = \quad 2f_1 \text{ (Hz)} \dots\dots\dots\dots\dots\dots\dots\dots\dots\dots\dots \quad (3)$$

$$f_{shv} \quad = \quad f_1 \left(\frac{R}{p} (1 - s) \pm 2(n - 1)\right) \text{ (Hz)} \dots\dots\dots\dots \quad (4)$$

If the rotor cage winding is asymmetric then sidebands appear around the fundamental current component and the slot harmonics of the current, end winding and axial flux, and vibration signals. (1,2).   An FFT analysis was initially applied to the transducer signals and a study made of the signature patterns. Where it was difficult to identify the difference between signature patterns for normal and abnormal operation, a zoom analysis was applied around specific frequency components. The frequency at which the zoom analysis is applied depends on the type of fault and signal being analysed.   "Equations (1) to (4) should be used for this purpose. Cepstrum analysis can be used to determine the sideband content of spectra. (2)

Test conditions. The spectra shown in "Figures (9) to (12)" were obtained using a specially designed 51-slot rotor (2) and the other experiments were conducted using a 28-slot rotor. The results shown in "Figures (2) to (15)" were recorded when the motor was delivering full-load output at the rated speed, the motor specification is as follows :

> 3-phase, 11-kW, 415-V, 50-Hz, 4-pole, squirrel cage induction motor
>
> 28-slot rotor; full-load rated speed 1 470 r.p.m.
>
> 51-slot rotor; full-load rated speed 1 430 r.p.m.
>
> 36-slot stator
>
> air-gap length - 0.381 mm (0.015 inches)

In addition, a 4-kW, SCIM was also used to investigate inter-turn winding faults.

Single-Phasing/Unbalanced Voltage Supply Fault Detection

A comparison of "Figures (2) and (3)" indicates that the 100-Hz component of vibration increases when one of the supply lines to the motor was open-circuited. The 100-Hz component of vibration also changes when a stator coil is short-circuited.   In addition, the $(2 - s)f_1$ component (approximately 100-Hz) of the axial flux increases with single-phasing or a short-circuited stator coil.(1) Hence the reliability of diagnosing a particular fault mechanism is suspect. Conversely, if the 100-Hz component changes in various interrelated signals then it can be used as a reliable indicator that a malfunction exists in the machine. If fundamental electrical machine concepts are considered then the condition of single-phasing will produce a standing wave flux pattern which should be reflected into the 100-Hz component of vibration. Further tests were conducted and "Figure (4)" shows the variation of the 100-Hz component between normal 3-phase operation and with one phase open-circuited.   The curves indicate that during the fault condition the level of the 100-Hz component varies dramatically with transducer

position - a standing wave pattern occurs around the periphery of the motor. The other phases were open-circuited in turn and the resulting curves were nearly coincident with the one shown in "Figure (4)". If this fundamental knowledge is used in a condition monitoring system then it is possible to improve the reliability of detecting a single-phasing fault. Further work is required to study the effect of varying the amount of supply voltage unbalance, motor mounting arrangements and pole numbers.

Identification of Broken Rotor Bars

The slot harmonic frequencies in the current and stray flux signals emanating from an induction motor with an asymmetric rotor can be calculated using "Equation (5)". (2)

$$f_{sh2} = f_1 \ (R \ (1 - s)/p \pm n) \pm 2sf_1 \ \dots\dots\dots\dots\dots\dots\dots\dots\dots \ (5)$$

The sidebands at twice the "slip" frequency also appear around the principal slot harmonic vibration components. This means similar signature patterns occur in four interrelated signals and can be used as a basis for identifying a rotor cage fault. Experimental tests have shown that this is the case, "see Figures (5) to (8)". However, one of the problems is the discrimination between rotor bar/end ring failures and inherent rotor asymmetries such as high resistance bar to end ring joints. In a recent paper by Thomson et al (3), a preliminary study of the effect of high resistance joints indicated that similar signature patterns occurred in four signals but when one bar was broken it was only the vibration which showed a significant change in the sideband content. A further series of tests have been conducted and the results show that as the number of high resistance joints is reduced the sideband content drops, and consequently the relative difference between the sideband content of a rotor having few high resistance joints and one broken bar is larger, "see Figures (9) to (12)". The reliability of fault discrimination is still suspect but it can be concluded that if all four signals exhibit this signature pattern then the rotor cage is asymmetric. If this condition develops while the motor is in-service it should be put under close surveillance.

Rotor-Stator Eccentricity

In contrast to the previous fault mechanisms the only significant change occurred at one of the slot harmonic components (885-Hz) of the vibration spectrum. The sense of the change was a function of transducer position around the periphery of the motor frame as shown in "Figure (13)". The results show that at least one of the four interrelated signals is sensitive to rotor-stator eccentricity. Further work is required to try and detect changes in the other signals and to investigate the effects of different motor mountings and dynamic eccentricity.

Inter-Turn Winding Faults

A comparison between "Figures (14) and (15)" shows that the 100-Hz, 200-Hz and 300-Hz vibration components increase when a coil is short-circuited in the stator winding, whereas in the current spectrum it was the 150-Hz and one slot harmonic component which increased. In the axial flux signal the 50-Hz, 100-Hz and 150-Hz components increased and the changes in the end winding leakage flux were a function of transducer position. Further test results taken from a 4-kW SCIM with a 4-pole winding show that it is possible to identify specific harmonic components in the axial flux signal when an inter-turn fault occurs. Using the methods suggested (10,11) it is predicted that time harmonics of order 1, plus all even orders should appear in addition to the usual 6n $\pm$ 1 orders. "Figures (16) and (17)" show that this is the case, particularly with reference to the fundamental and even harmonics. There is also growth in the third harmonic, most likely caused by local saturation effects in the vicinity of the shorted turns.

CONCLUSIONS

An investigation into the effectiveness of monitoring vibration, current and stray flux signals for detecting faults in a 3-phase squirrel cage induction motor has been carried out and reported. The fault mechanisms have been studied under controlled experimental conditions and a set of spectra presented for identifying a "healthy" and "unhealthy" motor. It has been verified that a similar signature pattern occurs in four interrelated spectra when a rotor cage

fault exists, consequently, this unified approach could improve the reliability of rotor cage fault detection. The results also show that the 100-Hz component of the vibration signal changes instantaneously when a single-phasing or inter-turn winding fault occurs, if the transducer is correctly positioned it is possible to discriminate between the two fault mechanisms. It has been verified by experiment that the predicted harmonic components (10,11) do appear in the axial spectrum when an inter-turn fault exists. In addition, the slot harmonic components in the vibration spectrum can be used to detect static rotor-stator eccentricity, further work is required to try and detect changes in the other signals and apply the techniques for detecting dynamic eccentricity. Finally, the concept of looking for changes in four interrelated spectra as opposed to only one, can, in certain cases, improve the reliability of fault detection.

ACKNOWLEDGEMENTS

SYMBOLS

B = flux density (Tesla)

f_1 = supply frequency (Hz)

f_{sh1} = slot harmonics of the flux (Hz)

f_{1v} = fundamental vibration component due to magnetic forces (Hz)

f_{shv} = vibration slot harmonics (Hz)

f_{sh2} = slot harmonics of the flux with an asymmetric rotor cage (Hz)

n = integer - 0, 1, 2, ----

p = pole pairs

R = rotor slots

s = per unit slip of the induction motor

REFERENCES

1. Thomson,W.T., Deans, N.D., Leonard, R.A., and Milne, A.J., 25 March,1983, "Condition Monitoring of Induction Motors for Availability Assessment in Offshore Installations", Fourth Euredata Conference Proceedings,Venice,Italy.

2. Thomson,W.T., Deans, N.D., Leonard, R.A., and Milne, A.J., 12 April,1983, "Monitoring Strategy for Discriminating between different types of Rotor Defects in Induction Motors", 18th Universities Power Engineering Conference Proceedings, University of Surrey, England.

3. Verma,S.P., Girgis, R.S., and Fleming, R.J., 1980, "The Problems and.Failures caused by Shaft Potentials and Bearing Currents in Turbogenerators; Methods of Prevention", CIGRE International Conference Proceedings on Large High Voltage Electric Systems, 11-10.

4. Howell, J.K., and Hogwood, E.E., 1981, "Electrified Oil Production", Penwell Publishing Company.

5. Brighton, R.J., and Ranade, P.N., 1982, "Why Overload Relays DO NOT Always Protect Motors", IEEE Transactions on Industry Applications, Vol. 1A-18, No. 6, 691.

6. Vincent, C.E., 1978, "Maintenance of Large Industrial Drives", IEE Conference Publication - Colloquium on The Design and Applications of Large Industrial Drives, No. 170, 16-17.

7. Burns, R.L., 1977, "Rotor Bar Failures in Large A.C. Squirrel Cage Rotors", Electr. Eng., 54, (19), 11.

8. Gaydon, B.G., and Hopgood, D.J., 1979,"Faltering Pulse can Reveal an Ailing Motor", Electrical Review, Vol. 205, No. 14, 37.

9. Binns, K.J., and Dye, M., 1973, "Identification of Principal Factors causing Unbalanced Magnetic Pull in Cage Induction Motors", Proc. IEE, Vol. 120, No. 3, 349.

10. Penman, J., Hadwick, J.G., and Stronach, A.F., 1980, "Protection Strategy against the Occurrence of Faults in Electrical Machines", Int. Confr. on Developments in Power System Protection, IEE Publ. 185, 54.

11. Penman, J., Dey, M., and Hadwick, J.G., 1980, "A Microcomputer Based Machine Protection System", 17th Universities Power Eng. Conf. Publ., Manchester.

12. Alger, P.L., 1965, "The Nature of Induction Machines", Gordon and Breach Science Publications.
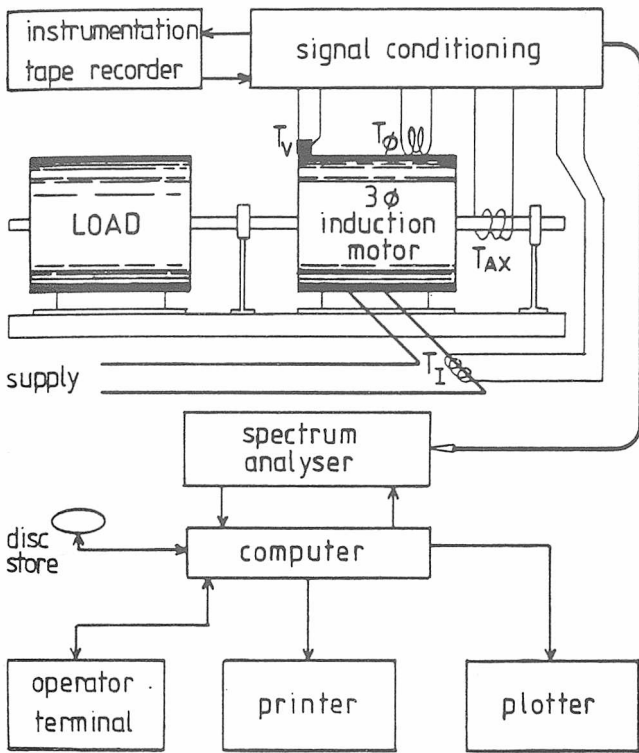
Figure 1 Test rig, data acquisition and processing equipment
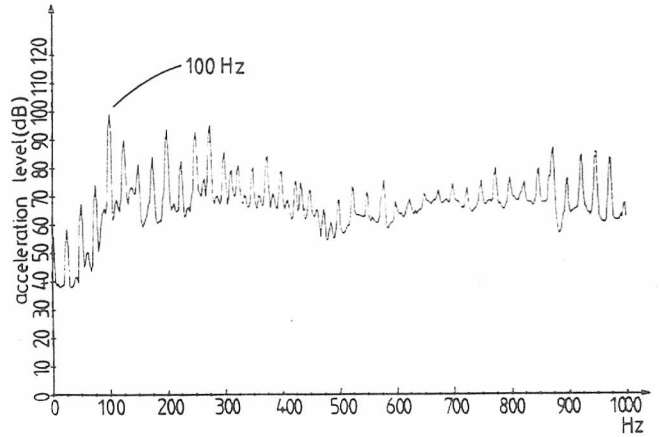
Figure 3 Acceleration spectrum 1-phase open circuit
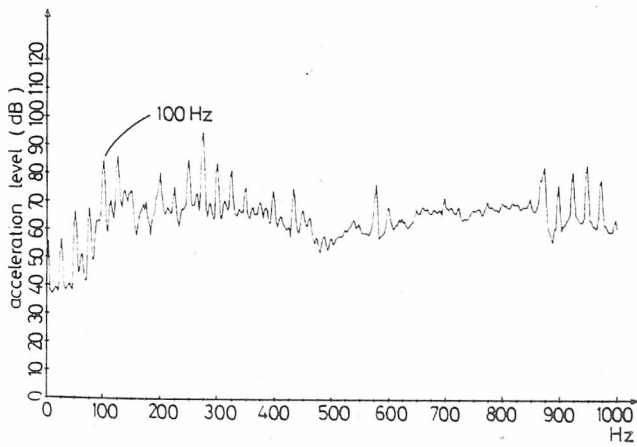
Figure 2 Acceleration spectrum normal supply
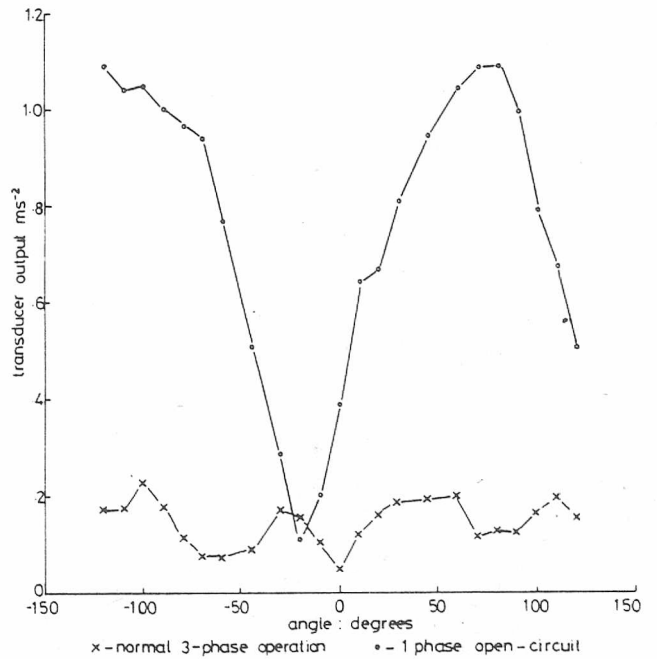
Figure 4 100 Hz vibration component as a function of position and operating condition
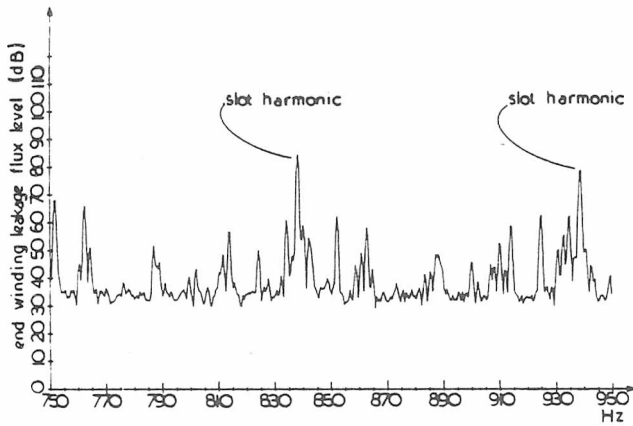
Figure 5 End winding leakage flux zoom spectrum, normal rotor
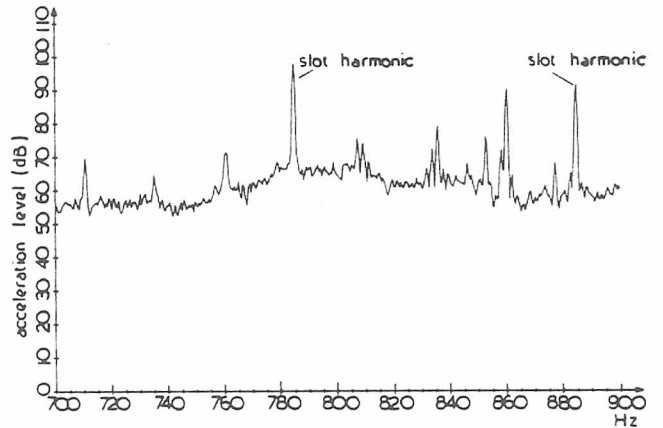
Figure 7 Acceleration zoom spectrum, normal rotor
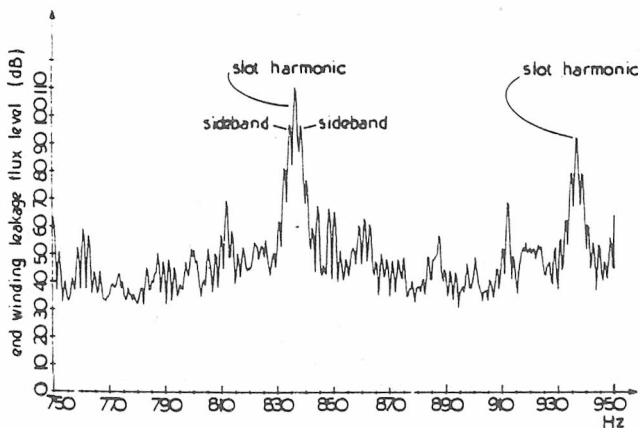
Figure 6 End winding leakage flux zoom spectrum, one broken bar
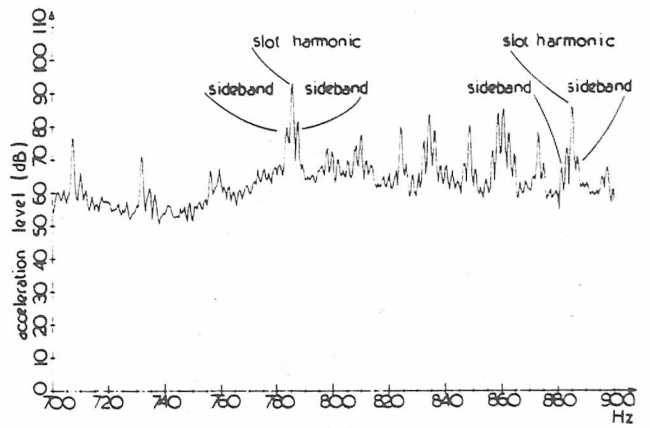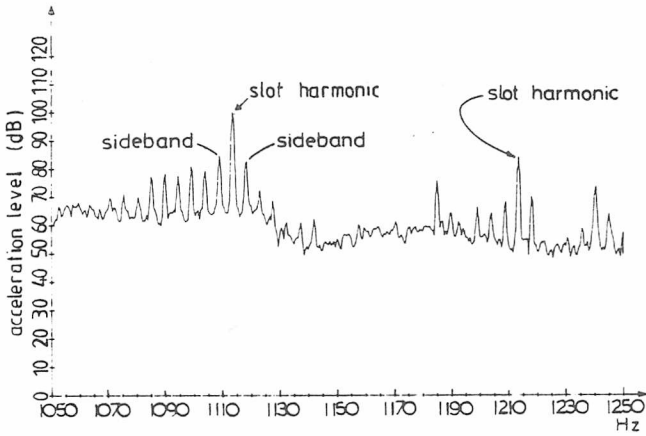

Figure 8 Acceleration zoom spectrum, one broken bar

Figure 9 Acceleration spectrum, 51 slot rotor, 8 high resistance joints
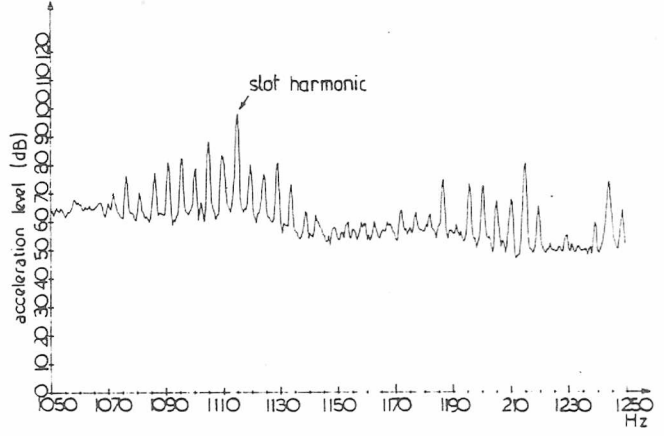
Figure 11 Acceleration spectrum, 51 slot rotor, 1 broken bar, 7 high resistance joints
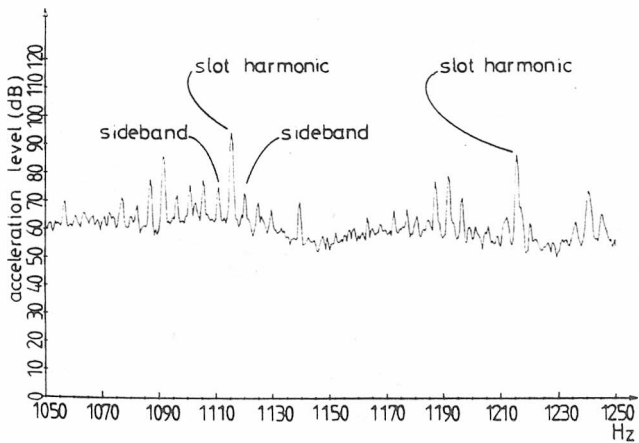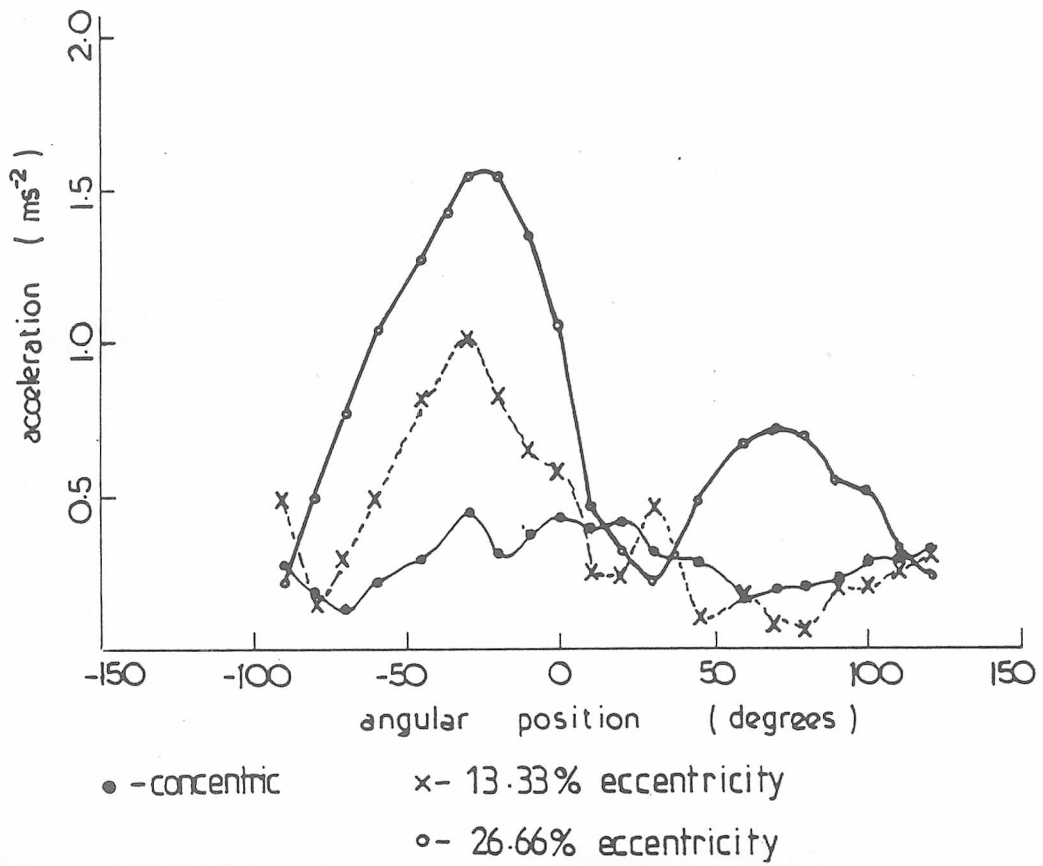

Figure 10 Acceleration spectrum, 51 slot rotor, 1 high resistance joint
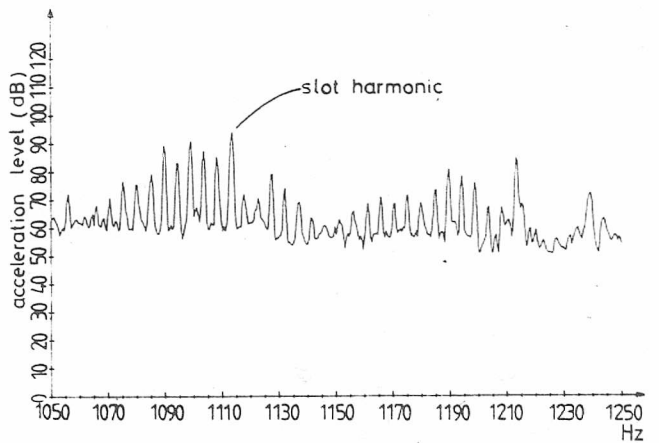
Figure 12 Acceleration spectrum, 51 slot rotor, 1 broken bar, no high resistance joints

Figure 13 Acceleration level of 885 Hz component versus transducer position with varying eccentricity
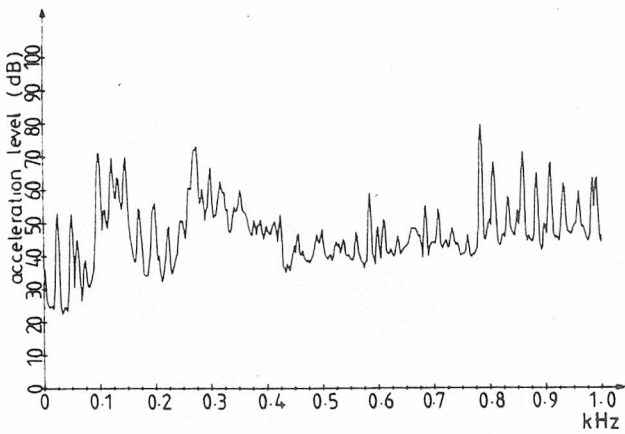

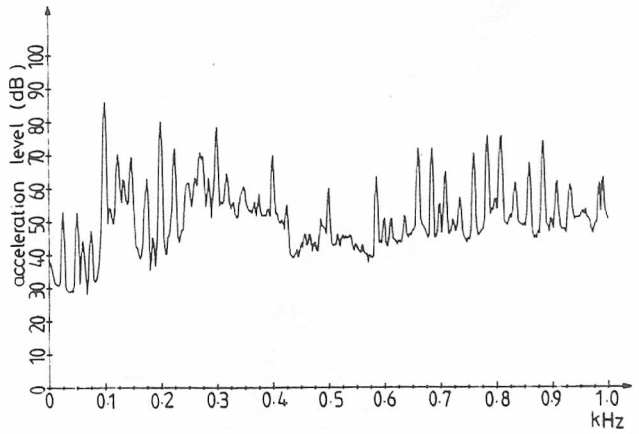Figure 14 Acceleration spectrum, normal winding

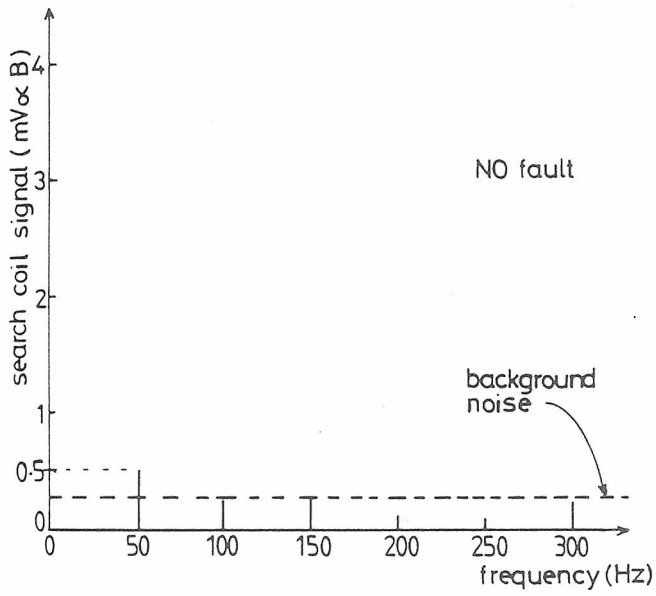Figure 15 Acceleration spectrum, short-circuited stator coil

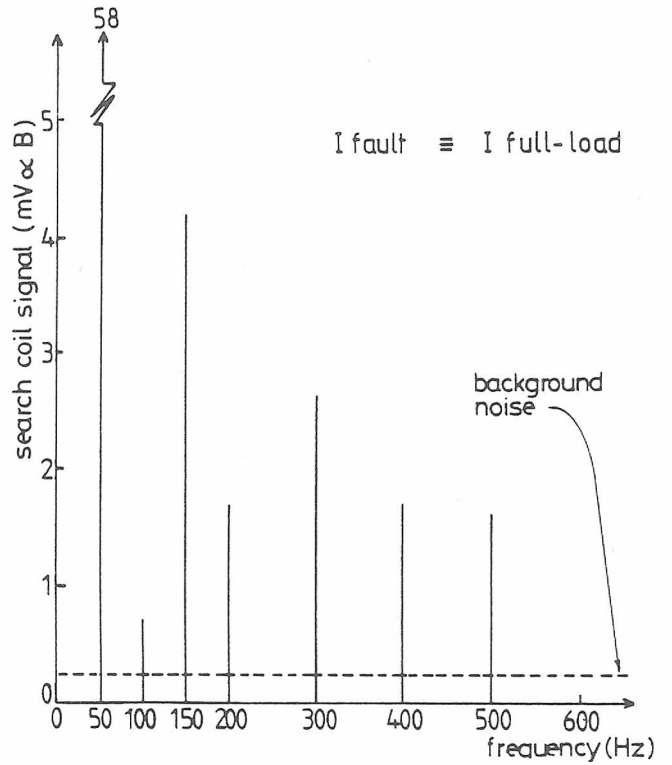Figure 16 Axial flux signal versus frequency with normal winding

Figure 17 Axial flux signal versus frequency with an inter-turn fault